Characterisation of CD3-enhanced gene-modified $CD4^+$ T cells for cancer immunotherapy

Alice Piapi

UCL

A thesis submitted to University College London (UCL) for the degree of

DOCTOR OF PHILOSOPHY

I, Alice Piapi confirm that the work presented in this thesis is my own. Where information has been derived from other sources, I confirm that this has been indicated in the thesis.

_____

Alice Piapi

Abstract

TCR gene transfer is used to redirect the antigen specificity of T lymphocytes towards known tumour antigens. TCR gene therapies in murine studies have shown promising results. However, in the clinic they have often generated sub-optimal responses, when compared to treatments with tumour infiltrating lymphocytes. Previous work to improve TCR gene therapy has demonstrated that transferring additional CD3 genes increases TCR expression of both endogenous and introduced TCR, in $CD4^+$ and $CD8^+$ T cells. *In vivo* experiments demonstrated that $CD8^+$ T cells, transduced with TCR and additional CD3 were more effective in tumour protection than T cells transduced with the TCR alone.

In this thesis the effects of CD3 (and as a consequence TCR) overexpression were studied in $CD4^+$ and $CD8^+$ T cells, that had been transduced with a retroviral vector containing the CD3 chains genes (CD3-GFP). *In vitro* analysis showed that $CD4^+$ T cell expressed higher levels of TCR compared to $CD8^+$ T cells, both before and after transduction with the CD3-GFP vector. This associated with higher Ca^{2+} and CD107a concentration, but no difference in T cell activation or proliferation. Unexpectedly, we found that increased TCR expression did not improve T cell functional avidity following polyclonal or peptide-specific stimulation. *In vivo* CD3-enhanced $CD4^+$ T cells survived for longer and were recovered in higher percentages, compared to CD3-enhanced $CD8^+$ T cells and mock transduced $CD4^+$ T cells, both in non-competition and competition experiments. Interestingly, this was observed despite a down-regulation of TCR levels in the CD3-enhanced $CD4^+$ T cells, compared to their pre-transfer TCR levels, which was not observed in the control-transduced $CD4^+$ T cells. The mechanism that drives TCR down-regulation and its biological meaning are unknown and require further investigation.

Acknowledgements

First, I would like to thank both my supervisors, Professor Emma Morris and Professor Hans Stauss for the opportunity to undertake my PhD in their lab. I'm very grateful for your supervision, patience and support. I now know that just because an experiment doesn't give the results I expect, it doesn't mean that it hasn't worked; and how to design experiments with a clear question in mind.

However, I truly believe I wouldn't be here writing the acknowledgments for a PhD thesis if it wasn't for the people in the lab, who made these past years VERY enjoyable, and were always there when things weren't going so well. Angelika, from day one you welcomed me in the lab and became my teacher. Thank you for all the advice and everything else you've done for me, from the endless (sometimes crazy) chats and discussions, to listening to my rants. Similarly, thank you to Alastair for being a great "consigliere" (his words, not mine) and friend. I'm glad I had the opportunity to learn from the "golden child", and I'm ever so thankful for your constant grammar checks! Thank you also to Sharyn, for all your help, for always testing my FlowJo, Prism and computer knowledge and for even more crazy conversations. I'm glad I chose to sit next to you three! Janani, thank you for your help, with both FACS related and non FACS related issues. I'm sorry about all the times I bothered you because your machines were not working and I couldn't figure out why. Sophie and Heather, you two also played a big part in making these years really fun! Thank you for our numerous tea-breaks and for your support in dealing with Alastair's sass. Last but not least, thank you to all the other lab and Institute members, both past and present, who contributed to a thoroughly enjoyable 4 years: Bea, Rachel, Rita, Jenny, Olivier, Aimee, Graham, Maria, and Bernardo.

Ringraziamenti

Grazie mille a tutti quelli che in un modo o nell'altro mi hanno supportato (e sopportato) in questi anni, non solo durante il dottorato, ma anche durante la triennale.

Prima di tutto grazie alla mia famiglia. Grazie ai miei genitori, per tutti i sacrifici che hanno fatto, per darmi l'opportunita' di studiare quello che volevo, dove volevo. Soprattutto a te papa' che nonostante tutto non mi hai mai fatto pesare niente in questi 8 anni, e mi hai sempre tranquillizzata e tenuta aggiornata su come andavano le cose a casa. Grazie ai fratelli migliori del mondo! Nonostante gli insulti e le battutacce, so di poter sempre contare su di voi. Questo dottorato e' la conferma che io sono decisamente la piu' intelligente dei 3!

Grazie ai miei nonni! Le vostre chiamate, i vostri messaggi, le cipolle e i funghi secchi, le berrette e i calzini di lana, i risotti in busta, i vostri "quando torni?" ecc., mi hanno sempre fatto sentire a casa. Non potevo desiderare nonni migliori di voi!

Grazie alla persona che probabilmente mi conosce meglio di chiunque altro, Angela. Nonostante gli anni trascorsi lontane e le mille esperienze diverse nulla e' cambiato, e adesso come in seconda superiore so di poter contare su di te per qualsiasi cosa, sempre. Non c'e' bff migliore di te! Grazie a Michael, Zanetta, Saviori e Bruno per gli anni passati sui banchi del Ghislandi, ma soprattutto per tutte le serate amarcord dal 2009 ad oggi!

L'ultimo pensiero pero' va a te Paola. Se sono arrivata qua e' grazie a te. Manchi.

Contents

List of Figures

List of tables

List of abbreviations

-/-	knock-out
ACT	adoptive cell therapy
AIRE	autoimmune regulator transcription factor
AP-1	activator protein 1
APC	antigen presenting cell
BAD	BCL-2 antagonist of cell death
BID	interacting domain death agonist
BIM	BCL-2-interacting mediator of cell death
BM	bone marrow
CAR	chimeric antigen receptor
CCR5, 7…	C-C chemokine receptor 5, 7…
CD3, 4...	Cluster of differentiation 3, 4, ..
CDR	complementarity determining region
CEA	carcinoembryonic antigen
CLIP	class II associated Ii peptide
cSMAC	central SMAC
cTEC	cortical thymic epithelial cell
CTL	cytotoxic T lymphocyte
CTLA-4	cytotoxic T lymphocyte antigen 4
CXCL9, 10…	C-X-C chemokine ligand 9, 10…
CXCR5	C-X-C chemokine receptor type 5
DAG	diacylglycerol
DC	dendritic cell
DN	double negative
DNA	deoxyribonucleic acid

DP	double positive
dSMAC	distal SMAC
ER	endoplasmic reticulum
ERAD	ER associated protein degradation
ERAAP	ER aminopeptidase associated with antigen processing
ERAP1, 2	ER aminopeptidase1, 2
FasL	fas ligand
FSC	forward scatter
GFP	green fluorescent protein
Gy	gray
HLA	human leukocyte antigen
i.p.	intra-peritoneal
i.v.	intra-venous
ICAM-1	intercellular adhesion molecule 1
IFNγ	interferon gamma
Ii	invariant chain
IL-1, 2…	interleukin 1, 2…
Iono	ionomycin
IP_3	inositol triphosphate
IRES	internal ribosome entry site
IS	immunological synapse
ITAM	immunoreceptor tyrosine-based activation motif
K_D	dissociation constant
LAT	linker for activation of T cells
Lck	lymphocyte-specific protein tyrosine kinase
LFA-1	leukocyte function associated antigen 1
LN	lymph node

LTR	long terminal repeats
MAGE-3	melanoma associated antigen 3
MAPK	mitogen activated protein kinase
MART-1	melanoma antigen recognised by T cells 1
MCA	Methylcholanthrene
MHC-I, -II	major histocompatibility complex class I, II
MIIC	MHC class II compartment
mRNA	messenger RNA
mTEC	medullary thymic epithelial cell
mTOR	mammalian target of rapamycin
NFAT	nuclear factor of activated T cells
NFκB	nuclear factor kappa light chain enhancer of activated B cells
NK cell	natural killer cell
PBMC	peripheral blood mononuclear cells
PBS	phosphate buffered saline
PI	propidium iodine
PI3K	phosphatidylinositol 4,5 bisphosphate 3 kinase
PIP-$_2$	phosphatidylinositol 4,5 bisphosphate
PLC-γ1	phospholipase C gamma 1
PMA	Phorbol 12-myristate 13-acetate
pSMAC	peripheral SMAC
RAG	recombination activating gene
SCID	severe combined immunodeficiency
Self-p:MHC	self-peptide:MHC complex
SLP-76	SH2 domain containing leukocyte protein of 76kDa
SMAC	supramolecular activation cluster
SSC	side scatter

TAA	tumour associated antigen
TAP	transporter associated with antigen processing
T_{CM}	central memory T cell
TCR	T cell receptor
TCR:pMHC	TCR:peptide-MHC complex
T_{EM}	effector memory T cell
Tfh	follicular helper T cell
TGF-β	transforming growth factor beta
Th1, 2...	Helper T cell type 1, 2…
TIL	tumour infiltrating lymphocyte
TNFα, β	tumour necrosis factor alpha, beta
TREC	TCR rearrangement excision circles
Treg	regulatory T cell
TRP1	tyrosinase-related protein 1
TSA	tumour specific antigen
ZAP70	ζ-chain-associated protein kinase of 70 kDa

1. Introduction

T cells, along with B cells, form the adaptive immune response that is mounted when the innate immune cells such as macrophages, neutrophils and NK cells are insufficient to deal with a pathogen. Whereas the innate response is quicker and of broad specificity, the adaptive immune response is typically slower, but highly specific and it recognises defined pathogen associated signals. In the case of T cells their specificity is determined by a unique T cell receptor, which defines what antigen will be recognised by that T cell.

1.1. The T cell receptor-CD3 complex

1.1.1. The T cell receptor

The T cell receptor (TCR) is expressed on the surface of all T cells and determines what antigen that T cell will be able to respond to (T cell specificity). The TCR is a heterodimeric membrane anchored protein composed of a disulphide linked α and β chain (figure 1.1). Both chains consist of two immunoglobulin like domains: a constant region domain that spans the cell membrane, and a variable region that projects outwards and is responsible for antigen binding (Davis and Bjorkman 1988). The variable domain binds, with relatively low affinity (~1-100 μM), short antigen fragments (peptides) when presented by major histocompatibility complex (MHC) molecules. The variation in TCR specificity is generated both by the assembly of the two different TCR chains and by a process known as V(D)J recombination. As T cells mature in the thymus they undergo a process of somatic recombination which rearranges the variable (V), joining (J) and, in the β chain, diversity (D) gene segments that comprise the variable region of the TCR. Additional nucleotides are also inserted or deleted in the rearranged regions during these recombination events (Schatz et al., 1992). The variability generated during the V(D)J recombination is mirrored in the complementarity determining region (CDR) of

the TCR variable chain. Each variable chain contains three CDRs: CDR1 and CDR2 bind the α-helix of the MHC molecule; CDR3, also known as hypervariable region, binds the peptide (Rudolph, 2006). Because V(D)J recombination is somewhat random, an enormous number of TCR and specificities can theoretically be generated and it is estimated to be in the range of about 10^{18} different TCRs, which to put things in perspective it is also the predicted number of grains of sand on planet Earth (Reddy, 2017). The initial understanding was that each TCR will only recognise one unique antigen. However, there are $>10^{15}$ potential foreign peptides that the immune system has to recognise and the human body contains only about 10^{12} T cells. More recent studies have estimated that the total number of TCR within this T cell pool is $<10^{8}$. Thus, it is now widely accepted that TCRs are degenerate and can bind multiple peptides and it is expected that one single antigen can be recognised by a variety of TCRs (reviewed in Sewell, 2012).

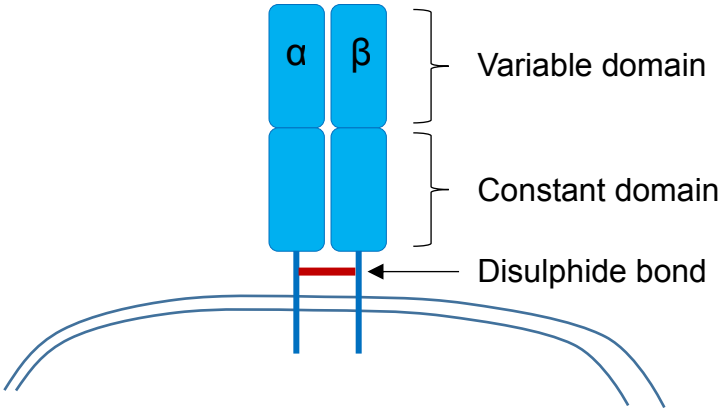

Figure 1.1– The T cell receptor (TCR).

1.1.2. The CD3 co-receptor

Signals transmitted via the TCR are the primary checkpoints controlling T cell activation, and the quality and strength of these signals determine the fate and ultimate function of the T cell. However, as the TCR does not contain any signalling domains within its

structure, TCR signalling is dependent upon association with the CD3 complex. In addition, cell surface expression of the TCR is dependent upon CD3 co-expression. The CD3 complex comprises 4 different chains: zeta (ζ), gamma (γ), epsilon (ε) and delta (δ) (figure 1.2).

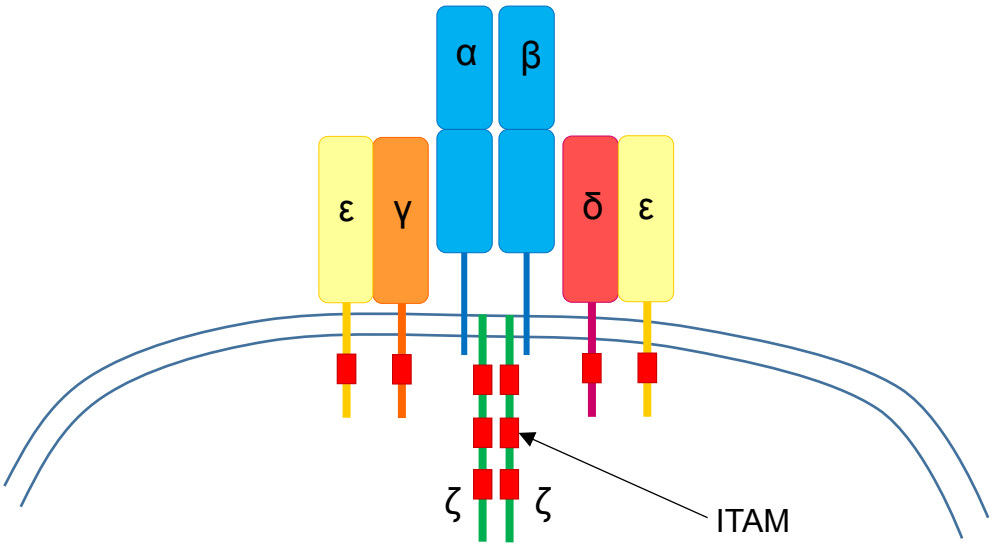

Figure 1.2– The TCR:CD3 complex.

All of the CD3 chains except for ζ are members of the immunoglobulin-like superfamily. CD3γ, ε and δ are structurally related and have significant sequence homology. They are encoded by genes on chromosome 11 (human) and chromosome 9 (mice). In contrast the CD3ζ chain has no structural or sequence homology to the other CD3 components and the gene coding for the ζ chain is found on chromosome 1 (in both human and mouse) (Baniyash, 2004). The cytoplasmic domains of each of the CD3 chains contain immunoreceptor tyrosine-based activation motifs (ITAMs) (YxxL/Ix6-12YxxL/I) through which the TCR signal is propagated inside the cell. Each ζ chain contains 3 ITAMs, whilst the other three chains contain one motif each. These signalling chains are known to form three distinct dimers: CD3δε, CD3γε and CD3ζζ. The TCR-CD3 complex assembles in the endoplasmic reticulum (ER) in an ordered process driven

by interactions among both transmembrane (TM) and extracellular domains of the CD3 and TCR subunits (Call et al., 2004). Studies carried out in Jurkat cells showed that the assembly of the CD3-TCR complex is a relatively rapid process, whereas the export of the complex from the ER to the Golgi apparatus is slow (Alarcon et al., 1988). The formation of a correct TCR-CD3 complex depends on the correct placement of nine ionizable residues within the TM domains of the TCR and the CD3 chains (figure 1.3). The TCRα chain first binds the CD3δε dimer by formation of a three-helix bundle, with each chain contributing one ionizable residue (2x acidic and 1x basic residues) to the interface among the three helices. A similar process allows the TCRβ chain to bind the CD3γε dimer. Once both CD3 dimers have assembled with the TCR, the ζζ dimer binds to the complex via a second distinct site in the TCRα chain (Call et al., 2004; Call et al., 2002). The α and β TCR chains dimerize via formation of disulphide bonds. Interaction of the two TCR chains only is not sufficient to prevent rapid degradation and such a dimer has a $T_{½}$ of 35-45 minutes in the ER. This degradation was shown to be a consequence of basic residues within the TM domains being exposed to the ER environment, as binding of the TCR chains with the CD3 dimers leading to shielding of such residues prevented degradation (Call et al., 2004). The sequestration of strongly polar residues at specific protein-protein interfaces, in addition to a specific ER retention signal present in the cytoplasmic domain of the CD3ε chain serve as a quality control mechanisms which determine the fate of the TCR-CD3 complex (Carrasco et al., 2001). Moreover, TCRαβ-CD3γε-CD3δε hexamers lacking the ζζ dimer that escape the ER are degraded by a second quality control step in the Golgi, thus preventing the expression of defective TCR-CD3 complexes on the cell surface (Sussman et al., 1988). Therefore, if one or more components of the TCR-CD3 complex are absent, the incomplete complex is retained and degraded within the ER or degraded once it reaches the Golgi complex. A fully functional and surface-expressed TCR-CD3 complex is thus composed of one TCRαβ heterodimer, one CD3γε homodimer, one CD3δε homodimer and one CD3ζζ heterodimer.

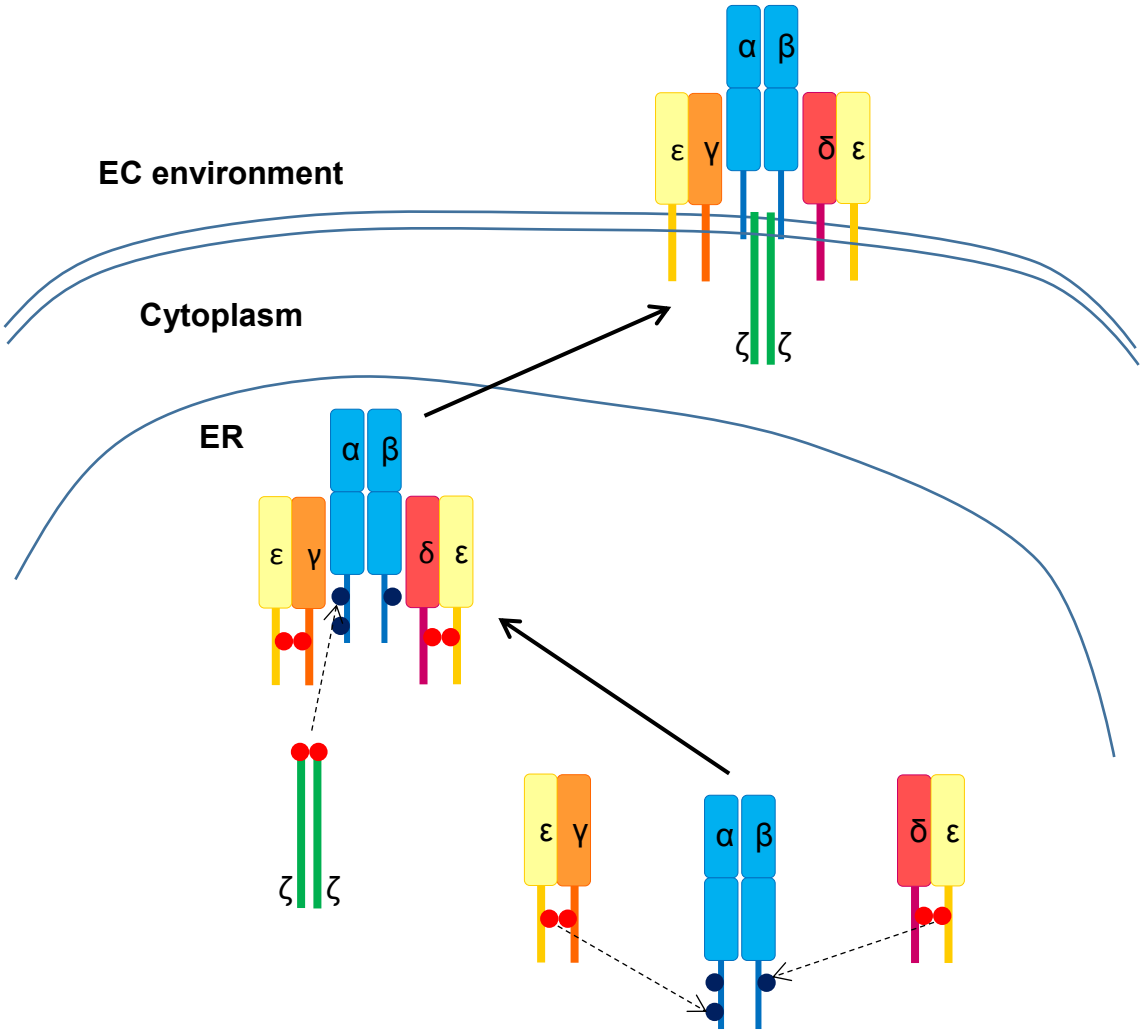

Figure 1.3 – The assembly of the TCD:CD3 complex.

1.1.3. The role of the CD3 co-receptor in thymocyte development and disease

Correct CD3 chain arrangement and expression was shown to be fundamental for thymocyte development. Genetically engineered mice deficient for any of the CD3 chains resulted in a block of thymocyte maturation at the double negative (DN) or double positive (DP) stage (Love et al., 1993; Malissen et al., 1995; Wang N. et al., 1998). The severity of this block and the phenotype of the mice changed depending on which CD3

chain was absent. The most important dimer for thymocyte maturation was CD3γε, followed by the ζζ dimer, whereas the CD3δε may be dispensable. Abrogation of expression of any of the CD3 chains causes a severe impairment in thymic output in mice. This study also suggested an overlapping role for CD3γ and CD3δ chains. Mice lacking either one of those chains developed only a small number of mature T cells. However, in mice deficient for both γ and δ chains mature T cells were not found (Wang B. et al., 1998). Additional genetic studies in which the ITAMs of the different CD3 chains were modified shed light on the importance played by these motifs in thymocyte development. In particular the efficiency of thymic selection was shown to correlate with the number of ITAMs (Shores et al., 1997; Love et al., 2000; Pitcher et al., 2005b). More recent studies showed that mutation of three or more ITAMs in one or more of any of the CD3 chains led to defective negative selection and development of fatal autoimmunity (Holst et al., 2008). This was thought to be a consequence of lower TCR signal strength during negative selection, allowing self-reactive T cells to escape the thymus leading to a breakdown of central tolerance. Notably, effector functions seem to be governed by different rules as cytokine production was relatively unaffected by a lower number of CD3 ITAMS, whereas lower proliferation had a linear correlation with the number of ITAMs present in the cell. These findings are in contrast with results from other studies, which have shown that ITAM-mutated CD3ζ and CD3γ transgenic mice did not exhibit autoimmunity and only a few cells showed mild auto reactivity (Shores et al., 1997; Ardouin et al., 1999; Haks et al., 2002; Pitcher et al., 2005a). The reason/s behind these discrepancies are not clear, but the different techniques used for genetic manipulation (retroviral transduction followed by adoptive transfer versus transgenesis) may explain the differences seen in the data sets. In addition, it has been shown that both other motifs in the CD3 chains and the length of the CD3 chain may play a role in thymocyte development, by influencing TCR-CD3 complex expression, signalling and trafficking (Dave, 2009).

Modulation of CD3 chains expression is also important for the correct functioning of mature T cells and their ability to mount an effective immune response. Patients with CD3 γ, δ, ε or ζ deficiencies have been reported and typically present with a severe combined immuno deficiency (SCID) phenotype, including absence of functional T cells and normal, but non-functional B cells. Recio et al. reported five patients with CD3γ deficiency, all of which presented with mild T lymphocytopenia, poor *in vitro* proliferative responses to antigens and very low TCR rearrangement excision circles (TRECs). However both intrafamilial and interfamilial variation was seen with some individuals reaching the third decade of life in healthy conditions, whereas others showed lethal SCID features and enteropathy in early life (Recio et al., 2007). More recently two siblings with autoimmunity were reported and upon genetic analysis it was discovered they both carried a mutation in the CD3γ gene (Tokgoz et al., 2013). Defects in CD3ε expression have also been reported in multiple patients. Three consanguineous patients all died within six months of age from viral infections and pneumonitis (Soudais et al., 1993). In contrast a two year old patient with CD3ε deficiency and recurrent pneumonia with otitis media was treated with antibiotics and no major infections were seen thereafter (de Saint Basile et al., 2004). The difference in survival between those two sets of patients may be explained by the different degree of CD3ε deficiency. A complete loss of expression (former three patients) correlated with severe immunodeficiency, whereas the latter patient's mutation did not totally prevent CD3ε expression. Several reports regarding CD3δ deficiency also exist. The thymus of a CD3δ-deficient fetus was analysed and it revealed that T cell differentiation was blocked at entry into the DP stage, indicating CD3δ may play an essential role in promoting thymocyte development (de Saint Basile et al., 2004). In another report describing three cousins, two died within the first three months of life due to multi-organ failure. The third one was diagnosed with CD3δ deficiency at birth, underwent bone marrow transplantation and was alive and well at three years of age (Dadi et a., 2003). As for deficiencies of the CD3ε chain, the degree of CD3δ loss seemed to correlate with patient outcome. CD3ζ deficiencies have been reported in a number of patients too. CD3ζ deficiency was linked to $T^- B^+ NK^+$ SCID in

two patients, both of whom received bone marrow transplantation to correct the immunodeficiency (Roberts et al., 2007; Rieux-Laucat et al., 2006). In a separate family two siblings were diagnosed with CD3ζ deficiency which caused lower expression of TCR-CD3 complex expression and a subsequent immunodeficiency. Lethal severe autoimmune haemolytic anaemia developed in one of the patients, who died at the age of three (Alarcon et al., 1988). Thus, a number of cases have been reported in which autoimmune disease developed as a consequence of CD3 chain deficiencies. The clinical features are highly variable and depend upon the affected chain and the type of mutation. Treatment has been aimed at infection control (where co-existing immunodeficiency exists) and where possible, a curative bone marrow transplantation can be attempted.

CD3 chain down-modulation leading to TCR-CD3 downregulation and T cell function impairment has been shown in mature T cells isolated from hosts with various chronic pathologies, including cancer, autoimmunity and chronic infection. Mutations causing this phenotype have been observed in all of the CD3 chain genes. A downregulation of the CD3γ gene, followed by a progressive impairment in TCR-CD3 complex expression and function was reported early upon HIV-1 and HIV-2 infection (Willard-Gallo et al., 1996; Segura et al., 1999; Willard-Gallo et al., 2001). HTLV-1, the agent known to cause T cell leukaemia and lymphoma, also has the capacity to impair T cell function upon infection. Akl et al., have shown that HTLV-1 infection initiates a process leading to complete loss of CD3 membrane expression by an epigenetic mechanism. The onset of this phenomenon coincided with a decrease of CD3γ followed by subsequent progressive reduction in CD3δ, then CD3ε and CD3ζ mRNA (Akl et al., 2007). However, in the majority of reported cases T cell dysfunction was a consequence of CD3ζ specific downregulation. The first report showing CD3ζ downregulation in the context of cancer came from an experimental model of colon carcinoma, in which cytotoxic T cells showed impaired effector function (Mizoguchi et al., 1992). Since then a number of reports describing aberrant T cell function in solid and non-solid tumours due to CD3ζ

downregulation have been published, from both human patients and animal models. These include colorectal cancer (Matsuda et al., 1995), renal cell carcinoma (Finke et al., 1993), ovarian carcinoma (Kuss et al., 2002), breast cancer (Kurt et al., 1998), prostate cancer (Healy et al., 1998), head and neck cancer (Kuss et al., 1999), melanoma (Dworacki et al., 2001) and acute lymphoblastic leukemia (Torelli et al., 2003). Ungefroren et al. suggested that CD3ζ downregulation may be one of the many mechanisms employed by tumour cells to evade immune surveillance. This hypothesis was based on the observation that factors secreted by malignant cells drive ζ downregulation (Ungefroren et al., 1999). Interestingly, initial CD3ζ downregulation was seen in tumour infiltrating lymphocytes (TILs) only, but upon cancer progression this phenomenon extended to peripheral blood lymphocytes (Baniyash, 2004). Moreover CD3ζ chain expression has been shown to correlate with cancer patients' outcomes, with low or absent ζ chain expression predicting poor prognosis and survival. Thus it could become a useful biomarker both for cancer prognosis and decisions on whether to administer immunotherapy or not (Whiteside, 2004). T cells isolated from patients suffering from systemic lupus erythematosus and rheumatoid arthritis also showed lower CD3ζ expression levels (Liossis et al., 1998; Maurice et al., 1997; Berg et al., 2000). Loss of ζ chain expression and dysfunctional T cells have also been reported in various infectious diseases. Patients who are infected with HIV (but have yet to develop AIDS) were found to have reduced CD3ζ levels in both $CD4^+$ and $CD8^+$ T cells (Stefanova et al., 1996; Trimble et al., 1998). A similar pattern of CD3ζ down modulation was seen in leprosy caused by Mycobacterium leprae (Zea et al., 1998) and in helminth infections (Appleby et al., 2015). Eleftheriadis et al. reported a selective downregulation of the ζ chain in chronic renal failure patients on haemodialysis (Eleftheriadis et al., 2008). Interestingly, in all the situations described above despite the absence of the CD3ζ chain, TCR levels on the cell surface were reported as normal. Studies have shown that the ζ chain can be replaced by the γ chain of the receptor for IgE (FcεR) leading to normal concentration of TCR on the cell surface but impaired T cell function after TCR:pMHC binding (Mizoguchi et al., 1992; Zea et al., 1998). As discussed above CD3ζ chain

downregulation can be driven by factors secreted by the tumour cells. In addition reports have shown that both oxidants secreted by macrophages within the tumour microenvironment but also chronic antigen exposure can cause ζ downregulation (Kono et al., 1996; Otsuji et al., 1996; Bronstein-Sitton et al., 2003). The reason behind ζ chain targeting may lie behind the central role played by CD3ζ in TCR signalling. In a fully functional T cell following TCR engagement the lymphocyte-specific protein tyrosine kinase (Lck) phosphorylates residues in the CD3ζ chain ITAMs, allowing the ζ-chain-associated protein kinase of 70 kDa (ZAP70) to bind and the signal to the transmitted downstream. Total or partial loss of CD3ζ expression thus prevents activation of the T cell (T cell signalling will be discussed in section 1.1.7) allowing disease progression.

1.1.4. The CD4 and CD8 co-receptors

The first indication that two different subsets of T lymphocytes exist came from studies in the mid 1970's, when it was shown that T cells express either the CD4 or CD8 co-receptor, and these receptors are mutually exclusive (Bach et al., 1976). With this came the discovery that the two subsets also had different functions: $CD4^+$ cells augmented the ability of B cells to produce antibodies (Cantor et al., 1977), whereas $CD8^+$ cells caused direct cytotoxicity of infected target cells (Cantor et al., 1975). Finally during the 1980's the discovery that CD4 binds to and recognises antigens on MHC-II and CD8 binds to recognises antigens on MHC-I was made (Doyle et al., 1987; Norment et al., 1988). It is now known that these co-receptors are glycoproteins which participate in both T cell development and antigen recognition. CD4 is a single chain composed of an intracellular domain and four extracellular Ig-like domains (D1 – D4) which binds via its D1 domain, a hydrophobic crevice at the junction between the α_2 and β_2 chains of the MHC-II molecule (figure 1.4 left). The CD8 co-receptor is a dimer composed of two different chains, one α and one β linked by a disulphide bond, and both chains interact with residues in the α_2 and α_3 domains of MHC-I (figure 1.4 right). The role played by the co-receptors has been intensively studied. Studies have shown that CD8 plays a role in stabilising the TCR:pMHC interaction, and such role is particularly important in the case

of lower affinity antigens whereas the requirement for CD8 is minimal in the case of strong TCR ligands with lower off-rates (Wooldrige et al., 2005). In contrast, it has been shown that CD4 does not play a stabilising effect on TCR:pMHC interactions. When the CD4:pMHC interaction was inhibited using anti-CD4 blocking antibodies, no change in the formation (kinetics and architecture) of immunological synapses was seen (Huppa et al., 2010). Both CD4 and CD8 co-receptors, however, play a critical role in enhancing TCR signalling by recruiting Lck to the TCR complex. When a TCR complex is engaged, the co-receptors in its proximity can bind Lck, preventing it from diffusing away (Chakraborty et al., 2014). Lck will then phosphorylate the ITAMs within the CD3ζ chains allowing ZAP70 to bind, initiating TCR signalling. TCR signalling will be discussed in further detail in section 1.1.7. The CD4 and CD8 co-receptors also contribute to naïve T cell survival and the homeostatic expansion of their relevant T cell subsets, as shown by studies where conditional loss of CD4 or mutation of the CD4 binding site on the MHC-II molecules inhibited the homeostatic expansion of $CD4^+$ cells in vivo (Strong et al., 2001; Ge et al., 2001).

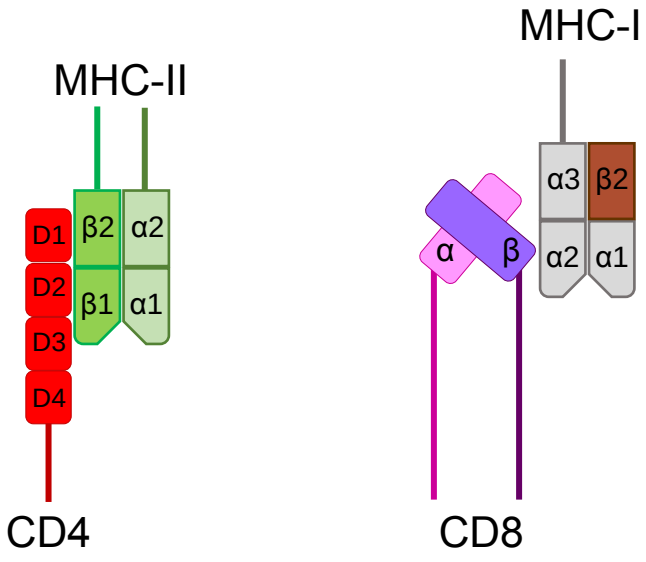

Figure 1.4 – The CD4 and CD8 co-receptors, and MHC-II and MHC-I molecules.

1.1.5. Antigen presentation and antigen recognition

T cells only recognize antigens that are displayed on cell surfaces and presented to them in the context of an MHC molecule, a process known as antigen presentation. The MHC molecules are encoded by genes in the major histocompatibility complex region, which is found on chromosome 6 in humans, and they were first identified in the context of transplantation. For that reason this cluster of genes and their protein output are known as the major histocompatibility complex. MHC molecules are divided into two classes: MHC class I and MHC class II. Both MHC-I and MHC-II molecules bind and present small peptides that derive from intact antigens. This process of peptide generation from a naïve protein is known as antigen processing. However, the structure, expression profile and function of these two classes of MHC are different. MHC-I molecules are expressed by all nucleated cells and the peptides they present originate in the intracellular milieu (cytoplasm or nucleus). MHC class I molecules are heterodimers composed of 2 chains: one heavy α chain formed of 3 different domains (α1-α3) and one light β_2-microglobulin chain (figure 1.4 right). The majority of peptides presented in the context of MHC-I are of intracellular origin (e.g. viral or nuclear antigens). In some circumstances peptides of extracellular origin can be presented on MHC-I molecules, via a process known as cross-presentation, which will be discussed later in this section. Proteins at the end of their functional life are degraded by the cellular proteasome-ubiquitin dependent system: proteins are conjugated with ubiquitin, which directs them to cytosolic and nuclear multicatalytic complexes, knows as proteasomes for subsequent degradation (Pickart et al., 2004). Proteasome activity is fundamental for antigen presentation by MHC-I molecules, as inhibitors of the proteolytic activity of the proteasome prevents MHC-I peptide presentation (Rock et al., 1994). Once a protein has been degraded the peptides that have been generated can either be destroyed by additional peptidases or pumped into the ER lumen via a specialised peptide transporter known as transporter associated with antigen processing (TAP). Inside the ER MHC-I molecules are stabilised by chaperone proteins such as tapasin, calreticulin and ERp57. These chaperones, the

MHC-I molecule and TAP form the so called peptide loading complex (PLC). Once inside the ER, peptides can then bind the MHC-I allowing the release of the chaperones and the export of the peptide:MHC-I complex to the cell's surface to facilitate antigen presentation. Since TAP translocates peptides that are between 8 and 16 amino acids in length (Parcej et al., 2010), and MHC-I complexes can only bind peptides of 8-10 residues in length due to their closed binding grove (York et al., 2002; Mohan et al., 2012), some peptides will need further "trimming" before loading onto the MHC-I molecule. This is carried out by ER aminopeptidases. One such enzyme has been identified in mice and it is known as ER aminopeptidase associated with antigen processing (ERAAP) (Serwold et al., 2002), and two of these enzymes have been discovered in humans and are known as ER aminopeptidase 1 and 2 (ERAP1 and ERAP2) (Saveanu et al., 2005). If a peptide that has entered the ER is not suitable for MHC-I binding, even after the action of ER aminopeptidases, it is transported back into the cytosol by the ER associated protein degradation (ERAD) system for destruction or for a new round of TAP translocation (Roelse et al., 1994; Neefjes et al., 2011) (figure 1.5). MHC class II molecules are primarily expressed by professional antigen presenting cells (APCs), such as dendritic cells (DCs) and B cells. However, expression of MHC-II can be induced by stimuli such as IFNγ in non-APCs, including fibroblasts and endothelial cells (Geppert et al., 1985) and mesenchymal stromal cells (Romieu-Mourez et al., 2007). The peptides presented by class II complexes are of extracellular origin and derive from proteins degraded via the endosomal pathway. The structure of MHC-II is similar to that of MHC-I: it is composed of two transmembrane chains, one α and one β, each consisting of two domains (figure 1.4 left). MHC-II α and β chains assemble in the ER and form a complex with the invariant chain (Ii). This prevents the premature binding of peptides but also contains two dileucine sorting motifs that direct MHC-II molecules to endosomal compartments (Landsverk et al., 2009). The dileucine motifs are recognised by the sorting adaptors AP1 (a Golgi adaptor) and AP2 (a plasma membrane adaptor). Thus the Ii:MHC-II heterotrimer can be transported to a late endosomal compartment named MHC class II compartment (MIIC), via either the Golgi complex (AP1) or by

endocytosis from the plasma membrane (AP2) (Hofmann et al., 1999). Once inside the MIIC the Ii is digested and a small peptide known as class II associated Ii peptide (CLIP) is left inside the peptide-binding groove of the MHC-II molecule. Exchange of CLIP with a specific peptide of endosomal origin is dependent upon activity of HLA-DM (humans) or H2-DM (mice). Class II complexes are able to accommodate longer peptides, typically 14-20 amino acids long thanks to their open binding grove (Mohan et al., 2012). Once a correct peptide is bound to MHC-II, the pMHC-II complex can translocate to the cell's surface for antigen presentation (Neefjes et al., 2011) (figure 1.6). As a general rule, intracellular peptides are presented to $CD8^+$ T cells by MHC-I molecules and antigens of extracellular origin are presented to $CD4^+$ cells by MHC-II molecules. However, as previously mentioned, in some cases MHC-I molecules can present peptides of extracellular origin, via a process known as cross-presentation, a mechanism discovered in the 1970's (Bevan, 1976). This process is fundamental for $CD8^+$ T cell cross-priming in response to viral infections and tumours that do not involve APCs. During cross-presentation DCs take up peptides by endocytosis mechanisms involving Fc and C-type lectin receptors, and present such peptides to both $CD4^+$ cells via MHC-II molecules and $CD8^+$ cells through MHC-I molecules (Kurts et al., 2010). Ever since its discovery cross-priming and cross-presentation has been shown to be required for defence against many viruses (Sigal et al., 1999) and tumours (Huang et al., 1994), and it is essential for many effective vaccination responses (Yewdell et al., 2005). Moreover, self-antigens can also be cross-presented resulting in deletion of self-reactive $CD8^+$ cells and cross-tolerance (Kurts et al., 1997). Thus, the specificities of MHC class I and class II molecules, in addition to cross-presentation make APCs able to present to T cells peptides of different origin, from almost all cellular compartments.

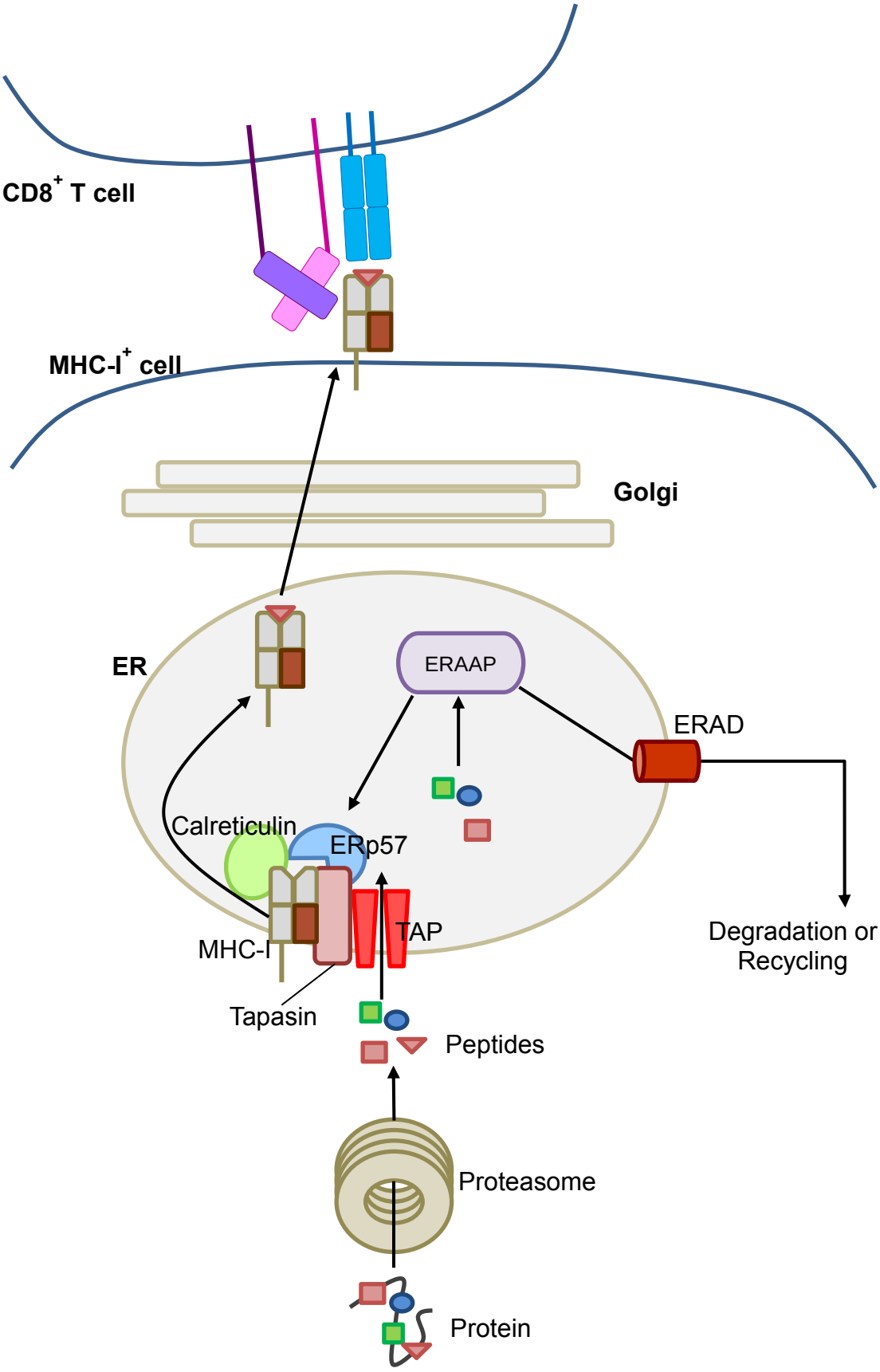

Figure 1.5 – Class I antigen processing and presentation (adapted from Neefjes et al., 2011).

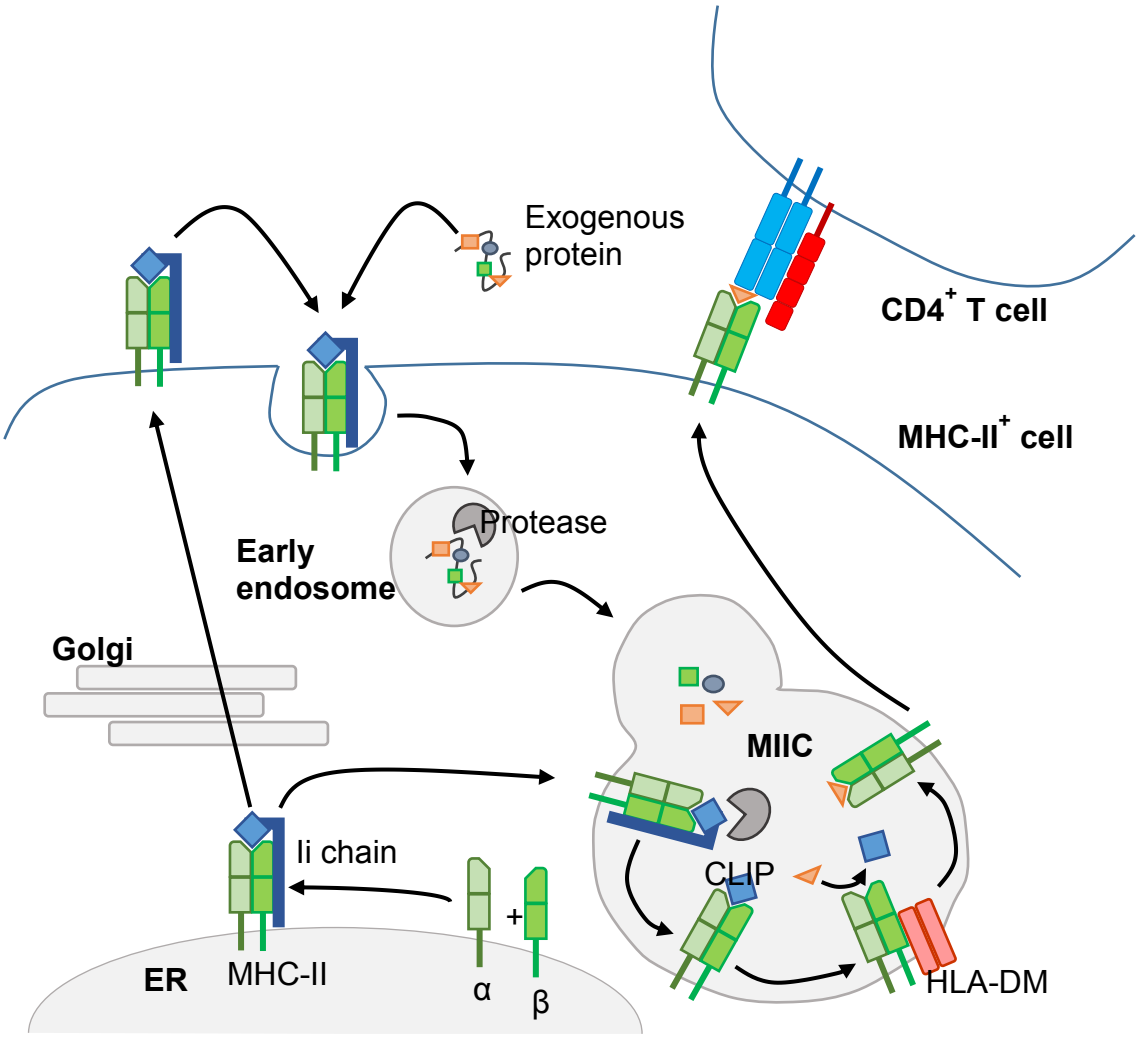

Figure 1.6 – Class II antigen processing and presentation (adapted from Neefjes et al., 2011).

1.1.6. The Immune Synapse

T cells constantly traffic throughout the body "looking" for their cognate antigen presented on a MHC molecule. Within minutes of the initial pMHC:TCR binding the T cell stops trafficking and forms a stable junction with the APC. This specialised junction is known as the immunological synapse (IS) as it bears many similarities to the classical synapse of the nervous system (Dustin et al., 2002) and it is arranged in a bulls-eye structure. The first step that leads to the formation of the IS is the recognition of a pMHC by the cognate TCR. This interaction causes an upregulation of the integrin leukocyte function associated antigen (LFA-1) on the surface of the T cell (Bromley et al., 2002). LFA-1 binds the intercellular adhesion molecule 1 (ICAM-1) on the APC, further slowing down T cell migration and stabilising the interaction between the T cell and the APC. All these receptors are arranged within three supramolecular activation clusters (SMACs): a distal SMAC (dSMAC), a peripheral SMAC (pSMAC) and a central SMAC (cSMAC) (Grakoui et al., 1999; Dustin et al., 2010). In the cSMAC on the surface of the T cell we find TCR micro-clusters, which are formed upon TCR signalling (Varma et al., 2006). Such clusters originally form in the dSMAC and gradually move centrally towards the cSMAC via an actin dependent process (Vardhana et al., 2010). In addition to TCRs we also find CD28, CD4 or CD8 and CD2 in the cSMAC. Importantly, such receptor arrangement within this central zone actively excludes the phosphatase CD45, one of the major negative regulators for TCR signalling (Varma et al., 2006). LFA-1 arranges around the c-SMAC, in the pSMAC. The outermost area is the dSMAC which represents an area of active membrane movement. TCR signalling is initiated with the formation of TCR micro-clusters so the formation of cSMAC is not necessary for TCR signal initiation (Monks et al., 1998). Is it now believed that the cSMAC mainly plays a role in signalling termination, by facilitating TCR ubiquitination and degradation (Lee at al., 2003). Finally, pSMAC may be important for cytolytic killing. It has been proposed that pSMAC might function as a "sealing ring" preventing cytolytic molecules secreted by the T cell to escape in the surrounding environment and focusing the killing on the target cell (Dustin et al., 2010).

1.1.7. TCR signalling

TCR signalling is initiated when a T cell encounters its cognate antigen presented in complex with a MHC-I or –II molecules on an APC. Upon TCR:pMHC interaction a number of changes (increased integrin binding, cytoskeletal rearrangements, production and mobilization of transcription factors and changes in metabolism) occur in the T cell which leads to cell's activation, proliferation and differentiation. The earliest modification that occurs upon TCR engagement is the phosphorylation of tyrosine residues in the CD3ζ chain ITAMs by the CD4/CD8 co-receptor-associated Lck. This in turns leads to the recruitment and activation of ZAP70, which is itself phosphorylated by Lck. ZAP70 phosphorylates two substrates: the linker for activation of T cells (LAT) and the SRC homology 2 (SH2)-domain-containing leukocyte protein of 76 kDa (SLP76). The activated forms of these molecules form a complex which activates phospholipase C-γ 1 (PLC-γ1). The active form of PLC-γ1 produces inositol triphosphate (IP_3) and diacylglycerol (DAG) from phosphatidylinositol 4,5-biphosphate ($PIP-_2$). These two secondary messenger molecules lead to T cell activation by three separate mechanisms. IP_3 causes the release of calcium ions (Ca^{2+}) from the ER and uptake of calcium from the microenvironment and activates calcineurin, which dephosphorylates and activates the transcription factor nuclear factor of activated T cells (NFAT). Conversely, DAG de-inhibits the transcription factor nuclear factor kappa-light-chain-enhancer of activated B cells (NFκB) and activates the mitogen-activated protein kinase (MAPK) cascade, leading to activation of the transcription factor activator protein 1 (AP-1). These transcription factors then translocate to the nucleus and induce transcription of genes involved in T cell proliferation, effector function and differentiation (Malissen et al., 2015; Smith-Garvin et al., 2009) (figure 1.7).

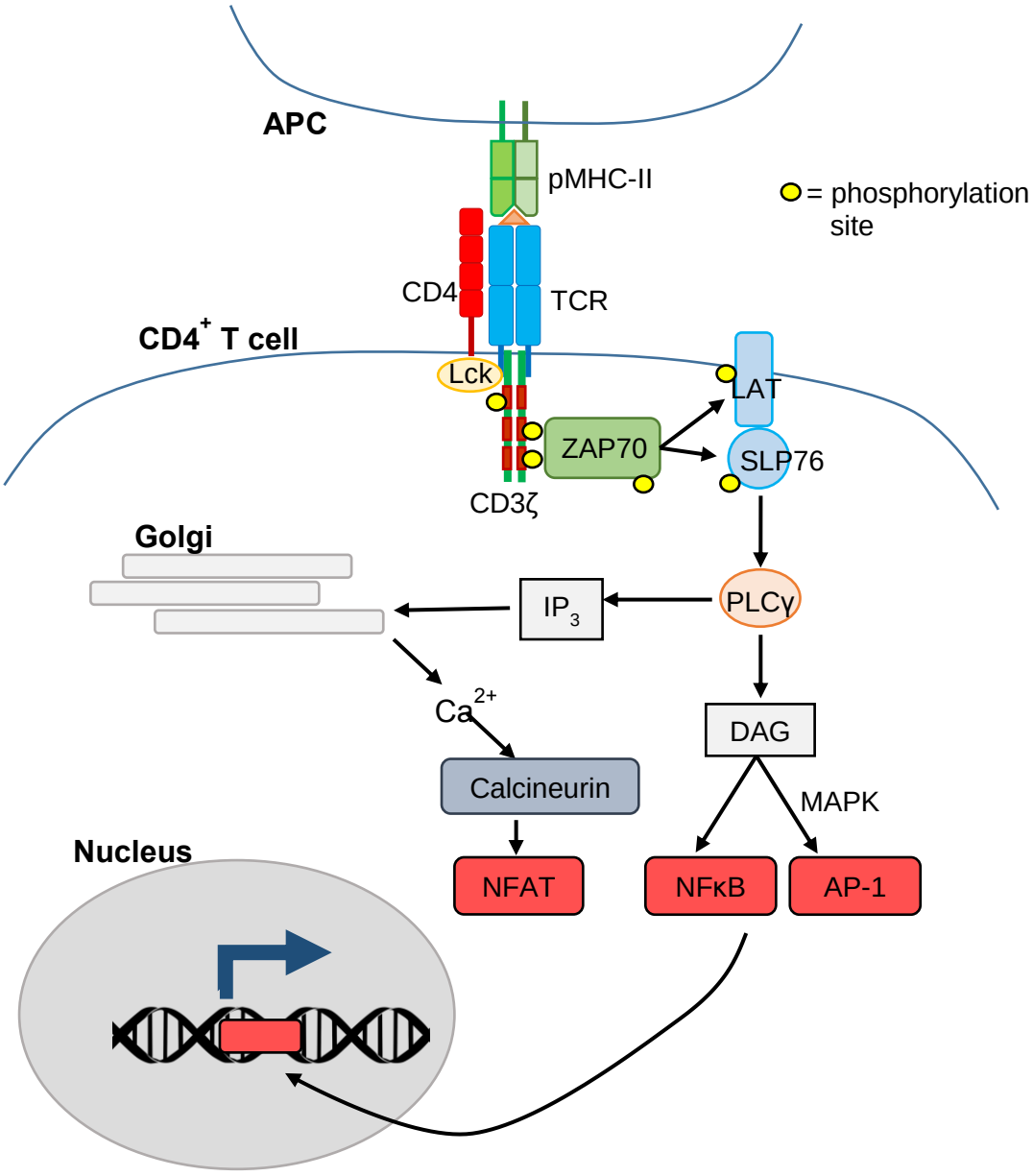

Figure 1.7 – TCR signalling

Although the molecular mechanisms behind T cell activation have been elucidated, the initial events that trigger TCR signalling are still poorly understood. Several models have been proposed which involve aggregation, conformational change and receptor segregation. Aggregation models propose that following TCR engagement, TCR-CD3 complexes aggregate in clusters enhancing phosphorylation. Data to support these models come from the finding that forced TCR aggregation through anti-TCR antibodies or soluble multimeric p:MHC complexes is sufficient to trigger TCR signalling (var der Merwe et al., 2011). The conformational change model suggests that binding of a p:MHC molecule alters the conformation of the TCR and initiates signalling (Xu et al., 2008). Segregation models such as the kinetic segregation theory suggest that TCR signalling is initiated when the TCR is clustered in areas of the plasma membrane that are rich in Lck and lack the phosphatase CD45 (Davis et al., 2006). This latter model corroborates the findings relative to the immune synapse. None of these models are mutually exclusive and it is likely that TCR triggering will involve a combination of these mechanisms. The initiation of signal transduction such as the phosphorylation of proximal signalling molecules, occurs within seconds and minutes after TCR engagement. However, for full activation and commitment to T cell proliferation and development of effector function, sustained signalling which involves p:MHC:TCR contact for several hours is required. Premature disruption of the TCR:cognate-antigen contact stops T cell progression into T cell division, despite effective initial signalling events. Thus, more than one threshold of activation needs to be exceeded for a T cell to become fully activated (Acuto et al., 2008).

1.1.8. Regulation of T cell activation

T cell maturation involves T cell binding to self-peptide:MHC complexes in the thymus. Therefore, all peripheral T cells express TCRs that can recognize “self” with low affinity. Moreover, self-p:MHC molecules are presented to T cells in greater numbers compared to foreign p:MHCs, indicating that T cells need to be able to not only discriminate between “self” and “non-self”, but also detect the very low number of foreign p:MHC ligands in the

presence of an excess of self-peptides. In addition, naïve, resting T cells continuously receive tonic signals from self-p:MHC molecules in the periphery, which are essential for their survival (Tanchot et al., 1997). A few models have been proposed to explain how T cell activation can occur despite low concentration of antigen, and how it is regulated to prevent autoimmune disease. The serial triggering model first described by Valitutti et al. may explain how T cells can mount an efficient response against a foreign peptide that is presented at a relatively low frequency. This study showed that a single p:MHC molecule can trigger up to 200 TCRs (Valitutti et al., 1995). How T cells can discriminate between self and non-self peptides can be explained by the kinetic proofreading model. According to this model, engagement of a TCR by a high-affinity p:MHC molecule with a lower dissociation rate results in a higher degree of TCR signalling, compared to low affinity peptides with higher dissociation rates that are present at higher concentrations (McKeithan, 1995; Rabinowitz et al., 1996).

However, full T cell activation requires three signals, of which TCR signalling is only one. The further two signals are provided by APCs in the form of co-stimulatory molecules (signal 2) and secreted inflammatory cytokines (signal 3). CD28 is the major costimulatory molecule present on T cells. Imaging studies have shown that upon TCR engagement CD28 forms micro-clusters with the TCR recruiting signalling molecules (Saito et al., 2010; Chen et al., 2013). CD80 and CD86 are the ligands for CD28 and are expressed on activated APCs. Binding of CD28 to either one of them activates the PI3K pathway, ultimately enhancing nuclear translocation of NFκB (Smith-Garvin et al., 2009). IL-12 and type I interferons (IFNα/β) are two of the major source of signal 3 in $CD8^+$ T cells, whereas IL-1 can also provide signal 3 to $CD4^+$ T cells. The molecular mechanisms behind signal 3 are still being elucidated, and appear to include cytokine-driven chromatin remodelling (Curtsinger et al., 2010). Importantly, signalling through the TCR alone in absence of co-stimulation and signal 3 results in a non-responsive state known as anergy. Anergic T cells are unable to optimally expand and acquire effector functions.

As with co-stimulatory molecules, co-inhibitory molecules that prevent T cell activation also exist. Cytotoxic T lymphocyte antigen 4 (CTLA-4) receptor is one of the main co-inhibitory molecules involved in T cell activation, and it competes with CD28 for the binding of CD80 and CD86. Upon binding, CTLA-4 can rip CD80 and CD86 from the surface of APCs, thereby preventing interaction of such ligands with co-stimulatory receptors (Qureshi et al., 2011). CTLA-4 binding to its ligand activates the phosphatases SH2 domain-containing tyrosine phosphatase 2 (SHP2) and serine/threonine protein phosphatase 2A (PP2A), which reduce proximal TCR signalling by dephosphorylating the CD3ζ chain. Whereas CD28 is constitutively expressed on T cells, CTLA-4 expression is upregulated upon T cell activation and its expression induces endocytosis and downregulation of CD28 (Rudd et al., 2009).

Thus, co-signalling molecules allow T cells to sense external environmental conditions and to promote T cell responses against harmful, non-self antigens, whist limiting or preventing aberrant and autoreactive responses.

1.2. T cell biology

1.2.1. T cell effector function

Upon activation through TCR signalling and co-stimulation a naïve T cell will proliferate and differentiate while assuming effector functions, allowing infections to be resolved. Within the naïve T cell population, only a few T cells specific for a given antigen will be present. However, upon encountering their cognate peptide these cells will undergo a massive burst of expansion. Using a murine LCMV infection model Blattman et al. showed that upon priming, antigen specific cells can divide more than 14 times in a week, going from 100-200 cells to approximately 10^7 cells (Blattman et al., 2002). Along with proliferation comes the acquisition of effector functions, thus antigen encounter generates a large population of antigen-specific, effector T cells. However, $CD4^+$ and $CD8^+$ T cells differ in their proliferative responses. Whereas $CD8^+$ T cells will rapidly proliferate and differentiate into cytotoxic T lymphocytes (CTLs), $CD4^+$ T cells have a lesser ability to divide and their proliferation begins after a slight delay (Foulds et al., 2002). Moreover, $CD4^+$ T cells have a broader differentiation repertoire which includes type 1 T helper (Th1), Th2, Th9, Th17, Th22, regulatory T cells (Treg) and follicular T helper cells (Tfh) (Wan et al., 2009; Rapahel et al., 2015). Some of the differences between $CD8^+$ and $CD4^+$ T cell effector functions will be described below.

1.2.1.1. $CD4^+$ T cells subsets

$CD4^+$ T cells are characterised by a different cytokine profile and transcription factor expression, both of which are used to define different $CD4^+$ T cell subsets. Originally it was thought that $CD4^+$ T cells simply differentiated into either Th1 or Th2 cells, the former characterised by the secretion of IFNγ and TNFα, the latter by IL-4, IL-15 and IL-13 expression (Mosmann et al., 1986). However, since the discovery of Th1 and Th2 subsets many additional Th subsets have been identified including Th17, Tregs, Th22,

Th9 and Tfh, and each one of these subsets plays a critical role in shaping the immune response (figure 1.8).

The role of Th1 cells is to stimulate innate and T cell responses by producing pro-inflammatory cytokines such as IFNγ, TNFα and TNFβ. Such cytokines induce CTL activation, IgG2a production by B cells and macrophage activation. Because of this pro-inflammatory profile, these cells are important in protecting the host from intracellular pathogens and help in immune-mediated tumour rejection (Wan et al., 2009). However, because of their pro-inflammatory profile they can cause tissue damage and elicit unwanted inflammatory diseases and self-reactivity. The transcription factor associated with Th1 cells is T-bet, and overexpression of T-bet activates IFNγ expression, while supressing IL-2, IL-4 and IL-5 production both in cell lines and primary cells (Dong et al., 2000).

Th2 cells are producers of IL-4, IL-5, IL-9, IL-10 and IL-13 and their master transcription factor regulator is GATA-3 (Zhang et al., 1997). Th2 responses are important to neutralise foreign organisms such as helminths and nematodes, as this type of response promotes IgG1 and IgE class-switching and eosinophil recruitment (Mossman et al., 1986). Just like Th1, Th2 cells can also promote pathology such as atopic asthma and allergy (Wan et al., 2009).

Th17 are so called because of their ability to produce IL-17 (A, E and F), but they can also produce IL-21 and IL-22. Th17 responses, which are able to indirectly induce the recruitment of neutrophils, are directed against extracellular bacterial and fungal infections, indirectly recruit neutrophils, but have also been implicated in autoimmune diseases such as multiple sclerosis and rheumatoid arthritis (Zambrano-Zaragoza et al., 2014; Wan et al., 2009; Pelletier et al., 2010). Rorγt is the transcription factor driving Th17 differentiation (O'Shea et al., 2010).

Both Th9 and Th22 were recently identified as new subtypes of helper T cells. Th9 cells were firstly reported in 2008 by Dardalhon et al. and Veldhoen et al., and are associated

with the production of high levels of IL-9 and IL-10 (Dardalhon et al., 2008; Veldhoen et al., 2008). Th22 cells are characterised by the secretion of IL-22 and TNFα, but not IFNγ, IL-4 or IL-17 and were first identified in the epidermis of individuals with inflammatory skin disorders (Eyerich et al., 2009).

Tregs are a specialised subset of helper T cells with regulatory functions, whose main role is to suppress the immune system. These can be thymically derived or natural Tregs (nTregs) which arise from self-reactive cells in the thymus; or can be induced in the periphery (iTregs). In both cases their signature transcription factor is Foxp3. Although nTregs and iTregs were shown to have similar transcriptional signatures, their TCR repertoires only minimally overlap. Thus, although both subsets of Tregs carry out similar immunosuppressive functions, the two populations are non-redundant with iTregs supplementing nTregs in part by expanding TCR diversity (Haribhai et al., 2011). Tregs can employ different mechanisms to exert their immunosuppressive functions: they can produce immunosuppressive cytokines such as IL-10 and TGF-β; they can suppress TCR-induced Ca^{2+}, NFAT and NF-κB signalling; they can suppress IL-2 consumption or induce cell death by perforin and granzyme; and they can drive down-modulation of co-stimulatory molecules on APCs by upregulating CTLA-4 (Schmidt et al., 2012). All these mechanisms are fundamental for the maintenance of self-tolerance and immune homeostasis. In fact, Treg depletion or dysfunction can lead to a variety of inflammatory and autoimmune diseases as shown some time ago by Sakaguchi et al. (1995).

Tfh are primarily found at the edge of the B cell zones and follicular regions and germinal centres of secondary lymphoid organs, due to their high expression levels of CXCR5. Tfh drive generation of high-affinity antibodies and memory B cells by expressing the B cell-promoting cytokine IL-10 and IL-21 (Wan et al., 2009; Fazilleau et al., 2009).

The different subsets described above have been classically viewed as distinct lineages. However, recent studies have shown that both transcription factor expression and cytokine production might not be as fixed as originally thought and flexibility in the

expression of master regulators and cytokines is relatively common (O'Shea et al., 2010). Nonetheless, despite questions remaining over $CD4^+$ T cell differentiation and plasticity, the different subsets all clearly play a diverse but important role the immune system.

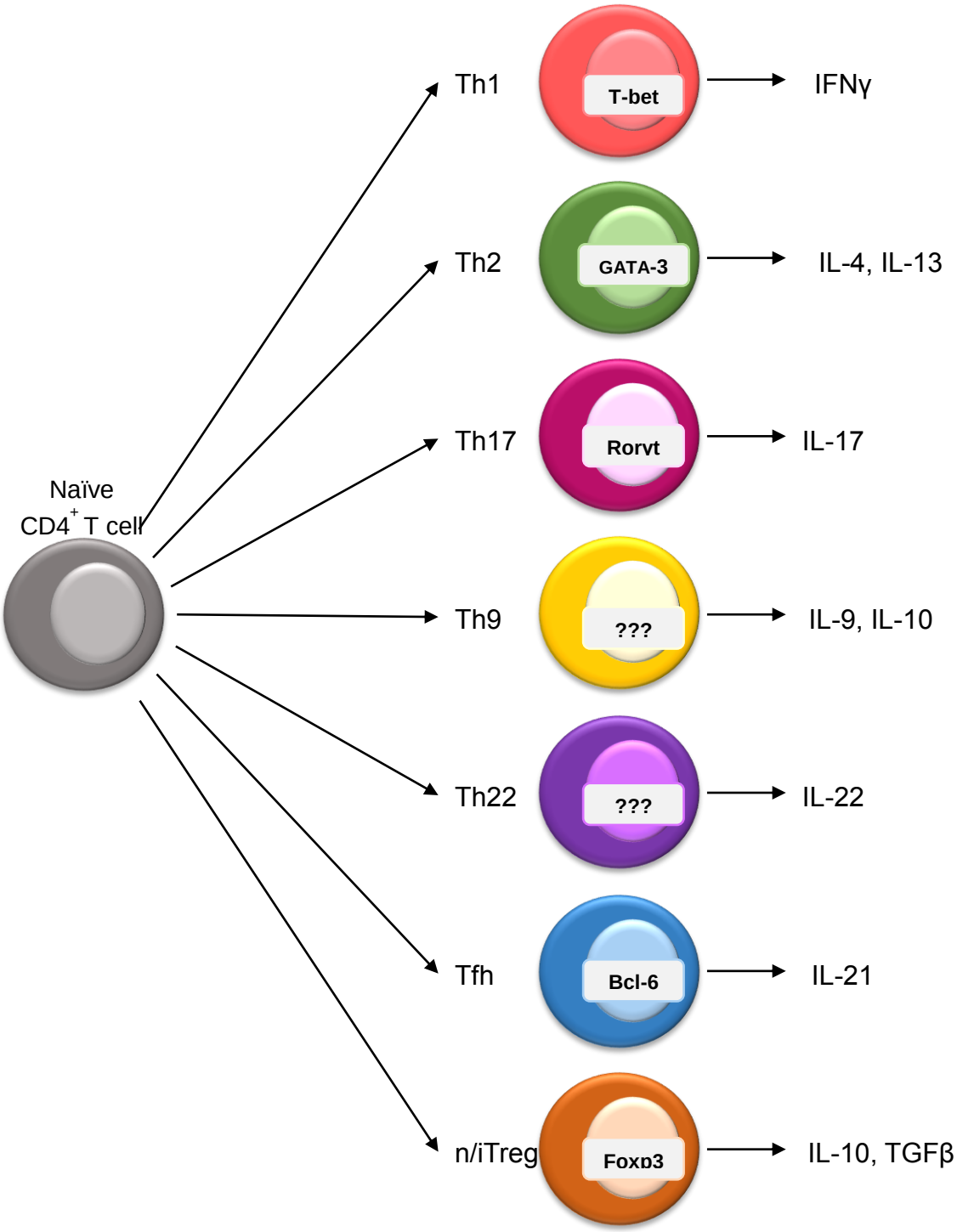

Figure 1.8 – CD4+ T cell subsets (adapted from O'Shea et al., 2010).

1.2.1.2. CD8$^+$ T cell subsets

CD8$^+$ T cells are commonly known as cytotoxic T lymphocytes and they are so named because of their ability to directly kill target cells. This killing is highly efficient and involves transient interactions (between 2-10 minutes) between the CTL and the target cell, through the formation of the immunological synapse. Killing occurs by induction of two separate apoptotic pathways. Firstly, upon target cell recognition and signalling through the CD8$^+$ T cell's TCR, a calcium-dependent mechanism is initiated by which the microtubule organisation centre reorganises, polarising the Golgi complex and lytic granules within the CTL's cytoplasm towards the target. Lytic granules are specialised secretory lysosomes containing cytolytic proteins such as granzymes and perforin. Upon polarisation, they move to the plasma membrane, where they dock and release their content onto the target cell. Perforin causes the formation of pores in the target cell's plasma membrane allowing granzyme to enter and trigger the mitochondrial apoptotic pathway by directly cleaving Bid (Sutton et al., 2000; Jenkins et al., 2010; Stinchcombe et al., 2001).

The second mechanism used by CD8$^+$ T cells to induce cytotoxicity involves the Fas-FasL lytic pathway. Fas is a transmembrane glycoprotein widely expressed on both lymphoid and non-lymphoid tissues, which contains an intracellular domain, homologous to the p55 TNF receptor death domain. FasL is a transmembrane protein of the tumour necrosis factor family that is expressed on activated T cells. Upon interaction with its ligand, Fas trimerises leading to caspase 8 activation, and ultimately cell apoptosis (Berke, 1995; Waring et al., 1999).

1.2.2. T cell central and peripheral tolerance

As described above, V(D)J recombination in the thymus is a quasi-random process through which millions of different TCR specificities can be generated. Many of the randomly rearranged TCR are useless as they will not be able to recognize and bind to the MHC molecules. Conversely, newly generated TCRs could also be potentially self-

reactive and harmful for the organism. To avoid both scenarios and to ensure generation of fully functional, non-self-reactive T cells during thymic maturation developing T lymphocytes undergo two selection steps known as positive and negative selection. Both steps occur simultaneously (Baldwin et al., 1999) and are crucial for the development of central tolerance.

Positive selection is the process by which the ability of newly generated TCRs to interact with self is tested. Indeed, cells expressing TCRs that are not capable of recognising and binding self-MHC molecules will not receive further survival signals through the TCR and will die by neglect. It has been estimated that the mouse thymus at the peak of its productivity generates around 50 million CD4 CD8 DP thymocytes each day. More than 90% of these precursors will die by neglect (Klein et al., 2014). Because this process enriches for self-reactive clones thus increasing the danger of autoimmunity, another process fundamental for central tolerance development is negative selection by clonal deletion. During negative selection T cell clones with high affinity for self are deleted. Alternatively some self-reacting T cells differentiate into Tregs upon strong interaction with self-p:MHC molecules. Thus, only clones with low-medium affinity for self-pMHC will proliferate and mature into functional conventional T cells.

Positive selection occurs in the thymic cortex and it is dependent on a single type of APC, known as the cortical thymic epithelial cells (cTECs). The ability of cTECs to play such a critical role in thymocyte development, is due both to their abundant surface expression of MHC molecules, and to the unique machinery they possess to process antigens. Indeed, for MHC-I antigen presentation, cTECs express a unique version of the proteasome (referred to as the “thymoproteasome”) which contains the catalytic subunit β5t. Mice lacking this subunit have a substantial defect in positive selection of $CD8^+$ T cells (Murata et al., 2007). In terms of MHC-II antigen presentation, cTECs express the unique lysosomal proteases cathepsin L and thymus-specific serine proteases (TSSP). Deficiency in these enzymes results in impaired positive selection of $CD4^+$ T cells (Nakagawa et a., 1998; Gommeaux et al., 2009). Thus, interaction of

thymocytes with cTECs also determines whether the CD4 CD8 DP precursors will mature into $CD4^+$ or $CD8^+$ T cells, depending on whether they bind MCH-II or MHC-I respectively. Negative selection occurs in the medulla and depends on another specific cell type, known as medullary thymic epithelial cells (mTECs). The peculiarity of mTECs is that collectively they express almost all peripheral tissue restricted antigens (TRAs), through their expression of the autoimmune regulator (AIRE) transcription factor. These self-antigens can be presented to thymocytes either by direct presentation on mTECs or by cross presentation on migratory DCs. Clonal diversion can also occur in the medulla, that is the process by which self-reactive T cells are imprinted with a regulatory function and become Tregs. What determines if a self-reacting cell will undergo clonal deletion or clonal diversification is still a matter of some debate.

Another key question that remains is how a TCR can discriminate between low and high affinity interactions, and as a consequence whether the T cell expressing that TCR will be deleted or not. It has been suggested that a high affinity interaction causes signal transduction leading to negative selection, whereas low affinity interactions result in a partial phosphorylation of the CD3 co-receptor, triggering positive selection (Palmer et al., 2009). Ca^{2+} and ERK signalling downstream of the TCR also seem important in determining negative versus positive selection. Indeed, rapid and robust ERK activation is associated with negative selection, whereas positive selection stimulates a lower intensity but sustained ERK activation (McNeil et al., 2005). The thymocyte expressed molecule involved in selection (Themis) also seems to be involved in determining the strength and kinetics of both ERK phosphorylation and Ca^{2+} influx, and its deficiency markedly impairs positive selection of thymocytes (Fu et al., 2009). Therefore, developing thymocytes integrate information from multiple inputs when deciding cell fate in the thymus.

Theoretically mature T cells that have left the thymus should either be naïve T cells that can recognise foreign antigens presented on self-MHC molecules, or self-reacting Tregs. However, low affinity self-reacting T cells continuously escape to the immune periphery

as shown by the occurrence of autoimmunity. These cells are subjected to peripheral tolerance, which is additional mechanisms that prevent self-reacting T cells from mediating autoimmunity in the periphery. Anergy is one such mechanism. T cells become activated in the presence of both a TCR (signal 1) and a co-stimulatory signal (signal 2). T cell activation in the absence of signal 2 induces a state of long term hypo-responsivness in the cells, termed anergy and characterised by active TCR signalling repression (Schwartz, 2003). Tolerogenic DCs can also induce tolerance, by presenting antigen without the adequate co-stimulatory signal. Evidence suggests that tolerogenic DCs are the results of incomplete DC maturation. For example, apoptotic cells unlike necrotic cells are insufficient to trigger DC maturation (Gallucci et al., 1999; Hawiger et al., 2001). Peripheral deletion of self-reacting clones can also occur. This is achieved through apoptotic cell death, via both the Fas- and the Bim-mediated apoptosis pathways, in T cells chronically stimulated by self-antigens (Xing et al., 2012). Finally, Tregs can also suppress self-reacting T cells via a variety a mechanisms including production of immunosuppressive cytokines and expression of inhibitory receptors such as CTLA-4 (described in section 1.2.1.1).

Thus, several mechanisms are in place, both in the thymus and in the periphery, to prevent the development of autoimmunity. These, together with the tightly regulated signalling sequences needed for full T cell activation (described in section 1.1.8.) ensure that effective immune responses are mounted only against foreign, harmful pathogens.

1.2.3. T cell homeostasis

After the process of positive and negative selection in the thymus, newly generated naïve, mature T cells exit the thymus and form the long-lived pool of naïve cells that recirculate within the peripheral tissues. Indeed, naïve murine T cells can persist for several weeks in the absence of antigenic stimulation. In the periphery, these cells are maintained without proliferating, and the number of T cells in the periphery remains fairly constant in young adult animals. This is in contrast with the maintenance of the human

naïve T cells pool, which is maintained by peripheral naïve T cell proliferation (den Braber et al., 2012). As with other cell types in the body, the composition and survival of the mature T cell pool are governed by complex homeostatic mechanisms. Post-thymic T cells retain a low degree of self-reactivity, and this is thought to be fundamental for their homeostatic survival. Much controversy exist in this field as different studies over the past few years, generated different conclusions. Initial studies suggested that T cell homeostatic signals rely on interactions between the TCR and self-p:MHC complexes (Brocker , 1997; Kirberg et al., 1997). Conversely, in later studies where MHC-II-deficient mice were used, normal maintenance of $CD4^+$ T cells was observed (Clarke et al., 2000; Grandjean et al., 2003). However, another study by Martin and colleagues contradicted this, as they found that MHC-II molecules were required for maintenance of the peripheral $CD4^+$ T cell pool in a non-lymphopenic environment (Martin et al., 2006). One caveat in the majority of these studies is that they involved sustained or transient lymphopenia, and it is now known that lymphopenic environments alter physiological T cell homeostasis, for example by generating a proliferative response and the acquisition of these cells of a memory-like phenotype (Takada et al., 2009a).

It has also been suggested that recognition of self-p:MHC complexes may control T cell function, and two contradictory models have been proposed. One study showed that $CD4^+$ T cells deprived of MHC-II molecules *in vivo*, showed a rapid decline in their ability to proliferate and produce IL-2 following *in vitro* stimulation. This suggests that self-peptide MHC complexes play a role in supporting T cell sensitivity to antigenic stimulation (Stefanova et al., 2002). However, data obtained from other studies showed that depriving $CD4^+$ T cells of contact with self-p:MHC complexes led to enhanced functional sensitivity (Smith et al., 2001). In the case of $CD8^+$ T cells, data suggests that lack of MHC-I molecules leads to upregulation of CD8 on the T cells, which makes T cells more responsive to weak antigens. In accordance with this data, it has been proposed that continuous interaction between the co-receptor and self-p:MHC complexes elevates the activation threshold of the T cells, a mechanism which may serve to prevent the

emergence of auto reactivity (Takada et al., 2009b). Thus, more studies are needed to dissect the role of TCR interactions with “self” in the context of naïve T cell reactivity.

Soluble factors also play a role in the maintenance of naïve T cell homeostasis. In particular, IL-7 is the major cytokine required for naïve T cell survival (Schluns et al., 2000; Hassan et al., 1998). Survival of naïve T cells is impaired if mice are injected with anti-IL-7 blocking antibodies, or after transfer into IL-7-deficient mice (Kondrack et al., 2003). In particular, IL-7 signalling enhances the expression of two anti-apoptotic factors, BCL-2 and MCL1, whilst inhibiting expression of the pro-apoptotic molecules interacting domain death agonist (BID), BCL-2-interacting mediator of cell death (BIM) and BCL-2 antagonist of cell death (BAD) (Wojciechowski et al., 2007). Moreover, IL-7 signalling through the PI3K-AKT pathway prevents T cell atrophy, by activating the mammalian target of rapamycin (mTOR) and sustaining the expression of the glucose transporter GLUT1 (Rathmell et al., 2001; Wofford et al., 2008).

TCR and IL-7 signalling seem to cooperate in the maintenance of the peripheral pool of naïve cells, as impairment of both mechanisms leads to more rapid decline of naïve T cell numbers, compared to inhibition of either pathway alone (Seddon et al., 2002).

To conclude, IL-7 and self-p:MHC complexes are known promoters of naïve T cell homeostasis. However the way in which these two signalling pathways are integrated is still unclear.

1.2.4. T cell memory formation

A T cell response to an antigen can generally be divided into four phases. As discussed above, on exposure to cognate antigen, naïve T cells are primed and undergo dramatic expansion. While proliferating they acquire effector functions and travel to the site of infection to mediate pathogen clearance (“effector phase”). During this expansion phase cells can divide up to 15-20 times, increasing up to 50,000-fold in number. This proliferation generally peaks around 7 days post infection, after which the second phase

of the T cell response occurs: the “contraction phase”. During this second phase the majority (90-95%) of the expanded T cell clones die by apoptosis. The remaining cells are maintained for years as long-lived memory cells, a phase known as the “memory maintenance phase”. The T cells that are left behind have an enhanced ability to control secondary infections by the same pathogen, due to their ability to rapidly acquire effector functions, and their localization at the site of infection. Indeed, the last phase of the T cell response occurs *if and when* the same pathogen re-infects the host. In this case the memory population that has been maintained throughout the life of the individual gives rise to a rapid recall response, providing better protection compared to that generated by antigen-inexperienced T cells (Williams et al., 2007).

The memory T cell compartment can be divided into central memory (T_{CM}) and effector memory T cells (T_{EM}), based on two criteria: the presence or absence of effector functions, and the expression of homing receptors which dictate the cell’s trafficking pattern (lymphoid or non-lymphoid organs). T_{CM} constitutively express CD62L and CCR7, two receptors required for extravasation which allow their migration to secondary lymphoid organs. This subset of memory cells displays limited effector functions, but upon TCR engagement they efficiently differentiate into effector cells. Moreover T_{CM} are less dependent on co-stimulation and provide a more effective feedback stimulatory mechanism to DC and B cells, via upregulation of CD40L. Upon activation they mainly produce IL-2, but can also produce large quantities of IFNγ or IL-4. On the other hand, T_{EM} no longer express CCR7 and their expression of CD62L is heterogeneous. In addition, they display different combinations of chemokine receptors and adhesion molecules, which promote their homing to different inflamed tissues. This subset of memory cells have a lower proliferative capacity, but can rapidly acquire effector functions within hours of antigen stimulation. Indeed, they can produce IFNγ, IL-4 and IL-5. $CD8^+$ T_{EM} also contain large amounts of intracellular perforin (Sallusto et al., 2004; Sallusto et al., 1999). In blood of healthy donors, T_{CM} are predominant in the $CD4^+$ T cell compartment; T_{EM} are predominant in the $CD8^+$ compartment. However within tissues

T_{CM} and T_{EM} display characteristic patterns of distribution, with T_{CM} being enriched in the lymph nodes and tonsils, while T_{EM} are primarily found in the lung, liver and gut (Campbell et al., 2001).

Although the four different phases that make up T cell responses are well established, the pathways that lead to memory formation are less well understood. Two studies have shown that that the transcription factors T-bet and Eomes determine the differentiation of T cells into either central or effector memory T cells. In particular, Joshi and colleagues showed that high levels of T-bet expression drive differentiation into T_{EM} cells; whereas Intlekofer and colleagues showed that Eomes expression is linked to T_{CM} maintenance (Joshi et al., 2007; Intlekofer et al., 2005).

The steps that lead to memory formation are still somewhat unclear. Two main models have been proposed. One model suggests that a subpopulation of the cells that differentiate into effector cells during an immune response, possibly those with greater effector function, will go on to become memory cells (Youngblood et al., 2013) (figure 1.9 A). Supporting data for this model comes from studies in which genetically marked, cytokine producing cells that were generated during the effector phase, were present in the subsequent memory pool (Harrington et al., 2008; Lohning et al., 2008).

An alternative model suggests that T cell differentiation follows a linear path, and memory cells can develop directly from naïve cells, without transitioning through an effector stage (figure 1.9 B). According to this theory, memory cells are generated from activated T cells that have never experienced full activation and effector state. Effector cells on the contrary, represent fully differentiated cells, which can only generate more effector cells or undergo apoptosis. (Restifo et al., 2013). Data supporting this “linear differentiation model” comes from a number of recent studies. D’souza and colleagues showed that naïve T cells adoptively transferred towards the end of an infection, preferentially differentiate into memory cells. This pattern of differentiation was promoted by reduced antigenic stimulation, which also correlated with fewer rounds of cell division. (D’souza

et al., 2006). Additionally, *in vivo* tracing studies showed that slowly proliferating cells generated long-lived memory cells; whilst increased levels of proliferation gave rise to short-lived effector cells. Rapidly expanding T cells were also found to be involved less in re-call responses (Buchholz et al., 2013; Gerlach et al., 2013).

Since memory T cells play a fundamental role in the adaptive immune responses, a deeper understanding of the processes involved in T cell differentiation is needed. Elucidation of the exact model, or models that drive differentiation of memory T cells is fundamental for the development of better therapies. Indeed, a number of studies have shown that transfer of T cells with a less differentiated phenotype correlates with a higher rate of objective responses. This will be discussed in more detail in section 1.4.3., in the context of tumour immunotherapy.

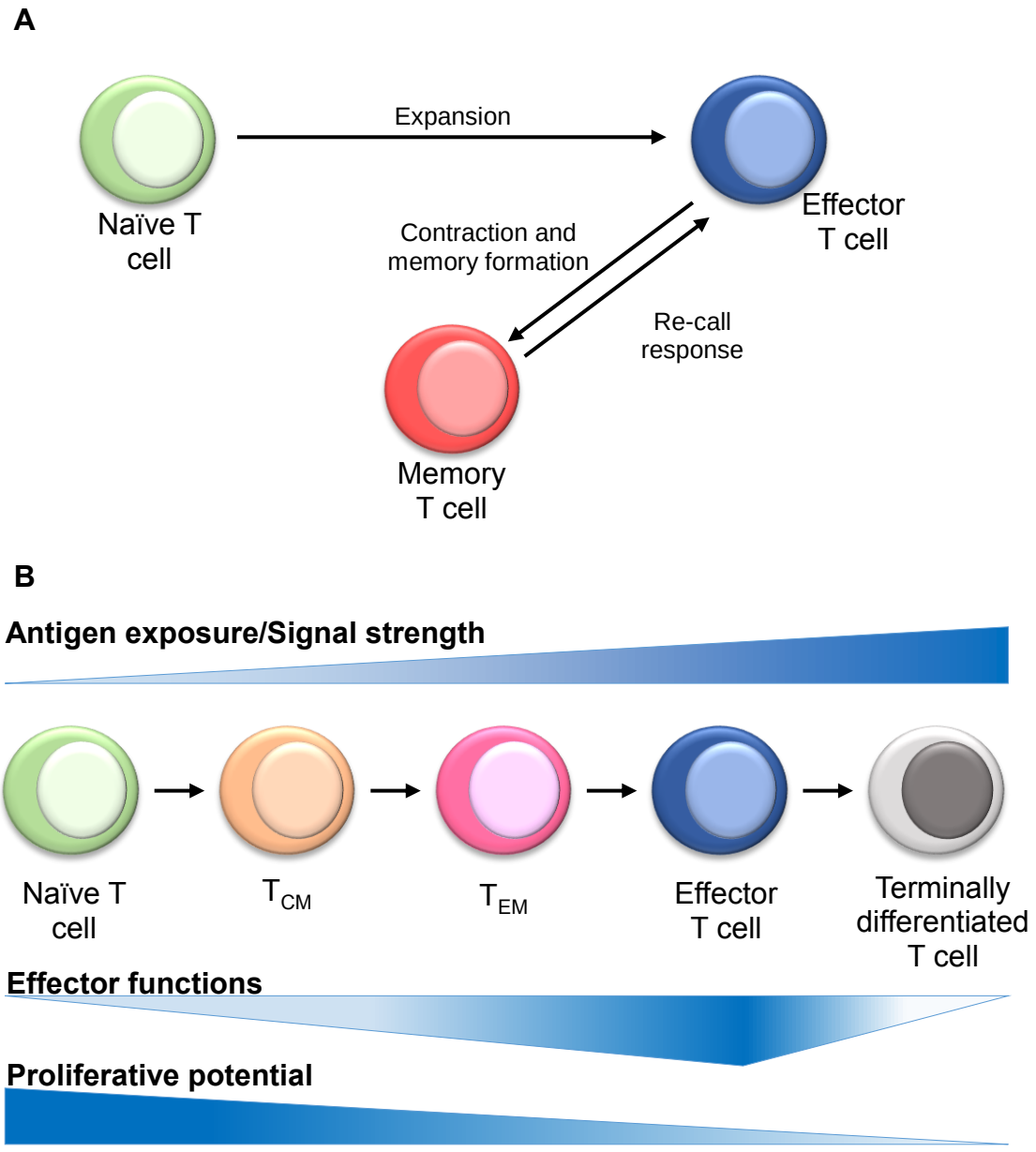

Figure 1.9 – Two models of memory T cell formation.

1.3. Tumour immunology

1.3.1. Immune surveillance

The role of the immune system in eradicating pathogens has long been understood. However the concept that the immune system could recognise and eradicate cancerous cells that arise in our bodies from transformed cells, was widely disputed until the mid-20th century.

The tumour surveillance hypothesis was first postulated by Paul Ehrlich in 1909. According to this theory the immune system is capable of distinguishing between healthy cells and transformed, cancerous cells, and is able to eliminate the latter before they develop into a clinically detectable disease (Ehrlich, 1909). However, convincing evidence did not emerge until the latter half of the 1900's, and this concept was formalised as the theory of "cancer immune surveillance" by Sir MacFarlane Burnet and Lewis Thomas in 1957.

The first conclusive evidence supporting a role of the immune system in tumour control came from mice lacking IFNγ. Dighe et al showed that in mice injected with a neutralising antibody against IFNγ, transplanted fibrosarcoma grew faster. Similarly, if the tumour cells expressed a dominant negative form of the IFNγ receptor α chain, they displayed enhanced tumorigenicity and lower immunogenicity when transplanted into syngeneic mice (Dighe et al., 1994). Later experiments showed that perforin-deficient mice were more susceptible to a variety of tumours (both transplanted tumour cell-lines and chemically-induced tumours), compared to wild type mice (van den Broek et al., 1996).

Subsequent work utilising knockout mice, built upon the notion that lymphocytes play a central role in tumour surveillance. Mice lacking the recombinase-activating-gene 2 (RAG2) were used to demonstrate that lymphocytes play a central role in the control of tumour growth. RAG2 deficient mice lack mature lymphocytes (T, B and NK T cells) due to their inability to initiate V(D)J rearrangement (Shinkai et al., 1992). Injection of the

chemical carcinogen methylcholanthrene (MCA) into these mice induced tumour formation at a higher frequency compared to wildtype mice. In addition RAG2 deficient mice showed an increase in the development of spontaneous neoplastic disease which, when then transplanted into immunocompetent hosts was shown to be more immunogenic compared to tumours that developed in the presence of an intact immune system. Interestingly, when RAG2 knockout mice were crossed with STAT1 deficient mice, which cannot respond to IFNγ, similar tumourigenesis kinetics were seen. Taken together this data suggests that there is an extensive overlap between these two tumour-suppressor systems, but also that an intact immune system shapes the growing tumours, eliminating the more immunogenic cells, favouring the growth of less immunogenic clones (Shankaran et al., 2001), a mechanism now known as “cancer immunoediting” (described in more detail in the next section). Finally, the fact that lymphocytes played a role in tumour control was given further credence by the identification of melanoma-specific cytotoxic T cells in the T cell pool derived from tumour-bearing patients (van der Bruggen et al., 1991).

1.3.2. Immunoediting

In the study by Shankaran described above, tumours developed even in the presence of a fully functional immune system. This led to the idea that a growing tumour is continuously edited and sculpted by the immune response to which it is subjected *in vivo*. Thus, tumours that are capable of developing despite an immune response, are likely to be (by default) less immunogenic. Therefore, the immune system plays a dual role by both protecting the host from, and promoting the growth of, tumours. This concept of immunoediting was originally proposed by Schreiber, and it can be divided into three different phases: elimination, equilibrium and escape (Schreiber et al., 2011).

The elimination phase can be described as an updated version of cancer immune surveillance, during which the innate and adaptive immune systems networks work together to detect and eliminate developing tumours before they become clinically

apparent. Invasive tumour growths cause inflammation in their surrounding tissues, leading to the recruitment of innate immune cells (NK cells, macrophages, etc.) into the site. These recently recruited innate cells recognise the transformed cells and produce IFNγ, which has both anti-proliferative and pro-apoptotic effects on the tumour cells. Moreover, IFNγ also induces the production of chemokines such as CXCL10 and CXCL9, which can prevent angiogenesis, leading to further tumour cell death. Tumour cell debris is taken up by DCs, which migrate to the draining lymph nodes and present tumour antigens to $CD4^+$ and $CD8^+$ T cells, priming antigen specific cells. Primed T cells are subsequently recruited to the tumour site where they exert their cytotoxic functions, killing additional tumour cells (Dunn et al., 2002). Although efficient, this immune response is not always sufficient to prevent tumour development.

In the equilibrium phase, the host immune system and any malignant cell clone that has survived the elimination phase enter into a dynamic equilibrium. During this process, potent selection pressure on the tumour cells is sufficient to control further tumour growth, but not fully eradicate the malignancy. Evidence for this process arose from *in vivo* experiments where mice were treated with small doses of MCA to induce tumour formation. Mice that after ~200 days were tumour-free were injected with either control antibodies, or anti-CD4/-CD8 or anti-IFNγ antibodies to deplete these populations or neutralise IFNγ, respectively. Following these weekly injections, 46% of the animals depleted of $CD4^+$ and $CD8^+$ T cells and treated to neutralised IFNγ, developed sarcomas. In contrast, no tumour growth occurred in the mice treated with control antibodies. This data supports the role of the adaptive immune system in preventing outgrowth of small MCA-induced sarcomas (Koebel et al., 2007). Which factors shift the balance towards subsequent tumour escape still needs to be determined. However during this process, as with Darwinian selection, new tumour variants carrying different, advantageous mutations arise, and these will go on to escape immune control (Greaves et al., 2012). The equilibrium phase is likely to be the longest of the three processes, and it has been suggested that this may occur over a period of many years.

Escape represents the final phase of immunoediting, during which the immune system fails to control the less immunogenic tumour cell variants, leading to uncontrolled growth and clinical presentation of a malignant disease. Tumour cells have developed multiple mechanisms to escape and evade recognition by the immune system. One of these mechanisms involves downregulation of antigen presentation. Indeed, reduced expression of, or mutations in proteins involved in antigen processing and presentation have been reported in a number of malignancies. These include mutations or down modulation of HLA, β2 microglobulin, TAP and components of the proteasome (Algarra, 2000; Seliger et al., 2000). Alternatively, immune pressure can cause tumour cells to silence the expression of tumour antigens. This was shown to be particularly relevant in the case of immunotherapies targeting a tumour antigen, often lost on non-responding or relapsing tumours (Verdegaal et al., 2016; Maude et al., 2014). Increased expression of anti-apoptotic molecules, such as Bcl-2, or decreased expression of receptors involved in apoptosis signalling, such as TRAIL, have also been reported as a mechanisms used by tumour cells to escape cell death (Fulda, 2009).

Tumour cells also have the ability to promote immune dysfunction by making the tumour microenvironment suppressive. Cancerous cells can over-express immunosuppressive cytokines such as IL-10 and transforming growth factor β (TGFβ) (Khong et al., 2002). In addition immunosuppressive cells such as Tregs, myeloid derived suppressor cells (MDSC), or dysfunctional DCs, can be recruited to the tumour site by malignant cells (Terabe et al., 2004; Gabrilovich et al., 2009; Pinzon-Charry et al., 2005).

1.4. Cancer immunotherapy

Over the past decades many attempts to utilise the potential of the immune system to treat and eradicate tumours in patients have been made. The responses generated by adaptive T cells are crucial to the anti-tumour immune response, and the biological characteristics of these effector cells make T cell immunotherapy a very attractive field. T cells can recognise tumour antigens and directly kill malignant cells. Moreover this recognition can occur systemically, potentially allowing T cells to cure metastatic diseases. Further, initial recognition of malignant cells leads to the formation of immunological memory, generating long lived protection. Indeed the majority of recent cancer immunotherapies have focused on the manipulation of T cell populations. The three main approaches used within the T cell immunotherapy field to generate anti-tumour responses are:

- Vaccination against tumour antigens to promote endogenous tumour-specific T cell responses
- Expansion and adoptive transfer of tumour infiltrating lymphocytes
- Genetic modification of T cells to generate new anti-tumour T cell populations

Briefly, while vaccines have proved potent at inducing durable responses against infectious disease, their use in cancer immunotherapy has proved more challenging. Vaccination in this context can be used both prophylactically, and therapeutically. Perhaps the best known prophylactic cancer vaccine to date is the HPV vaccine, which protects against high-risk types of the human papilloma virus (HPV), well known agents that can drive cervical cancer development upon long term infection. In the case of therapeutic vaccines, these are given to patients with an established disease, to boost their anti-tumour immune responses, and DCs are at the centre of these technologies thanks to the role they play in the initiation of T cell responses.

The rest of this section will describe the foundations of and recent developments in the other two approaches.

1.4.1. Adoptive T cell therapy (ACT)

T cells capable of recognising cancer cells have been identified in multiple patients, burdened with a number of different malignancies. These T cells are commonly referred to as tumour infiltrating lymphocytes or TILs. Autologous TILs can be isolated from the patient, expanded *ex vivo* using tumour specific peptides and/or cytokines, and re-infused back into the patient where they can carry out their effector functions and mediate tumour control. The first evidence that adoptive transfer of sensitised, *ex vivo* cultured T cells could induce cancer regression came from a murine lymphoma study, in which 93% of mice with disseminated tumours were cured with ACT (Eberlein et al., 1982). This anti-tumour effect was improved by co-administration of IL-2 (Rosenberg et al., 1985). Soon after these initial studies, the efficacy of TILs isolated from surgically removed tumours and grown *ex vivo*, was also shown (Rosenberg et al., 1986). Importantly, these therapies were shown to be effective only when administered in combination with lymphodepletive chemotherapy. Depletion of the endogenous pool of immune cells is now known to favour homeostatic proliferation and expansion of the transferred cells by providing “space”; by removing “cytokine sinks”, that is endogenous immune cells, thereby giving the transferred cells greater access to IL-15 and IL-7; and by reducing Treg mediated immune-suppression, through depletion of endogenous Tregs (Dummer et al., 2002; Gattinoni et al., 2005a; Antony et al., 2005). The promising results shown by these pre-clinical experiments, led to the design of clinical trials to treat patients with metastatic melanoma. In these crucial studies, co-administration of TILs and exogenous IL-2, in combination with lymphodepletion, resulted in objective responses in 50-70% of patients with progressive, refractory, metastatic disease (Dudley et al., 2002; Dudley et al., 2008). One of the benefits of ACT using TILs, is that the population of isolated tumour reactive lymphocytes is polyclonal and may contain cells with reactivity to a number of tumour antigens. Some TILs may recognise antigens that are dispensable for tumour survival, and may be downregulated due to immune pressure, thus giving short-term responses; others may recognise antigens derived from genes indispensable for cancer

progression, mediating durable regressions (Lu et al., 2014). However, isolation of, and treatment with TILs is not technically feasible for all patients. The location of the tumour may make surgical resection and TIL extraction difficult in some cases; moreover isolation of sufficient numbers of TILs may not always be possible, especially from patients with less immunogenic malignancies. In addition, the immunosuppressive characteristics of the tumour microenvironment in addition to the lengthy *ex vivo* culture to which TILs are subjected, may limit the efficacy of these therapies. Lastly, in the case of cancers expressing self-antigens, TILs may not be available, as self-reacting T cells would have been eliminated during their development in the thymus, or may have been rendered tolerant. Therefore, alternative ways to generate tumour specific T cells, by genetically modifying T lymphocytes to re-direct their specificity, have been developed.

1.4.2. TCR gene therapy

The antigen specificity of a T cell is defined exclusively by the TCR it expresses. Therefore the specificity of a T cell can be re-directed, for example towards tumour antigens, by introducing the genes coding for an anti-tumour TCR. Once a T cell clone with the desired specificity is isolated, its TCR α and β chains can be sequenced, and cloned into vectors which can be used to transduce peripheral blood lymphocytes. The use of retroviral vectors to introduce the genes encoding for the αβ TCR of desired specificity, has been tested in many studies. In all of these, the retrovirally transduced cells were functional, exhibited the same specificity as the original T cell clones from which the TCR was derived, and were able to recognise and reject antigen-expressing tumours *in vivo* (Clay et al., 1999; Cooper et al., 2000; Stanislawski et al., 2001; Kessels et al., 2001; Ahmadi et al., 2011; Xue et al., 2005). These initial studies, and the successful treatment of melanoma patients with ACT, led investigators to design similar clinical trials with TCR-modified T cells. TCR genes were isolated from a HLA-A2 restricted T cell clone that recognised the antigen “melanoma antigen recognised by T cells 1” (MART-1) (from Dudley et al., 2002). Patients’ own PBMCs were transduced with the MART-1 TCR, and then infused back into the patients, after a lymphodepleting

conditioning regimen. Objective regression of metastatic melanoma lesions was seen in four patients (13%). Two of these patients remained disease-free at 20 months after treatment (Morgan et al., 2006). Shortly afterwards a follow-up study was performed using a higher avidity MART-1 TCR, and an anti-gp100 TCR, which recognises the gp100 melanoma antigen. In this study 30% and 19% of patients treated with the MART-1 and the anti-gp100 TCR, respectively, showed objective cancer regression (Johnson et al., 2009). Similar results were obtained in a study were a TCR targeting the NY-ESO-1 cancer/testis antigen, expressed in 80% of patients with synovial cell sarcoma and 25% of patients with melanoma and other common epithelial tumours, was used. In particular, objective clinical responses were seen in 67% and 45% of synovial cell carcinoma patients, and melanoma patients, respectively (Robbins et al., 2011). Since these initial studies, others, more or less successful, have been carried out targeting a number of different antigens. These include p53, the carcinoembryonic antigen (CEA), another melanoma antigen, MAGE A-3, and the hepatitis B surface antigen (HBsAg) (reviewed in Duong et al., 2015). The clinical trials described above have shown that treatment with TCR transduced T cells can indeed induce clinical responses, and control tumour progression, but only in a subsets of patients. Therefore new strategies to improve the efficacy of these therapies, and also to limit their side effects, are urgently needed.

1.4.3. Strategies to improve TCR gene therapies

Since the initial studies described above, using TCR modified T cells, different strategies have been devised in order to improve the efficacy of the engineered T cells.

Antigen selection

First of all, the choice of a suitable antigen to target is fundamental. Tumour antigens can be divided into two families: tumour associated antigens (TAAs), and tumour specific antigens (TSAs).

TAAs are non-mutated self-antigens that are expressed both by tumour cells, and by healthy cells of specific tissues. Furthermore, this family of antigens can be divided into 3 more sub-families. A first class represents antigens whose expression is restricted to male germline cells, such as the cancer testis antigen NY-ESO-1, and often expressed by cancers. The second class is represented by differentiation antigens, that is epitopes expressed by both the tumour cells and the healthy tissues these originate from. An example of these is the MART-1 antigen, expressed both on melanoma cells, but also on healthy melanocytes. Finally, the last class of TAAs include epitopes derived from proteins expressed in healthy tissues such as the Her-2/Neu antigens (Heemskerk et al., 2013). The benefit of TAAs is their potential to be targeted by the same TCR, in different patients. On the other hand, the downside of using such antigens, is that TAA arise from self-antigens. Thus, TAA-specific T cells may either be deleted during development, or have low affinity for the TAA, or they may be subject to peripheral tolerance mechanisms, to prevent the onset of autoimmunity. Indeed, Zhu and colleagues showed that AIRE deficiency correlates with lower TRP1 thymic expression, a melanocyte-specific self-antigen, also expressed in melanoma cells. This translated into a greater ability of AIRE-deficient mice to reject $TRP1^{+}$ melanoma (Zhu et al., 2013). Similarly, T cells specific for the melanoma antigen gp100 were tolerant to a B16 melanoma model in mice, unless these were also given an antigen-specific vaccination (Overwijk et al., 2003). Finally, targeting of TAAs may lead to “off-tumour, on-target” side effects, where the therapeutic T cells attack healthy tissues which express the target antigen. This has indeed been reported in a number of clinical trials were MART-1, gp100 or MAGE A-3 specific T cells caused adverse side effects (in some cases leading to the death of the patient) as a consequence of the transduced T cells targeting the antigen on healthy tissues (skin, inner ear, retina, brain) (Johnson et al., 2009; Morgan et al., 2013).

Therefore TSAs are the preferred target of choice for TCR gene therapy. TSAs, also referred to as neoantigens, are generated as a consequence of mutations in the genome of the cancer cells, leading to the production of novel protein sequences. Alternatively in

the case of virus-associated tumours, such as cervical cancer, TSAs can derive from the viral open reading frames (Schumacher et al., 2015). Thanks to their restricted expression on tumour cells, targeting of neoantigens cannot lead to “on-target, off-tumour” side effects. Moreover, T cells specific for such antigens, are not subject to central or peripheral tolerance mechanisms. Thus, theoretically neoantigens represent the perfect target for cancer immunotherapy. T cells specific for neoantigens have now been found in a number of patients. Moreover, Lennerz and colleagues showed that tumour-reactive T cells isolated from the blood of a melanoma patient predominantly reacted against patient specific neoantigens, rather than shared, known TAAs (Lennerz et al., 2005). This showed that it is feasible to isolate patient-specific, anti-tumour neoantigens T cells. However, unless these neoantigens represents driver mutations, the immune pressure exerted by the tumour infiltrating T cells may lead to loss of the T-cell-recognised neoantigen from the tumour cell population, as previously shown in two melanoma patients (Verdegaal et al., 2016). It is now well known that extensive heterogeneity exists between individual tumours, and within the same tumour too. Therefore, identification of driver mutations (sometimes referred to as “trunk” mutations), indispensable for the survival of the cancer cells, and expressed ubiquitously in the tumour microenvironment, is fundamental to prevent immune escape (Gerlinger et al., 2012). However, the major downside of neoantigen targeting is that the vast majority of these are patient-specific (Heemskerk et al., 2013). The use of neoantigens is therefore considered a form of personalised medicine, and the feasibility of this approach will need to be addressed if therapies targeting those antigens are to enter the clinic.

Increasing TCR expression

Another approach to try and improve the efficacy of TCR gene therapies, consists of increasing the expression levels of the introduced TCR. Increased TCR surface expression correlates with increased sensitivity for the target p:MHC complex, and increased anti-tumour activity *in vivo* (Jorritsma et al., 2007; de Witte et al., 2008). When a new TCR is introduced into a T cell, both this new TCR and the endogenous TCR will

be expressed on the cell surface. The ability of a TCR to be expressed depends on the intrinsic ability of its α and β chain to pair, and its ability to associate with the CD3 complex (Heemskerk et al., 2007). This results in some TCRs being better expressed ("strong" TCRs), compared to others ("weak" TCRs). The level of CD3 within a cell are also rate-limiting for TCR expression. This is particularly obvious in the case of TCR transfer, when an exogenous TCR has to compete with the endogenous TCR population for CD3 complexes and cell surface expression (figure 1.10 B and C). Indeed, our lab has previously shown that providing T cells with additional CD3 genes leads to increased TCR surface expression (both endogenous and introduced TCR). This translates into greater functional avidity *in vitro*, and greater anti-tumour activity *in vivo* (Ahmadi et al., 2011).

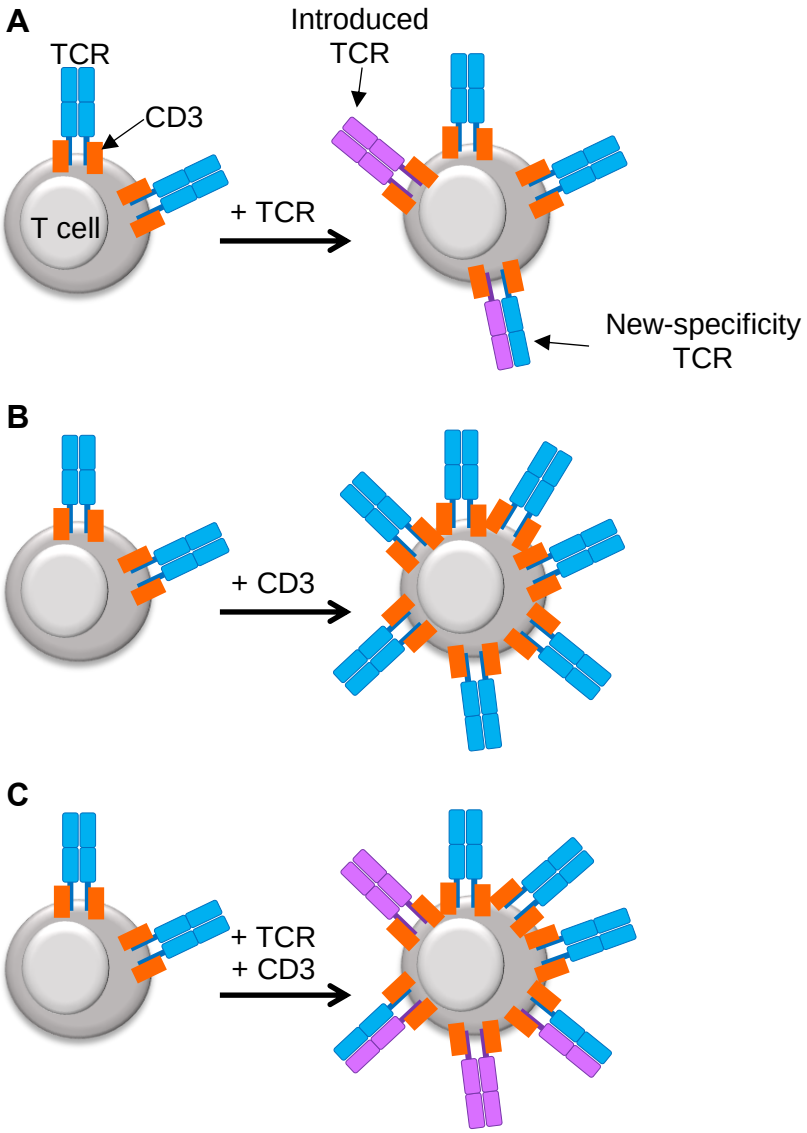

Figure 1.10 – TCR mispairing and the competition for CD3 molecules.

Preventing αβ chain mispairing is another approach used to increase the expression of the introduced TCR. When a second TCR is introduced into a T cell, the new α and β chain can potentially pair with the endogenous TCR chains, and form TCRs of new, unknown, potentially autoreactive specificities, with the overall effects of reducing the expression of the wanted TCR (Bendle et al., 2010) (figure 1.10 A). Nowadays the introduced TCRs are frequently genetically engineered to express additional cysteine residues in their constant regions, leading to the formation of an additional disulphide bond between the constant α and constant β chains, promoting preferential pairing of

those and increasing TCR functional avidity (Kuball et al., 2007; Cohen et al., 2007). Alternatively, in the case of human TCRs, these can be modified and their constant α and constant β regions replaced with murine constant regions, to favour correct αβ pairing. In addition the murine chains bind the CD3 complex more efficiently, with the overall result of greater anti-tumour activity (Cohen et al., 2006).

Improvements in the design of the vectors may also lead to better TCR expression levels. Codon optimisation of the introduced TCR sequences has been shown to increase gene expression, allowing the exogenous TCR to outcompete the endogenous TCR for CD3 binding, leading to improved TCR surface expression (de Witte et al., 2008; Kerkar et al., 2011). In addition, providing the cell with equimolar amounts of the α and β chains, through the use of viral self-cleaving 2A peptide sequences to separate the genes, promotes specific pairing, as both chains are expressed equally (Szymczak et al., 2004). This approach differs from the use of an internal ribosome entry site (IRES), which requires two transcription events to produce the α and β chains.

Expression of the introduced TCR may also be increased by the suppression of endogenous TCR expression. This can be achieved using a variety of methods, including RNA interference (Bunse et al., 2014); zinc-finger nucleases (Provasi et al., 2012); TALEN or CRISPR/Cas9 technologies (Knipping et al., 2017). In brief, these technologies suppress the expression of the endogenous TCR by distorting the TCR genes or its mRNA, preventing its successful transcription and translation into a functional protein.

Increasing TCR affinity

Whereas the avidity of a TCR for its cognate antigen determines how strongly the interaction will be, the affinity of a TCR for its cognate peptide determines how well the TCR will recognise, and a consequence bind to, its cognate peptide. Thus, much effort has been put towards the generation of TCR with higher affinities for its cognate p:MHC complexes, to generate better immune responses. The affinity of a naturally occurring

TCR for its cognate p:MHC complex is normally in the micromolar range, with K_D values between 1-100 μM. TCR with higher affinity for their p:MHC complexes can be generated, by mutating the protein sequence of the CDR regions, followed by selection using phage display. This methods allows the creation of TCRs whose affinities are in the picomolar region (Li et al., 2005). Higher affinity TCRs have higher on-rates, suggesting which may impair specificity, and perhaps not surprisingly, they can also be stimulated by self-peptides. This correlates with the notion that TCRs with high affinities are normally negatively selected in the thymus, due to their potential to become auto-reactive (Holler et al., 2003). If the affinity of a TCR is pushed beyond the natural TCR affinity range (1-100 μM), these TCRs initiate T cell responses faster compared to wild type TCRs, but they also lose their ability to respond to low antigen density, suggesting higher affinity correlates with decreased off-rates, impairing serial triggering (Thomas et al., 2011). Thus, the designing of affinity matured TCRs should concentrate on the production of TCRs with only marginal increases in their affinity, which falls within the natural affinity range, compared to that of wild-type TCRs. Indeed, the generation of TCRs with ultra-high affinities may be detrimental.

Increasing TCR-transduced T cell persistence

Another factor influencing the outcome of TCR engineered T cell therapies, is the ability of the adoptively transferred cells to persist in the periphery. It is now well documented that longer persistence, and in greater numbers, correlates with better anti-tumour responses (Robbins et al., 2004). Multiple rounds of *in vitro* stimulation before adoptive transfer drive T cells to acquire an end stage effector phenotype, which correlates with pronounced *in vitro* tumour killing, but impaired *in vivo* T cell activation, proliferation and survival (Gattinoni et al., 2005b). Transfer of less-differentiated cells may be more efficacious at providing tumour protection. Indeed, Klebanoff et al. have shown that transfer of tumour specific T_{CM} cells translated into more effective anti-tumour responses, compared to T_{EM} cells. This correlated with a greater ability of T_{CM} cells, compared to T_{EM} cells, to recirculate through secondary lymphoid organs and encounter APCs, thanks to

their expression of CD62L and CCR7 (Klebanoff et al., 2005). Data supporting the notion that less differentiated cells may generate better anti-tumour responses also came from a study from Hinrichs and colleagues. In this study it was shown that effector cells derived from naïve progenitors, rather than T_{CM} progenitors, possessed greater proliferative potential and greater ability to produce IFNγ, which in turn correlated with greater anti-tumour responses (Hinrichs et al., 2009).

Finally, as previously described, lymphodepletion prior to adoptive transfer, also promotes the expansion and persistence of the transferred cells (Dudley et al., 2005; Dummer et al., 2002; Gattinoni et al., 2005a; Antony et al., 2005).

1.4.4. CAR-T cell therapy

An alternative strategy to redirect T cell antigen specificity, is to transduce T cells with a novel class of receptors called chimeric antigen receptors (CARs). The basic structure of a CAR consists of an extracellular binding domain, linked to an intracellular signalling domain (figure 1.11), via a transmembrane domain. Antigen specificity is typically provided by a single chain antibody variable fragment (scFv), although other receptors, such as cytokine receptors can be used (Kong et al., 2012). The first generation of CARs, contained the CD3ζ intracellular signalling domain; however T cells transduced with such constructs proliferated poorly and failed to elicit a robust cytokine response, due to poor T cell activation (Brocker et al., 1995; Cong et al., 1999). CARs were then modified, and the second generation of these receptors contained both CD3ζ and the cytoplasmic domain of a co-stimulatory receptor, such as CD28, 4-1BB or OX40. Addition of these co-stimulatory domains improved T function by conferring greater strength of signalling and persistence to the transduced lymphocytes (Finney et al., 2004; Sadelain et al., 2013). This translated into better persistence in patients (Savoldo et al., 2011). More recently third generation CARs have been designed and tested in the clinic. These receptors contain 2 co-stimulatory domains combined with an activation domain, in their

cytoplasmic region. In some mouse models these receptors seem to confer yet greater potency to anti-tumour cells (Zhong et al., 2012; Tammana et al., 2010).

The advantage of CAR gene therapy over TCR gene therapy is that CAR recognition of antigen is not dependent on presentation by MHC, meaning they are not restricted by a particular HLA molecule and can be used in patients of different HLA types. Moreover they are not associated with mispairing risk, inherent in TCR gene therapy.

However, the disadvantage of CAR therapy is that the antigen recognised by the receptor must be expressed as an intact molecule on the surface of the target cell, limiting the range of targetable antigens.

Nevertheless, clinical trials using anti-CD19 CAR-T cells to treat patients with a number of haematological malignancies showed very promising results. For example, in one study by Maude and colleagues 30 patients suffering from relapsed or refractory acute lymphoblastic leukaemia were treated with anti-CD19 CAR transduced T cells. Complete remission was achieved in 27 of those (90%) (Maude et al., 2014).

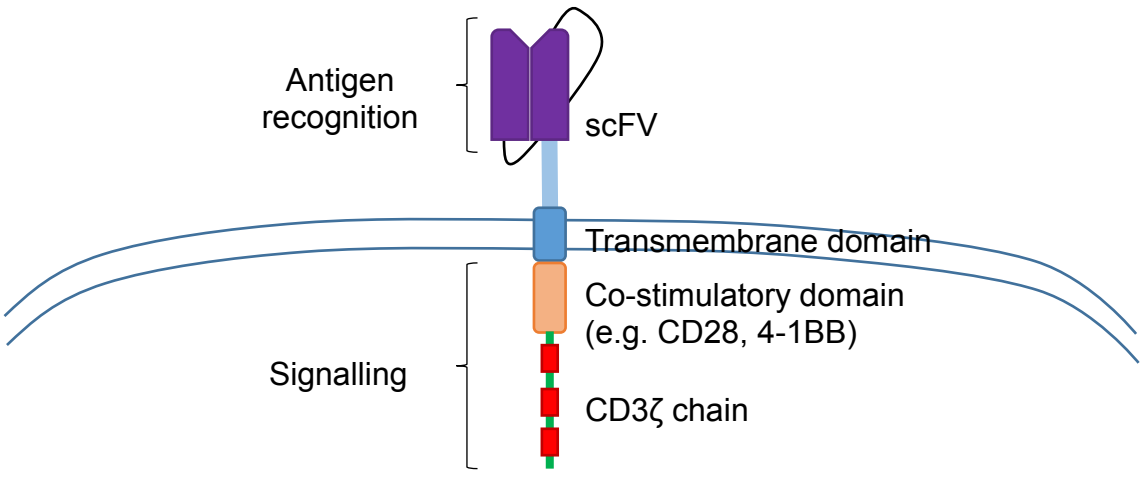

Figure 1.11 – Chimeric antigen receptors (CARs).

1.5. Limitations of mouse immunology for the study of human immunology

Thanks to their genetic and physiological relatedness to humans, mice are the experimental tool of choice to study the human immune system. However significant differences exist between them, and these have been highlighted by the failure to translate a number of therapies from murine models into the clinic. In this section some of the differences between human and mouse, and some of the limitation of murine models will be discussed.

The overall structure of the immune system is quite similar between mice and human (reviewed in Haley et al., 2003), but the expression and/or function of some of its components varies. For example, although ZAP-70 mutations are found both in humans and in mice, the phenotype caused by these mutations are different; in humans mutations in this signalling molecule results in normal numbers of CD8+ and CD4+ T cells, although the latter are non-functional. On the contrary, ZAP-70 mutations in mice result in a block in differentiation of both T cell subsets at the double positive stage (Elder et al., 2001). This difference was suggested to be a consequence of the “leakiness” of the Syk kinase which is seen in humans, but not in mice (Chu et al., 1999). The expression of the co-stimulatory molecule CD28 is also different, with the expression in murine CD4+ and CD8+ T cells being close to 100%, while only 80% of human CD4+ and 50% of human CD8+ T cells express this receptor. This in turn was suggested to play a role in the efficacy of anti-CTLA-4 blocking antibody treatments, which are more efficient in mice compared to humans (Lenschow et al., 1996). Thus, although mice and human express the same proteins, their function and the pathways in which these are involved may be different.

Similarly to the study of single molecules and pathways, mice are the tool of choice to study the biology of cancer, among other diseases. Although these models have been useful tools to validate gene function, to identify novel cancer genes and to test novel

therapeutic strategies, significant limitations still exist. These include species-specific differences and inaccurate representation of de novo tumour development and progression. For example, telomerases are active in mice, whereas are largely inactive in adult human cells. As a consequence murine cells can transform and become immortalised more easily than human cells do. Thus, murine tumours require fewer genetic alterations for malignant transformation than human malignancies do. Species to species differences also results in mouse tumours with different histology and/or spectrum from human tumours. For example Rb heterozygous mutant mice develop pituitary adenocarcinomas, unlike children with the same mutation who develop retinoblastoma (Jacks et al., 1992). In addition, the metastatic potential of murine cancers is different compared to human tumours: mouse models tend to develop relatively few metastases, or metastases with different tissue specificities, which suggests the metastatic process in mouse and human might follow different mechanisms. The number and type of genetic mutations are also different: many mouse models rely on mutations in the germ-line or in a large proportion of somatic cells. The latter are often promoted by the use of carcinogens, such as MCA, which don't mimic the human tumorigenesis process. Moreover in human cancers germ-line mutations are rare, and most somatic mutations are quite rare. In humans, point mutations in onco- or tumour-suppressive genes normally cause and/or drive the disease; in mice cancer often develops as a consequence of gene/s deletion or overexpression. Thus, murine malignancies are generally more homogeneous compared to human cancers. (Cheon et al., 2011). Whether the development of ideal mouse models is achievable is still unclear, and all the limitations of the current systems need to be taken into consideration when designing experiments, interpreting the data and developing new therapeutic strategies. Currently, mouse models are unlikely to replace research based on patients' samples, and no one best model in which to study cancer exists. Therefore, combinatorial approaches using multiple systems are necessary to study and understand human cancers.

1.6. Background to PhD project

The amount of endogenous TCR expressed by a T cell on its surface, is dictated early on during development in the thymus. How this level changes in the periphery, during an immune response, and after pathogen clearance is not known.

Thanks to their ability to be genetically modified, and because of the central role they play in an adaptive immune response, T cells are at the centre of the cancer immunotherapy field.

Over the past decades a number of technologies have been developed to improve the anti-tumour efficacy of genetically transduced T cells. In particular, our group has shown that CD3 overexpression, leading to TCR overexpression, in $CD8^+$ T cells, correlates with greater functional avidity *in vitro* and better anti-tumour responses *in vivo* (Ahmadi et al., 2011); similar results were obtained with $CD4^+$ T cells (Nicholson, unpublished data). However in the latter case, preliminary evidence suggested that CD3-overepressing $CD4^+$ T cells may be toxic *in vivo*.

This project was therefore designed to investigate the consequences of CD3 (and as a consequence endogenous TCR) overexpression in $CD4^+$ T cells. We hypothesised that increasing the levels of TCR on the T cell surface lowers the activation threshold of $CD4^+$ T cells, which in turn may promote their *in vivo* survival due to greater interaction with self-p:MHC complexes. Consequently the co-transfer of additional CD3 molecules may be a viable strategy to improve $CD4^+$ T cell cancer immunotherapies.

1.6.1. The role of $CD4^+$ T cells in adoptive immunotherapy

Although $CD4^+$ T cells are critical for orchestrating immunological responses, cancer immunotherapy has until recently focused primarily on tumour reactive $CD8^+$ cytotoxic T cells, mainly because of their capacity to directly kill cancerous cells. A number of groups have now demonstrated that $CD4^+$ T cells not only enhance $CD8^+$ T cell responses, but are themselves capable of eradicating tumours.

1.6.2. $CD4^+$ T cells in tumour immunity

Our understanding of the role played by $CD4^+$ T cells in tumour immunity comes from both animal models and from patients. Greenberg and colleagues demonstrated that adoptive transfer of $CD4^+$ T cells into mice burdened with MHC-I^+ metastatic acute leukaemia, and which lacked both $CD4^+$ and $CD8^+$ T cells, lead to tumour eradication, even in absence of CTLs (Greenberg et al., 1985). Moreover, a melanoma model was used to demonstrate that whereas $CD4^+$ T cell deficient mice failed to reject tumours, a significant proportion of $CD8^+$ T cell deficient mice mounted successful tumour rejection. This led the authors to conclude that $CD4^+$ T cell-dependent effector mechanisms existed, in addition to the MHC-I restricted $CD8^+$ T cell killing mechanisms (Hung et al., 1998).

In patients, tumour specific $CD4^+$ T cells have been isolated from a number of different malignancies. In a study looking at small cell carcinoma and adenocarcinoma patients, it was found that a decreased CD4/CD8 ratio was significantly associated with a worse prognosis (Nakamura et al., 2002). In breast cancer patients, an increase in $CD4^+$ T cells in axillary lymph nodes correlated with disease-free survival (Kohrt et al., 2005). Rosenberg et al. showed that adoptive transfer of a heterogeneous population of TILs, containing both $CD4^+$ and $CD8^+$ T cells, to treat patients suffering from metastatic melanoma, led to an objective clinical response in 77% of patients. This was in contrast to previous studies were no objective response was seen in metastatic melanoma patients treated with an anti-tumour $CD8^+$ T cell only population (Rosenberg et al., 2004). Adoptive transfer of autologous $CD4^+$ T cells specific for the melanoma-associated NY-ESO-1 antigen, into a patient with refractory metastatic melanoma mediated a durable clinical remission, with the patient remaining in remission 2 years post adoptive transfer (Hunder et al., 2008).

1.6.3. Mechanisms of action of tumour specific $CD4^+$ T cells

From the data described above it is clear that $CD4^+$ T cells play a central role in tumour eradication. Indeed, they can coordinate both innate and adaptive immune responses, both of which are important for tumour rejection. $CD4^+$ T cells can activate tumour-specific CTL, APCs, macrophages and NK cells, and can themselves also be cytotoxic.

It is well established that *in vivo* priming of antigen specific $CD8^+$ T cells depends on "help" provided by the $CD4^+$ T cells. This "help" comes from APC-licensing by activated $CD4^+$ T cells. CD40L is expressed on the surface of activated $CD4^+$ T cells. Its interaction with CD40 on the surface of APCs, B cells and macrophages increases their ability to present antigen and upregulate their co-stimulatory molecules. Thus, after interaction with $CD4^+$ T cells, APCs can more efficiently present antigens and stimulate cytotoxic $CD8^+$ T cells, which become activated. The role played by the CD40:CD40L interaction was demonstrated by both Bennett et al. and Schoenberger et al. Both groups showed that in CD4 deficient mice, $CD8^+$ T cell responses could be restored by administering activating anti-CD40 antibodies. Conversely, blockade of CD40L abrogated priming (Bennett et al., 1998; Schoenberger et al., 1998).

Quezada et al. investigated the mechanisms of tumour protection by $CD4^+$ T cells in a murine model of melanoma. Transgenic $CD4^+$ T cells expressing the TRP1-TCR, which recognises a melanoma antigen, were transferred into animals with established melanoma. Transfer of as few as 50,000 $CD4^+$ TRP1-TCR^+ T cells was sufficient to induce initial regression of the tumours. However, in 60% of the cases the tumour recurred. This was prevented by co-injecting the animals with anti-CTLA-4 antibodies, at the time of adoptive transfer. CTLA-4 blockade increased the expansion of the transgenic cells by up to 3 fold, and prevented the differentiation of the adoptively transferred $CD4^+$ T cells into $Foxp3^+$ cells. The adoptively transferred cells acquired a Th1 phenotype, and produced large amounts of both IFNγ, TNF and IL-2, which were further increased with CTLA-4 blockade. IFNγ was shown to be fundamental for tumour rejection, as IFNγ

neutralisation prevented rejection of tumours. Moreover, it was shown that at least initially, IFNγ produced by the TRP1-TCR^{+} CD4^{+} T cells directly targeted the tumour cells, as transfer into IFNγ receptor-deficient did not alter the kinetics of tumour rejection. However, in this case 100% of recipients regrew tumours, suggesting IFNγ-sensitive cells, besides tumour cells, are potentially important for complete tumour eradication. Further experiments with RAG-deficient and perforin-deficient recipient mice indicated that tumour rejection was independent of endogenous T, B and NK cells. Cytotoxic activity also required direct MHC-II recognition by the adoptively transferred cells, which exerted their cytotoxic activity by degranulation of granzyme-containing lytic granules (Quezada et al., 2010).

Similar results using the TRP1-TCR melanoma model were also obtained by Xie and colleagues. They demonstrated that after adoptive transfer into lymphopenic hosts, CD4^{+} T cells differentiated into Th1 cytotoxic cells, which expressed genes normally associated with effector cells, such as perforin, granzyme B and LAMP-1 (Xie et al., 2010).

IFNγ produced by CD4^{+} T cells has also been shown to act on non-haematopoietic IFNγ receptor^{+} cells. In particular, IFNγ acts on stromal cells to inhibit angiogenesis, leading to tumour necrosis (Qin et al., 2000). Moreover, Corthay et al. also showed that CD4^{+} T cells could mediate rejection of MHC-II$^{-/-}$ myeloma. The IFNγ produced by CD4^{+} T cells was a potent activator of macrophages at the tumour site, which in turn suppressed tumour growth (Corthay et al., 2005).

Perez-Diez compared tumour protection efficiency by two transgenic populations of CD8^{+} (MataHari) and CD4^{+} (Marilyn) T cells which both recognise the H-Y antigen. Mice were challenged with a bladder carcinoma which expressed both MHC-I and MHC-II H-Y antigens, recognised by the transgenic CD8^{+} and CD4^{+} cells respectively. Surprisingly, MataHari CD8^{+} T cells were no capable of mediating tumour rejection, whereas 80% of the Marilyn CD4^{+} T cells cleared the tumour. Moreover, lack of MHC expression by the tumour cells did not lessen the anti-tumour effects of the CD4^{+} cells, but MHC-II

expression on host cells was fundamental to mediate tumour rejection. In addition, NK cells were fundamental for long-term tumour rejection, and these co-localised with the $CD4^+$ Marilyn cells in the tumour mass, suggesting they worked in concert at the tumour site (Perez-Diez et al., 2007).

1.7. Research aims and hypothesis

This project was designed to investigate the effects of CD3 overexpression in $CD4^+$ T cells. We hypothesised that CD3 overexpression leading to increased expression of the endogenous TCR may alter the triggering threshold of $CD4^+$ T cells and enhance their *in vivo* survival. To address this, we used retroviral vectors to provide additional CD3 genes to bulk populations of $CD4^+$ T cells (with or without additional TCR), which were then examined *in vitro* and transferred into lymphopenic mice, in both competitive and non-competitive settings. The survival and differentiation of CD3-transduced $CD4^+$ T cells was tracked overtime, and compared to those of control-transduced $CD4^+$ T cells.

2. Materials and Methods

2.1. Cell culture

2.1.1. Tissue culture and cell counting

All tissue culture was performed under sterile conditions in Biohit Biological Safety Cabinet Class 2 hoods. All cells were cultured at 37 ºC with 5% CO_2 unless otherwise stated.

Cell counting was performed using a haemocytometer (Immune Systems, BVS100). Cells were diluted in Trypan Blue 0.4% (Life Technologies, 15250-061) and live cells (cells that did not uptake the dye) were counted under a light microscope.

Cell counting in flow cytometric analyses were performed using CountBright™ Absolute Counting Beads (Life Technologies, C36950). A fixed number of counting beads were added to each sample allowing the total number of cells in each sample to be calculated.

2.1.2. Phoenix eco (p.eco) cells

P.eco cells, the packaging cells used for the production of retroviruses, derive from the human 293T cell line (a human embryonic kidney line transformed with the adenovirus E1a). 293T cells were stably transfected, by the Nolan laboratory, with the DNA encoding for the gag-pol proteins as well as the ecotropic virus envelope. Cells were grown in tissue culture flasks 75 cm^2 (TPP, 90076) with Isocove's Modified Dulbecco Medium (IMDM) (Lonza, BE12722F), supplemented with 10% Foetal Calf Serum (FCS) (Biosera), 1% Penicillin/Streptomycin (100 U/ml; GIBCO, 15070) and 1% L-Glutamine 200 mM (2 mM; GIBCO, 25030). Cells were detached by treating them with 3 ml of 0.05% Trypsin-EDTA (GIBCO, 25300) for 1 minute before neutralisation with culture medium. Cells were split 1/8 every 2 days, according to cell growth.

2.1.3. Murine T cell culture

Murine spleens were mashed through a 40 µM cell strainer (BD Falcon, 352340) into a 50 ml Falcon centrifuge tube (TPP, 91050) and washed with PBS. Red blood cells were lysed by resuspending the pellet in 2 ml of ammonium-chloride-potassium (ACK) lysing buffer (Lonza, 10-548E) for 2 minutes. Cells were then washed with 10x PBS. Cells were MACS sorted (see below) if needed, and cultured in RPMI 1640 medium (Lonza, BE12-167F) supplemented with 10% Foetal Calf Serum (FCS) (Biosera), 1% Penicillin/Streptomycin (100 U/ml; GIBCO, 15070), 1% L-Glutamine 200 mM (2 mM; GIBCO, 25030) and 0.5% 2-Mercaptoethanol (complete RPMI 1640 medium).

2.2. Transduction of murine splenocytes/T cells

2.2.1. Retroviral vectors

The retroviral vectors pMP71-CD3ζ-2A-CD3ε-2A-CD3δ-2A-CD3γ-IRES-GFP (CD3-GFP), pMP71-iCre-IRES-GFP (control-GFP), and pMP71-TRP1-IRES-CD19 (TRP1-TCR) were available in the laboratory and were used for transduction (figure 2.1 and 2.2). The CD3-GFP vector contains all four chains of the CD3 complex, linked by 2A sequences. The control-GFP vector contains the Cre sequence in reversed orientation, so not to give any transcription. Both vectors contain an IRES-GFP sequence so that transduction efficiency of both vectors can be assessed by GFP expression. The TRP1-TCR vector encodes the α and β chains of the TRP1-TCR, separated by a 2A sequence. The TRP1-TCR recognizes a peptide ($TRP1_{113-127}$) derived from the tyrosinase related protein 1, on MHC-II. All TCRs were codon optimised and the TRP1-TCR also contain an extra cysteine residue in the constant chain to facilitate preferential pairing of the introduced TCR.

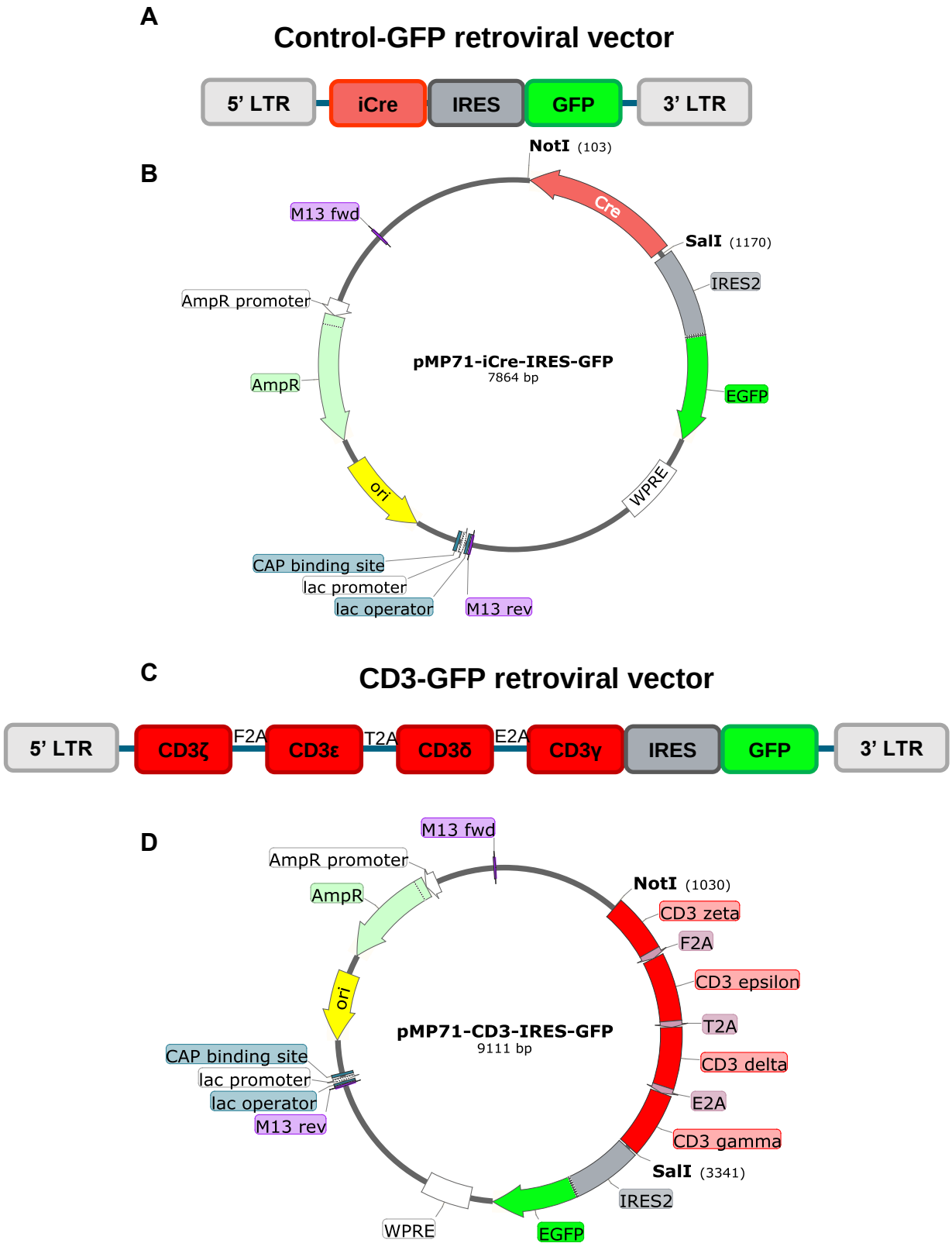

Figure 2.1 – control-GFP and CD3-GFP retroviral vectors. (A) Schematic outline and (B) vector map of the pMP71-iCre-IRES-GFP (referred to as "control-GFP") retroviral vector. (C) Schematic outline and (D) vector map of the pMP71-CD3ζ-F2A-CD3ε-T2A-CD3δ-E2A-CD3γ-IRES-GFP (referred to as "CD3-GFP") retroviral vector.

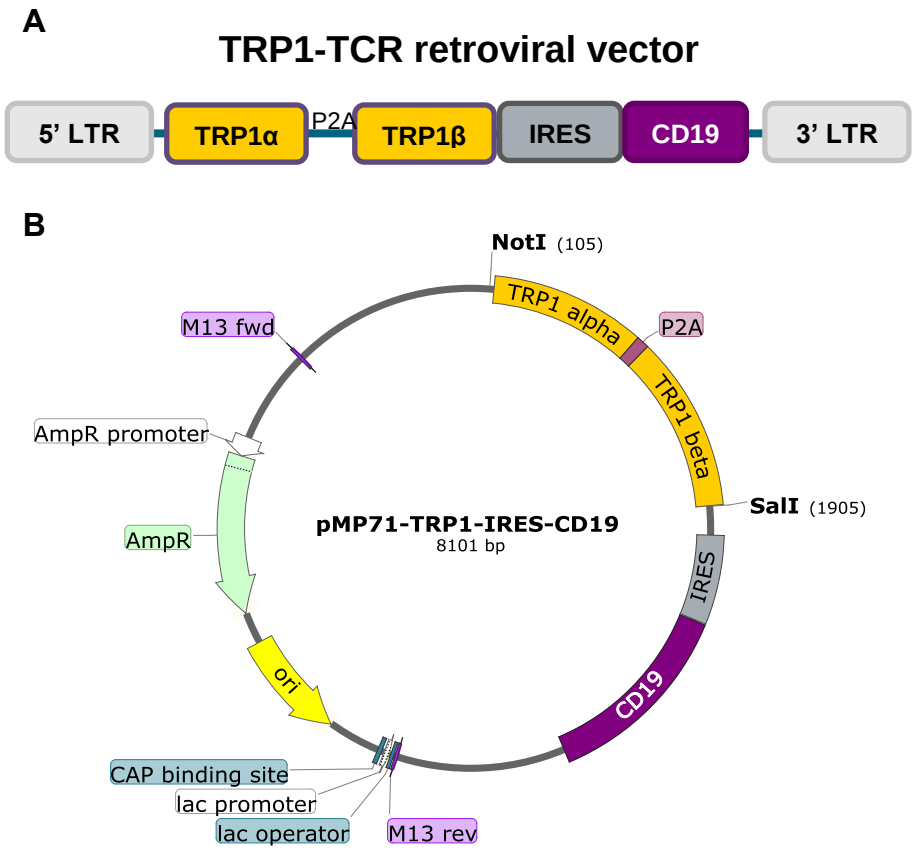

Figure 2.2 – TRP1-TCR retroviral vector. (A) Schematic outline and (B) vector map of the pMP71-TRP1-IRES-CD19 (referred to as "TRP1-TCR") retroviral vector.

2.2.2. Retrovirus production

1.5 x 10^6 p.eco cells were plated on a 60.1 cm^2 tissue culture treated dish (TPP, 93100) in 8 ml of complete IMDM. The next day the medium was replaced with 5 ml of fresh IMDM 30-60 minutes before transfection. The transfection mix was set up as follows: 10 µl of Fugene HD Transfection Reagent (Roche, 04709713001) was added to 150 ul OPTIMEM media (GIBCO, 31985) in a 1.5 ml Eppendorf tube. In a separate Eppendorf the DNA mix was set up: 2.6 µg of vector DNA and 1.5 µg of pCl-Eco DNA were added to a total volume of 50 µl water. The DNA mix was gently added to the Fugene-OPTIMEM mix and incubated at room temperature for 15-20 minutes, before dripping it onto the p.eco plates. After 24 hours the medium on the p.eco cells was replaced with 5 ml of complete RPMI 1640 medium. Two days after transfection the viral supernatant was

harvested from the p.eco plates and spun down to remove debris. Viral supernatant was used fresh or cryopreserved and stored at -80 °C for future transductions.

2.2.3. Purification and activation of murine T cells

$CD4^+$ and $CD8^+$ T cells were sorted from bulk splenocytes using CD4 (L3T4) (Miltenyi, 130-049-201) MicroBeads or CD8a (Ly-2) MicroBeads (Miltenyi, 130-049-401). Splenocytes single cells suspensions were prepared as described above and resuspended in 630 µl of MACS buffer (0.5% Bovine Serum Albumin (BSA) and 2 mM Ethylendiamintetraacetat (EDTA)) per spleen. 70 µl of relevant MicroBeads were added per spleen and incubated at 4 °C for 15 minutes. LS magnetic separation columns (Miltenyi, 130-042-401) were equilibrated with 3 ml of MACS buffer. Cells were washed with 15 ml of MACS buffer and then resuspended in 500 µl of MACS buffer per 10^8 cells/per spleen. Cells were loaded onto the equilibrated columns prior to washing three times with 3 ml of MACS buffer. Cells were eluted with 5 ml of MACS buffer into a sterile 30 ml Universal container. The sorted cells were resuspended at 1.5 x 10^6/ml in complete RPMI 1640 medium supplemented with 30 U/ml IL-2 (Roche, 11011456001), and activated with Dynabeads® Mouse T-Activator CD3/CD28 (Thermo Fisher, 11456D) (20 µl per million of cells) for 24 hours before transduction.

2.2.4. Retroviral-mediated transduction of T cells

24 hours after activation, T cells were counted and 4-6 x 10^6 cells resuspended in 1.5 ml of neat retroviral supernatant. Non-tissue culture treated plates were prepared by coating with 2.5 ml of RetroNectin (Takara, T100B) for 3 hours at room temperature, then blocked with filter sterilised 2% BSA/PBS for 30 minutes at room temperature and finally washed twice with PBS. The activated cells were resuspended in the retroviral supernatant, added to the retronectin-coated plates and spun at 2000 rpm for 90 minutes at 32 °C. For co-transductions, activated cells were resuspended in an equal volume of TRP1-TCR supernatant and Control-GFP or CD3-GFP supernatant. At the end of the spin, 4.5 ml of complete RPMI 1640 medium and 10 U/ml of Roche IL-2 were added and the cells

were cultured in a 37 °C incubator. Fresh complete RPMI 1640 medium and IL-2 were added every 2-3 days. The process of retrovirus production and transduction is shown in figure 2.3 below.

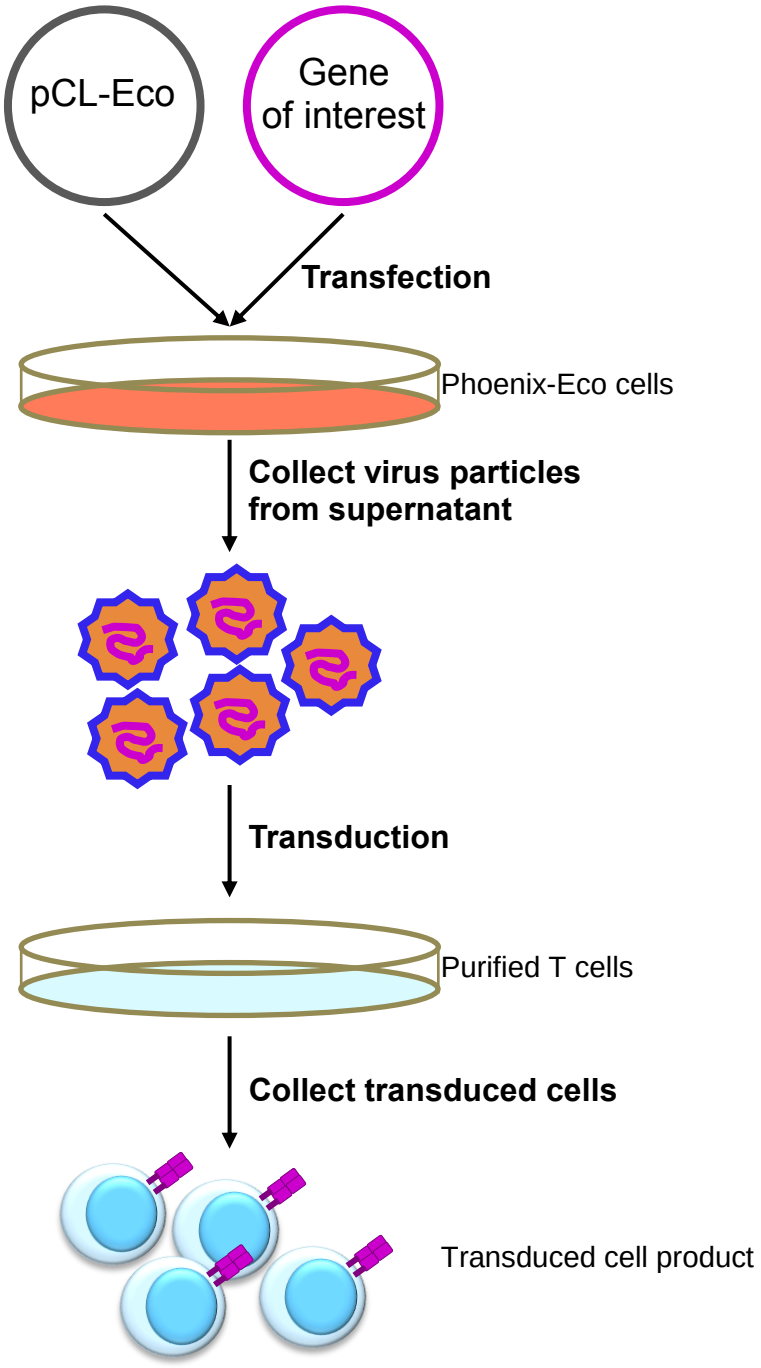

Figure 2.3 – Transfection and Transduction. Schematic representation of the phoenix eco transfection and T cell transduction steps.

2.3. Flow cytometry

2.3.1. Surface staining

Prior to FACS analysis all cells were washed once with PBS and resuspended in 50 µl FACS buffer (1% FCS/PBS) containing the monoclonal antibodies of interest in the appropriate dilutions (see table 2.1 below for details). Cells were incubated in the dark at 4 °C for 30 minutes, before a further wash in FACS buffer. FACS data acquisition was performed on BD Fortessa or LSRII flow cytometers. FCS flow cytometry files were analysed using FlowJo v10 software (Treestar).

Annexin V staining was performed using the Annexin V Apoptosis Detection Kit (Thermo Fisher, 88-8008-72), as per manufacturer's instructions. Cells were stained for surface molecules as described above, washed once in FACS buffer and once in Annexin V binding buffer 1x. Cells were resuspended in 100 µl Binding buffer containing the Annexin V antibody diluted 1/20. Cells were incubated in the dark at room temperature, for 10-15 minutes, before being washed and then resuspended in binding buffer. Cells were analysed by flow cytometry within 4 hours of Annexin V staining.

2.3.2. Intracellular staining

Cells were initially stained for surface molecules as described above and then fixed with 300 µl IC Fixation buffer (eBioscience, 00-8222-49) for 30 minutes at 4 °C. Cells were washed with 1 ml 2% BSA/PBS. Cells were permeabilised with 300 µl/sample of 0.1% IGEPAL® CA-630 (Sigma Aldrich, I8896) for 3 minutes on ice. Cells were washed once more, then resuspended in 50 µl FACS buffer (1% FCS/PBS) containing the monoclonal antibodies of interest in the appropriate dilutions (see table 2.1 for details).

For p-ERK intracellular staining cells (up to 1 x 10^6 cells) were fixed with 1 ml 2% PFA/PBS for 10 minutes at 37 ºC. Cells were permeabilised with 0.9 ml of ice-cold 90%

MeOH for 30 minutes on ice, washed once and simultaneously stained for both surface markers and p-ERK, as described above.

Ki67 staining was performed using the FoxP3 staining kit (eBioscience, 00-5523-00). Cells were surface stained as above and fixed with 300 ul of FoxP3 Fix/Perm solution for 30 minutes on ice. Cells were washed with perm wash and stained with Ki67 eFluor660 diluted in Perm wash for 30 minutes at room temperature. Cells were then washed again in Perm wash and resuspended in BSA/PBS for analysis.

Specificity	Fluorochrome	Manufacturer	Catalogue number	Dilution
CD3	BUV395	BD	563565	1/50
CD3	BV605	BD	563004	1/50
CD3	BV711	BD	563123	1/50
CD4	APC-H7	BD	580181	1/400
CD4	PerCP	BD	553052	1/100
CD8	v500	BD	560778	1/200
CD8	v450	BD	560469	1/400
CD25	PE	BD	553075	1/100
CD45.1	BV650	BD	563754	1/200
CD62L	Alexa Fluor700	BD	560517	1/400
CD69	APC-Cy7	BD	561240	1/100
CD127	eFluor660	eBioscience	50-1271-80	1/100
TCRβ	APC	BD	553174	1/50
TCRβ	PE	BD	555548	1/100
Thy1.1	PE-Cy7	eBioscience	25-0900-82	1/10000
Annexin V	PerCP-eFluor710	Invitrogen	88-8008-72	1/20
Ki67	eFluor660	Invitrogen	50-5698-80	1/200
Live/Dead	PI	BD	556463	1/300
Live/Dead	APC-Cy7	Thermo Fisher	L10119	1/800
IFNγ	APC	BD	554413	1/200
IL-2	APC	BD	554429	1/100
p-ERK (Thr202/Tyr204)	N/A	CST	4377S	1/50
goat anti-rabbit IgG	PE	Invitrogen	P-2771MP	1/50
Vβ14	PE	Miltenyi Biotec	130-110-051	1/100

Table 2.1 – FACS antibodies

2.4. *In vitro* functional assays

2.4.1. CD107a assay

$CD4^+$ and $CD8^+$ T cells were MACS purified from C57Bl/6 spleens, as described above. After purification cells were resuspended at 1 x 10^6/ml in complete RPMI 1640 medium supplemented with 0.7 µl/ml Golgi stop (BD Biosciences; 554724), 0.2 µl/ml Brefeldin A (Brefeldin A blocks the transport of proteins from the Golgi apparatus preventing secretion of cytokines) and 1:100 dilution of anti-CD107a APC-conjugated antibody. Cells were restimulated with anti-CD3/CD28 beads (20 µl/million of cells), or 200 ng/ml PMA plus 2000 ng/ml ionomycin (positive control) or PBS (negative control), up to 4 hours and samples taken at 5, 15, 30 minutes and 1, 1.5, 2, 3 and 4 hours. Each sample was washed with 2 ml ice-cold PBS, followed by two further washes in FACS buffer. Cells were stained and analysed by flow cytometry.

2.4.2. Stimulation of T cells soluble anti-CD3 antibody

Polyclonal $CD4^+$ and $CD8^+$ T cells were purified by magnetic sorting from C57Bl/6 spleens, as described above. After purification up to 1 x 10^6 purified cells were restimulated by addition of 50 µg/ml soluble anti-CD3 antibody (BD, 553057) for 1-60 minutes, for ERK phosphorylation analysis. At the end of the stimulations cells were fixed, permed and stained for p-ERK as described above.

2.4.3. Stimulation of T cells with plate-bound anti-CD3 antibody

Polyclonal T cells transduced with the control-GFP or the CD3-GFP vectors (see figure 2.1) were cultured for 6 days post-transduction in the presence of IL-2 prior to CD3 stimulation for *in vitro* functional analysis. Non-tissue culture treated 96-well plates were coated with 10 µg – 0.001 µg of anti-CD3 antibody (BD, 553057) or PBS, overnight at 4 °C. The following day wells were washed once with PBS before 0.1 x 10^6 transduced cells were transferred to the coated wells and were incubated for 4 hours or overnight in

a 37 °C incubator. At the end of the restimulation cells were spun and 150-180 µl of supernatant was harvested and stored at -20 °C for subsequent analysis by ELISA. Where stated, the cells were stained for intracellular cytokines, as described in section 2.3.2. If intracellular cytokine staining was performed, Brefeldin A was added to the cells after 2 hours from initial stimulation (referred to as “4 hours stimulation”) or the following morning (referred to as an “overnight stimulation”).

2.4.4. Stimulation of T cells with peptide-loaded splenocytes

$CD4^+$ MACS purified T cells transduced with the TRP1-TCR and the control-GFP or the CD3-GFP vectors (See figure 2.1 and 2.2) were cultured for 6 days post transduction in the presence of IL-2 prior to peptide stimulation for *in vitro* functional analysis. Single cell suspensions of C57Bl/6 spleens were generated and splenocytes were loaded with 10 µM-100 pM $TRP1_{113\text{-}127}$ peptide (CRPGWRGAACNQKI), or 10 µM pNP_{366} peptide (ASNENMDAM; irrelevant peptide for negative control) for 2-3 hours at 37 ºC in complete RPMI 1640 medium. After loading 5 x 10^4 peptide-loaded stimulator cells were added to 5 x 10^4 transduced $CD4^+$ T cells. The cells were initially co-cultured in complete RPMI 1640 medium for 2 hours, after which 5 µg/µl brefeldin A was added; the cells were then co-cultured overnight. The next morning the cells were washed, fixed and permeabilised for intracellular staining as described above. For positive control, transduced T cells were incubated overnight with PMA and ionomycin in absence of stimulator cells.

2.4.5. Enzyme-linked Immunoabsorbent Assay (ELISA)

Cytokine-containing supernatants were generated as described in section 2.4.3. IL-2 and IFNγ concentrations were measured using the BD OptEIA kits (IFNγ, 555138; IL-2, 555148), according to manufacturer’s instructions. Supernatants were diluted 1/4 in complete RPMI 1640 media before used in the assay.

2.4.6. Calcium flux assay

10 x 10^6 $CD4^+$ and $CD8^+$ purified T cells per sample were resuspended in IMDM supplemented with 5% FCS and loaded with Indo-1 AM (Thermo Fisher, I1223) (4 µg/ml) for 1 hour at 37 °C. Indo-1 AM is a UV light-excitable, ratiometric Ca^{2+} indicator (see chapter 3, section 3.3 for mechanism of action). Cells were re-suspended in a final volume of 2 ml IMDM supplemented with 1% BSA prior to analysis on the BD Fortessa at 37 °C. To determine baseline levels of intracellular calcium, cells were acquired for an initial 2-4 minutes, after which stimulation was provided by adding 10 or 5 µg/ml of anti-CD3 purified antibody (BD, 553057), or PMA/ionomycin. Data was recorded for a further 15 minutes. FCS flow cytometry files were analysed using FlowJo v10 software (Treestar).

2.4.7. LEGENDplex™ bead-based immunoassay

Murine peripheral blood was collected into eppendorf tubes on day 3 and day 11 post T cell transfer. Blood was left to clot for 30 minutes and spun for 10 minutes at 13000 rpm; serum was removed from each sample and stored at -80 °C until analysis. The LEGENDplex™ bead-based immunoassay (BIolegend) assay was performed on serum to determine the concentration of the following cytokines: MCP-1; GM-CSF; IFN-β; IFN-γ; IL-1α; IL-1β; IL-6; IL-10; IL-12 (p70); IL-17A; IL-23; IL-27; TNF-α and IL-2. The assay was performed according to manufacturer's instructions.

2.5. *In vivo* experiments

2.5.1. Mice

Animal protocols were approved by local institutional research committees and in accordance with UK Home Office guidelines. C57BL/6 female mice aged between 8 and 10 weeks were obtained from the in-house Comparative Biology Unit at the Royal Free

Hospital, London. Similarly aged Thy1.1 luciferase$^+$ C57BL/6 mice, Thy1.1 C57BL/6 mice and CD45.1 C57BL/6 congenic mice from the same animal facility were also used as donors in multiple experiments. All experiments were carried out under home office licenses (project licence numbers PPL 70/7300 and PA41AA614).

2.5.2. *In vivo* bioluminescence imaging of T cells

$CD4^+$ and $CD8^+$ T cells were MACS sorted from C57BL/6 Thy1.1 luciferase$^+$ mice and transduced with the CD3-GFP vector as described in sections 2.2.3 and 2.2.4. Three days post transduction, wild-type C57BL/6 mice were sub-lethally irradiated with 5.5 Gy and then 3-4 hours post irradiation the mice were injected with 5 x 10^6 transduced luciferase$^+$ cells in a total volume of 200 µl PBS, intravenously (i.v.) On day 8 post T cell transfer mice were injected with 200 µl D-Luciferin Firefly (15 mg/ml) (Biosynth, L-8220), anaesthetized, and after 10 minutes post injection, imaged with a Xenogen IVIS-100 (Caliper Life Sciences). Bioluminescent Imagining was performed as per local institutional operating procedures.

2.5.3. *In vivo* competition experiments

C57BL/6 mice were sublethally irradiated with 5.5 Gy on day 0 and then 3-4 hours later received an i.v. injection of a mixture of CD45.1 and hy1.1 congenically marked $CD4^+$ T cells, transduced with the control-GFP and the CD3-GFP vector respectively. The proportion of control-GFP and CD3-GFP cells in the injection mixture was analysed by flow cytometry prior to injection. Mice's weight was monitored over time and animals were sacrificed at day 5, 10, 15 and 20 post T cell transfer. Spleen, inguinal lymph nodes, bone marrow (pooled from 1 tibia and 1 femur per mouse) and liver were harvested from each culled animal and single cell suspensions prepared as follows: tissues were mashed through a 40 µM cell strainer (BD Falcon, 352340) into a 50 ml Falcon centrifuge tube (TPP, 91050) and washed with PBS. Red blood cells were lysed by resuspending the pellet in 2 ml of ammonium-chloride-potassium (ACK) lysing buffer (Lonza, 10-548E)

for 2 minutes. Cells were then washed with 20 ml PBS. Cells were analysed by flow cutometry as described in section 2.3.

2.6. Statistical analysis

Data was analysed in GraphPad Prism 6, which was also used to generate graphs and perform statistical analysis. Unpaired student t-tests was calculated for all data sets, except for *in vitro* restimulations (sections 3.9 and 3.10), where two-way ANOVA analysis was applied. Differences were considered statistically significant when p values were <0.05 (significance was represented by *: ≤0.05; **:≤0.01; ***:≤0.001; ****≤0.0001).

3. *In vitro* phenotype and function characterisation of CD3 engineered $CD4^+$ and $CD8^+$ T cells

3.1. Introduction

The functional avidity of a T cell for its cognate peptide is dependent on the "fitness" of the T cell, the affinity of the TCR for its peptide:MHC complex (p:MHC) and the density of TCR on the T cell's surface. The density of the TCR plays a major role in determining whether a T cell will be activated or not. Irrespective of the affinity of the TCR for its p:MHC, a T cell will not be activated unless a threshold number of TCR has been engaged. Viola et al. showed that T cell activation in absence of co-stimulation will occur only when ≥8000 TCRs are engaged, whereas if CD28 co-stimulation is present ligation of 1000 TCRs is sufficient for activation (Viola et al., 1996). Other studies have also shown that the level of T cell activation correlates with TCR density. A transgenic mouse model where T cells express different levels of the same TCR was used to show that calcium mobilization, proliferation and IFNγ production are reduced by approximately 3 fold when the number of TCR per cell is reduced from $5x10^4$ to $1x10^4$ (Blichfeldt et al., 1996).

Our laboratory has previously shown that concentration of CD3 in T lymphocytes is rate limiting for TCR-CD3 surface expression. In fact provision of additional CD3 molecules to T cell is an effective strategy to increase TCR expression. When CD3 is co-transduced with a therapeutic TCR into $CD8^+$ T cells, expression of both introduced and endogenous TCRs is increased. This improved TCR expression augments TCR functional avidity, which correlates with better peptide specific responses *in vitro* (cells respond to lower concentration of peptide and produce more cytokines upon stimulation). This translates to better anti-tumour responses *in vivo*: more cells traffic to the tumour site and they

persist for longer, leading to faster tumour eradication (Ahmadi et al., 2011). Similarly $CD4^+$ T cells co-transduced with a class I-restricted therapeutic TCR and CD3 showed increased functional avidity which in turn gives better *in vivo* anti-tumour responses. However mice receiving $CD4^+$ cells co-transduced with TCR + CD3 developed fatal toxicity, which was independent from tumour burden. Interestingly preliminary results also showed $CD4^+$ transduced with CD3-only cells could also cause toxicity *in vivo* (Nicholson, unpublished data).

Thus the aim of the experiments reported in this chapter was to characterise the consequences of CD3 overexpression in $CD4^+$ and $CD8^+$ T cells. Initially we investigated the phenotype of non-manipulated $CD4^+$ and $CD8^+$ T cells. We then assessed if and how their phenotype and *in vitro* functions are changed after transduction with CD3.

3.2. Polyclonal $CD4^+$ T cells express higher levels of endogenous TCR than $CD8^+$ T cells

TCR and CD3 expression were measured in freshly isolated $CD4^+$ and $CD8^+$ T cells isolated from spleen, inguinal lymph nodes (LN), bone marrow (pooled from one tibia and one fibula; BM) and liver, of a untreated C57Bl/6 mouse. Tissues were harvested and single cell suspensions generated as described in chapter 2, section 2.5.3.

$CD4^+$ and $CD8^+$ T cell populations were identified by flow cytometry in the four tissues (figure 3.1A) and their expression levels of TCR and CD3 were analysed, using antibodies recognising the TCR murine constant β (Cβ) chain and CD3ε respectively. Figure 3.1B shows typical expression levels (median fluorescent intensity; MFI) of TCR and CD3 in freshly isolated lymphocytes. $CD4^+$ T cells express significantly higher levels of TCR, on average 2.5 fold more, compared to $CD8^+$ T cells ($CD4^+$ TCR MFI=11066.7; $CD8^+$ TCR MFI=5772.57; $CD4^+$ CD3 MFI=1856; $CD8^+$ CD3 MFI=1306). Mean values are

shown in figure 3.1C. Thus resting, unmanipulated CD4⁺ T cells physiologically express significantly higher levels of TCR-CD3 complex compared to CD8⁺ T cells.

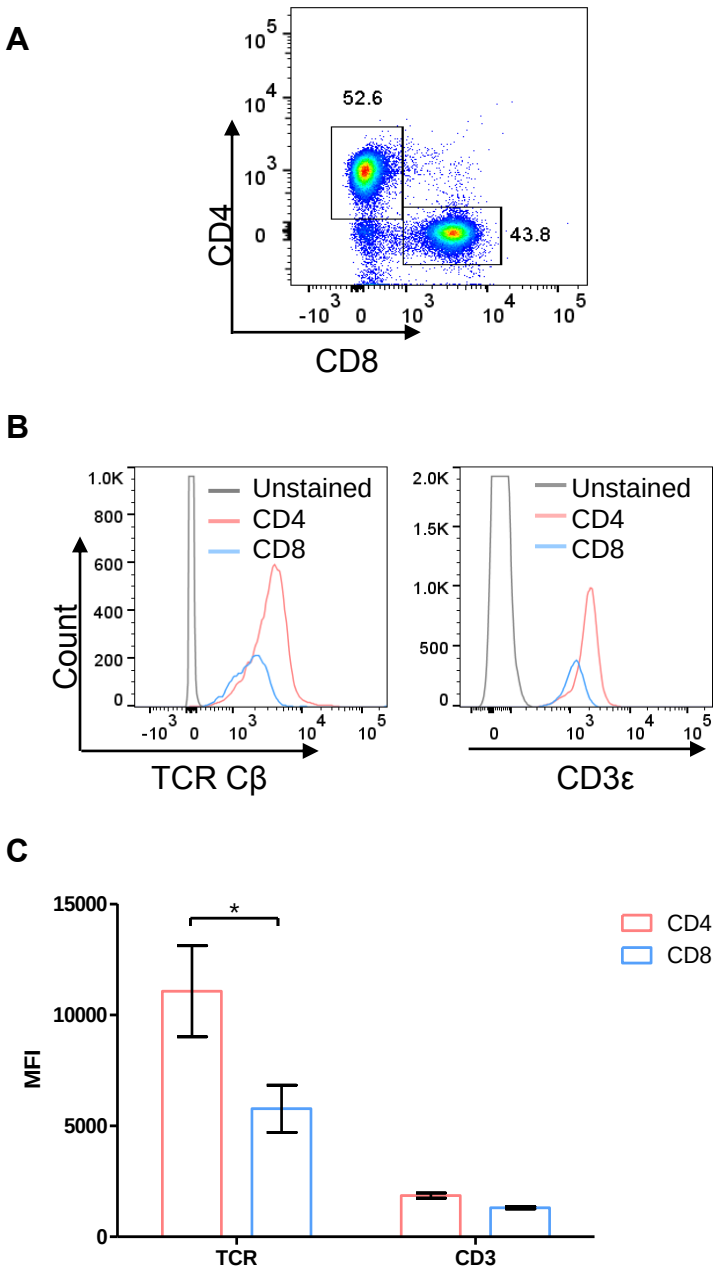

Figure 3.1 – Polyclonal CD4⁺ T cells express higher levels of endogenous TCR than CD8⁺ T cells. Single cell suspensions from spleen, LN, BM and liver were stained for CD4, CD8, TCR Cβ and CD3ε. (A) Representative plot showing CD4⁺ and CD8⁺ cells FACS gating used for TCR and CD3 expression analysis. (B) Representative plot of TCR and CD3 MFI levels in unstained controls, CD4⁺ and CD8⁺ T cells isolated from the above tissues. (C) Mean values (TCR n=8, CD3 n=2) showing significantly higher expression of TCR in CD4⁺ T cells compared to CD8⁺ T cells. (p=*≤0.05; unpaired t test; standard error of the mean (SEM) is plotted).

3.3. Higher levels of TCR associates with higher cytoplasmic Ca^{2+} concentration

Previous experiments showed that unmanipulated $CD4^+$ T cell express higher levels of TCR than $CD8^+$ T cells. To investigate whether this correlates with stronger TCR signalling we analysed calcium signalling in unmanipulated T cells. Ca^{2+} ions are universal second messengers in eukaryotic cells. Indeed after TCR engagement one of the earliest signalling events to take place is an increase in intracellular calcium concentration. This rise in concentration is caused by both calcium influx from the extracellular environment and calcium release from the ER.

To analyse the influx of calcium in the cytoplasm of T lymphocytes, cells were loaded with Indo-1 AM, a cell permeable dye that binds to calcium. The peculiarity of this dye is that its emission shifts from about 475 nm (Indo-1 Blue) in Ca^{2+} free conditions to about 400 nm (Indo-1 Violet) when it is saturated with calcium. The different emission spectra MFIs and their shift can be measured in real time by flow cytometry. Similarly the ratio between the calcium-bound to calcium-unbound dye and its moving median can be calculated. Thus the MFI of the dye in the calcium bound and unbound state can be used to indirectly quantify the intracellular calcium concentration. Figure 3.2 shows how the emission spectrum of the dye changes upon addition of a stimulus, and how the two emission spectra can be plotted and their ratio and its moving median calculated.

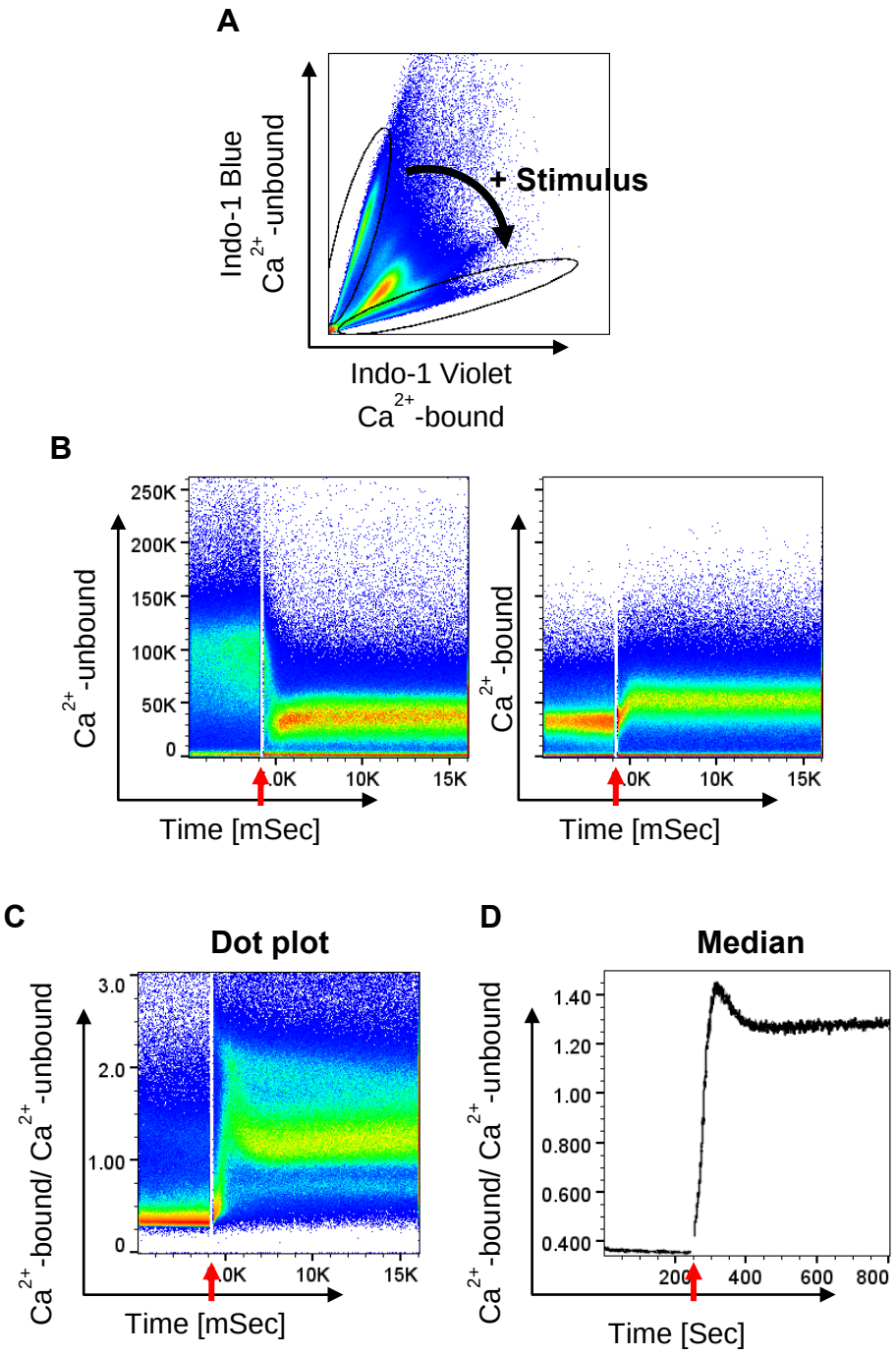

Figure 3.2 – Indo-1 AM dye is used to study intracellular calcium levels. Indo-1 AM is a UV excitable, cell-permeant, ratiometric calcium indicator. (A) The emission spectrum of the dye changes from 475 nm to 400 nm when the dye becomes saturated with calcium. (B) The changes in the two emission spectra can be monitored overtime and (C) their ratio can be calculate and plotted as a function of time. (D) The ratio's moving median can be calculated and it can be used to indirectly analyse intracellular calcium concentration. The red arrow indicates addition of the stimulus. Plots are representative of 5 independent experiments.

$CD4^+$ and $CD8^+$ T cells were MACS purified and loaded with Indo-1 AM dye as described in chapter 2, section 2.2.3 and section 2.4.6. Soluble anti-CD3 antibody was used for stimulation. Cells were acquired for 2-4 minutes to record cytoplasmic calcium baseline levels, after which the stimulus was added and data acquired for a further ~15 minutes. Plots in figure 3.3A are representative of the purity (typically ≥95%) of $CD4^+$ and $CD8^+$ populations used to run the assays. From each reaction the ratio of calcium-bound: calcium-unbound ratio can be calculated and plotted as moving average (figure 3.3B). The ability of both $CD4^+$ and $CD8^+$ T cells to upregulate intracellular calcium concentration after stimulation was assessed by measuring the change in the ratio of Ca^{2+}-bound:$Ca2^+$-unbound before and after the addition of the stimulus (figure 3.3 C). Stimulation with culture medium doesn't trigger calcium influx or calcium release from intracellular storages and the intracellular calcium concentration remains unchanged as shown but the similar values of Ca^{2+}-bound:$Ca2^+$-unbound ratio before and after stimulation. Addition of the PKC-activator PMA causes a rapid increase in intracellular calcium concentration which is similar in both $CD4^+$ and $CD8^+$ cells, and it is shown by the increase in Ca^{2+}-bound:$Ca2^+$-unbound ratio. High affinity stimulation with 10 µg/ml anti-CD3 antibody only marginally causes an increase in intracellular calcium concentration. Lowering the concentration of anti-CD3 antibody to 5 µg/ml doesn't give any detectable change in cytoplasmic Ca^{2+} concentration. The average changes in calcium ratio are summarised in 3.1 below.

	10 µg/ml anti-CD3		**5 µg/ml anti-CD3**		**PMA**		**Culture medium**	
	$CD4^+$	**$CD8^+$**	**$CD4^+$**	**$CD8^+$**	**$CD4^+$**	**$CD8^+$**	**$CD4^+$**	**$CD8^+$**
Unstimulated	0.39	0.4	0.33	0.35	0.34	0.38	0.37	0.36
Stimulated	0.67	0.54	0.41	0.36	1.62	1.78	0.4	0.38

Table 3.1 – Average changes in intracellular calcium concentration ratios

Analysis of Indo-1 Violet's MFI, the Ca^{2+}-bound form of the dye, allowed us to study the changes in cytoplasmic concentration of $CD4^+$ and $CD8^+$ T cells. The first ~12 minutes of the analysis were divided into 7 sections: from time 0 to the addition of the stimulus

(section 0), followed by 6 100-seconds-long sections (1-6); this allowed us to study the early signalling events occurring after stimulation (figure 3.3D). Although the kinetics of calcium upregulation and the ability to upregulate intracellular calcium are similar between the two populations of T lymphocytes, the cytoplasmic calcium concentration of $CD4^+$ T cells is higher to that of $CD8^+$ T cells, both at baseline and after stimulation (figure 3.3E). The average Ca^{2+}-bound (Indo-1 Violet) MFI in $CD4^+$ T cells at baseline is 30400, whereas in $CD8^+$ T cells the same dye has an average MFI of 16416. After stimulation both $CD4^+$ and $CD8^+$ T cells upregulate their intracellular calcium levels according to the strength of stimulation: the stronger the stimulus the higher the increase in cytoplasmic calcium. Indeed PMA causes the highest increase in Indo-1 Violet MFI, in both $CD4^+$ and $CD8^+$ cells, followed by stimulation with 10 µg/ml of anti-CD3 antibody. Stimulation with 5 µg/ml anti-CD3 antibody or PBS does not cause a detectable increase in Indo-1 Violet MFI. Overall even after PMA stimulation, the highest intracellular calcium concentration reached by $CD8^+$ T cells is lower than that of $CD4^+$ cells stimulated with either 10 µg/ml of anti-CD3 or PMA.

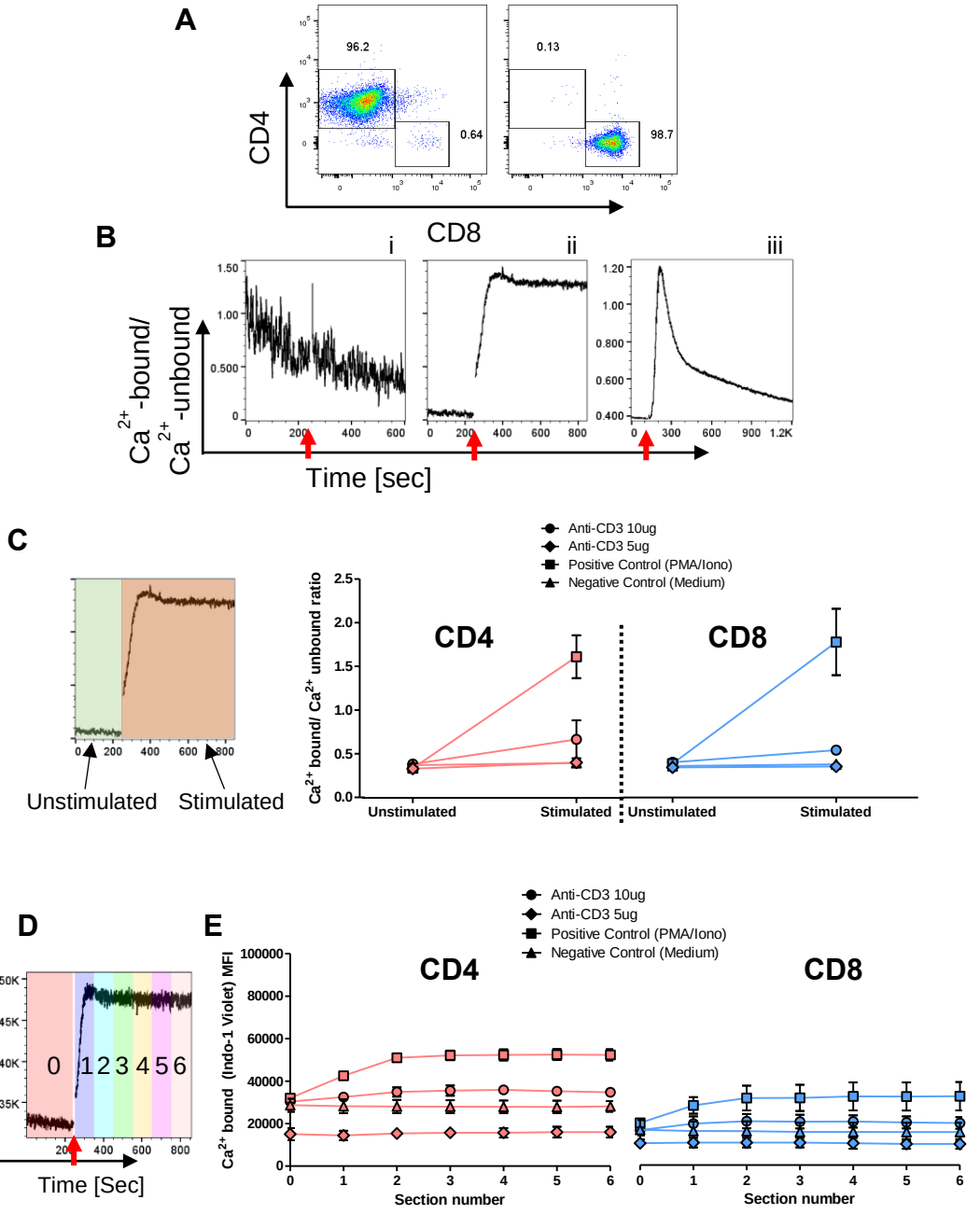

Figure 3.3 – CD4⁺ T cells exhibit higher intracellular Ca^{2++} concentration compared to CD8⁺ T cells after stimulation. (A) Representative plot of MACS sorted CD4⁺ and CD8⁺ T cells used for calcium analysis. (B) Representative moving averages from negative (i; culture medium), positive (ii; PMA/Ionomycin) and anti-CD3 stimulation (iii) are shown. The red arrow indicates the addition of the stimulus. (C) The moving average was used to calculate the change in Indo-1 Violet:Indo-1 Blue ratio before and after the addition of the stimulus. Summary data for CD4⁺ and CD8⁺ cells is shown on the right. (D) Each stimulation was split into 7 time windows. (E) The MFI for Indo-1 Violet (Ca^{2+}-bound) was calculated for each section for both CD4⁺ and CD8⁺. Data from 5 independent experiments. SEM is shown.

3.4. $CD4^+$ and $CD8^+$ T cells have similar kinetics of ERK phosphorylation

The ERK pathway is a major pathway induced by TCR stimulation at it plays an important role in the regulation of T cell activation and differentiation. TCR signalling leads to DAG activation, which in turns activates the guanine nucleotide-binding protein Ras. After its activation Ras activates Raf, which initiates MAP kinase phosphorylation and the MAPK signalling cascade, leading to ERK1/2 phosphorylation and activation. In previous experiments the kinetics of calcium flux were studied as representative of early TCR signalling events. Phosphorylation of ERK occurs downstream of calcium mobilisation and it can be used as a model for late TCR signalling events. Thus we investigated whether higher TCR expression in $CD4^+$ T cells translated into increased ERK phosphorylation following stimulation.

$CD4^+$ and $CD8^+$ T cells were MACS purified and stimulated with anti-CD3 antibody as described in chapter 2 section 2.2.3 and section 2.4.2. Cells were stimulated for 1, 5, 10, 15, 30, 45 and 60 minutes, or left unstimulated. Stimulation with PMA/Ionomycin for 15 minutes was used as positive control; PBS stimulation was used as negative control. Reactions were stopped with PFA and cell permeabilised for p-ERK staining with MeOH, as described in chapter 2, section 2.3.2. The antibody used for intracellular staining recognised both phospho-44 and phospho-42 ERK (Thr202/Tyr204).

The kinetics of ERK phosphorylation are similar between $CD4^+$ and $CD8^+$ T cells. Stimulation with PMA/Ionomycin gives a strong p-ERK signal with, on average, ≥80% of cells becoming p-ERK^+ after 15 minutes of stimulation. Anti-CD3 stimulation, albeit with a high concentration (50 µg/ml) of antibody, only gives marginal ERK phosphorylation (~30%) in both cell populations. The kinetics of phosphorylation are the same in $CD4^+$ and $CD8^+$ T cells, with the peak of ERK phosphorylation occurring after 15 minutes of stimulation. After this time point p-ERK levels are downregulated and quickly return to baseline values (figure 3.4B).

Similarly, the levels of p-ERK within the cell are comparable between $CD4^+$ and $CD8^+$ cells, as shown in figure 3.4C. Stimulation with PMA for 15 minutes causes more than a 9 fold increase in p-ERK MFI in both $CD4^+$ and $CD8^+$ cells (from 28.5 to 495.9 in $CD4^+$ and from 65.75 to 594 in $CD8^+$). Increase in p-ERK signal following stimulation with anti-CD3 is minimal, even at the peak of the stimulation (15 minutes), going from 28.5 and 65.75 to 96.25 and 125.9 in $CD4^+$ and $CD8^+$ cells respectively (figure 3.4C).

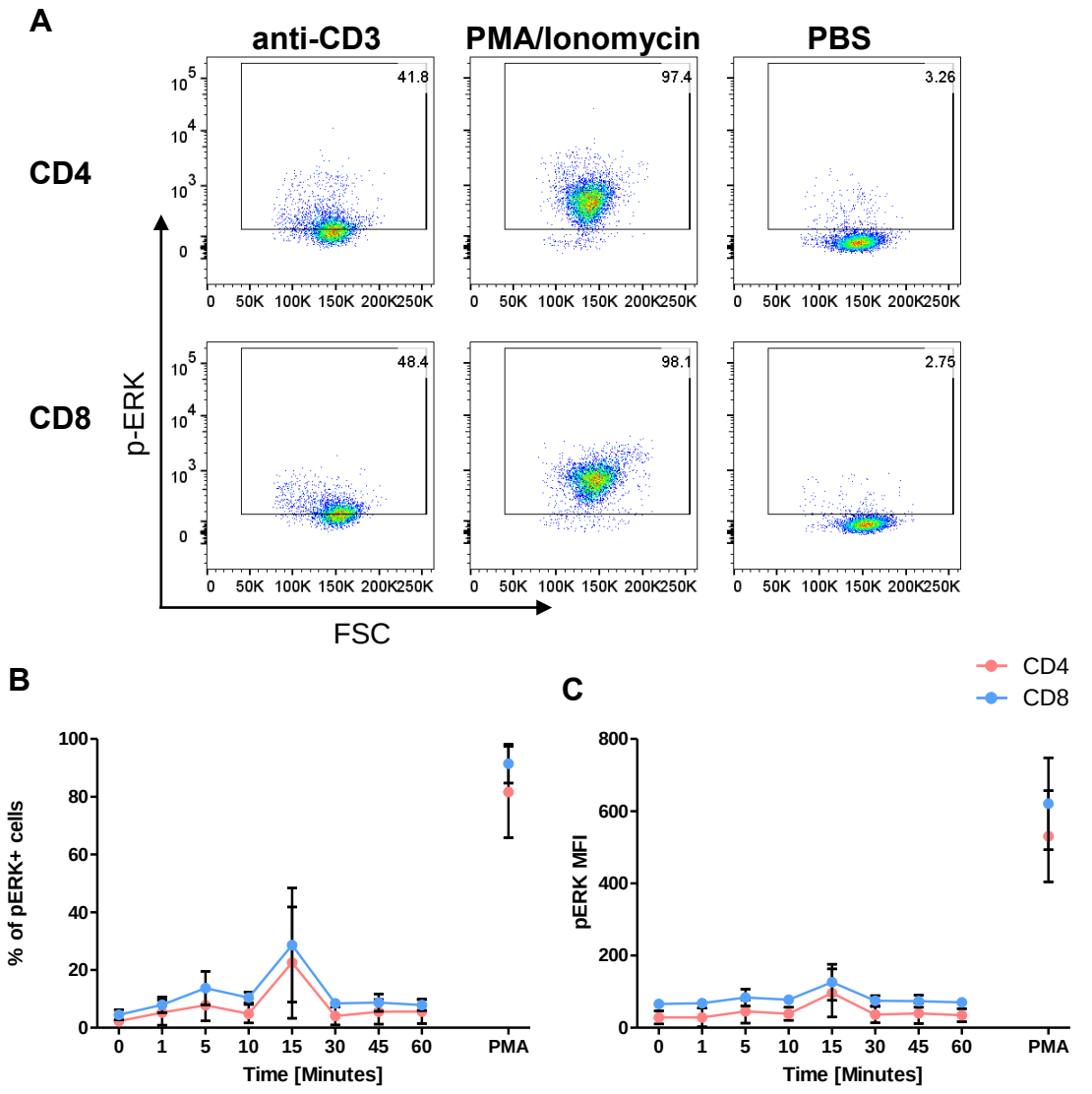

Figure 3.4 – ERK phospshorylation levels and kinetics are similar in CD4+ and CD8+ T cells. (A) Representative plots used to calculate p-ERK^+ % and p-ERK MFI are shown. (B) Summary data of p-ERK phosphorylation and (C) p-ERK MFI following stimulation is shown. Data from 2 independent experiments.

3.5. No difference in CD107a expression is seen between polyclonal $CD4^+$ T cells and polyclonal $CD8^+$ T cells

Previous experiments showed that $CD4^+$ T cells express higher levels of TCR compared to $CD8^+$ T cells. In addition preliminary data suggested that $CD4^+$ cells with increased TCR expression can be toxic *in vivo*, whereas $CD8^+$ T cells in the same setting are not. To assess whether higher TCR expression is associated with a higher cytotoxic potential, we decided to analyse the expression of the degranulation marker CD107a in both $CD4^+$ and $CD8^+$ T cells.

C57Bl/6 splenocytes were resuspended in complete RPMI 1640 medium supplemented with Golgi stop, Brefeldin A and anti-CD107a antibody. Cells were re-stimulated with anti-CD3/anti-CD28 beads, or PMA and ionomycin (positive control) or PBS (negative control) as described in chapter 2, section 2.4.1. Cells were stimulated for up to 4 hours with samples taken and reactions stopped at 5, 15, 30 minutes and 1, 1.5, 2, 3 and 4 hours.

Figure 3.5A shows a typical CD4 and CD8 gating used for subsequent CD107a analysis. Figure 3.5B shows the staining given by the IgG2ak isotype control, the CD107a staining control. Both at baseline at upon stimulation no statistically significant difference is seen in the percentage of $CD107a^+$ $CD4^+$ or $CD8^+$ T cells (figure 3.5C). On average 15.3% of resting $CD4^+$ T cells (PBS negative control) express CD107a, compared to 3.4% of $CD8^+$ T cells. Stimulation with the PKC-activator PMA, leads to a gradual increase of CD107a expression in both $CD4^+$ and $CD8^+$ T cells, which in both populations peaks at 4 hours from initial stimulation. At this time point 26% of $CD4^+$ T cells express CD107a, compared to 20% of $CD8^+$ T cells. The kinetics of CD107a expression after triggering of the T cells with anti-CD3/CD28 beads are different between the two T cell subsets. CD3/CD28 stimulation causes a rapid upregulation of CD107a in $CD4^+$ T cells and the percentage

of $CD4^+$ $CD107a^+$ cells peaks (29.25%) at 15 minutes post initial stimulation. On the other hand the peak (10.6%) of CD107a upregulation in $CD8^+$ T cell is reached at 1 hour after initial stimulation. The levels of CD107a expressed in the cells were also compared by looking at the MFI of CD107a (figure 3.5D). No difference in the MFI of CD107a was seen between $CD4^+$ and $CD8^+$ T cells ($CD4^+$ CD107a average MFI=100.6; $CD8^+$ CD107a average MFI=62.9). Similarly to the kinetics described above, after stimulation with CD3/CD28 beads, CD107a expression in $CD4^+$ T cells peaks at 15 minutes (MFI=126). $CD4^+$ stimulation with PMA doesn't lead to changes in CD107a MFI, the levels of which remain relatively stable overtime. In $CD8^+$ T cells CD3/CD28 stimulation causes a sharp upregulation of CD107a expression which is downregulated by 1.5 hours post initial stimulation. PMA stimulation in $CD8^+$ T cells causes a gradual increase in CD107a expression, which peaks at 4 hours post stimulation. PMA-stimulated $CD8^+$ T cells express the highest CD107a levels (CD107a MFI=133) observed in all of the assays.

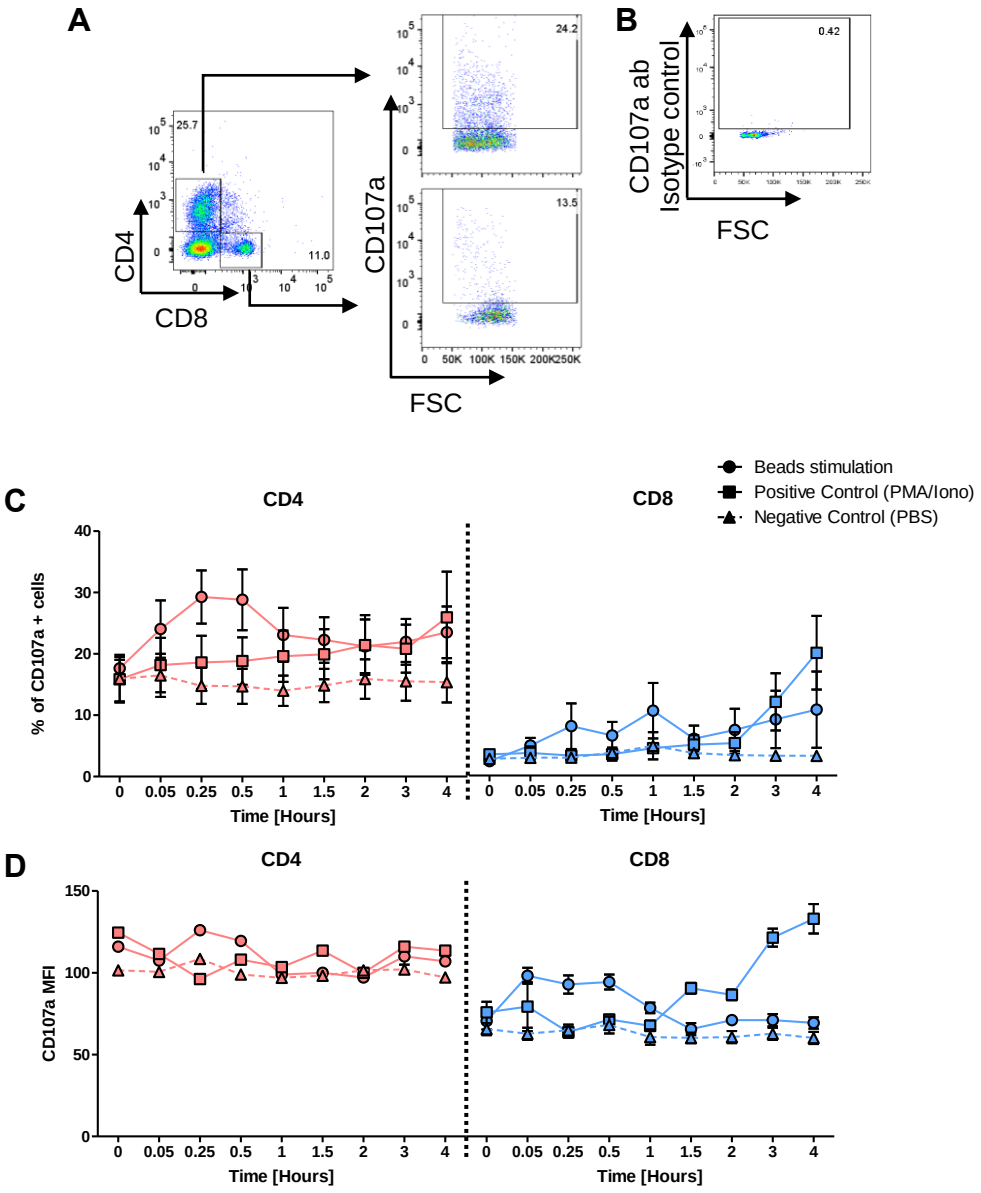

Figure 3.5 – CD4⁺ and CD8⁺ T cells express similar levels of CD107a at resting state and upon polyclonal stimulation. (A) Splenocytes were stained for CD4 and CD8 and their expression of CD107a was analysed by flow cytometry. (B) The isotype IgG2ak was used as control for CD107a staining. (C) The percentage of CD4⁺ and CD8⁺ T cells expressing the degranulation marker CD107a, at rest and upon stimulation is shown. (D) CD107a MFI of CD4⁺ and CD8⁺ T cells at rest and upon stimulation is shown. Mean data + SEM from 2 independent experiment are plotted.

3.6. CD3-engineered CD4$^+$ T cells have higher levels of TCR expression compared to CD3-engineered CD8$^+$ T cells

Following characterisation of non-manipulated CD4$^+$ and CD8$^+$ T cells, we wanted to investigate which changes, if any, occur in T lymphocytes following CD3 overexpression.

Previous experiments showed that naïve, resting CD4$^+$ T cells express higher levels of TCR compared to their CD8$^+$ counterparts. Firstly we the wanted to study whether this difference was maintained upon transduction with additional CD3 genes. CD4$^+$ and CD8$^+$ splenocytes were MACS sorted, activated and transduced as described in chapter 2, sections 2.2.3 and 2.2.4, and their TCR levels were analysed by flow cytometry at day 3, 5 and 7.

Purified CD4$^+$ and CD8$^+$ cells were transduced with either the control-GFP vector or the CD3-GFP vector. GFP was used as a marker for transduction which allowed us to compare both transduced and untransduced cells. Cell's purity was typically ≥95% for both CD4$^+$ and CD8$^+$ populations (figure 3.6A); transduction efficiency was more variable, with CD4$^+$ normally having a higher transduction efficiency compared to CD8$^+$, in both cases typical transduction efficiency was over 50% (figure 3.6B). Transduction with the control-GFP vector did not alter TCR expression and both GFP- (untransduced) and GFP+ cells (transduced) expressed similar levels of TCR (figure 3.6C; summary data in figure 3.6D). However upon transduction with the CD3-GFP vector TCR expression increased by 2 to 2.5 folds in both CD4$^+$ and CD8$^+$ cells, as shown in figure 3.6D. The statistically significant increase in TCR expression after CD3 transduction was maintained for up to a week post transduction. TCR levels were similar between day 3 and day 5 post transduction. At day 7 lower TCR levels were seen in all cell populations.

The difference between TCR levels in CD4$^+$ and CD8$^+$ T cells was maintained even after transduction with the CD3-GFP vector: transduced CD4$^+$ cells still expressed higher

levels of TCR compared to CD8⁺ T cells transduced with the same vector, up to 7 days post transduction (figure 3.6D).

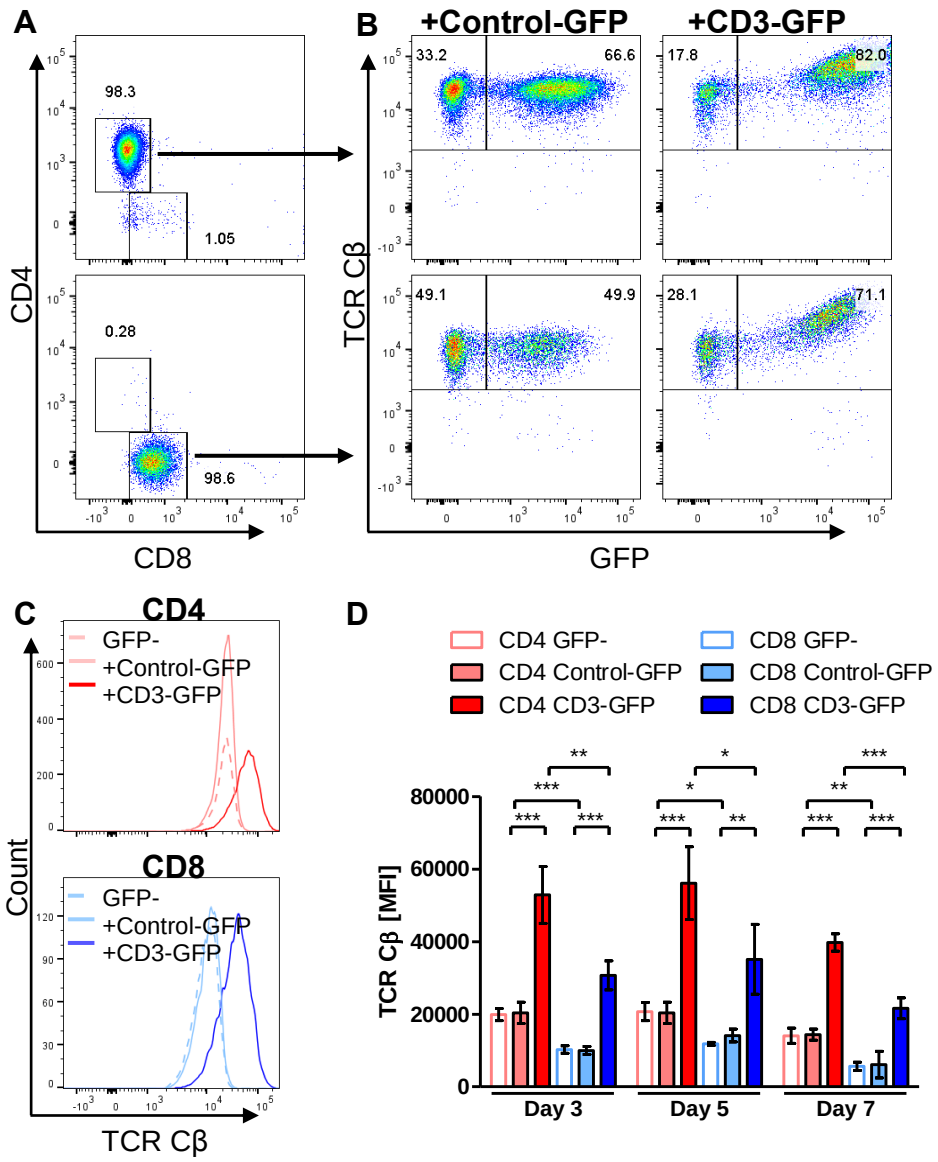

Figure 3.6 – Transduction with the CD3-GFP retroviral vector increases TCR expression in both CD4⁺ and CD8⁺ T cells. (A) Representative plot of MACS purified CD4⁺ and CD8⁺ cells used for transduction. (B) Purified cells were transduced with either the control-GFP or the CD3-GFP retroviral vector, and their transduction efficiency and TCR expression measured by flow cytometry. (C) Histograms showing TCR expression increase in both CD4⁺ and CD8⁺ T cell transduced with the CD3-GFP vector, compared to cells transduced with the control-GFP vector, or non-transduced (GFP-). (D) TCR levels were analysed at day 3, 5 and 7 post transduction; mean values from 3 independent experiments is shown. (p=* ≤0.05; ** ≤0.01; ***≤0.001; unpaired t test. SEM is shown).

3.7. CD3 overexpression does not enhances in vitro proliferation in $CD4^+$ or $CD8^+$ T cells

In vivo TCR signals from contact with self-ligands induce anti-apoptotic signals to promote survival of naïve T cells in a resting state. Similarly *in vitro* T cells don't survive unless a stimulation signal is provided. Increasing the density of the TCR-CD3 complex on the cell surface may overcome the need for such extrinsic. TCR-CD3 complexes may form micro clusters on the cell's surface which may provide the tonic signalling needed for survival. To investigate whether this was the case, we monitored cell's numbers overtime (up to 7 days post transduction).

$CD4^+$ and $CD8^+$ T cells were purified and activated for transduction as described in chapter 2, section 2.2.3. Cell numbers were recorded on day 0 (transduction day) and day 3, 5 and 7 post transduction. At each time point cell number was plotted as variation from day 0, which was considered to be 100%.

No significant differences were seen between $CD4^+$ and $CD8^+$ cells transduced with either the control-GFP or the CD3-GFP vector (figure 3.7). Three days post transduction all 4 different populations expanded. $CD4^+$ T cells expanded to a lesser extent compared to $CD8^+$ T cells: the former population typically doubled in size, whereas the latter population generally expanded by 3.5-4 folds. The differences in cell numbers however weren't significant. By day 5 post transduction all four populations contracted and cell numbers decreased reaching similar or lowers figures to those at day 0. Between day 5 and day 7 no change in cell numbers was seen in any of the four different populations. Average values for each population at the 4 different time points are shown in 3.2 below (n=8 $CD4^+$ cells; n=2 $CD8^+$ cells).

		Day 0	Day 3	Day 5	Day 7
CD4⁺	**Control-GFP**	100	333.46	72.24	95.94
	CD3-GFP	100	324.08	85.37	82.99
CD8⁺	**Control-GFP**	100	387.5	74	64.5
	CD3-GFP	100	417.5	47	46

Table 3.2 – Changes in cell numbers post transduction.

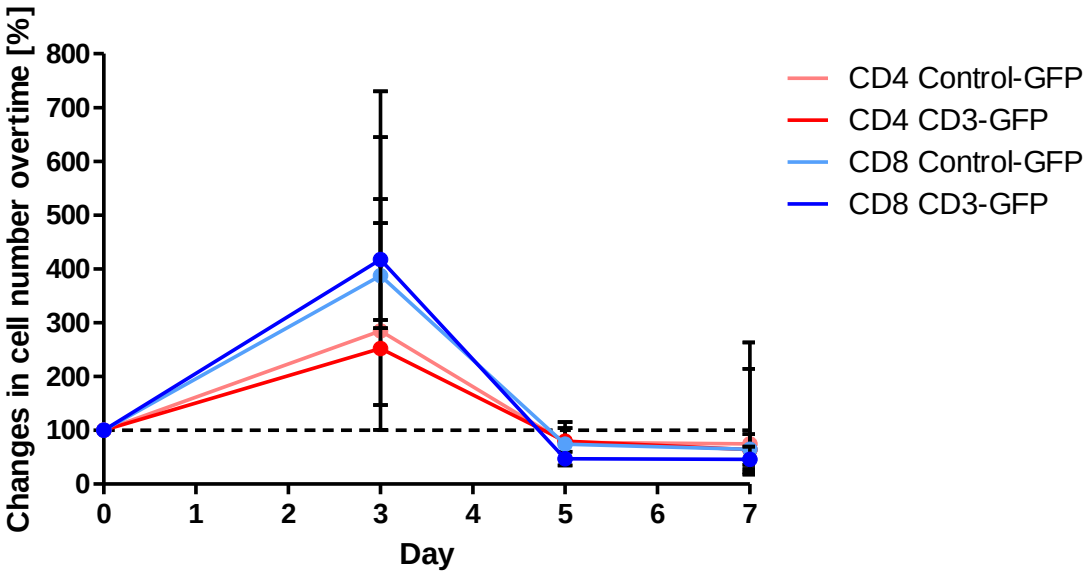

Figure 3.7 – Overexpression of CD3 does not enhances *in vitro* proliferation in neither CD4⁺ nor CD8⁺ cells following stimulation with anti-CD3/CD28 beads. Purified CD4⁺ and CD8⁺ T cells were transduced with either the control-GFP or the CD3-GFP vector and their cell numbers (cell/ml) were monitored at day 3, 5 and 7 post transduction (day 0). On day -1 cells were stimulated with anti-CD3/CD28 beads. Data is plotted as a variation from the concentration at day 0 (100%). Data from 8 independent experiments (CD4⁺) or 2 independent experiments (CD8⁺).

3.8. Overexpression of CD3 in $CD4^+$ and $CD8^+$ polyclonal T cells does not alter their activation status or phenotype

Previous experiments showed that both naïve and CD3-transduced $CD4^+$ T cells express higher levels of TCR compared to naïve and CD3-transduced $CD8^+$ T cells. This was not associated with an advantage in *in vitro* persistence as cell numbers were similar overtime. However previous experiments indicated that polyclonal $CD4^+$ T cells overexpressing CD3 can be toxic *in vivo*, whereas $CD8^+$ cells with the same modification are not. Thus *in vitro* studies were performed to investigate the phenotype and activation status of CD3-overexpressing $CD4^+$ and $CD8^+$ T cells overtime.

$CD4^+$ and $CD8^+$ splenocytes were purified and transduced as described in chapter 2, section 2.2.3 and section 2.2.4, and their CD25, CD69, CD62L and CD127 expression monitored overtime by flow cytometry.

CD25 is the IL-2 receptor α chain, and it is expressed on activated T cells. CD25 expression at day 3 following transduction is similar between GFP^- (activated but not transduced) $CD4^+$ and $CD8^+$ T cells and $CD8^+$ cells transduced with either the control-GFP or the CD3-GFP. At this time point a trend showing higher CD25 expression in both $CD4^+$ transduced populations compared to the other 4 populations was seen. CD25 expression increased in both GFP^- populations and in GFP^+ $CD8^+$ T cells by day 5, reaching similar levels to those in $CD4^+$ T cells. At day 7 no significant difference in CD25 expression was seen among the different populations. Overall CD25 expression was stable in $CD4^+$ GFP^+ cells between day 3 and day 5; it increased in GFP^- cells and GFP^+ $CD8^+$ cells between the same two time points; and slightly decreased in all populations by day 7 (figure 3.8A).

CD69 is another activation marker expressed on T cells. In these *in vitro* settings the expression pattern of CD69 follows that of CD25. No significant difference was seen in

CD69 expression among the six populations at any of the analysed timepoints (figure 3.8B).

The homing receptor CD62L and the IL-7 receptor α chain CD127 were used to divide the cells into naïve-like, memory and effector populations, as shown in figure 3.8C. Naïve-like cells were so called as the cells were previously activated with anti-CD3/CD28 for transduction, and thus they were not strictly naïve; they were identified as $CD127^+$ $CD62L^+$. Effector cells were identified as $CD127^-$ $CD62L^-$; memory cells were characterised as $CD127^+$ $CD62L^-$.

The percentages of naïve-like, effector and memory cells were similar among the six different populations, but different across the three time points. At day 3 post transduction the majority of the cells presented with an effector phenotype, followed by naïve-like cells and memory cells. Two days later (day 5 post transduction) the percentage of effector cells had expanded in all populations, whereas the portion of naïve-like cells had decreased to similar levels of that of memory cells. By day 7 post transduction the effector population had expanded further all six populations. The percentage of memory cells also increase in the four transduced populations, whereas is remained constant in the GFP^- cells. Naïve-like cells accounted for the lower percentage of differentiated cells at day 7.

The level of TCR expression in the three differentiated population was also analysed to determine whether a trend in TCR expression was associated with a specific differentiation profile. However no difference in TCR expression was seen among the three differentiated populations across the three time points, as shown in figure 3.9. The kinetics of TCR expression were similar between the 3 differentiated subsets in all

populations, with relative constant TCR expression levels between day 3 and day 5, and decrease in TCR expression at day 7.

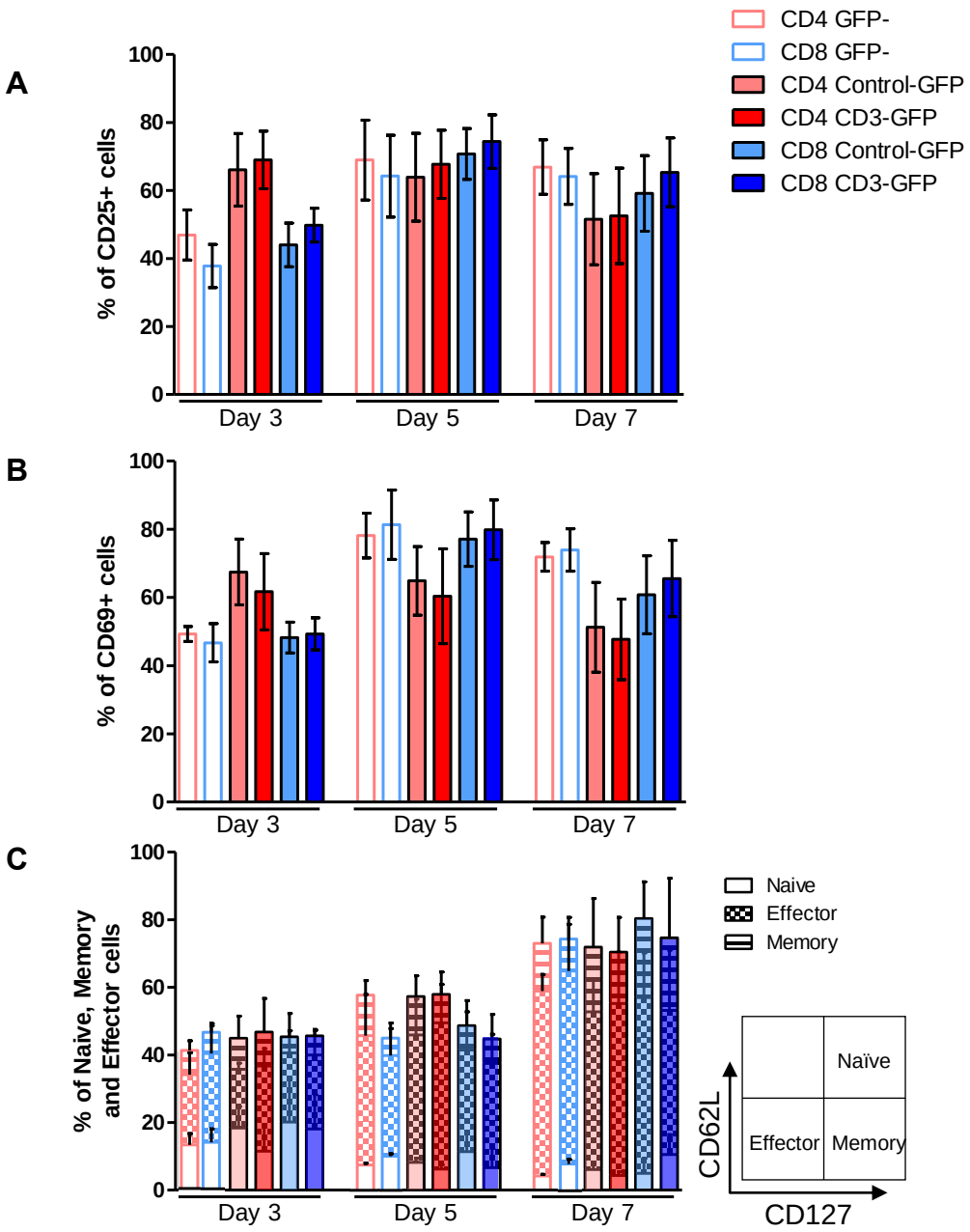

Figure 3.8 – Transduction with the CD3-GFP vector does not alter CD25 and CD69 expression or the differentiation status of CD4⁺ and CD8⁺ T cells, after stimulation with anti-CD3/CD28 beads. Untransduced, control-GFP transduced and CD3-GFP transduced CD4⁺ and CD8⁺ T cells express similar levels of both CD25 (A) and CD69 (B), following stimulation with anti-CD3/CD28 beads at day -1. Stimulus was removed on day 3. (C) Similarly their differentiation status based on CD127 and CD62L expression does not change upon transduction with either one of the vectors, and after stimulation. Mean values + SEM from 3 independent experiments are plotted.

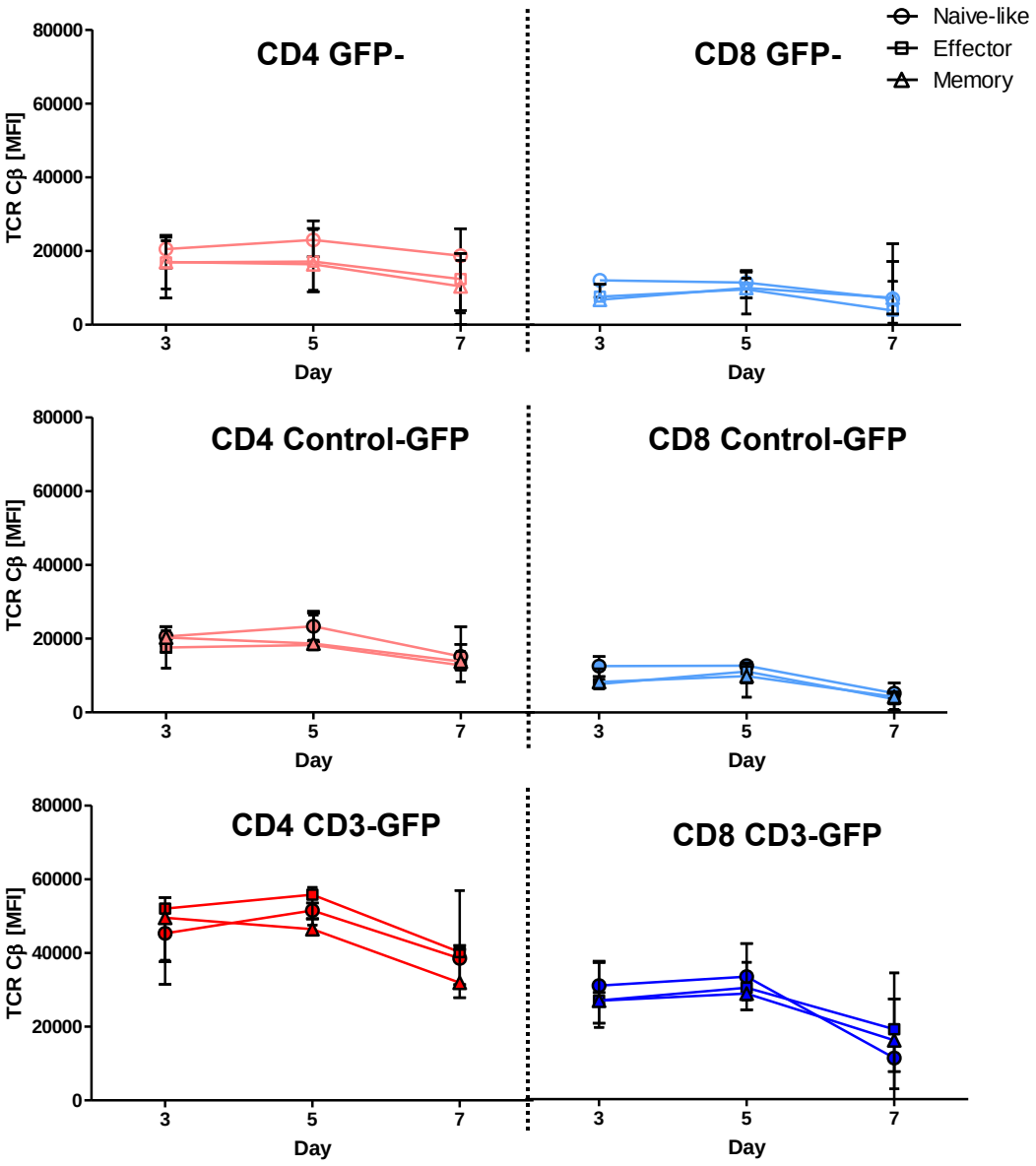

Figure 3.9 – Naïve-like, effector and memory subsets express the same level of TCR. Analysis of naïve-like, effector and memory T cells show that all 3 differentiated subsets express similar levels of TCR, independently of transduction status (non-transduced, control-GFP transduced or CD3-GFP transduced), following stimulation with anti-CD3/CD28 beads at day -1. Stimulus was removed on day 3. Moreover the kinetics of TCR expression are the same across the 3 differentiated subsets and across the 6 populations. Mean values + SEM from 2 independent experiments are shown.

3.9. Increased TCR expression is not associated with improve effector function in polyclonal CD4$^+$ T cells

To determine whether the increased levels of TCR on CD4$^+$ cells transduced with the CD3-GFP vector compared to control-GFP transduced CD4$^+$ cells has a functional implication, we examined the triggering threshold and cytokine (IL-2 and IFNγ) production of transduced CD4$^+$ cells.

Polyclonal CD4$^+$ splenocytes were purified and transduced as described in chapter 2, sections 2.2.3 and 2.2.4. Seven days post transduction (8 days post initial activation) the cells were restimulated for 4 hours or overnight with plate-bound anti-CD3 antibody, or PMA/ionomycin or left unstimulated, as described in chapter 2, section 2.4.3. At the end of the stimulation the supernatant was collected and analysed by ELISA; the cells from the 4 hours restimulation were also harvested and analysed for cytokine production by flow cytometry. Representative FACS analysis from one experiment is shown in figure 3.11A.

Contrary to what we expected, CD4$^+$ cells overexpressing CD3 and TCR do not show lower triggering threshold compared to control-GFP transduced CD4$^+$ cells. On the other hand increased TCR density seems to be detrimental to cell activation and cytokine production. Indeed CD3-GFP transduced cells produce significantly less IL-2 compared to control-GFP transduced cells in 4 out of the 5 tested, anti-CD3 antibody concentrations for 4 hours restimulation. IFNγ production is similar between the two CD4$^+$ populations after 4 hours restimulation (figure 3.10A). After overnight stimulation IL-2 production follows the same trend seen in the 4 hours restimulation, albeit more IL-2 is produced. Control-GFP transduced cells produce more cytokine compared to CD3-GFP transduced cells, with a significant difference seen at the lowest, tested concentration of anti-CD3 (0.01 μg/ml). More IFNγ is produced during overnight stimulation compared to the 4

hours stimulation, but no notable differences between the two populations of transduced $CD4^+$ cells are seen (figure 3.10B).

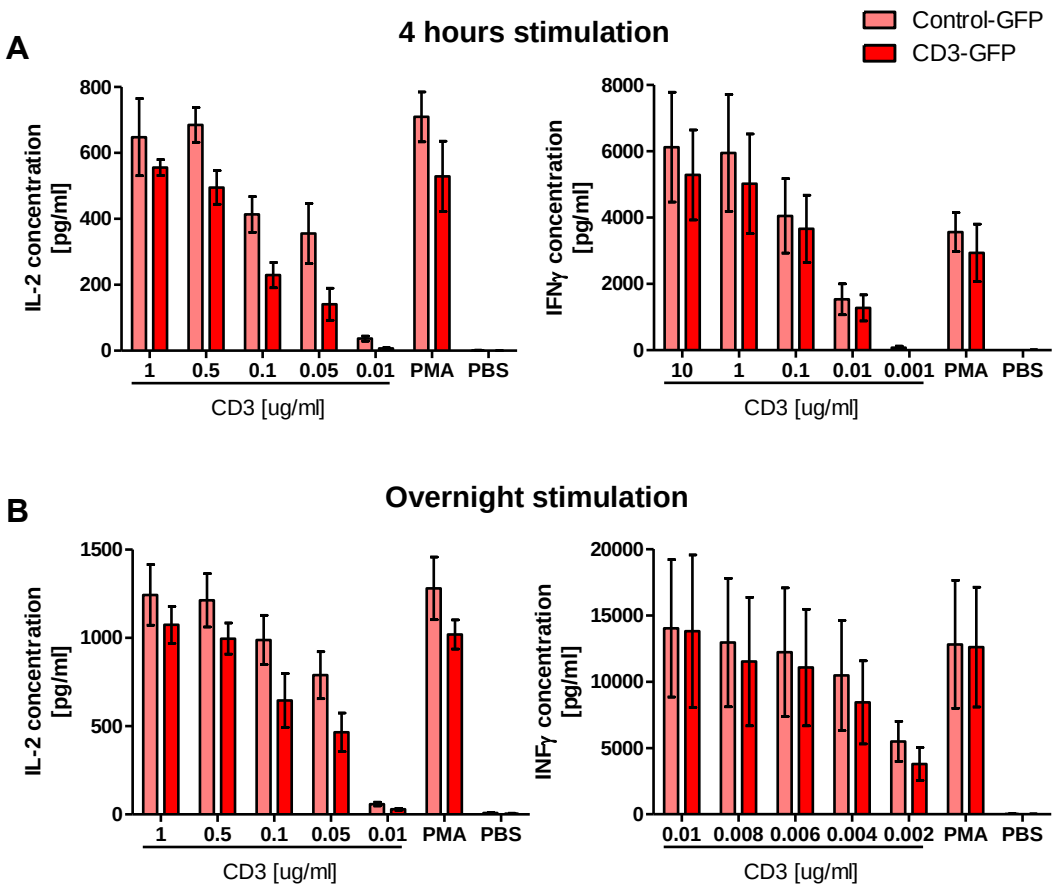

Figure 3.10 – Transduction with the CD3-GFP vector does not increase $CD4^+$ T cells functional avidity - ELISA. No statistically significant difference in IL-2 and IFNγ production after (A) 4 hours or (B) overnight polyclonal stimulation (with plate-bound anti-CD3 antibodies), by control-GFP and CD3-GFP transduced $CD4^+$ T cells was seen (as measured by ELISA). The number of cells in each well was adjusted based on the transduction efficiency, so to have 1 x 10^5 transduced cells (GFP^+) in each well. Data from 3 independent experiments, each re-stimulation was performed in duplicates. SEM is plotted. Two-way ANOVA statistical analysis was performed and no difference was determined to be statistically significant.

Intracellular (IC) cytokine staining after 4 hours stimulation showed similar results to those seen by ELISA for both IL-2 and IFNγ production. No significant differences were seen in either IL-2 or IFNγ production, with generally higher percentages of IL-2^+ or IFNγ^+ cells in the control-GFP $CD4^+$ population (figure 3.11B and C).

The lack of difference in IL-2 and IFNγ production between the two populations was seen despite CD3-GFP transduced cells expressing higher levels of TCR compare to control-GFP transduced $CD4^+$ cells, both at baseline and upon stimulation (figure 3.11D).

Stimulation through the TCR-CD3 complex is known to cause TCR downregulation. Indeed TCR downregulation upon stimulation was observed in both $CD4^+$ populations in these assays. The extent of TCR downregulation was proportional to the strength of stimulation: the stronger the stimulation, the greatest the TCR downregulation. For example cells stimulated with 10 μg/ml of anti-CD3 antibody almost completely downregulate their TCR levels; T cells stimulated with the lowest concentration of anti-CD3 (0.001 μg/ml) have TCR levels that are comparable to the TCR levels seen in unstimulated $CD4^+$ cells (PBS negative control) (figure 3.11D).

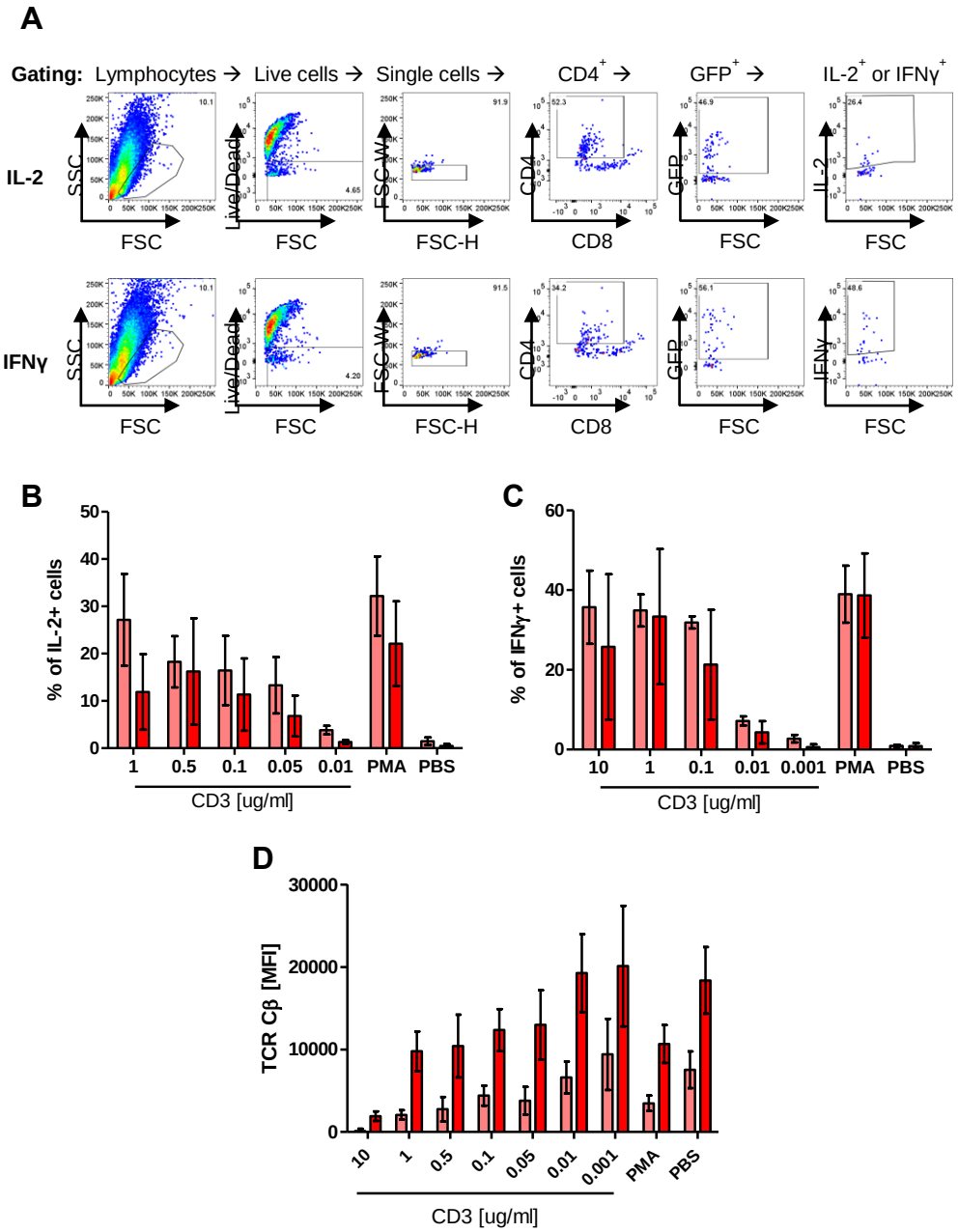

Figure 3.11 – Transduction with the CD3-GFP vector does not increase CD4⁺ T cells functional avidity – IC cytokine staining. (A) The gating strategy for IL-2 and IFNγ expression analyses are shown. IL-2 (B) and IFNγ (C) production after 4 hours polyclonal stimulation with plate-bound anti-CD3 antibody was measured by IC cytokine staining. The number of cells in each well was adjusted based on the transduction efficiency, so to have 1 x 10^5 transduced cells (GFP^+) in each well. (D) TCR downregulation following anti-CD3 stimulation was analysed by flow cytometry. Data from 3 independent experiments, each stimulation was performed in duplicates. SEM is shown.

3.10. Increased TCR expression is not associated with improved CD4$^+$ antigen-specific effector functions

Since transduction with the CD3-GFP vector did not alter cytokine production, nor the triggering threshold of polyclonal CD4$^+$ cells restimulated with anti-CD3 antibody, we sought to investigate whether increased TCR expression improves functional avidity in the context of antigen-specific restimulations.

CD4$^+$ splenocytes were purified and co-transduced with the MHC-II restricted TRP1-TCR vector and the control-GFP or the CD3-GFP vector as described in chapter 2, sections 2.2.3 and 2.2.4. Seven days post transduction (8 days post initial activation) the cells were restimulated overnight with peptide-loaded splenocytes, or PMA and ionomycin, as described in chapter 2, section 2.4.4. At the end of the stimulation the cells were harvested and analysed for cytokine production by flow cytometry. Representative FACS analysis from one experiment is shown in figure 3.12A.

On restimulation day, the expression levels of the TRP1-TCR were analysed in both co-transduced populations. The β chain used in the TRP1-TCR complex is the murine β14; thus anti-Vβ14 antibodies were used to indirectly assess TRP1-TCR expression. TRP1-TCR + CD3-GFP double transduced CD4$^+$ cells expressed higher levels of the Vβ14 chain compared to TRP1-TCR + control-GFP transduced cells, before restimulation (Figure 3.12B). On average TRP1-TCR + CD3-GFP transduced cells expressed 5 folds more Vβ14 compared to the control transduced population. TRP1-TCR downregulation following peptide stimulation was also analysed, and the data from the two experiments is summarised in figure 3.12C. At all stimulation conditions TRP1-TCR + CD3-GFP cells expressed higher levels of Vβ14 compared to TRP1-TCR + control-GFP transduced cells. However contrary to what we observed during polyclonal stimulation, no TCR downregulation correlating with the strength of the stimulation was observed, in neither one of the populations. Peptide stimulation of the TRP1-TCR + control-GFP co-transduced cells caused a small decrease in TCR surface expression, compared to the

stimulation with the irrelevant peptide (pNP_{366}). No Vβ14 down modulation was seen in the TRP1-TCR + CD3-GFP co-transduced population, at any of the tested stimulation conditions.

Despite higher TRP1-TCR expression in the CD3-GFP transduced cells, no difference in functional avidity (cytokine production or triggering threshold) was seen between the two populations of $CD4^+$ transduced cells. Both populations demonstrated IL-2 and IFNγ production both all tested TRP1-peptide concentrations and after stimulation with PMA and ionomycin. Less than 1% of the cells responded to stimulation with pNP_{366} loaded cells.

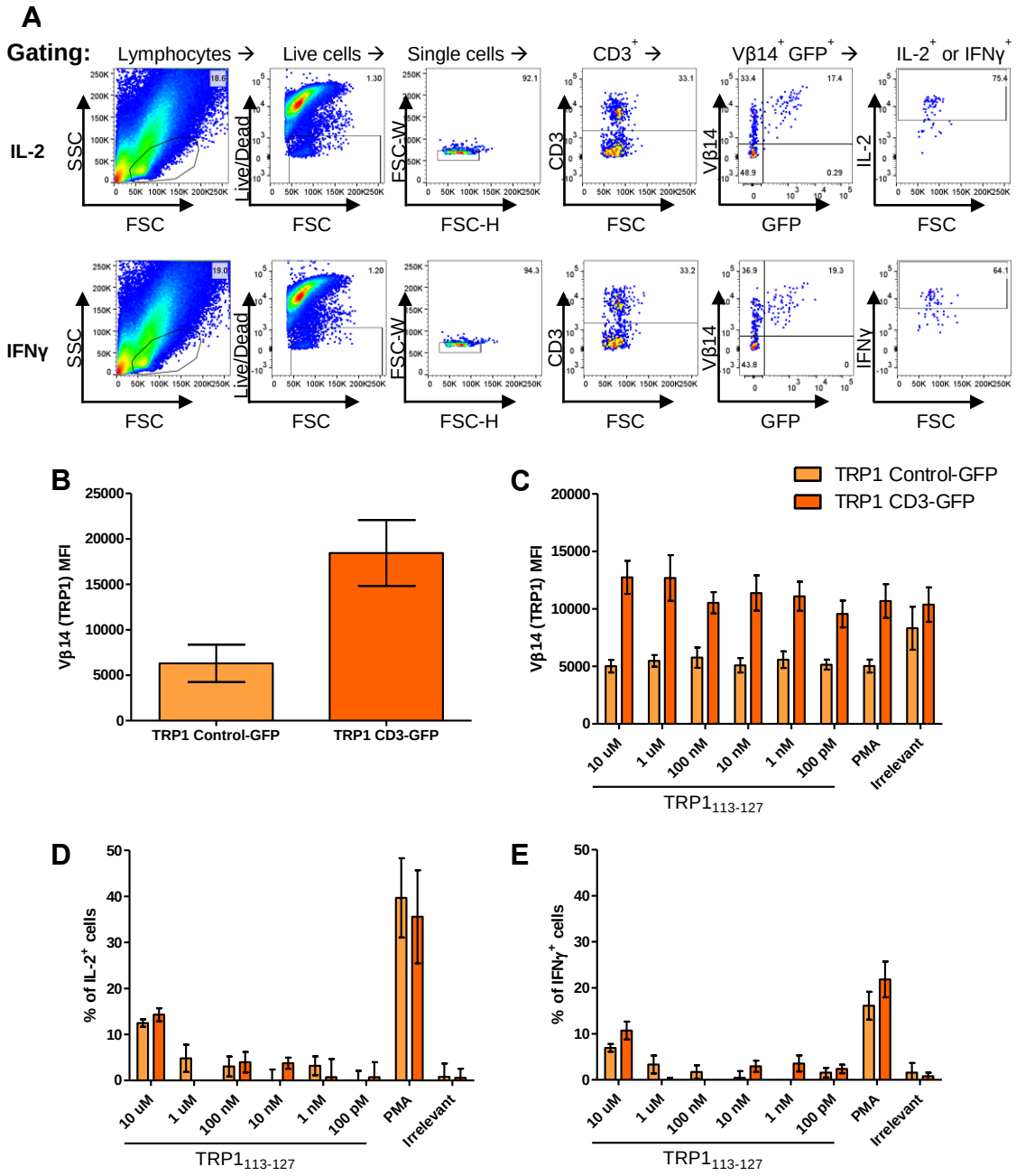

Figure 3.12 – TRP1-control and TRP1-CD3 transduced CD4⁺ T cells do not show differences in functional avidity. (A) The gating strategy for IL-2 and IFNγ expression analysis are shown. (B) The expression TRP1-TCR before restimulation was measured using an anti-Vβ14 antibody. (C) TCR expression levels following stimulation with TRP1-loaded splenocytes was analysed by flow cytometry. The number of cells in each well was adjusted based on the transduction efficiency, so to have 1 x 10^5 double transduced cells (Vβ14⁺ GFP⁺) in each well, and 1 x 10^5 stimulator cells. (D) IL-2 and (E) IFNγ production after overnight stimulation was measured by IC cytokine staining. Data from 2 independent experiments, each experiment was performed in duplicates. SEM is shown.

3.11. Summary and Discussion

Preliminary data from our laboratory showed that $CD4^+$ T cells overexpressing endogenous TCR can become toxic when adoptively transferred *in vivo*. The aim of the experiments described in this chapter was to phenotype $CD4^+$ and $CD8^+$ cells both in their unmanipulated state and after transduction with either the control-GFP or the CD3-GFP vectors.

Firstly, phenotypic and functional analysis of unmanipulated $CD4^+$ and $CD8^+$ cells was carried out. These experiments showed that resting $CD4^+$ T cells isolated from spleen, inguinal lymph nodes, bone marrow and liver of untreated C57Bl/6 mice, express higher levels of surface TCR compared to their $CD8^+$ counterparts, as demonstrated by flow cytometry (figure 3.1). Typically $CD4^+$ T cells express 1.5 fold more TCR compared to $CD8^+$ T cells; the same difference in TCR expression was maintained even after transduction with the CD3-GFP vector. Transduction with the control-GFP vector did not alter TCR expression, and its levels are comparable to that of untransduced (GFP^-) cells (figure 3.6). Both $CD4^+$ and $CD8^+$ T cells have the ability increase TCR expression by 1 to 1.5 folds, suggesting the lower TCR levels seen in $CD8^+$ cells are not due to TCR being rate-limiting. This increased TCR expression was associated with higher intracellular Ca^{2+} levels in $CD4^+$ T cells compared to $CD8^+$ T cells, both at baseline and upon stimulation. However both T cell populations could increase their intracellular calcium levels by the same extent, as shown by the similar increase in Ca-bound:Ca-unbound ratio (figure 3.3C). ERK phosphorylation levels did not differ between the two populations, suggesting late TCR signalling events are not influenced by the higher expression of TCR. Surprisingly $CD4^+$ T cells expressed higher levels of the degranulation marker CD107a compared to $CD8^+$ T cells (figure 3.5). The kinetics of CD107a upregulation upon polyclonal stimulation with CD3/CD28 beads were also different, with $CD4^+$ cells peaking at 30 minutes post stimulation, compared to 60 minutes in $CD8^+$ T cells. The *in vitro* survival of $CD4^+$ and $CD8^+$ transduced with either the control-GFP or the CD3-GFP vector was not significantly different. All cells populations

expanded by day 3 post activation and by day 5 the proliferation kinetics were identical, and remained so at day 7 (figure 3.7). Similarly, the expression levels of the activation markers CD25 and CD69, and the differentiation markers CD62L and CD127 were similar in all populations, at all time points (day 3, 5 and 7 post transduction). Transduced $CD4^+$ T cells expressed higher levels of CD25 and CD69 3 days post transduction, but this difference was not significant. The kinetics of TCR expression followed the same trend in both non-transduced and transduced cells, with expression levels similar between day 3 and day 5 and a decrease in TCR at day 7 (figure3.9). Finally increase in TCR expression was not associated with increase functional avidity in either polyclonal or antigen-specific $CD4^+$ cells (figure 3.10-3.12).

Although the density of TCR on a T cell is known to change during its lifetime (Finkel et al., 1989), to our knowledge this disparity in TCR expression between $CD4^+$ and $CD8^+$ cells has yet to be reported, and the reason behind $CD4^+$ cells expressing more TCR than $CD8^+$ cells is unknown. Recently it has been suggested that different threshold may exists for the activation of $CD4^+$ and $CD8^+$ cells, with $CD4^+$ T cells needing longer to reach such threshold (Kaech et al., 2002). Whether this difference is triggering threshold is dictated by extrinsic or intrinsic factors is unknown. Higher TCR expression in $CD4^+$ T cells may account for this difference in activation threshold: if the same proportion of TCR needs to be engaged in $CD4^+$ and $CD8^+$ cells to promote T cell activation, it will take longer for $CD4^+$ T cells to reach this result, if the cells are stimulated with the same amount of antigen. However Viola et al., showed that the minimum number of TCRs that need to be engaged for a T cell to become activated is 8000. Above this number both $CD4^+$ and $CD8^+$ T cells start to proliferate and produce IFNγ (Viola et al., 1996). Thus, in this setting $CD4^+$ and $CD8^+$ T cells showed the same triggering threshold.

One important contributing factor affecting TCR expression levels might be the different *in vivo* interactions $CD4^+$ and $CD8^+$ have with “self”. MHC-I molecules are ubiquitously expressed, providing $CD8^+$ T cells with more opportunities to encounter MHC-I complexes. In contrast, MHC-II molecules are expressed on a more limited set of cells,

meaning $CD4^+$ T cells have a lower probability to encounter their MHC complex. It is now well established that TCR stimulation leads to TCR downregulation, and that T cells continuously interact with "self" over their lifetime. Thus, the higher interaction rate of $CD8^+$ with MHC-I molecules *in vivo* may keep TCR levels in $CD8^+$ T cells low, compared to $CD4^+$ T cells that have less chances to encounter MHC-II molecules.

Our results also suggest that increased TCR expression is associated with higher intracellular calcium concentration. Although the intracellular calcium concentration in T cells is known to be tightly controlled, and kept between ~100 nM in resting cells and ~1 μM following TCR stimulation (Feske, 2007), little is known about how Ca^{2+} concentration changes in $CD4^+$ and $CD8^+$ T cells. Previous studies have shown that both lymphocyte motility and immunological synapse formation are Ca^{2+}-dependent processes. In particular calcium increase in $CD4^+$ cells as a consequence of T cell:APC contact needs to last for several hours to induce changes in $CD4^+$ T cell gene expression. On the other hand CTL-mediated killing by release of lytic granules is faster and occurs within the first 5 minutes of target-cell recognition (Lyubchenko et al., 2001). Our data does not quantify the concentration of intracellular calcium, but it indicates that the cytoplasmic concentration of Ca^{2+} in $CD4^+$ T cells is higher compared to that of $CD8^+$ T cells. Higher levels of intracellular calcium at baseline and upon stimulation might facilitate sustained calcium signalling needed for $CD4^+$ T cell activation, and $CD4^+$ calcium-depletion experiments would indicate whether this is the case or not. However neither intracellular calcium concentration, nor different TCR expression seem to influence Ca^{2+} mobilization, as both $CD4^+$ and $CD8^+$ T cell can upregulate their cytoplasmic calcium concentration to the same extent (figure 3.3C). This is in contrast with results from Blichfeldt et al. who reported that a decrease in TCR numbers resulted in reduction in cytosolic $Ca2^+$ mobilization (Blichfeldt et al, 1996). However in their system TCR expression is downregulated below physiological levels; our system increases the levels of TCR. The TCR levels that are set in $CD4^+$ and $CD8^+$ T cells during thymic development and *in vivo* homeostasis may be the minimum required level for effective TCR signalling, and

increasing these levels might not affect TCR signalling in terms of calcium mobilisation. More physiological stimulation, such as peptide specific stimulation, or analysis of $CD4^+$ and $CD8^+$ sorted cells that express the same level of TCR are needed to further understand the biology of cytoplasmic calcium upregulation and if this is influenced by the levels of TCR expression.

Contrary to Ca^{2+} levels, phospho-ERK (p-ERK) levels are similar between $CD4^+$ and $CD8^+$ cells despite their different TCR expression. This suggests that increased TCR levels are not associated with stronger, late TCR signalling, and regulatory mechanisms might be in place to prevent aberrant T cell activation in response to increased TCR triggering. Indeed studies in human T lymphocytes have shown that p-ERK has the capacity to induce LAT phosphorylation and attenuation of T cell signalling. However such mechanism has not been observed in mouse lymphocytes, but other mechanisms might be in place (Matsuda et al., 2004). Moreover in our assays activation was achieved with a high affinity antibody stimulus, bypassing TCR:p-MHC interaction. To note is that soluble anti-CD3 stimulation, in the absence of CD28 co-stimulation, may not be sufficient for full T cell activation. In these assays a higher concentration of anti-CD3 (50 µg/ml) was required to detect phosphorylation of ERK; lower concentrations, for example 10 µg/ml anti-CD3 (the same concentration used for calcium signalling assays) did not give detectable levels p-ERK (data not shown). Thus late TCR signalling events may not occur unless a strong signal 1 and signal 2 are delivered to the T cell.

CD107a, also known as lysosome-associated membrane protein-1 (LAMP-1), is a common marker of degranulation and cytotoxic activity. As degranulation occurs, secretory lysosomes are released and CD107a is transported to the plasma membrane. Although cytotoxic activity as traditionally being associated with $CD8^+$ T cells, the existence of distinct population of $CD4^+$ cytotoxic T cells is now well established (Mucida et al., 2013). Since uptake of extracellular calcium is required for lymphocyte cytolytic activity (Maul-Pavicic et al., 2011), the higher cytosolic calcium concentration in $CD4^+$ may account for their increased expression of CD107a. However previous studies

looking at LCMV-specific $CD4^+$ and $CD8^+$ effector cells showed that after 5 hours stimulation ~80% of $CD8^+$ T cells expressed CD107a, compared to ~25% of $CD4^+$ T cells. Nonetheless, their *in vivo* killing capacity was similar (Hildemann et al., 2013). The discrepancy between this study and our results may be due to the type of stimulation used for CD107a measurement, a peptide specific stimulation versus our polyclonal high affinity stimulation. Stimulation with high-affinity antibodies might give a response that is stronger than the normal physiological response. However this still doesn't explain the higher CD107a levels at baseline seen in $CD4^+$, compared to $CD8^+$ cells. Notably, this data is from two experimets only; more repeats are necessary in order to obtain significant results. Another limitation of these assays is represented by the expression of the CD4 co-receptor, as this is not limited to $CD4^+$ T cells. Monocytes, macrophages, NK cells, eosinophils and basophils all express CD4 (Biswas et al., 2003), in addition to CD107a. Our gating strategy cannot distinguish between $CD4^+$ T cells and the other cell populations. Therefore, it is possible that our CD107a data is not representative of a pure $CD4^+$ T cells population. Further experiments looking at CD107a expression in $CD4^+$ T cells, after manipulation of both TCR expression and cytoplasmic Ca^{2+} are required to increase our understanding of how these influence CD107a expression. Moreover cytolytic assays are required to test whether the higher CD107a expression in the $CD4^+$ cell population correlates with improved killing activity.

As previously described, transduction with the control-GFP vector did not increase TCR expression levels in either $CD4^+$ or $CD8^+$ T cells; CD3-GFP transduction on the other hand lead to a significant increase in TCR density in both T cell populations, but with $CD4^+$ T cell still expressing higher levels of TCR compared to $CD8^+$ T cells. However this increase in TCR expression was not associated with an advantage in cell proliferation or *in vitro* cell survival. Although effective T cell stimulation was achieved with anti-CD3/CD28 stimulation (as seen by initial T cell expansion) this was not sufficient to promote "stimulus-independent" (similar to antigen-independent) proliferation. Indeed, removal of the CD3/CD28 beads on day 3 lead to a quick loss of cell numbers on day 5

and day 7. Moreover increasing TCR density on the cell's surface does not induce antigen-independent tonic signalling, which may promote antigen-independent survival.

The notion that increased TCR expression in the context of high affinity stimulation with antibodies does not induce any changes in T cell activation, is corroborated by our activation and differentiation markers expression data. To investigate whether increased TCR expression favoured T cell activation or differentiation into a particular phenotype, CD25, CD69, CD62L and CD127 expression was analysed at day 3, 5 and 7 post transduction. CD69 is an early activation marker and it is detectable within hours of TCR ligation; *in vitro* its expression returns to baseline levels by 72 hours post activation (Simms et al., 1996). CD25 is detectable about 24 hours post stimulation and upregulated from day 2 onwards. CD69 expression is higher in the transduced $CD4^+$ populations at day 3 post transduction suggesting a stronger activation in these two T cell populations, compared to the other populations. However this difference is lost by day 5 as both GFP^- and $CD8^+$ GFP^+ upregulate their expression of CD69. Interestingly this upregulation occurs after removal of the stimulus as CD3/CD28 beads are removed at day 3 post stimulation. CD69 expression levels are downregulated between day 5 and day 7. Since CD69 expression returns to baseline levels by 72 hours post activation, analysis of CD69 expression at earlier time points (between day 0 and day 3 post transduction) may reveal differences in its expression. Similar kinetics are seen for CD25 expression throughout the analysis. Interestingly CD69 and CD25 expression peaks at day 5 post transduction, whereas cell proliferation has stopped by day 5. Between day 5 and day 7 CD69 and CD25 expression remains relatively constant, as does cell proliferation. Thus TCR overexpression in $CD4^+$ or $CD8^+$ cells is not associated with increased expression of activation markers, suggesting increased TCR density does not promote tonic signalling in the absence of antigen/stimulation. CD62L and CD127 expression was used to determine naïve-like, effector and memory subsets. Perhaps not surprisingly the differentiation status is very similar among the 6 different populations at every time point, as all populations have undergone the same activation protocol. By day

5 post transduction the majority of the cells has acquired an effector phenotype ($CD62L^-$ $CD127^-$) and this differentiation can be attributed to the CD3/CD28 activation steps, needed for transduction, which also explains why GFP^- cells also present with a similar phenotype. The differentiation into effector cells continues up to day 7 when in all 6 populations ~50% of the cells lose the expression of both CD62L and CD127. Thus, similarly to CD69 and CD25 expression, increasing the TCR levels on $CD4^+$ or $CD8^+$ T cells does not alter their differentiation program upon activation. Moreover the three different subsets of differentiated cells express comparable levels of TCR and acquisition of an effector phenotype continues even upon TCR downregulation, as seen between day 5 and day 7. This corroborates the hypothesis that differentiation occurs independently from TCR expression levels and increasing the levels of TCR does not promote tonic signalling and antigen-independent T cell activation.

To test whether increasing endogenous TCR levels is associated with augmented functional avidity, we setup both polyclonal and antigen-specific restimulations. Control-GFP and CD3-GFP transduced $CD4^+$ cells were restimulated with plate-bound anti-CD3 antibody; TRP1-TCR + control-GFP and TRP1-TCR + CD3-GFP double transduced cells were restimulated with peptide-loaded splenocytes. Our data suggests that increasing the levels of TCR does not lower the triggering threshold of either polyclonal or antigen-specific $CD4^+$ cells. IL-2 and IFNγ production was seen after stimulation with all of the tested concentrations of both anti-CD3 antibody and TRP1 peptide (10-0.001 μg/ml anti-CD3; 10 μM-100 pM TRP1-peptide), in both control-GFP and CD3-GFP transduced polyclonal and antigen specific cells (figure 3.11 and 3.12). In addition increasing TCR density does not increase the frequency of IL-2 or IFNγ producing cells. On the contrary, the percentage of IL-2 producing cells after 4 hours polyclonal restimulation was significantly higher in the control-GFP transduced population. All other stimulation conditions, both with anti-CD3 and with TRP1 peptide, gave similar frequencies of IL-2 and IFNγ producing cells in both control-GFP and CD3-GFP transduced populations. This pattern of cytokine expression was confirmed by both ELISA and IC cytokine

staining for the polyclonal stimulation; and by IC cytokine staining for the antigen specific stimulation. Our peptide-specific restimulation data is discordance with previously published results from our lab, where it was shown that increased TCR expression following transduction with the CD3-GFP results in increased functional avidity (Ahmadi et al., 2011). However previous studies were carried out in the context of class-I restricted peptides and TCRs. Because the TRP1-TCR is a class-II restricted TCR, a "cleaner" restimulation system may be required to appreciate differences, if any, between the two double transduced populations. In a population of splenocytes only a small proportion of cells (DCs and B cells) will be capable of presenting the TRP1 peptide in a MHC-II context to $CD4^+$ cells. Restimulation with peptide-loaded purified DCs for example, may be a more efficient system for $CD4^+$ restimulation.

Higher TCR expression on CD3-GFP-transduced polyclonal and TRP1-TCR cells, was confirmed by flow cytometry; thus the absence of increased cytokine production was not due to a lack of increased TCR expression in the CD3-GFP transduced cells. Published studies have shown that TCR downregulation after initial T cell activation correlates with antigen avidity (Itoh et al., 1999). Accordingly, restimulation through the TCR-CD3 complex by anti-CD3 antibody lead to TCR downregulation, the extent of which was associated with the strength of the stimulus: restimulation with 10 µg/ml anti-CD3 leads to downregulation of ≥90% of surface TCR in both control-GFP and CD3-GFP transduced cells, a greater downregulation to that seen with PMA stimulation; PBS and 0.01-0.001 µg/ml anti-CD3 restimulations did not give any detectable TCR down modulation. However analysis of Vβ14 chain levels after stimulation with peptide-loaded splenocytes did not show TRP1 downregulation. This suggests that the stimulation conditions were not ideal and that the strength of the stimulation was insufficient to activate TRP1-TCR transduced cells. This supports our hypothesis that this stimulation setup may not be ideal to study functional avidity of $CD4^+$ T cells and a more specific system is needed.

Notably although PMA is regarded as a strong T cell agonist, TCR downregulation following PMA stimulation is not as strong as that seen after stimulation with 10 µg/ml anti-CD3. This discrepancy might be due to the fact that different mechanisms are responsible for TCR down modulation following PMA or TCR-CD3 stimulation (Salio et al., 1997). Whether the observed TCR downregulation is permanent or transient we don't know. However it has been previously suggested that stimulation with specific ligands leads to TCR degradation (Valitutti et al., 1997), whereas downregulation following PMA stimulation is transient and downregulated TCR are sequestered inside the cell and can be expressed on the cell surface when the stimulus is removed (Salio et al., 1997).

Finally, as described repeatedly above one of the major caveats with polyclonal *in vitro* restimulation analysis is the use of high affinity anti-CD3 antibodies. Antibodies' affinities are normally in the nanomolar concentrations (k_D ~10^{-9}), compared to the micromolar affinities (k_D 10^{-6}) of TCRs for their antigens. This non-physiological stimulation might trigger particular regulatory mechanisms. In addition high affinity stimulation may mask subtle differences in T cell activation, which could be seen in the context of peptide-specific stimulations.

To conclude our data showed that $CD4^+$ T cells express higher levels of endogenous TCR and intracellular Ca^{2+}, compared to $CD8^+$ T cells. However this was not associated with increased proliferation, or increased expression of activation markers or increased differentiation into a particular phenotype. In addition effector functions of $CD4^+$ T cells are not improved upon transduction with additional CD3 genes. Whether these differences play a role in the development of toxicity in mice receiving $CD4^+$ T cells is unknown. Since all of the above characterisations were performed *in vitro*, experiments were carried out to characterise the behaviour of CD3-overexpressing $CD4^+$ and $CD8^+$ T cells *in vivo*. Such experiments are described in chapter 4.

4. In vivo functional analysis of CD3-engineered CD4$^+$ and CD8$^+$ T cells

4.1. Introduction

The data described in chapter 3 demonstrated that CD4$^+$ T cells express higher levels of endogenous TCR compared to CD8$^+$ T cells, both before and after transduction with the CD3-GFP vector. Previous experiments from our lab showed that provision of additional CD3 genes to TCR gene-modified CD8$^+$ T cells promotes *in vivo* cell persistence and accumulation (Ahmadi et al., 2011). Moreover, tonic signalling through the TCR is fundamental for T cell homeostatic survival (Takada et al., 2009a). Therefore, we next investigated whether the difference in TCR expression between CD4$^+$ and CD8$^+$ T cells translated into different *in vivo* behaviour. In particular, we investigated whether the levels of TCR expression influenced the *in vivo* persistence, homing and differentiation profiles of CD4$^+$ and CD8$^+$ T cells.

Although our *in vitro* experiments did not show any difference in T cell activation and survival, physiological homeostatic signals received by the T cells *in vivo* may unmask subtle functional differences between the CD4$^+$ and the CD8$^+$ T cell populations. Thus, the experiments described in this chapter explore the consequence of CD3 overexpression in both CD4$^+$ and CD8$^+$ T cells in an *in vivo* setting. Sub-lethally irradiated mice received syngeneic CD4$^+$ and CD8$^+$ T cells that had been transduced with the CD3-GFP vector (CD4$^+$ CD3-GFP and CD8$^+$ CD3-GFP, respectively), or untransduced CD4$^+$ T cells (CD4$^+$ mock). Their homing, accumulation and differentiation were then analysed at two time points: one early time point, day 10 post T cell transfer; and one later time point, day 16 post adoptive transfer. We hypothesised that the higher levels of TCR expression in CD4$^+$ T cells may lead to stronger survival signalling, promoting CD4$^+$ T cell accumulation and survival, compared to similarly modified CD8$^+$ T cells.

4.2. CD3-engineered CD4$^+$ T cells accumulate in greater proportion *in vivo* compared to CD3-engineered CD8$^+$ T cells

Initial experiments were performed to compare *in vivo* persistence and differentiation of CD4$^+$ mock, CD3-engineered CD4$^+$ and CD8$^+$ T cells, during early T cell engraftment. On day 0 C57Bl/6 Thy1.2$^+$ recipient mice were sub lethally irradiated with 5.5 Gy; 2-3 hours post irradiation they received adoptive transfer of 5 x 10^6 luciferase$^+$ Thy1.1$^+$ CD4$^+$ mock, or luciferase$^+$ Thy1.1$^+$ CD3-engineered CD4$^+$ (CD4$^+$ CD3-GFP), or luciferase$^+$ Thy1.1$^+$ CD3-engineered CD8$^+$ (CD8$^+$ CD3-GFP) transduced T cells. Because transduction efficiency was not 100%, and because the transduced T cells were not sorted before injection, the number of adoptively transferred cells was adjusted according to the efficiency of transduction, with all mice receiving the same number of transduced cells. At day 8 post injection the adoptively transferred cells were tracked by bioluminescent imaging; on day 10 post injection the mice were sacrificed and the homing of Thy1.1$^+$ cells investigated in four tissues: spleen, inguinal lymph nodes (LN), bone marrow (from one tibia and one fibula; BM) and liver. Prior to sacrifice, mice's weight was monitored daily, and as per Home Office regulations, mice with > 20% body weight loss were culled. Figure 4.1 shows a schematic representation of the experimental *in vivo* set up.

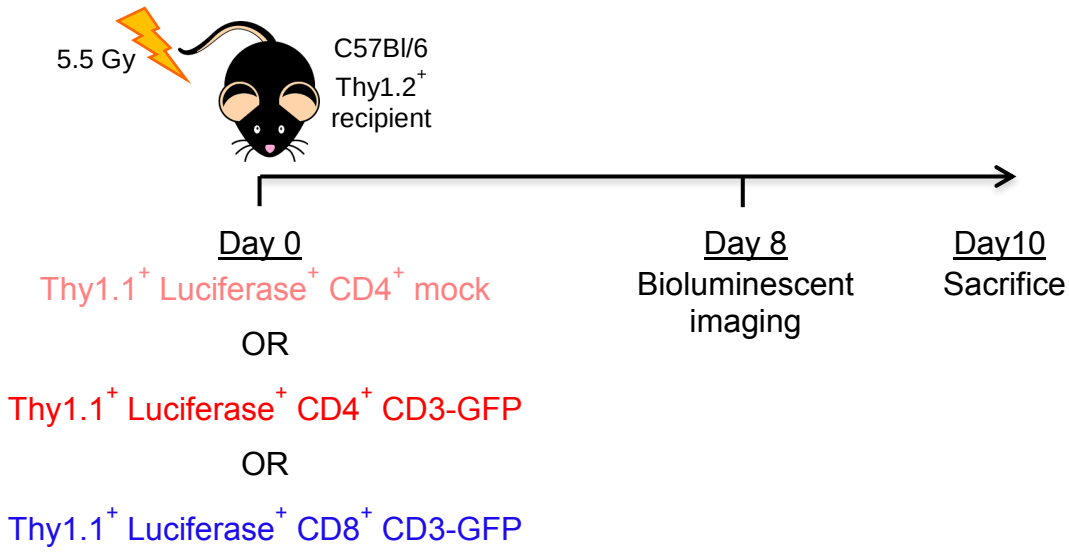

Figure 4.1 – Schematic representation of experimental set up for *in vivo* persistence, homing and differentiation studies at day 10 post T cell transfer.

$CD4^+$ and $CD8^+$ T Cells were MACS sorted and transduced as described in chapter 2 sections 2.2.3 and 2.2.4, prior to injection on day 3 post transduction. Figure 4.2A shows typical purity of adoptively transferred cells, which in all populations was >95%. Transduction efficiency was also similar between the CD3-engineered $CD4^+$ and $CD8^+$ T cells (84% and 72% respectively). In these experiments $CD4^+$ mock cells were not transduced with the control-GFP vector, hence the lack of GFP signal (figure 4.2A). The differentiation status based on CD127 and CD62L expression was also analysed before injection (figure 4.2B). All three populations presented with identical proportions of naïve-cells ($CD127^+$ $CD62L^+$), ≥80%, $CD127^-$ $CD62L^-$ effector cells (≤1%) and $CD127^+$ $CD62L^-$ memory cells ≤20% (figure 4.2C).

Weight was used to monitor the wellbeing of the animals and to track potential toxicity onset. No toxicity was seen in any of the animals in these experiments; the changes in body weight are plotted in figure 4.2D.

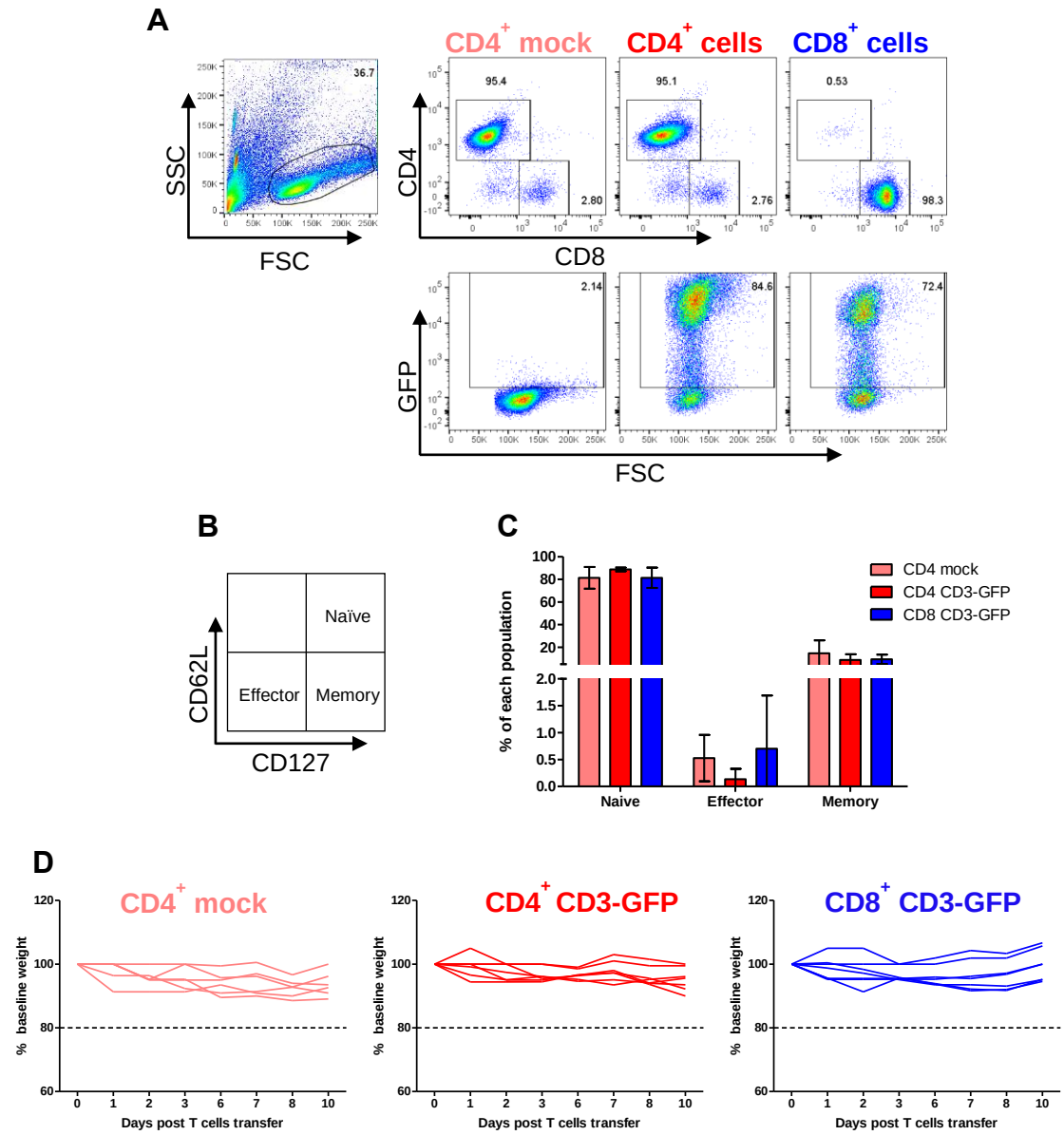

Figure 4.2 – Purity, transduction efficiency, differentiation status of adoptively transferred cells and mice weights. (A) Typical purity and transduction efficiency of adoptively transferred cells are shown. (B) Schematic representation of the gating strategy used to identify naïve, effector and memory cells based on CD62L and CD127 expression. (C) The differentiation status of the adoptively transferred cells is shown (SEM is plotted). (D) The changes in mice weight overtime are plotted for the three experimental groups. Data from 2 independent experiments. The total number of animals/group was $CD4^+$ mock n=6; $CD4^+$ CD3-GFP n=7; $CD8^+$ CD3-GFP n=7.

On day 8 post T cell transfer, homing of the transferred cells was tracked *in vivo* by bioluminescent imaging, as described in chapter 2, section 2.5.2. Adoptively transferred cells were luciferase$^+$; when recipient mice are injected with luciferin, this is broken down by the luciferase enzyme in a two-step reaction, causing light to be emitted, as shown by the reaction below.

$$\text{LUCIFERIN} + \text{ATP} \rightarrow \text{LUCIFERYL ADENYLAYE} + PP_i$$

$$\text{LUCIFERYN ADENYLATE} + O2 \rightarrow \text{OXYLUCIFERIN} + \text{AMP} + \text{LIGHT}$$

At this time point (day 8 post adoptive T cell transfer) CD4$^+$ CD3-GFP T cells were readily detectable compared to CD4$^+$ mock and CD3-engineered CD8$^+$ cells, as shown by the increased bioluminescent signal (figure 4.3). In 4 out of 5 mice that received CD4$^+$ mock T cells, luciferase$^+$ T cells were observed in the thymic/cervical lymph nodes area and around the mucosal membrane of the snout (figure 4.3A). In the experimental group receiving CD8$^+$ CD3-GFP T cells a weak bioluminescent signal was observed in the thymic area in 3 out of 5 mice. No other signal was detected (figure 4.3C). In contrast, a strong bioluminescent signal was observed in all mice receiving CD3-engineer CD4$^+$ T cells. Luciferase$^+$ T cells were present in the thymic/cervical lymph nodes area, mucosal membrane of the snout, inguinal lymph nodes, splenic area and in the skin (tail, ears, and paws) (figure 4.3B).

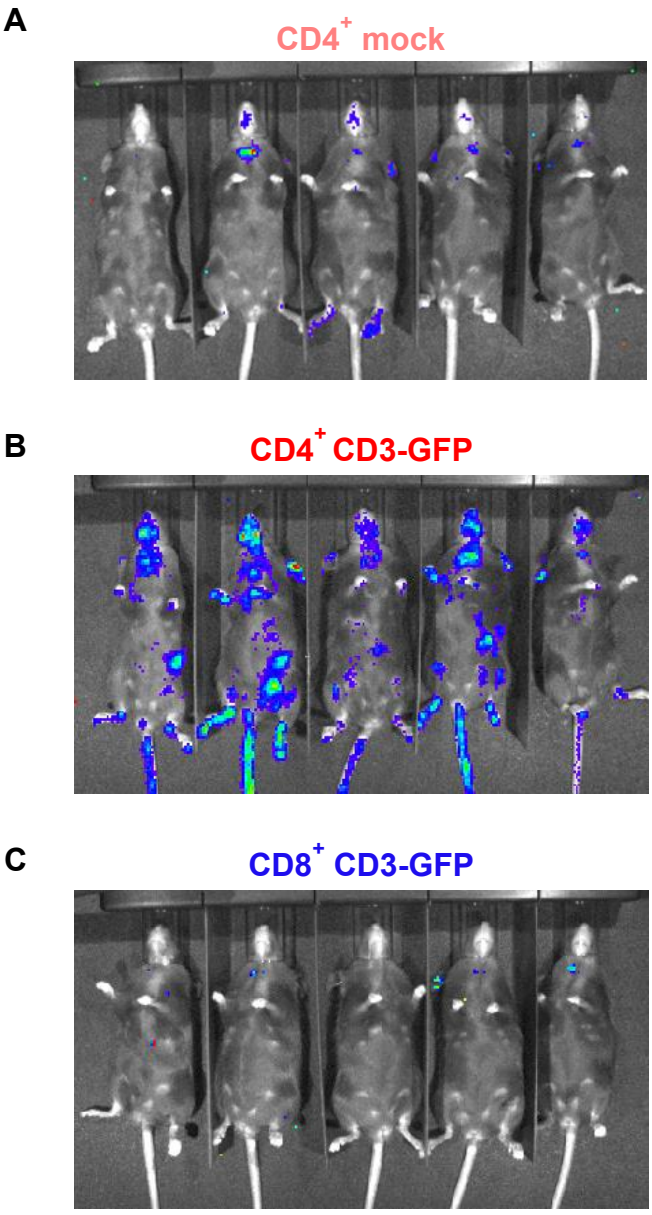

Figure 4.3 – Bioluminescent imaging at day 8 post adoptive transfer. Mice in all experimental groups were imaged to track the homing and survival of the adoptively transferred cells. (A) $CD4^+$ mock group. (B) $CD4^+$ CD3-GFP group. (C) $CD8^+$ CD3-GFP group.

Two days after bioluminescent imaging was performed all mice were humanely killed and their spleens weighted. Mice that received CD3-engineered $CD4^+$ T cells had significantly heavier spleens ($p \leq 0.05$) compared to the other two experimental groups. This was not due to higher body weight, as these were comparable to the weights of mice receiving $CD4^+$ mock cells, and were significantly lower to those mice receiving $CD8^+$ CD3-GFP T cells (figure 4.4).

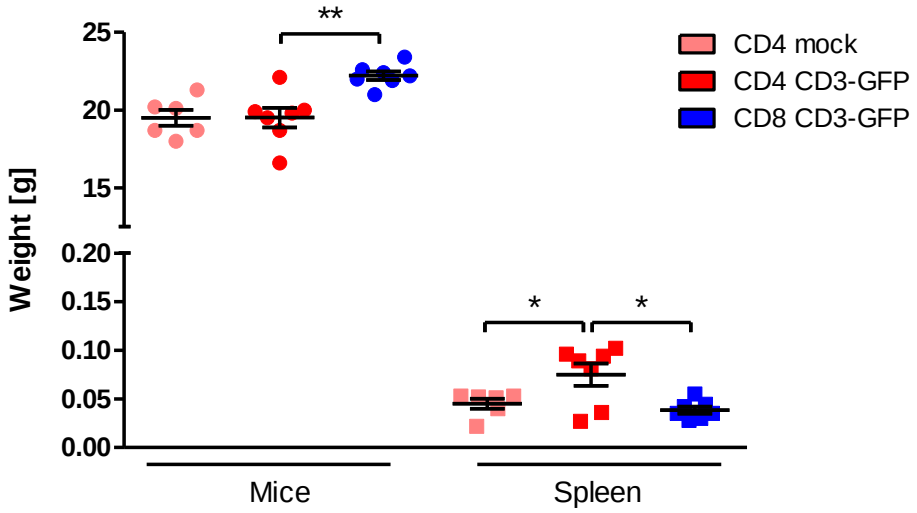

Figure 4.4 – Weight of whole mice and resected spleens at day 10 post T cell transfer. 10 days post T cell transfer the mice were culled, and their spleens were weighted. Data from 2 independent experiments. $CD4^+$ mock n=6; $CD4^+$ CD3-GFP n=7; $CD8^+$ CD3-GFP n=7. (p=* ≤0.05; ** ≤0.01; unpaired T test. Lines represent mean + SEM).

Single cell suspensions of spleen, inguinal LNs, BM and liver were prepared and analysed by flow cytometry, as described in chapter 2, sections 2.5.3 and 2.3, respectively. Using congenically marked Thy1.1$^+$ cells for adoptive transfer into Thy1.2$^+$ recipients allowed us to discriminate the transferred cells from the endogenous Thy1.2$^+$ T cell population. GFP expression permitted comparison of transduced CD4$^+$ and CD8$^+$ T cells. Thus the expansion and persistence of transduced cells in different tissues could be assessed. Figures 4.5A and B show the gating strategy used to analyse the single cell suspension from the four tissues of mice receiving CD4$^+$ mock T cells and CD3-engineered T cells, respectively. Summary data showing the percentage of transferred cells recovered from each tissue is shown in figure 4.5C and D. In mice receiving CD4$^+$ mock T cells, the transferred cells accounted for less than 60% of the total viable CD4$^+$ population, in all analysed organs (spleen:42.4%; LN: 35.9%; BM: 42.5%; liver: 58.5%). Similar percentages of transferred CD8$^+$ CD3-GFP T cells were recovered from the tissues (spleen: 44.6%; LN: 40%; BM: 51.8%; liver: 66%). Conversely, CD3-engineered CD4$^+$ T cells were isolated in significantly higher proportions compared to both CD4$^+$ mock and CD3-engineered CD8$^+$ T cells, from all analysed tissues. On average they represented 60% or more of the total CD4$^+$ Thy1.1$^+$ population found in the spleen (66.4%), LN (60.3%), BM (73%) and liver (83.8%). Summary of mean percentages is shown in figure 4.5 D.

Absolute numbers of transferred cells were also calculated using counting beads as described in chapter 2, section 2.1.1. Similar to the trend seen in the percentages of recovered cells, CD3-engineered CD4$^+$ T cells were recovered in significantly higher numbers compared to CD3-engineered CD8$^+$ T cells, in all analysed organs, except the liver. In the liver no difference was seen in the number of recovered CD4$^+$ CD3-GFP T cells compared to CD8$^+$ CD3-GFP T cells. No difference in the absolute number of cells recovered from animals receiving the CD4$^+$ mock or the CD3-engineered CD4$^+$ T cells was seen. Figures 4.5 E and F show the mean absolute number of

transferred cells recovered from each tissue.

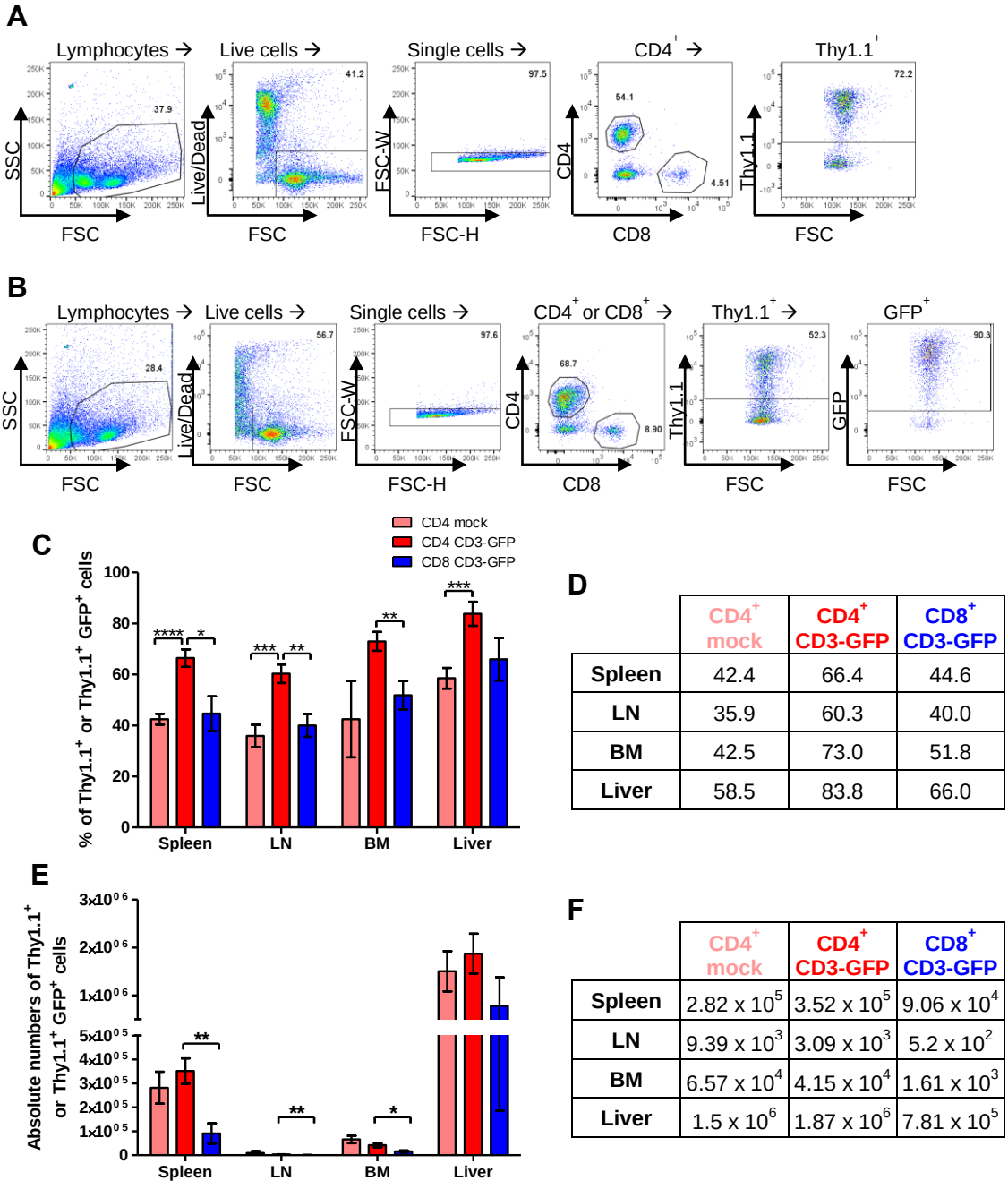

	CD4+ mock	CD4+ CD3-GFP	CD8+ CD3-GFP
Spleen	42.4	66.4	44.6
LN	35.9	60.3	40.0
BM	42.5	73.0	51.8
Liver	58.5	83.8	66.0

	CD4+ mock	CD4+ CD3-GFP	CD8+ CD3-GFP
Spleen	2.82×10^5	3.52×10^5	9.06×10^4
LN	9.39×10^3	3.09×10^3	5.2×10^2
BM	6.57×10^4	4.15×10^4	1.61×10^3
Liver	1.5×10^6	1.87×10^6	7.81×10^5

Figure 4.5 – Increased TCR expression in CD4⁺ cells is associated with increased *in vivo* persistence. (A) The gating strategy to analysed CD4⁺ mock and (B) CD3-engineered CD4⁺ and CD8⁺ T cells is shown. (C, D) The mean percentages + SEM of recovered transferred cells are shown. (E, F) The mean absolute numbers + SEM of recovered transferred cells are shown. Data from 2 independent experiments. CD4⁺ mock n=6; CD4⁺ CD3-GFP n=7; CD8⁺ CD3-GFP n=7. (p=* ≤0.05; ** ≤0.01; ***≤0.001; **** ≤0.0001; unpaired t test).

4.3. *Ex vivo* phenotype of adoptively transferred CD4$^+$ and CD8$^+$ T cells is determined by both T cell lineage and their eventual homing site

The data described above suggests that CD3 and TCR overexpression in CD4$^+$ T cells promotes their *in vivo* persistence, compared to CD3-overexpressing CD8$^+$ T cells. To determine whether this was associated with distinct differentiation profiles, flow cytometry was used to analyse the phenotype of the transferred T cells at day 10 post injection. CD62L and CD127 expression was analysed to determine whether the isolated cells presented with a naïve (CD62L$^+$ CD127$^+$), effector (CD62L$^-$ CD127$^-$) or memory (CD62L$^-$ CD127$^+$) phenotype (figure 4.6A).

Analysis of CD62L and CD127 revealed that the phenotypic profile of the experimental T cells evolved after adoptive transfer, as shown by the different differentiation statuses observed on injection day and at day 10 post T cell transfer.

CD62L and CD127 expression was analysed on viable, CD4$^+$ Thy1.1$^+$ (CD4$^+$ mock group) or viable CD4$^+$/CD8$^+$ Thy1.1$^+$ GFP$^+$ (CD4$^+$ and CD8$^+$ CD3-GFP groups) T cells. In the spleen no significant difference in the proportion of naïve (16.6%-46%) or effector (20.3%-22.1%) cells was seen among the three populations. The proportion of CD3-engineered CD8$^+$ T cells demonstrating a naïve phenotype was slightly higher (46%), but not significantly. Memory cells were present in significantly higher proportions in the two CD4$^+$ populations (57% CD4$^+$ mock; 63% CD4$^+$ CD3-GFP), compared to the proportion of recovered CD8$^+$ T cells with a memory phenotype (28%) (figure 4.6B).

In the inguinal LNs (figure 4.6C) no difference in the percentage of naïve cells was seen between the CD4$^+$ mock and the CD8$^+$ CD3-GFP population (37% and 30% respectively), whereas the percentage of recovered naïve CD4$^+$ CD3-GFP T cells was significantly lower (12%). No difference in the proportion of effector cells were seen among the three populations, and it varied between 9.1% and 21.1%. Similar to the trend

seen in the splenic T cell population, the percentage of memory $CD4^+$ T cells recovered from both the $CD4^+$ mock and $CD4^+$ CD3-GFP experimental groups was not significantly different (48% and 64% respectively). In addition, the latter was significantly higher than the proportion of memory $CD8^+$ T cells (38%) recovered from the mice receiving the $CD8^+$ CD3-GFP control T cells.

The highest percentage of transferred cells recovered from the bone marrow of the three experimental groups, had an effector phenotype; no difference in the percentage of effector cells was seen among the three groups ($CD4^+$ mock: 51%; $CD4^+$ CD3-GFP: 49%; $CD8^+$ CD3-GFP: 41%). The second highest proportion of recovered cells were memory cells as defined by our cell surface staining. In this case, no significant difference was seen in the percentage of $CD4^+$ mock and $CD4^+$ CD3-GFP memory T cells (38% and 45% respectively), suggesting increased TCR expression in $CD4^+$ T cells did not affect differentiation status. In addition the proportions of $CD4^+$ mock and CD3-engineered $CD4^+$ memory T cells were significantly higher compared to that of CD3-engineered $CD8^+$ memory T cells (18%). No significant difference was seen in the percentage of naïve cells recovered from the two $CD4^+$ experimental groups ($CD4^+$ mock: 6.8%; $CD4^+$ CD3-GFP: 3.7%). The proportion of T cells with a naïve phenotype recovered from the CD3-engineered $CD8^+$ experimental group was significantly higher than both $CD4^+$ groups, and was 20.5% (figure 4.6D).

In the liver (figure 4.6E) the percentage of adoptively transferred cells with an effector phenotype was not significantly different among the three different experimental populations (25.6%-38.7%). $CD8^+$ CD3-GFP T cells with a naïve phenotype were recovered in higher percentages (40%) compared to both $CD4^+$ populations ($CD4^+$ mock: 9%; $CD4^+$ CD3-GFP: 6%). On the other hand the percentage of isolated, transferred cells presenting with a memory phenotype from both $CD4^+$ experimental populations was significantly higher compared to the percentage of memory $CD8^+$ T cells recovered from the CD3-engineered $CD8^+$ population ($CD4^+$ mock: 51%; $CD4^+$ CD3-GFP: 61%; $CD8^+$ CD3-GFP: 20%).

Thus, analysis of the *ex vivo* $CD4^+$ mock, CD3-engineered $CD4^+$ and CD3-engineered $CD8^+$ T cells, from the four examined tissues revealed that the differentiation profile of the transferred cells, 10 days post T cell transfer is determined both by T cell lineage, and their homing site. Broadly speaking, the differentiation of the two $CD4^+$ T cell subsets is similar in all analysed organs (with the exception of the naïve population in the LN), suggesting the cell's lineage determines the phenotypic status, not the level of TCR expression (as altered by co-transfer of additional CD3); $CD8^+$ T cells followed a distinct differentiation trend, which was organ specific. Figure 4.13 summarised the percentages of naïve, effector and memory cells isolated from the tissues of the three experimental groups.

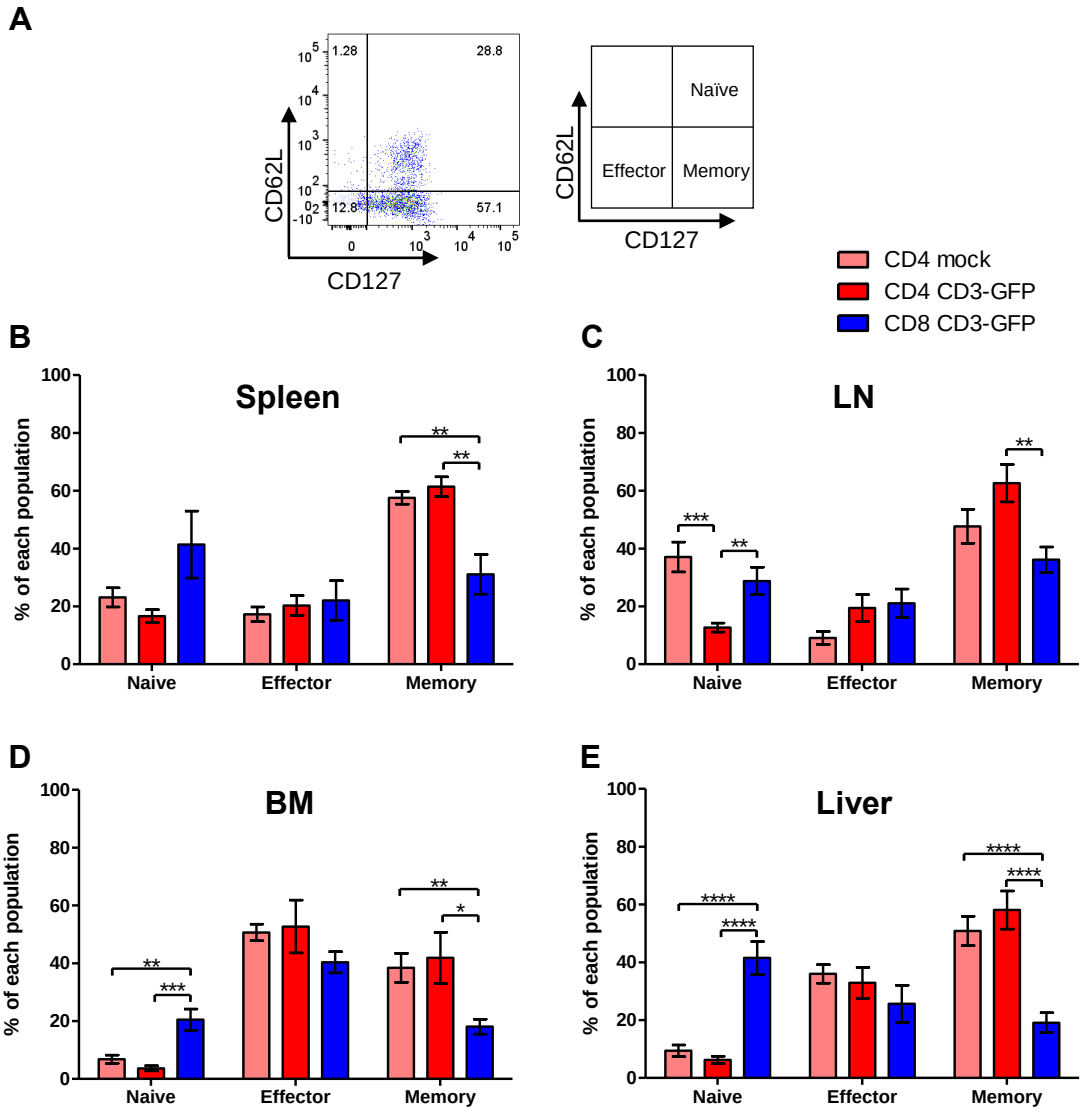

Figure 4.6 – Day 10 *ex vivo* differentiation status of adoptively transferred cells. (A) The expression profiles of CD62L and CD127 were used to determine the phenotype of the recovered, transferred cells. A representative plot of the gating strategy is shown. (B-E) The differentiation profile was examined in adoptively transferred cells ($CD4^+$ mock: $Thy1.1^+$; $CD4^+$ and $CD8^+$ CD3-GFP: $Thy1.1^+$ GFP^+) recovered from the spleen, inguinal lymph nodes (LN), bone marrow (BM) and liver. Mean values + SEM from 2 independent experiments are shown. $CD4^+$ mock n=6; $CD4^+$ CD3-GFP n=7; $CD8^+$ CD3-GFP n=7.

4.4. CD3-engineered $CD4^+$ T cells accumulate in greater numbers *in vivo* compared to CD3-engineered $CD8^+$ T cells, 16 days post adoptive transfer

The experiments described above aimed to analyse the kinetics of T cell persistence and differentiation during the first 10 days following T cell transfer. To determine whether a longer exposure to "self" induced changes in the accumulation or differentiation of the experimental T cells, a similar experiment to the one described above was performed. On day 0, C57Bl/6 $Thy1.2^+$ recipient mice were sub lethally irradiated with 5.5 Gy; 2-3 hours post irradiation they received adoptive transfer of 5 x 10^6 $Thy1.1^+$ $CD4^+$ mock or $Thy1.1^+$ CD3-engineered $CD4^+$ ($CD4^+$ CD3-GFP) or $Thy1.1^+$ CD3-engineered $CD8^+$ ($CD8^+$ CD3-GFP) transduced T cells (cell number was adjusted to transduction efficiency, based on GFP expression). On day 16 post T cell injection the mice were sacrificed and the homing of $Thy1.1^+$ cells investigated in the following four tissues: spleen, inguinal lymph nodes (LN), bone marrow (from one tibia and one fibula; BM) and liver. In addition at day 3 and day 11 post injection serum samples were obtained from peripheral blood, to examine the concentration of inflammatory cytokines, and how their concentration changes over time. Mouse weight was monitored overtime, and as per Home Office regulations mice with > 20% body weight loss were sacrificed. Figure 4.7 shows a schematic representation of the experimental set up.

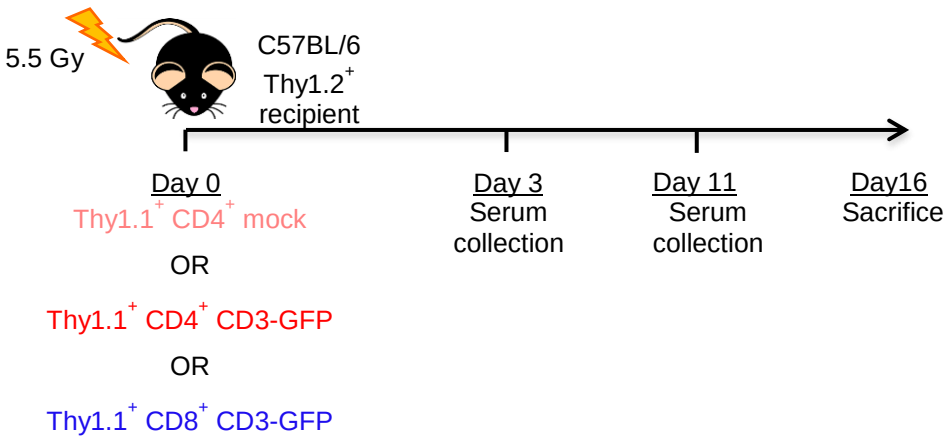

Figure 4.7 – Schematic representation of experimental set up for *in vivo* persistence, homing, differentiation at day 16 post T cell transfer, and cytokine studies.

T cells were MACS sorted and transduced as described in chapter 2 sections 2.23 and 2.2.4, prior to injection on day 3 post transduction. Figure 4.8A shows typical purity of adoptively transferred cells, which in all populations was >90%. Transduction efficiency was twice as much in the CD3-engineered $CD4^+$ population (69%) compared to the CD3-engineered $CD8^+$ population (33%). As with the previous experiments $CD4^+$ mock cells were not transduced with the control-GFP vector, hence the lack of GFP signal in this population. The differentiation status based on CD127 and CD62L expression was also analysed before injection. All three populations presented with identical proportions of naïve-cells ($CD127^+$ $CD62L^+$), ≥70%, $CD127^-$ $CD62L^-$ effector cells (≤1%) and $CD127^+$ $CD62L^-$ memory cells ≤20% (figure 4.8B).

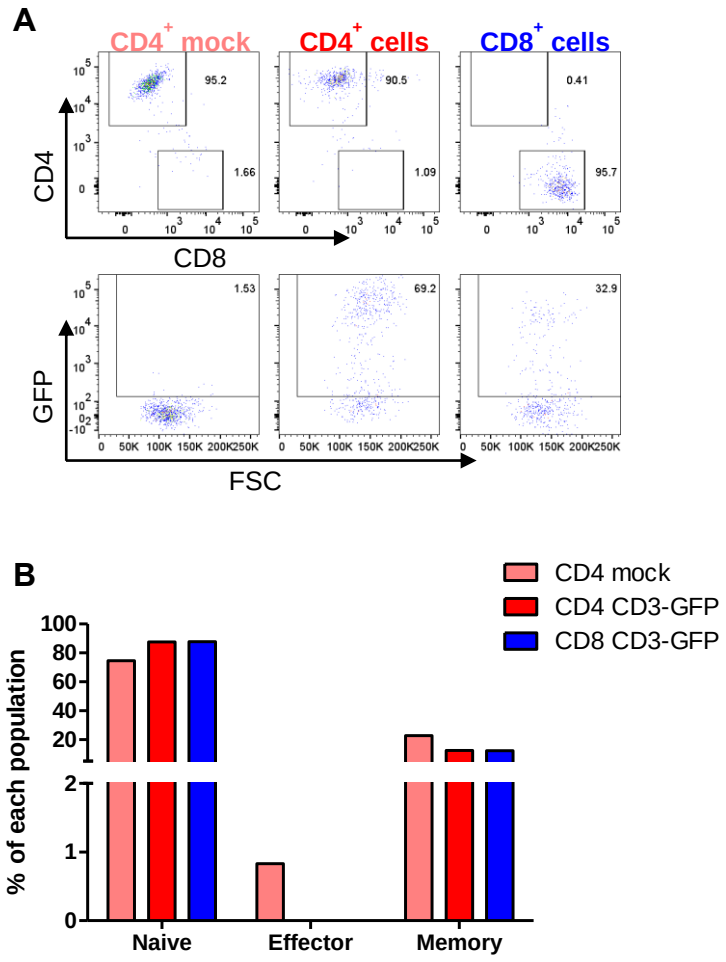

Figure 4.8 – Purity, transduction efficiency and differentiation status of adoptively transferred cells. (A) The purity (top) and transduction efficiency (bottom) of the three populations of experimental cells were analysed on day 3 post transduction, before their injection into recipient mice. (B) CD62L and CD127 expression was examined to determine the phenotype of the injected cells (naïve: $CD62L^{+}$ $CD127^{+}$; effector: $CD62L^{-}$ $CD127^{-}$; memory: $CD62L^{-}$ $CD127^{+}$). Mean values are shown. Data from 1 experiment.

Animal weight was monitored to track their wellbeing and to check for toxicity development. Contrary to the experiments above where the weight of the mice did not drop by more than 20%, by day 16 (the set end point) one of the animals had lost more than 20% of its body weight and for the others there was a downward trend. Figure 4.9A shows the changes of weight compared to baseline.

Ex vivo, spleens were weighed, as previous experiments had shown that mice in the $CD4^+$ CD3-GFP group had significantly enlarged spleens. However no difference in spleen (or mouse) weight was observed in this experiment (figure 4.9B).

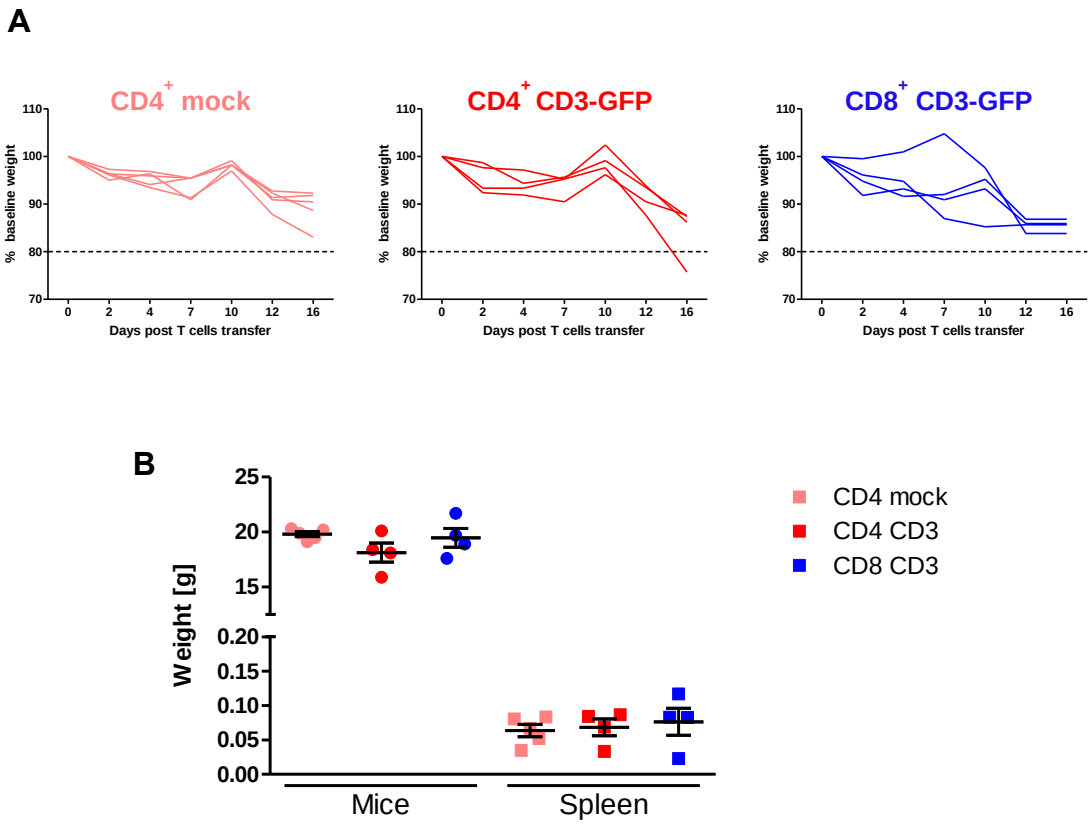

Figure 4.9 – Percentage of mice's body weight overtime and spleen weight. (A) The changes in mice weight are plotted for the three experimental groups. (B) 16 days post T cell transfer the mice and their spleens were weighed. Data from one experiment; $CD4^+$ mock n=5; $CD4^+$ CD3-GFP n=4; $CD8^+$ CD3-GFP n=4. Lines represent mean + SEM.

As for previous experiments, the congenic marker Thy1.1 allowed discrimination of the adoptively transferred cells from the endogenous Thy1.2$^+$ T cells; GFP permitted comparison of CD4$^+$ and CD8$^+$ T cells transduced with CD3-GFP vector. Figures 4.10A and B show the gating strategy used to analyse the single cell suspensions from the four tissues of mice receiving CD4$^+$ mock cells and CD3-engineered T cells, respectively. Summary data showing the percentage of transferred cells recovered from each tissue is shown in figures 4.10C and 4.10D.

The trend in the percentage of Thy1.1$^+$ (CD4$^+$ mock group) or Thy1.1$^+$ GFP$^+$ (CD4$^+$ and CD8$^+$ CD3-GFP groups) isolated at day 16 post T cell transfer was similar to that seen at day 10 post T cell transfer. In all tissues, with the exception of the bone marrow, CD3-engineered CD4$^+$ T cells were recovered in significantly higher percentages compared to CD4$^+$ mock and CD3-engineered CD8$^+$ T cells, and represented 50% or more of the total population of viable Thy1.1$^+$ cells (spleen: 55.78%; LN: 50%; liver: 69.1%) . In the bone marrow the highest percentage of transferred cells was recovered from the CD4$^+$ mock group (89.8%), followed by the CD4$^+$ CD3-GFP group (63.6%), and the CD8$^+$ CD3-GFP group (35.9%). No difference in the proportion of recovered T cells was seen between the CD4$^+$ group and the CD4$^+$ CD3-GFP group in the liver (67.9% and 69.1% respectively). However the percentage of transferred cells recovered from liver-derived single cell suspensions in animals receiving the CD3-engineered CD8$^+$ T cell product was significantly lower compared to both CD4$^+$ experimental groups (41.7%). In both the spleen and lymph nodes the percentage of isolated, experimental T cells was significantly higher in the CD4$^+$ CD3-GFP group compared to either one of the other two experimental groups. In particular, in the spleen 55.78%, 45.9% and 28.9% of transferred cells were recovered from the CD4$^+$ CD3-GFP group, CD4$^+$ mock group and CD8$^+$ CD3-GFP group, respectively. In the lymph nodes the percentage of recovered Thy1.1$^+$ GFP$^+$ cells from the CD4$^+$ CD3-GFP group was 50%; followed by 36.3% of Thy1.1$^+$ cells recovered from the CD4$^+$ mock group; and 31.43% of Thy1.1$^+$ GFP$^+$ cells recovered from the CD8$^+$ CD3-GFP group.

However, no significant difference in the absolute number of transferred cells recovered was seen among the three groups, in any of the tissues (figure 4.10E and F).

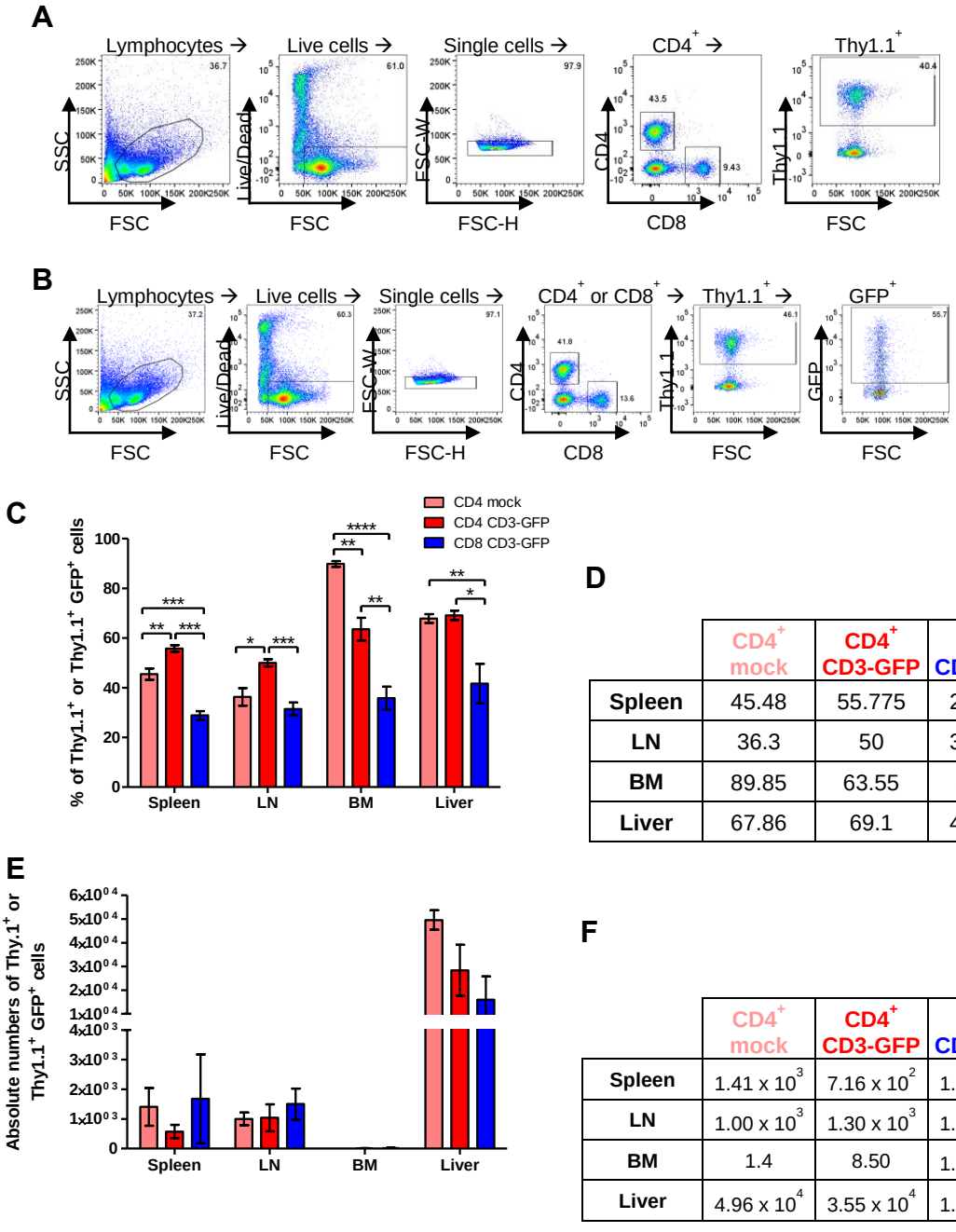

	CD4+ mock	CD4+ CD3-GFP	CD8+ CD3-GFP
Spleen	45.48	55.775	28.875
LN	36.3	50	31.425
BM	89.85	63.55	35.85
Liver	67.86	69.1	41.675

	CD4+ mock	CD4+ CD3-GFP	CD8+ CD3-GFP
Spleen	1.41×10^3	7.16×10^2	1.68×10^3
LN	1.00×10^3	1.30×10^3	1.50×10^3
BM	1.4	8.50	1.28×10^1
Liver	4.96×10^4	3.55×10^4	1.60×10^4

Figure 4.10 – Increased TCR expression in CD4⁺ cells is associated with *in vivo* accumulation. (A) The gating strategy to analysed CD4⁺ mock and (B) CD3-engineered CD4⁺ and CD8⁺ T cells is shown. (C, D) The mean percentages + SEM of recovered transferred cells are shown. (E, F) The mean absolute numbers + SEM of recovered transferred cells are shown. CD4⁺ mock n=5; CD4⁺ CD3-GFP n=4; CD8⁺ CD3-GFP n=4. (p=* ≤0.05; ** ≤0.01; ***≤0.001; **** ≤0.0001; unpaired t test).

4.5. *Ex vivo* phenotype of transferred cells is similar between day 10 and day 16

As for the previous experiment the differentiation phenotype of the recovered cells was examined by looking at their CD62L and CD127 expression. The Thy1.1$^+$ or Thy1.1$^+$ GFP$^+$ cells recovered from the tissues were divided into naïve (CD62L$^+$ CD127$^+$), effector (CD62L$^-$ CD127$^-$) and memory (CD62L$^-$ CD127$^+$) cells.

The phenotypic profile of the transferred cells isolated at day 16 was different to that observed in the experimental populations at the time of injection.

The proportion of naïve T cells recovered from the spleen of mice receiving CD3-engineered CD4$^+$ T cells was significantly lower (21.6%) compared to percentage of naïve cells recovered from both the CD4$^+$ mock group (30.3%) and the CD8$^+$ CD3-GFP group (71%). On the other hand the percentage of adoptively transferred memory CD8$^+$ T cells recovered from the CD8$^+$ CD3-GFP group was the lowest (19.1%) among the three experimental groups. The proportion of memory T cells in the spleen of two CD4$^+$ experimental groups was similar (CD4$^+$ mock: 57%; CD4$^+$ CD3-GFP: 65.8%). Lastly the percentage of effector T cells recovered from the spleen was similar among the three different experimental groups (CD4$^+$ mock: 11.6%; CD4$^+$ CD3-GFP: 12%; CD8$^+$ CD3-GFP: 8.1%) (figure 4.11A). This phenotypic differentiation followed the same trend to that seen in the cells isolated 10 days post T cell transfer (figure 4.6A).

Similarly the percentages of naïve, effector and memory cells isolated from the LN of the three experimental groups, followed the same trend both on day 10 and day 16 (figure 4.11B). Noticeably the lowest percentage of naïve cells was recovered from the CD4 CD3-GFP group (10.5%). This value was significantly lower than both proportions of naïve cells isolated from the CD4$^+$ mock (31.2%) and the CD3-engineered CD8$^+$ group (40.6%). No differences were seen in the percentage of effector cells, which was 5% in the CD4$^+$ mock T cell population, 7.8% in the CD4$^+$ CD3-GFP T cell population, and 8.2% in the CD8$^+$ CD3-GFP T cell population. Finally contrary to the trend seen with naïve

cells, transferred T cells isolated from the CD3-engineered $CD4^+$ group presented with the highest proportion of memory cells (80.9%) out of the three experimental groups. This was significantly higher than the percentage of memory cells recovered both from the $CD4^+$ mock group (62.4%) and the $CD8^+$ CD3-GFP group (49.3%).

Figure 4.11C summarises the phenotype of cells isolated from the bone marrow. The highest proportion of naïve cells was recovered in the $Thy1.1^+$ GFP^+ population isolated from the CD3-engineered $CD8^+$ group (26%); this proportion was significantly higher than that seen in both $CD4^+$ groups ($CD4^+$ mock: 2.7%; $CD4^+$ CD3-GFP: 4.9%). The percentage of effector CD3-engineered $CD4^+$ T cells was 27; that of CD3-engineered $CD8^+$ T cells was 44. The percentage of effector cells isolated from the $CD4^+$ mock group was 43.2% and significantly higher to that of effector CD3-engineered $CD4^+$ T cells. Similarly to the trend seen in both the spleen and the LN, the highest percentage of memory cells was recovered from the population of $CD4^+$ CD3-GFP T cells (63.4%); this value was significantly higher than that of $CD4^+$ mock T cells (53.6%), which in turn was significantly higher to the percentage recovered from population of CD3-engineered $CD8^+$ T cells (24.9%).

The trends seen in the liver for naïve, effector and memory cells were identical to those seen in the spleen, and are summarised in figure 4.11D. Adoptively transferred cells recovered from the $CD8^+$ CD3-GFP group had the highest percentage of naïve cells (28.2%), which was significantly higher than that seen in the population of $CD4^+$ mock T cells (5.9%), which in turn was significantly higher than the percentage of naïve $CD4^+$ CD3-GFP T cells (2.7%). No significant difference in percentages of effector cells was seen between the groups ($CD4^+$ mock: 27.8%; $CD4^+$ CD3-GFP:23.2%; $CD8^+$ CD3-GFP: 38.7%); the highest proportion of memory cells was found in the population of transferred cells isolated from the livers of mice receiving CD3-engineered $CD4^+$ T cells (73.9%). The proportion of memory cells recovered in the $CD4^+$ mock population was 65.9%; the proportion recovered from the $CD8^+$ CD3-GFP cells was 29%.

The analysis of the differentiation profiles of *ex vivo* $CD4^+$ mock, CD3-engineered $CD4^+$ and CD3-enginerrred $CD8^+$ T cells at day 16 post T cell transfer revealed that the T cell phenotype at this time point are comparable to that observed at day 10; at day 16, both $CD4^+$ populations in the bone marrow presented with a memory phenotype, compared to the effector phenotype seen at day 10; and the majority of $Thy1.1^+$ GFP^+ $CD8^+$ T cells isolated from the liver of the $CD8^+$ CD3-GFP group present with an effector phenotype, compared to the naïve phenotype seen at day 10. In addition similar to the trends seen at day 10, $CD4^+$ T cells (both mock transduced and CD3-engineered) followed the same differentiation pattern across all four analysed organs. CD3-engineered $CD8^+$ T cells differentiation is more varied and it's tissue specific. Figure 4.13 summarised the percentages of cells with the different phenotypes, from all tissues and experimental groups.

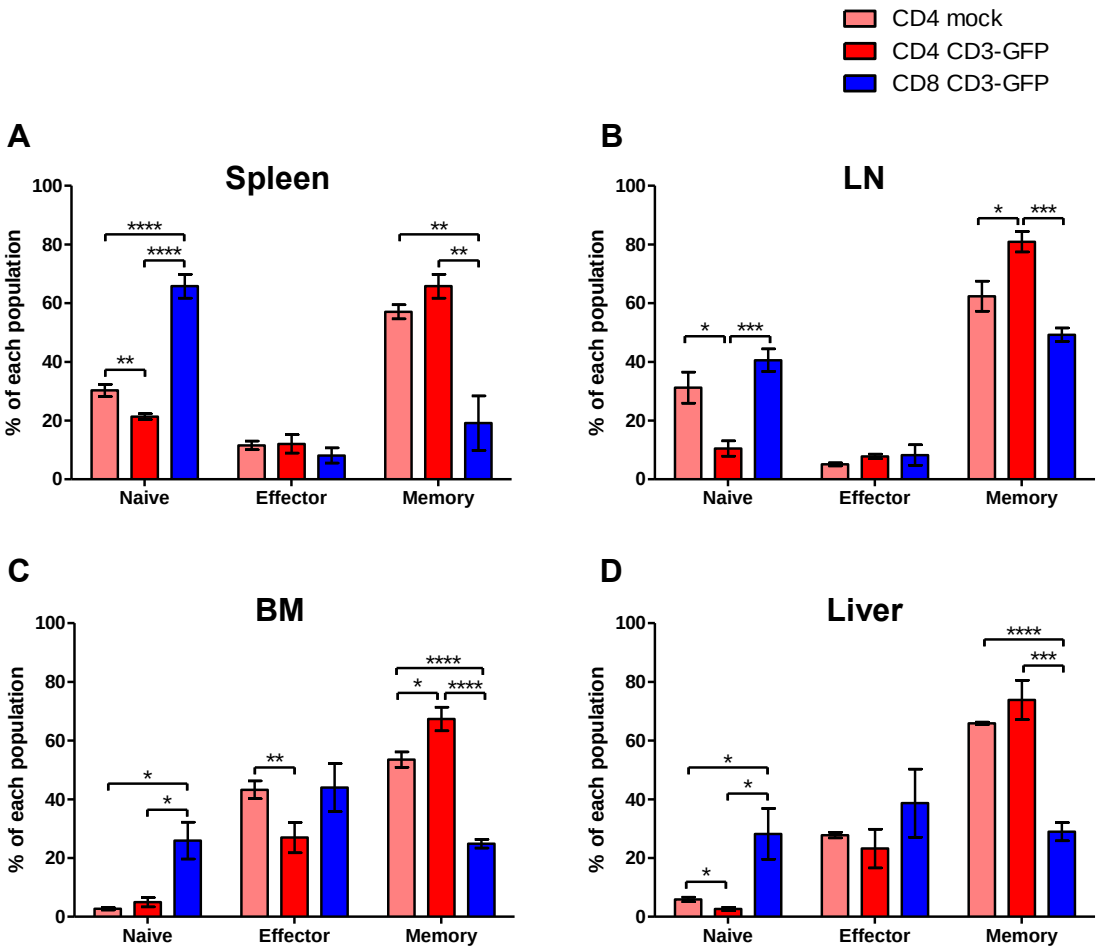

Figure 4.11 – Day 16 ex vivo differentiation status of the adoptively transferred cells. (A-D) The differentiation profile was examined in adoptively transferred cells recovered from the spleen, inguinal lymph nodes (LN), bone marrow (BM) and liver. Cells were divided into naïve ($CD62L^+$ $CD127^+$), effector ($CD62L^-$ $CD127^-$), and memory cells ($CD62L^-$ $CD127^+$). $CD4^+$ mock n=5; $CD4^+$ CD3-GFP n=4; $CD8^+$ CD3-GFP n=4 (p=* ≤0.05; ** ≤0.01; ***≤0.001; **** ≤0.0001; unpaired t test. Mean values + SEM are plotted).

4.6. The *ex vivo* phenotype of transferred $CD4^+$ and $CD8^+$ cells is different from that of $CD4^+$ and $CD8^+$ T cells isolated from the tissues of untreated C57Bl/6 mice

We next examined whether the transferred $CD4^+$ and $CD8^+$ T cells homing to the four different tissues acquire similar phenotypes to those of endogenous $CD4^+$ and $CD8^+$ T cells found in the same tissues, in untreated animals. Single cell suspensions of spleen, LN, BM and liver were generated from the tissues of untreated, non-irradiated C57Bl/6 animals. The expression levels of CD62L and CD127 were analysed in $CD4^+$ and $CD8^+$ populations from the four different tissues, as for previous experiments.

Similar differentiation profiles from $CD4^+$ and $CD8^+$ T cells from the spleen (figure 4.12A) and the lymph nodes (figure 4.12B) were seen.

In the spleen no significant difference in the proportion of naïve or effector cells were seen between the $CD4^+$ and $CD8^+$ T cells. 58.4% of $CD4^+$ T cells isolated from the spleen presented with a naïve phenotype, whereas the proportion of $CD8^+$ T cells with the same phenotype was 72.8%. Effector $CD4^+$ T cells from the same organ accounted for 0.93%, compared to 1.86% of $CD8^+$ effector cells. However memory $CD4^+$ T cells were present in the spleen in a significantly higher proportion compared to $CD8^+$ T cells (33.7% and 8% respectively; $p \leq 0.001$).

74.3% of naïve $CD4^+$ T cells were recovered from the inguinal lymph nodes, compared to 73.9% naïve $CD8^+$ T cells. No difference was seen in the percentages of effector cells, with $CD4^+$ effector T cells accounting for 0.29%, and $CD8^+$ effector T cells accounting for 0.19% of the total $CD4^+/CD8^+$ T cell population. A significantly higher proportion of memory $CD4^+$ T cells were recovered from the lymph node, compared to $CD8^+$ memory T cells (9.76% and 3.24% respectively).

The patterns of $CD4^+$ and $CD8^+$ differentiation in the bone marrow (figure 4.12C) and the liver (figure 4.12D) were also very similar to one another. In both organs significantly higher proportions of $CD8^+$ naïve and effector T cells were recovered, compared to their $CD4^+$ counterparts. Higher proportions of memory $CD4^+$ memory T cells were recovered, compared to $CD8^+$ T cells from both tissues.

In the bone marrow naïve $CD4^+$ T cells accounted for 26.9% of the total viable $CD4^+$ population, compared to 62.6% of naïve $CD8^+$ T cells; in the same tissue 0.49% of $CD4^+$ T cells presented with an effector phenotype, compared to 6.3% of $CD8^+$ T cells. The percentage of $CD4^+$ T cells with a memory phenotype was 65.5%, compared to 11.3% of $CD8^+$ T cells.

In the liver, 37.25% and 0.43% of $CD4^+$ T cells presented with a naïve and effector phenotype, respectively, compared to 71.7% and 3.1% of naïve and effector $CD8^+$ T cells. Lastly, 58.8% $CD4^+$ cells isolated from the liver presented with a memory phenotype, compared to 15.1% of $CD8^+$ cells.

Figure 4.13 summarised the percentages of the different cells' phenotypes, from all tissues and experimental groups.

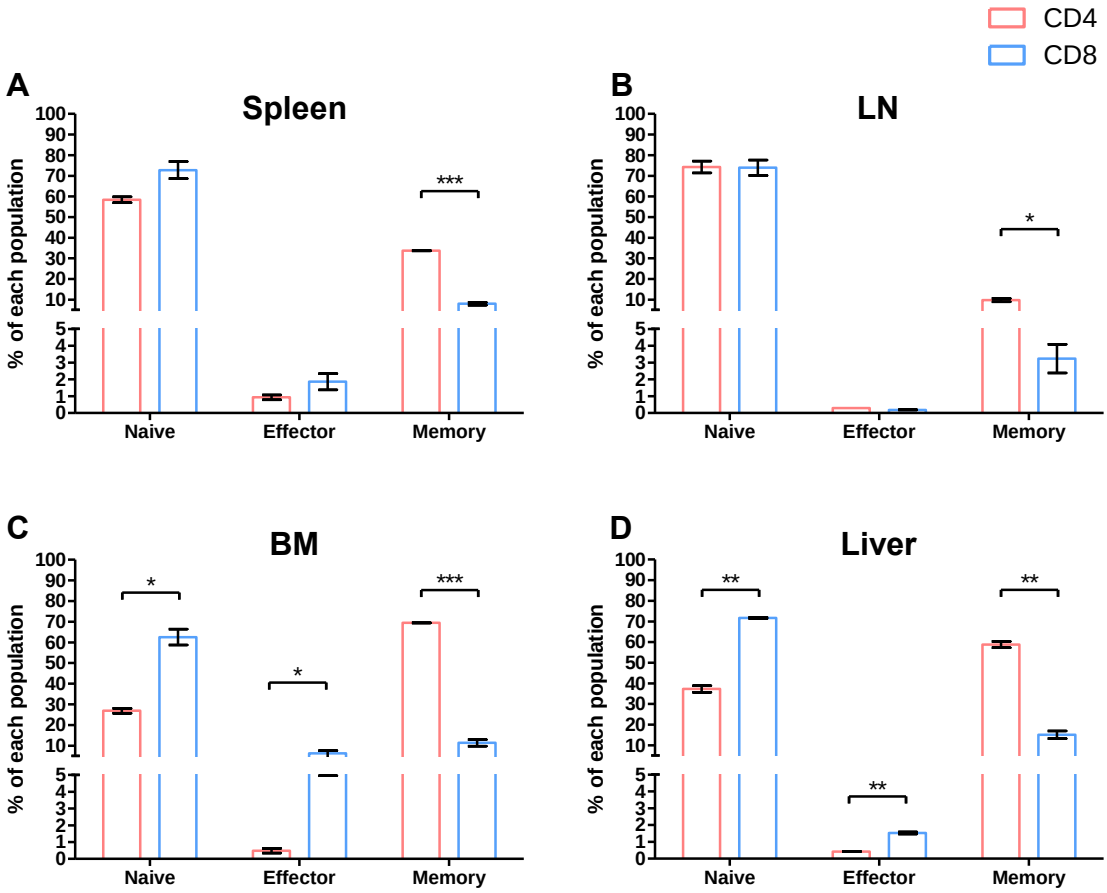

Figure 4.12 – Ex vivo differentiation status of CD4⁺ and CD8⁺ T cells from untreated mice. (A-D) The differentiation profile was examined in CD4⁺ and CD8⁺ T cells isolated from the tissues of untreated mice, to determine the percentage of naïve, effector and memory T cells normally found within those tissues. Cells were divided into naïve (CD62L⁺ CD127⁺), effector (CD62L⁻ CD127⁻), and memory cells (CD62L⁻ CD127⁺). n=2 for each tissue (p=* ≤0.05; ** ≤0.01; ***≤0.001; unpaired t test. Mean + SEM are plotted).

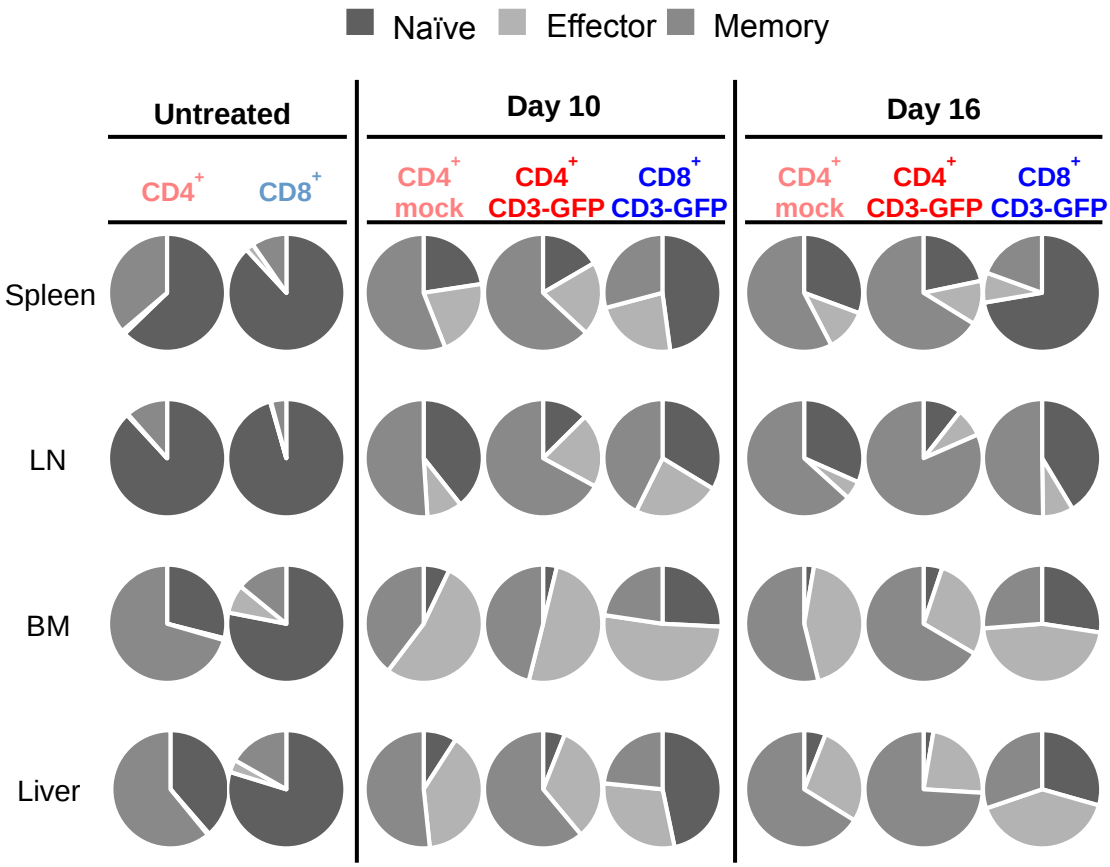

Figure 4.13 – Differentiation status summary data. The average percentage of naïve, memory and effector $CD4^+$ and $CD8^+$ T cells isolated from untreated animals, and at day 10 and 16 post adoptive transfer are shown.

4.7. No difference in serum cytokine profiles observed between mice receiving $CD4^+$ mock, CD3-engineered $CD4^+$ or CD3-engineered $CD8^+$ T cells

Previous experiments showed that $CD4^+$ T cells with enhanced CD3 and TCR expression have a survival advantage over both $CD4^+$ mock and CD3-engineered $CD8^+$ T cells. To investigate if this accumulation is driven by systemic T cell activation, driven by cytokines, we analysed the levels of 13 signature inflammatory cytokines in the serum of the recipient mice (*in vivo* experimental set up is described in figure 4.7). Peripheral blood samples were collected at an early time point (day 3 post adoptive transfer) and a late time point (day 11 post T cell transfer), and the serum isolated as describes in chapter 2, section 2.4.7. Day 3 and day 11 were chosen based on previous experiments, where mice receiving CD3-engineered $CD4^+$ T cells, developed toxicity as early as day 12 post T cell transfer. Day 3 represented an early, baseline time point; day 11 represented the peak of a potential cytokine storm syndrome. LEGENDplex™ technology was used to analyse the serum levels of IL-1α; IL-1β; IL-6; IL-10; IL-12(p70); IL-17A; IL-23; IL-27, GM-CSF; IFNβ; IFNγ; MCP-1 and TNFα, as described in chapter 2, section 2.4.7. This particular set of cytokines was chosen as it contains classical inflammatory cytokines produced upon T cell activation, which are capable of driving both further T cell activation, and also pathology.

Despite the differences in T cell accumulation, no difference in the serum concentration of any of the analysed cytokines was seen, at either day 3 or day 11 post adoptive T cell transfer (figures 4.14, 4.15 and summary data in figure 4.16). Although the levels of some cytokines increased (e.g. IL-6 and TNFα) between day 3 and day 11, this change in concentration was seen in all recipient animals. The mean concentration of the different cytokines, in the mice receiving $CD4^+$ mock, CD3-engineered $CD4^+$ or $CD8^+$ T cells, at day 3 and day 11 are summarised in the figure 4.16.

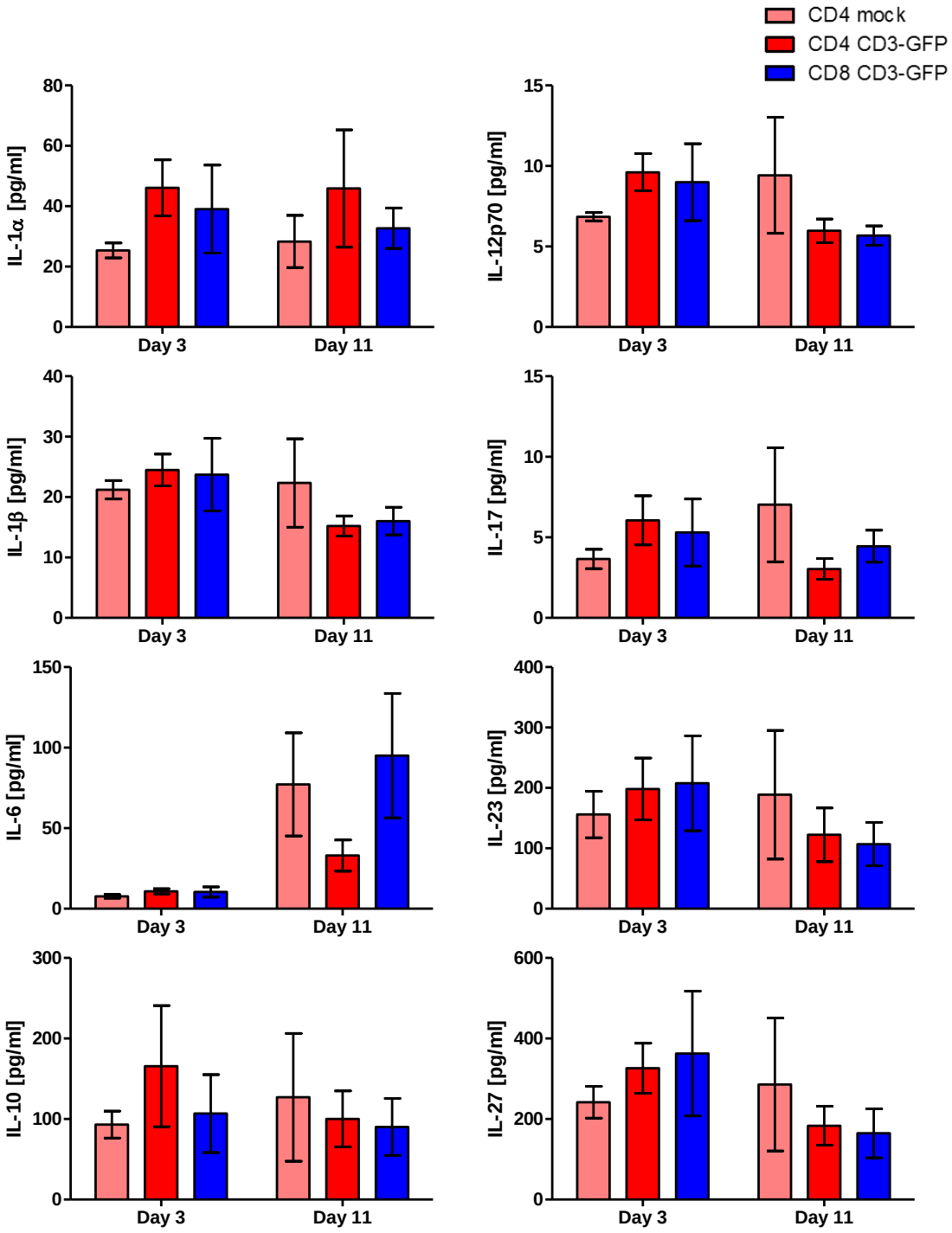

Figure 4.14 – Serum cytokine concentrations. The concentration (pg/ml) of IL-1α; IL-1β; IL-6; IL-10; IL-12(p70); IL-17A; IL-23 and IL-27 in the serum of treated animals, at day 3 and day 11 post T cell transer is shown. Mean values + SEM are plotted.

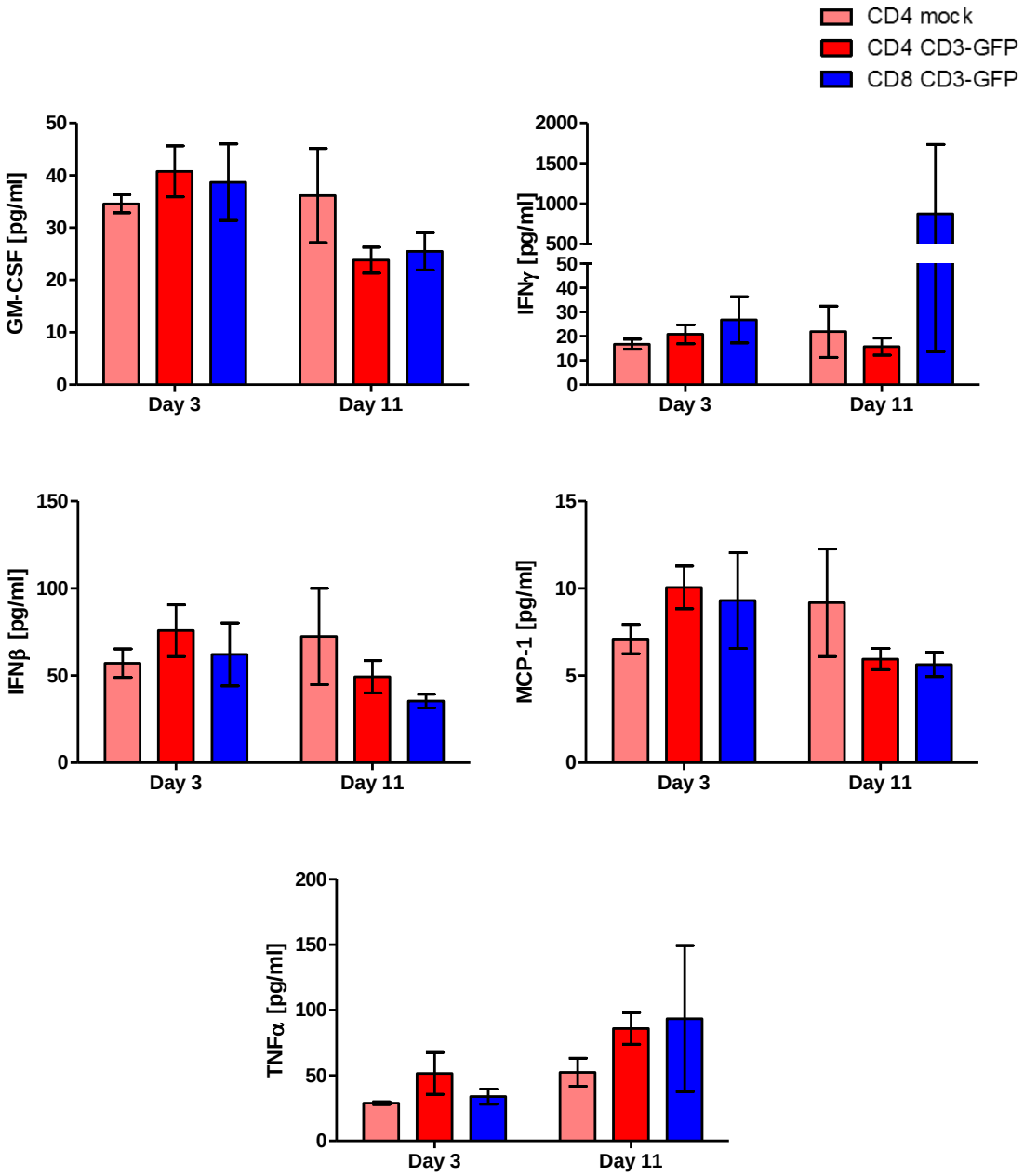

Figure 4.15 – Serum cytokine concentrations. The concentration (pg/ml) of GM-CSF; IFNβ; IFNγ; MCP-1 and TNFα in the serum of treated animals, at day 3 and day 11 post T cell transfer is shown. Mean values + SEM are plotted.

IL-1α		
	Day 3	Day 11
CD4+ mock	25.352	28.324
CD4+ CD3-GFP	46.072	45.88
CD8+ CD3-GFP	39.04	32.73

IL-27		
	Day 3	Day 11
CD4+ mock	241.806	285.776
CD4+ CD3-GFP	326.238	183.454
CD8+ CD3-GFP	362.565	164.625

IL-1β		
	Day 3	Day 11
CD4+ mock	21.226	22.338
CD4+ CD3-GFP	24.478	15.21
CD8+ CD3-GFP	23.7175	16.03

GM-CSF		
	Day 3	Day 11
CD4+ mock	34.57	36.162
CD4+ CD3-GFP	40.776	23.802
CD8+ CD3-GFP	38.705	25.4925

IL-6		
	Day 3	Day 11
CD4+ mock	7.668	77.182
CD4+ CD3-GFP	10.816	33.03
CD8+ CD3-GFP	10.4025	95.065

IFNβ		
	Day 3	Day 11
CD4+ mock	57.122	72.388
CD4+ CD3-GFP	75.756	49.298
CD8+ CD3-GFP	62.1575	35.4175

IL-10		
	Day 3	Day 11
CD4+ mock	93.07	127.026
CD4+ CD3-GFP	165.602	100.096
CD8+ CD3-GFP	106.755	90.1775

IFNγ		
	Day 3	Day 11
CD4+ mock	16.706	21.916
CD4+ CD3-GFP	20.844	15.732
CD8+ CD3-GFP	26.82	874.58

IL-12(p70)		
	Day 3	Day 11
CD4+ mock	6.85	9.42
CD4+ CD3-GFP	9.608	5.976
CD8+ CD3-GFP	8.9925	5.68

MCP-1		
	Day 3	Day 11
CD4+ mock	7.098	9.18
CD4+ CD3-GFP	10.058	5.946
CD8+ CD3-GFP	9.305	5.6375

IL-17		
	Day 3	Day 11
CD4+ mock	3.654	7.026
CD4+ CD3-GFP	6.058	3.036
CD8+ CD3-GFP	5.3	4.4475

TNFα		
	Day 3	Day 11
CD4+ mock	28.922	52.496
CD4+ CD3-GFP	51.596	85.996
CD8+ CD3-GFP	33.87	93.49

IL-23		
	Day 3	Day 11
CD4+ mock	156.042	188.672
CD4+ CD3-GFP	198.286	122.438
CD8+ CD3-GFP	207.7	106.888

Figure 4.16 – Serum cytokines concentration summary data. The mean concentration (pg/ml) of cytokines found in the serum of $CD4^+$ mock, $CD4^+$ CD3-GFP and $CD8^+$ CD3-GFP treated animals are summarised.

4.8. Summary and discussion

The aim of the experiments described in this chapter was to examine whether the higher TCR expression in $CD4^+$ T cells observed *in vitro*, translated into different *in vivo* behaviour. Mature T cells in the periphery continuously interact with self-p:MHC complexes. These interactions, alongside IL-7 signalling, may play a role in T cell maintenance in the periphery (Takada et al., 2009a). Thus we hypothesised that increased TCR expression may favour $CD4^+$ T cell survival over $CD8^+$ cells, as they may be subjected to stronger interaction with "self and stronger TCR signalling.

To test our hypothesis, we set up *in vivo* experiments which allowed us to study the persistence, homing and differentiation profile of adoptively transferred mock transduced $CD4^+$ T cells, CD3-engineered $CD4^+$ T cells and CD3-engineered $CD8^+$ T cells. Indeed $CD4^+$ T cells overexpressing CD3 were recovered in higher percentages (from the spleen, inguinal lymph nodes, bone marrow and liver) compared to mock transduced $CD4^+$ T cells and CD3-engineered $CD8^+$ T cells, both at day 10 and day 16 post T cell transfer. The accumulation of CD3-engineered $CD4^+$ cells was confirmed by both *in vivo* bioluminescent imaging and *ex vivo* analysis of tissues' single cell suspensions. CD3-engineered $CD4^+$ T cell accumulation was also associated with splenomegaly at day 10 in the mice receiving these cells. However no enlarged spleens were seen if the mice were sacrificed at 16 days post T cell transfer. The phenotype of the recovered cells was also analysed *ex vivo* by flow cytometry. Broadly speaking $CD4^+$ T cells, both mock and CD3-engineered, followed the same pattern of differentiation, and this was identical at both day 10 and day 16 post T cell transfer. CD3-engineered $CD8^+$ T cells had a different maturation phenotype (compared to the $CD4^+$ T cells), but again was similar at day 10 and day 16. Analysis of $CD4^+$ and $CD8^+$ T cell populations from the tissues of untreated mice allowed us to examine whether adoptively transferred T cells repopulating these tissues, present with the same differentiation profiles. What we found was that the proportion of naïve cells was lower in the populations of adoptively transferred cells (both $CD4^+$ and $CD8^+$), compared to the percentage of naïve $CD4^+$ and $CD8^+$ T cells found at

steady state; the percentage of effector cells was higher in the *ex vivo* populations of experimental cells, compared to untreated $CD4^+$ and $CD8^+$ T cells. Lastly the percentages of memory cells recovered from the $CD4^+$ and $CD8^+$ populations differs both between themselves, and also from the percentages seen in untreated tissues.

The endpoints of the experiments were set based on previous observations regarding toxicity onset. In previous studies, mice conditioned with the same irradiation dose and receiving a lower dose (1×10^6 transduced T cells) of $CD4^+$ T cells transduced with the CD3-GFP vector, developed toxicity as early as day 12, with the average onset day being between day 15 and 17. Therefore day 10 was determined to be an early time point when adoptively transfer T cells start to infiltrate tissues; day 16 represented the peak time of T cell infiltration into target tissues. However no toxicity, as determined by weight loss, was seen in these set of experiments. Only one mouse lost more than 20% body weight by day 16. In addition other experiments were mice where kept for up to 30 days did not show any sign of pathology (data not shown).

Despite the lack of toxicity, $CD4^+$ T cells modified to express higher levels of CD3 and thus higher levels of TCR accumulated in higher percentages, compared to the other two experimental cell products, in all analysed tissues. Accumulation was confirmed by both *in vivo* bioluminescence and *ex vivo* flow cytometry analysis. *Ex vivo* analysis of the transferred cells at day 10 and day 16 post T cell injection, showed that the greatest accumulation is seen in the $CD4^+$ CD3-GFP population. At day 10 no difference is seen in the accumulation of $CD4^+$ mock and CD3-engineered $CD8^+$ T cells. 16 days post T cell transfer the accumulation of $CD4^+$ mock T cells is inferior to that of CD3-engineered $CD4^+$ T cells, but significantly higher than that of CD3-engineered $CD8^+$ T cells.

In our *in vivo* studies the biological level of TCR is increased to supraphysiological levels in both $CD4^+$ and $CD8^+$ T cells. We hypothesised that increasing TCR expression promotes T cell survival, either by increasing the number and the strength of TCR:self-p:MHC interactions, or by increasing ligand-independent survival signals. A number of *ex vivo* studies have demonstrated that naïve T cells in the periphery exist with basal

levels of CD3ζ phosphorylation (van Oers et al., 1994; Witherden et al., 2000). This was suggested to be a consequence of T cell interaction with self-p:MHC complexes. However whether TCR engagement by self-peptides is required for prolonged *in vivo* survival of naïve T cells is still matter of debate. Dorfman et al. revealed that lack of self-p:MHC:TCR interaction and loss of CD3ζ phosphorylation did not impair T cell persistence (Dorfman et al., 2000). Other studies involving inducible TCR loss showed that absence of TCR leads to a gradual decay of T cells, with $CD8^+$ T cells decaying faster ($t_{1/2}$ 16 days) compared to $CD4^+$ T cells ($t_{1/2}$ 78 days) (Labrecque et al., 2001; Polic et al., 2001); Thus, despite controversial evidence regarding a potential role for TCR engagement by self-p:MHC complexes, TCR expression is fundamental for T cell survival in the periphery.

Our data does not indicates whether the accumulation of CD3-engineered $CD4^+$ T cells is a consequence of increased interaction with "self", or increased ligand-independent signalling. To determine what mechanism is indeed driving T cell accumulation *in* vivo, analysis of the cell surface protein CD5 expression could be useful. Increasing evidence shows that differences in the expression of CD5 can be used to assess the strength of TCR;self-p:MHC interactions (Fulton et al., 2015; Tarakhovsky et al., 1995; Smith et al., 2001; Wong et al., 2001). In particular high CD5 levels correlate with stronger interaction with MHC molecules. Indeed *ex vivo* analysis of CD5 levels on the transferred cells would allow us to determine whether T cell persistence requires TCR:self-p:MHC contact, or whether it is a ligand-independent mechanism. In the first case, higher CD5 expression would be expressed on the accumulating cells, compared to mock $CD4^+$ and CD3-engineered $CD8^+$ T cells; in the latter case similar levels of CD5 would be expected on all experimental T cells populations. Alternatively, the experimental cells could be adoptively transferred into MHC-II deficient hosts, and their survival analysed. Lack of accumulation in this setting would suggest TCR:self-p:MHC interactions play a role in *in vivo* T cell persistence. Analysis of CD3ζ phosphorylation levels may also indicate the extent of interaction with self, as discussed above.

One controversy however is generated by our *in vitro* data. *In vitro* analysis showed that $CD8^+$ T cells transduced with the CD3-GFP vector express higher TCR levels compared to $CD4^+$ mock cells (figure 3.6). However, we cannot determine from our *in vivo* data what were the TCR levels on the adoptively transferred cells were at takedown day. TCR downregulation occurs after TCR engagement and prevents aberrant T cell activation. Indeed a recent report by Gallegos et al. has shown that activated $CD4^+$ and $CD8^+$ T cells at the peak of their clonal expansion after antigenic stimulation, downregulate their TCR. The proportion of TCR downregulation correlates with the strength of stimulation, with higher affinity and higher avidity TCRs, being downregulated to a greater extent compared to lower affinity TCRs, recognising the same antigen (Gallegos et al., 2016). Although our system does not alter the affinity of the TCR pool, nor provides foreign antigenic stimulation, TCR avidity is greatly increased, as shown in the context of antigen-specific stimulations (Ahmadi et al., 2011). Increasing the avidity of the endogenous TCR pool leading to an increase in the strength of interaction with "self" may initiate a negative feedback mechanism in our experimental CD3-engineered T cells, similar to that described by Gallegos and colleagues. TCR downregulation in turn may correlate with decrease $CD8^+$ T cell survival and a lower percentage of recovered experimental $CD8^+$ T cells. TCR downregulation may also occur in CD3-engineered $CD4^+$ T cells as between day 10 and day 16 there's a 10% drop in the percentage of recovered cells. This decrease in recovered cells is more profound in $CD8^+$ T cells where in all organs but the lymph nodes, it's 15% or more. CD3-engineered $CD4^+$ T cells subjected to TCR downregulation may still express enough TCR (and a higher level of it compared to CD3-engineered $CD8^+$ T cells) to promote their persistence. The physiological TCR levels and avidity of the unmanipulated $CD4^+$ mock T cells may allow for these cells to persist for longer *in vivo*. Indeed in the spleen and lymph nodes no difference in the percentage of recovered $CD4^+$ mock cells was seen between day 10 and day 16 (figures 4.5D and 4.10D).

Alternatively $CD8^+$ T cells may be subjected to greater TCR downregulation. As suggested in chapter 3, the ubiquitous expression of MHC-I molecules may lead to a higher number of interactions between $CD8^+$ T cells and self-peptides, which may maintain TCR levels low and may correlate with a lower activation threshold, compared to $CD4^+$ T cells. Thus this latter population may be subjected to less TCR downregulation, allowing accumulation of the $CD4^+$ T cell population to a greater extent.

TCR downregulation kinetics studies by Gallegos et al. showed that TCR is downregulated by day 15 post T cell transfer. This finding is in line with the kinetics of decrease cell accumulation we see at day 16 post T cell transfer in our *in vivo* experiments.

Similar *in vivo* experiments where adoptively transferred $CD4^+$ and $CD8^+$ T cells express the same levels of TCR, or where TCR downregulation is prevented, for example by modifying the CD3 motifs involved in TCR downregulation, would allow us to test our hypothesis regarding TCR downregulation playing a role in T cell persistence.

All of our *in vivo* experiments were carried out in lymphopenic animals, as a consequence of the 5.5 Gy sub lethal irradiation, a step that is necessary for the engraftment of the adoptive T cells. Once injected the cells will undergo lymphopenia induced proliferation (LIP). Increasing evidence suggests that the homeostatic proliferation in a lymphopenic environment is radically different to that seen in physiological, non lymphopenic conditions (Almeida et al., 2005; Surh et al., 2008). Lack of endogenous immune cells in lymphopenic animals means adoptively transferred T cells have greater access, and increased sensitivity to the available homeostatic factors (IL-7 and self-p:MHC complexes). Indeed polyclonal T cells rely on interaction with self-p:MHC complexes and IL-7 signalling for proliferation in lymphopenic settings, as LIP is impaired in mouse models where either one of those is absent (Tan et al., 2001; Ernst et al., 1999). Although we can't rule out the presence of different signals in the different recipient animals in our system, the conditions in the three different experimental groups were constant. Syngeneic animals were used as recipients in all experimental groups, and they all

received 5.5 Gy sub lethal irradiation. Thus we can assume that our adoptively transferred T cells were transferred into the same lymphopenic environment, and experienced the same survival and expansion signals. Therefore any difference in their survival could be attributed to their different TCR expression.

The differences in the numbers of transferred cells recovered at day 10, mirror the differences in the percentages of recovered cells. However no difference is seen among the numbers of recovered cells at day 16, despite significant differences in the percentages. The absolute number of cells was calculated as the number of transferred cells in the total lymphocytes population (determine by FACS gating; figures 4.5A and B, and 4.10A and B). Similar number of cells but lower percentages indicate that in the mice receiving the $CD4^+$ mock cells or the CD3-engineered $CD8^+$ cells the lymphocyte population contains a higher proportion of host lymphocytes. Since this is only seen at day 16 post T cell transfer, it may indicate a repopulation of the lymphocyte pool (T and B cells, NK cells, DCs, macrophages) following irradiation. However why this repopulation is not seen in the mice receiving the CD3-engineered $CD4^+$ T cells is not known. Since the absolute numbers of recovered cells are the same, lack of “space” in the tissue should not be the cause. Tanchot et al. have shown that adoptively transferred transgenic T cells are rapidly replaced by host thymic emigrants when transferred into lymphopenic congenic hosts (Tanchot et al., 2002). The repopulation of the tissues described above may be an indication of this replacement taking place. However our injected cells represent a polyclonal population, thus they might be subjected to different survival mechanisms, which may lead to a different outcome compared to that seen by Tanchot and colleagues. How CD3-overexpressing $CD4^+$ T cells interact with their surroundings and prevents niche repopulation is unknown.

Overall the number of recovered cells from all experimental groups, from all analysed tissues, is lower at day 16 compared to day 10. Thus the higher percentage of cells is either a consequence of increased proliferation, with similar levels of cell death; or increased cell death, with similar levels of proliferation. Further experiments analysing

cell proliferation (e.g. Ki67 expression), or the levels of cell death (e.g. Annexin V expression) are needed to investigate which one of the scenarios described above is responsible for the differences seen in T cell accumulation.

At both analysed endpoints the majority of CD3-engineered $CD4^+$ T cells were recovered from the liver, followed by the bone marrow, the spleen and the lymph nodes. Similar accumulation trends were also seen for the other two experimental groups. The decision to look at those four tissues as targets for T cell trafficking was based on previous experimental data which indicated CD3-overexpressing T cells preferentially home to these tissues. Other tissues (e.g. dermis and epidermis) were analysed for T cell homing, but no transferred cells were recovered, suggesting they were not homing targets (data not shown), or our assays were not sensitive enough to detect very small numbers of transferred cells at these sites. What promotes T cell trafficking into the spleen, lymph nodes, bone marrow and liver, over other tissues may reside in the organs' primary functions. The spleen, lymph nodes and bone marrow are classic lymphoid organs, through which T lymphocytes normally circulate and where lymphocytes home. In addition abundant evidence now supports the concept that the liver acts as a secondary lymphoid organ too (Crispe, 2009).

Naïve unstimulated lymphocytes normally spend between half a day to a day within a lymphoid organ, surveying it for antigen presence, after which they return to the circulation (Cyster, 2003). However the trafficking pattern of T cells changes after their differentiation into memory cells. Increased availability of homeostatic factors during lymphopenia is thought to drive not only expansion but also differentiation into a memory-like phenotype (Jameson, 2002). Indeed memory cell phenotype was confirmed by our *ex vivo* differentiation data (discussed later in this section). In particular our memory cells were L-selectin (CD62L) low, and IL-7 receptor (CD127) positive, suggesting they were effector memory T cells (T_{EM}). T_{EM} are found both in all secondary lymphoid tissues (Weninger et al., 2001) and can also enter peripheral tissues (Mora et al., 2006), thus corroborating our trafficking data. Analysis of homing receptors expressed on our

subsets of cells would give better insights on what specific interactions drive their homing into these specific tissues. For example expression of CXCR4, the CXCL12 receptor, on the transferred cells would account for their trafficking into the CXCL12-rich bone marrow environment. Otherwise, although no specific liver homing molecules have been identified yet, high levels of the vascular adhesion protein-1 (VAP-1) may promote trafficking into this tissue (Lalor et al., 2002).

The differentiation status of the $CD4^+$ mock, CD3-engineered $CD4^+$ and CD3-engineered $CD8^+$ T cells was also analysed, both before injection and *ex vivo*. The expression of L-selectin (CD62L), a cell adhesion molecule driving homing of T lymphocytes into secondary lymphoid tissues; and the IL-7 receptor (CD127), a protein fundamental for IL-7 signalling and T cell survival, was analysed by flow cytometry. For successful retroviral transduction the target cells need to be proliferating, as retroviruses will not infect quiescent cells. Thus all of our cells produced for adoptive transfer, including the $CD4^+$ mock population were initially stimulated with anti-CD3/CD28 beads, in the presence of IL-2. Despite this initial activation, the majority of the cells maintained a naïve phenotype, as demonstrated by their $CD62L^+$ $CD127^+$ phenotype (figures 4.2B and 4.8B). In both cases 80% or more of the cells presented with a naïve phenotype; memory cells accounted for 20% or less; and the percentage of effector cells was negligible (1% or less).

Adoptive transfer of the cells promoted T cell differentiation into effector and memory T cells (figures 4.6B-E and 4.11A-D). The differentiation followed by the adoptively transferred cells is distinct from that which naturally occurs during an antigen response. In our experimental model, no external antigen was present to activate T cells, and the mice were lymphopenic. As previously described during LIP, T cells not only expand but also acquire a memory-like phenotype (Jameson, 2002). This is thought to be a consequence of stronger TCR and IL-7 signalling, caused by the lower competition for survival signal to which the adoptive transferred cells are exposed to. Moreover, it has

been suggested that the LPS released from the gut after irradiation may promote T cell activation and differentiation (Ferreira et al., 2000).

Indeed, our data has shown that the majority of $CD4^+$ T cells (both from the $CD4^+$ mock and $CD4^+$ CD3-GFP group) isolated from the tissues had a memory phenotype, both at day 10 and day 16 post T cell transfer. However $CD8^+$ T cell differentiation followed different trends compared to $CD4^+$ T cells, and memory $CD8^+$ T cells were recovered from the lymph nodes only. The reason behind this difference is unknown. Previous reports suggested that $CD8^+$ T cells may survive better and undergo homeostatic proliferation faster than $CD4^+$ T cells (Jameson, 2002), suggesting $CD8^+$ T cells undergoing LIP should acquire a memory phenotype faster than $CD4^+$ T cells. This higher proliferation rate may be the consequence of the different mechanisms that support $CD4^+$ and $CD8^+$ T cell LIP. $CD8^+$ T cells require IL-7 produced by stromal cells; $CD4^+$ T cells require IL-7 production by haematopoietic cells. Guimond and colleagues showed that IL-7R signalling on DCs limits their IL-7 production, thus limiting $CD4^+$ T cell expansion (Guimond et al., 2009). However it has been shown that T cells with high-affinity TCR for self-p:MCH ligands undergo LIP at faster rates, compared to low affinity T cells, as shown by Kassiotis and colleagues (Kassiotis et al., 2003). Higher affinity TCR lead to stronger TCR signalling compared to lower affinity ones; as previously discuss, increasing the levels of TCR expression and avidity of a T cell by providing extra CD3 genes may have the same overall results (stronger TCR signalling) to that of increasing TCR affinity. Thus in our model the rate at which CD3-engineered $CD4^+$ T cells undergo LIP may be higher than that of CD3-engineeered $CD8^+$ T cells, due to their higher TCR expression, promoting their differentiation into memory cells.

What our data has demonstrated is that $CD4^+$ and $CD8^+$ T cell differentiation is determined by the T cell lineage ($CD4^+$ or $CD8^+$), by LIP, and also by the site of homing. Indeed both $CD4^+$ mock and CD3-engineered $CD4^+$ T cell population, independently of their TCR expression levels, follow the same pattern of differentiation, which is however different in different tissues, and at different time points. Influence of homing on the

differentiation is more marked in the $CD8^+$ T cell population, where cells with different phenotypic profiles are recovered from different tissues. However whether the transferred cells acquire the specific phenotype once in the tissue, or whether they differentiated elsewhere and are then recruited into the specific tissues due to their phenotype is not known.

Broadly speaking the differentiation profiles of the transferred $CD4^+$ and $CD8^+$ T cells do not change between the two takedown time points. This suggests that the cells differentiate early after adoptive transfer, and maintain their differentiated profile up to 16 days post T cell transfer. Whether this phenotype represents a fully differentiated and terminal state, or whether T cells are only temporarily expressing this phenotype due to the signal they are receiving, is unknown. In similar adoptive transfer experiments where transgenic T cells were transferred into congenic hosts, the injected naïve T cells acquired a memory-like phenotype which remained stable with time, even in the absence of antigenic stimulation (Tanchot et al., 2002).

Notably the time window between the two takedown points (day 10 and day 16) is not substantial. This may explain the lack of a difference in both T cell differentiation profile and T cell accumulation, between day 10 and day 16. Lengthier experiments, during which the adoptively transferred T cells are exposed to "self" for longer, may give different results, both in terms of T cell persistence, and T cell differentiation.

Indication that the differentiation pattern is not fully dictated by the T cell lineage or CD3-overexpression also comes from *in vitro* analysis of the transduced cells. CD3/CD28 activated T cells cultured in the presence of IL-2 for up to 7 days post transduction, mainly differentiate into an effector phenotype (figure 3.8C), a different trend from that observed *in vivo*. A role for LIP in influencing T cell differentiation, is suggested by the different *ex vivo* differentiation profiles of adoptively transferred $CD4^+$ and $CD8^+$ T. These differ from the phenotypic profiles of $CD4^+$ and $CD8^+$ T cells isolated from untreated naïve animals. Perhaps not surprisingly, in the spleen and lymph nodes of unchallenged mice over 50% of the isolated $CD4^+$ and $CD8^+$ T cells present with a naïve ($CD62L^+$ $CD127^+$) phenotype.

The same is true for $CD8^+$ T cells isolated from the bone marrow and the liver. In contrast $CD4^+$ T cells isolated from the bone marrow and liver of unchallenged mice presented with a memory phenotype. Indeed, it has been previously shown that the bone marrow is a reservoir for both central and effector memory T cells (di Rosa et al., 2016). Similarly the liver can act as a secondary lymphoid organ and memory cells are found within this organ (Crispe, 2009). After irradiation and adoptive T cell transfer, the cells reconstituting the spleen, lymph node, bone marrow and liver lymphocyte pools, are phenotypically different from the T cells originally found in the tissues. Based on our data and on what has been discussed previously, we can attribute this difference to the conditioning regime (5.5 Gy irradiation) of the mice that drives LIP.

Suggestion that tissue specific signals rather than systemic ones, impart different phenotypic profiles on the T cells is also suggested by the lack of increased systemic cytokines. Blood samples were collected at day 3 and day 11 post T cell transfer, and the serum was isolated. Day 3 and day 11 time points were chosen to track any change in the systemic cytokine profile, which may drive adoptive T cell proliferation. The concentration of classical inflammatory cytokines (IL-1α; IL-1β; IL-6; IL-10; IL-12(p70); IL-17A; IL-23; IL-27, GM-CSF; IFNβ; IFNγ; MCP-1 and TNFα) was analysed. All of these cytokines have a role in promoting inflammation by triggering the expression of genes involved in cell's activation, cell's trafficking, and secondary cytokine production, among others. Increase in the concentration of inflammatory cytokines may also indicate the onset of a cytokine storm. For example, increased serum cytokine levels in the serum of mice receiving CD3-engineered $CD4^+$ T cells, but not in that of animals receiving CD3-engineered $CD8^+$ T cells, may indicate a potential mechanism to drive the previously observed toxicity. However our data did not show changes in the concentration of any of the analysed cytokines. IL-6 and TNFα were the only two cytokines whose concentration increased between day 3 and day 11. However the increase was seen in all three experimental groups. Whether this increase was caused by the adoptive transfer of the cells or by the conditioning regimen was not tested in our experiment. Irradiation has

previously shown to cause an increase in TNFα production in wildtype mice irradiated with 2 Gy (Kang et al., 2009). Similarly IL-6 production is also increased after *in vivo* irradiation (Neta et al., 1992). To conclude our data does not indicate that adoptive transfer of $CD4^+$ mock, or CD3-engineered $CD4^+$, or CD3-engineered $CD8^+$ T cells alters serum cytokine concentration, nor initiates a cytokine storm.

Notably, in the experiments examining the transduced cells 16 days post adoptive transfer, the transduction efficiency of the $CD8^+$ population was significantly lower to that of the CD3-engineered $CD4^+$ population (70% and 32% respectively). Although the number of transduced (GFP^+) cells that was injected was the same (5×10^6), the number of bystander cells in this groups will be more than double, compared to the $CD4^+$ CD3-GFP group. Thus the frequency of transduced cells in the total population is lower. Whether this low concentration of experimental cells, and the high number of untransduced, bystander cells affects the *in vivo* behaviour of the experimental cells is unknown. It can be postulated that transduced cells will have less access to the homeostatic signals because of a higher number of competitor cells. Indeed this would affect their *in vivo* persistence and differentiation. Whether adoptive transfer of a $CD8^+$ population with better transduction efficiency will have led to different results is unknown. However, *ex vivo* analysis at day 10 post T cell transfer, in experiments were transduction efficiencies were similar between CD3-engineered $CD4^+$ and $CD8^+$ T cells showed that CD3-engineered $CD8^+$ T cells still accumulate to a lower extent compared to their $CD4^+$ counterparts.

In conclusion what our *in vivo* experiments have shown is that $CD4^+$ T cells engineered to express higher levels of CD3 and as a consequence higher levels of endogenous TCR. They accumulate in greater percentages than $CD4^+$ cells expressing physiological levels of TCR (mock $CD4^+$) or CD3-overexpressing $CD8^+$ T cells. Because of the similar differentiation kinetics between mock $CD4^+$ T cells and CD3-engineered $CD4^+$ T cells we proceeded to determine whether TCR expression favours accumulation in the context of *in vivo* competition assays. The results of these experiments are described in chapter 5.

5. *In vivo* functional analysis of $CD4^+$ control-GFP and $CD4^+$ CD3-GFP T cells

5.1. Introduction

The data described in the previous chapters demonstrated that $CD4^+$ T cells engineered to express higher levels of CD3 and TCR accumulate in higher percentages compared to CD3-engineered $CD8^+$ T cells, at both 10 days and 16 days post adoptive transfer, when the proportion of CD3-engineered $CD8^+$ T cells was also significantly lower than that of $CD4^+$ mock T cells. We hypothesised that this difference in T cell accumulation was a consequence of higher TCR expression in the $CD4^+$ T cells overexpressing CD3.

These experiments were carried out using lymphopenic recipients, receiving only one population of transduced T cells (mock $CD4^+$, or $CD4^+$ CD3-GFP, or $CD8^+$ CD3-GFP). As a consequence the adoptively transferred T cells did not have to compete with endogenous cells for survival signals. The only cells competing with the transduced cells for survival signals, were the untransduced cells present in the same population.

To examine whether the supraphysiological levels of TCR expressed by CD3-engineered $CD4^+$ T cells drive accumulation of this population in competitive settings too, a new set of *in vivo* studies was set up. In particular, $Thy1.2^+$ $CD45.2^+$ C57Bl/6 recipient mice received a known mix (1:1, 2:1 or 1:2) of $CD45.1^+$ control-GFP transduced $CD4^+$ T cells and $Thy1.1^+$ CD3-GFP transduced $CD4^+$ T cells. The changes in the proportion of $Thy1.1^+$ and $CD45.1^+$ cells in the total GFP^+ population, were then tracked over time.

Previous reports have shown that transgenic T cells after antigenic stimulation downregulate their TCR at the peak of their clonal expansion (Gallegos et al., 2016). The extent of TCR down-regulation correlates with the affinity and the avidity of the TCR for its cognate p:MHC complex. Thus, we hypothesised that although CD3-overexpressing

$CD4^+$ T cells will have a persistence advantage over $CD4^+$ control-GFP cells, their continuous, stronger interaction with "self" may drive TCR down-regulation.

The levels of $Ki67^+$ and Annexin V^+ within the two transduced cells populations were also tracked over time, to determine whether any difference in T cell accumulation was driven by increased cell proliferation, or decreased cell death.

5.2. CD3 overexpression promotes accumulation of $CD4^+$ T cells in 1:1 competition settings

Initial experiments were performed to compare in vivo persistence of CD3-engineered $CD4^+$ T cells, when these are transferred into a lymphopenic recipient in a 1:1 mix with control-GFP transduced $CD4^+$ T cells. On day 0 C57Bl/6 $Thy1.2^+$ $CD45.2^+$ recipient mice were sub lethally irradiated with 5.5 Gy; 2-3 hours post irradiation they received adoptive transfer of a mix of 2.5×10^6 $CD45.1^+$ control-GFP transduced $CD4^+$ and 2.5×10^6 $Thy1.1^+$ CD3-GFP transduced $CD4^+$ T cells in a 1:1 ratio. Because transduction efficiency was not 100% the number of adoptively transferred cells was adjusted according to the efficiency of transduction, in order to inject 5×10^6 total transduced cells. At day 10 post injection the mice were sacrificed and the homing of GFP^+ $CD45.1^+$ and GFP^+ $Thy1.1^+$ cells to four tissues was investigated: spleen, inguinal lymph nodes (LN), bone marrow (from one tibia and one fibula; BM) and liver. Mouse total weight was monitored on over time, and as per Home Office regulations mice with > 20% body weight loss were culled. Figure 5.1 shows a schematic representation of the *in vivo* experimental set up.

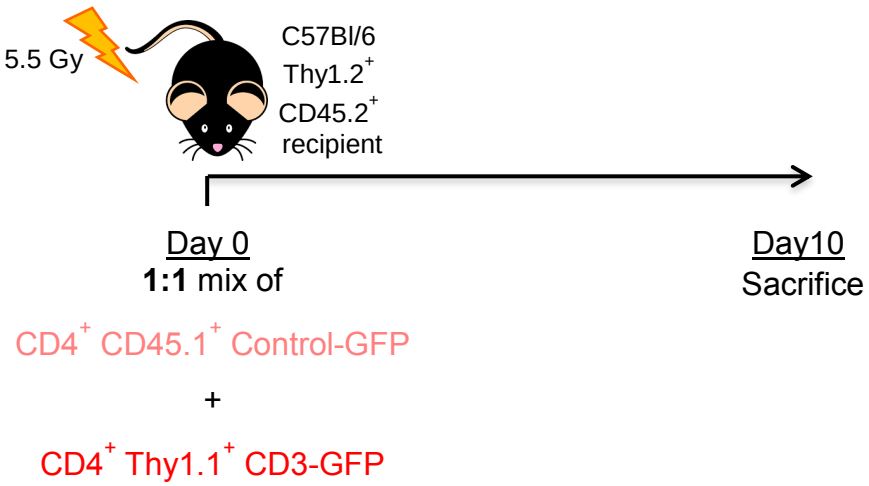

Figure 5.1 – Schematic representation of experimental set up for in vivo persistence, homing and differentiation studies in a 1:1 competition environment.

$CD4^+$ T Cells were MACS sorted and transduced as described in chapter 2 sections 2.2.3 and 2.2.4, prior to injection on day 3 post transduction. Figure 5.2A shows typical purity of adoptively transferred cells, which was >95%. The injection mix was analysed by flow cytometry to check the ratio of control-GFP to CD3-GFP cells. GFP expression allowed us to compare transduced cells from both the control-GFP and the CD3-GFP transduction. The congenic markers CD45.1 and Thy1.1 allowed us to separate control-GFP and CD3-GFP transduced cells respectively (figure 4.2A). The average proportion of control-GFP and CD3-GFP cells injected is shown in figure 4.2B. The injection mixes contained on average very similar proportions of control-GFP (48.15%) and CD3-GFP (47.6%) transduced $CD4^+$ T cells. The differentiation status based on CD127 and CD62L expression was also analysed before injection (figure 5.2C). Figure 5.2D shows representative plots of CD62L and CD127 expression in the control-GFP and CD3-GFP populations. At the time of injection both populations had similar proportions of $CD127^+$ $CD62L^+$ naïve cells (control-GFP: 74.15%; CD3-GFP: 62.1%); $CD127^-$ $CD62L^-$ effector cells (control-GFP: 2.27%; CD3-GFP: 5.94%) and $CD127^+$ $CD62L^-$ memory cells (control-GFP: 15.35%; CD3-GFP: 13.65%) (figure 5.2E).

Weight was used to monitor the wellbeing of the animals. No toxicity was seen in these experiments and the changes in body weight observed throughout the experiments are plotted in figure 5.3.

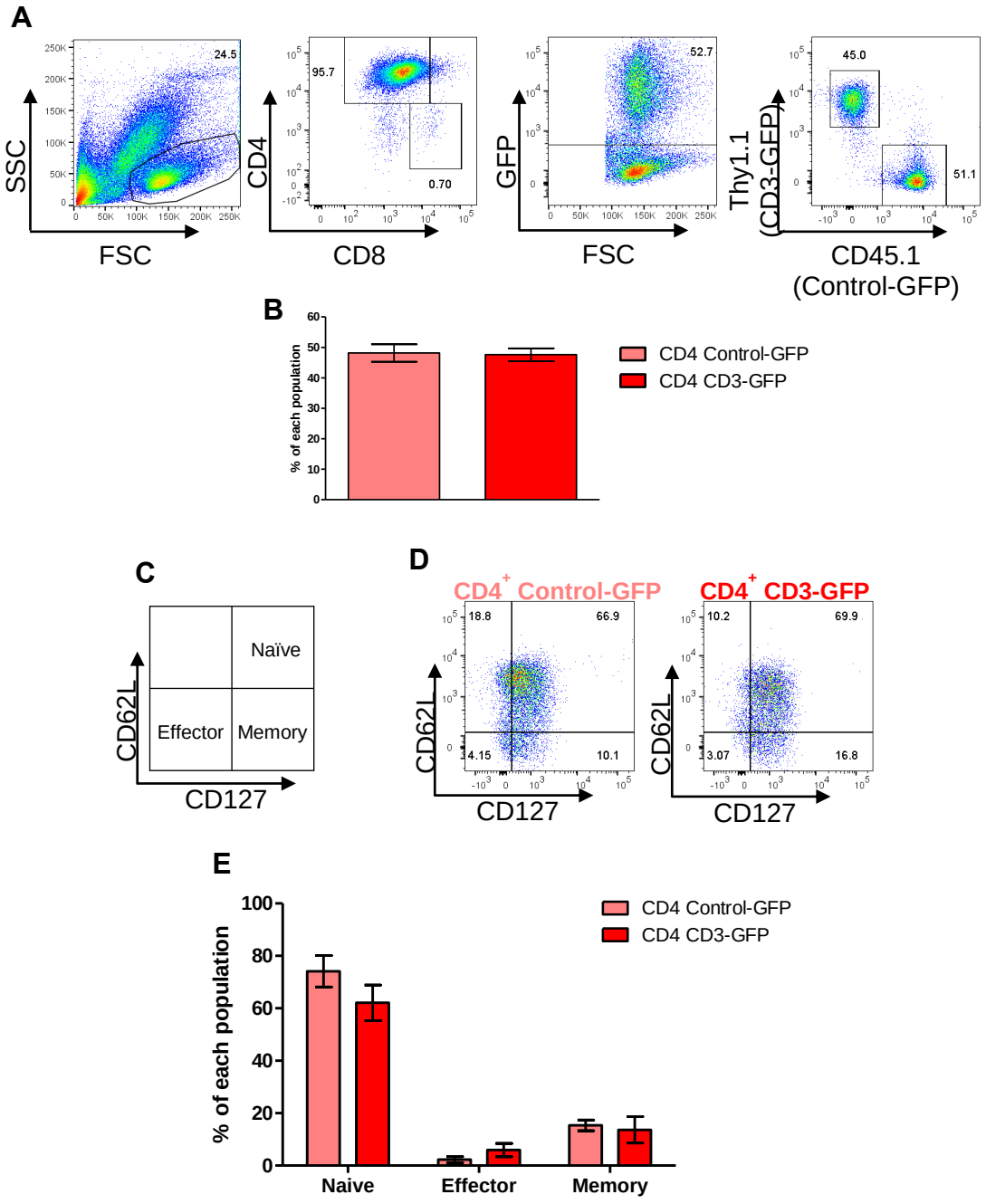

Figure 5.2 – Purity, transduction efficiency, injection mix ratio and differentiation status of adoptively transferred cells, in the 1:1 competition experiments. (A) Typical purity, transduction efficiency and control-GFP:CD3-GFP ratio of adoptively transferred cells are shown. (B) The mean proportion + SEM of Control-GFP and CD3-GFP cells in the injection mixes is shown. (C) The differentiation status of the adoptively transferred cells was determined by examining CD62L and CD127 expression, as shown by the gating strategy diagram. (D) Representative plots of the differentiation profile seen in the two $CD4^+$ populations used for adoptive transfer are shown. (E) The average percentage + SEM of naïve, effector and memory cells in the adoptively transferred cells are shown. Data from 2 independent experiments.

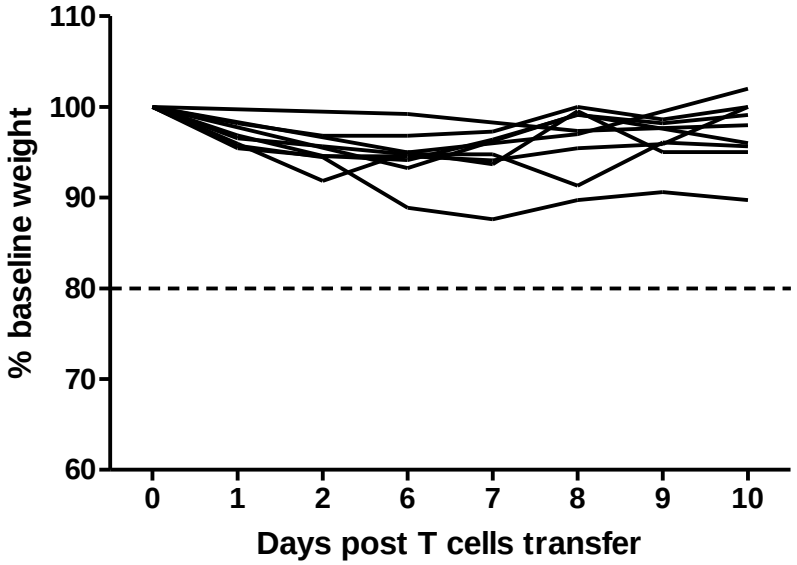

Figure 5.3 – Mice's body weight. The changes in mice weight are plotted as a function of time. Data from 2 independent experiments, n=9.

On day 10 post T cell transfer all mice were culled and single cell suspensions of the spleen, inguinal lymph nodes (LN), bone marrow (pooled from one tibia and one fibula; BM) and liver generated, as described in chapter 2, section 2.5.3. This allowed us to study the proportion of $CD45.1^+$ GFP^+ and $Thy1.1^+$ GFP^+ cells infiltrating in the tissues, and to determine whether any changes from the initial 1:1 ratio of the injected T cells had occurred. To analyse the isolated, transduced cells the gating strategy that was used is shown in figure 5.4A. Briefly, $CD45.1^+$ and $Thy1.1^+$ populations were identified in the total population of live, singlets, $CD4^+$ GFP^+ lymphocytes.

On average the percentage of $CD4^+$ CD3-GFP T cells isolated from the tissues was ≥ 1.5 fold higher than that of $CD4^+$ control-GFP T cells. In the total population of GFP^+ cells isolated from the spleen, control-GFP cells accounted for 25.35%, whereas CD3-GFP cells accounted for 71.3%; in the LN, the control-GFP and CD3-GFP cells accounted for 38.3% and 60.1% of the total GFP^+ population, respectively; in the bone marrow control-

GFP cells accounted for 29.8%, and CD3-GFP cells accounted for 66.9% of the total GFP^+ population; lastly the proportion of control-GFP cells in the total GFP^+ population isolated from the liver was 37.1%, compared to 71.3% of CD3-GFP cells (figure 5.4B).

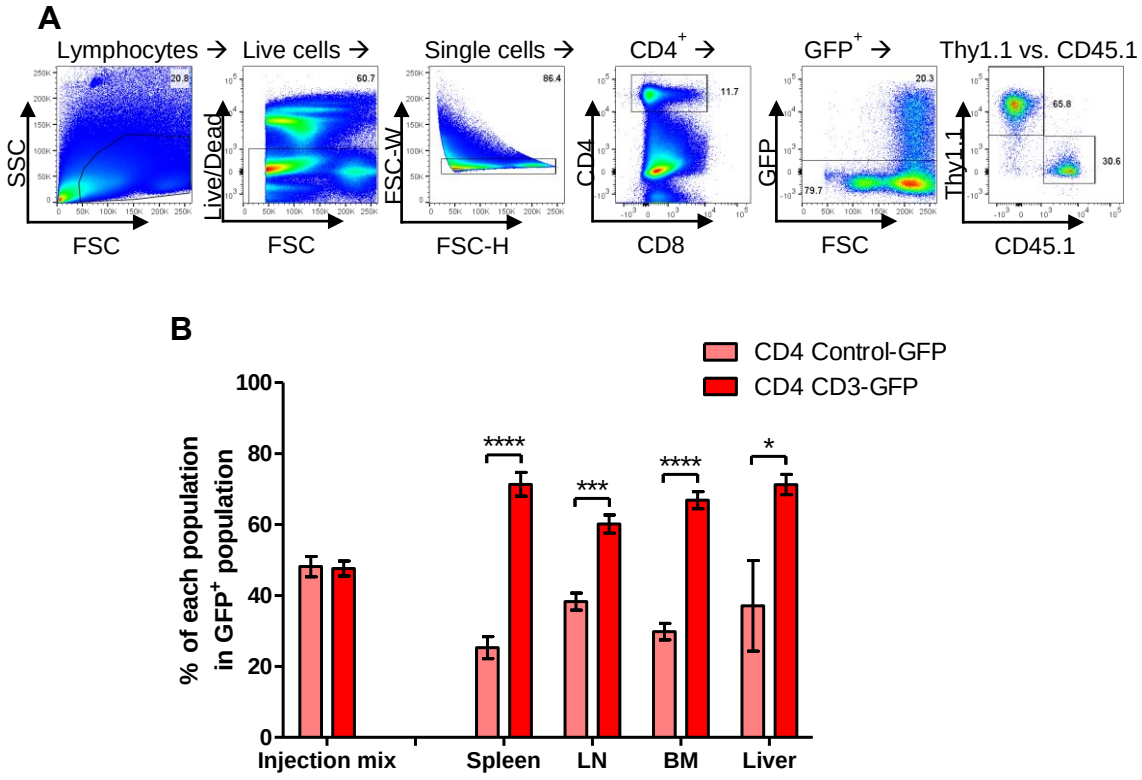

Figure 5.4 – Percentages of CD4+ control-GFP and CD4+ CD3-GFP T cells recovered from the tissues, 10 days post T cell transfer. (A) 10 days post T cell transfer the infiltration of $CD4^+$ control-GFP and $CD4^+$ CD3-GFP T cells into the spleen, inguinal lymph nodes, bone marrow and liver was analysed, using the gating strategy shown here. (B) Summary data of the percentage of adoptively transferred cells isolated from the tissues is shown. Data from two independent experiments, n=11 (p=* ≤0.05; ***≤0.001; **** ≤0.0001; unpaired t test. Mean + SEM are shown).

5.3. The *ex vivo* phenotype of adoptively transferred $CD4^+$ T cells is not influenced by the levels of TCR expression, but is determined by the homing site and T cell lineage

The data described above showed that CD3 overexpression in $CD4^+$ T cells promotes their *in vivo* persistence, compared to $CD4^+$ T cells expressing normal levels of CD3 and TCR. To confirm the finding that TCR expression does not influence the activation phenotype of the $CD4^+$ T cells (originally observed in chapter 4), the *ex vivo* phenotype of the adoptively transferred cells was analysed 10 days post T cell transfer. CD62L and CD127 expression was analysed to determine whether the isolated cells presented with a naïve ($CD62L^+$ $CD127^+$), effector ($CD62L^-$ $CD127^-$) or memory ($CD62L^-$ $CD127^+$) phenotype. The data is summarised in figure 5.5A-D.

No difference in the percentage of naïve, effector and memory cells was seen between the two populations of $CD4^+$ T cells, in any of the analysed organs. As seen previously, cells isolated from different tissues, had a different phenotype.

In the spleen 49.7% of control-GFP and 59.3% of CD3-GFP cells presented with an effector phenotype. The percentage of memory cells form the GFP^+ population in this tissue was 39.2% in the control-GFP population and 33% in the CD3-GFP population. Naïve cells represented 7.5% and 4.8% of the control-GFP and CD3-GFP population, respectively (figure 5.5A).

Similar proportions of effector cells were found in the LN (control-GFP: 42.3%; CD3-GFP: 49.2%). The proportion of memory cells in this tissue was ~10 folds lower than that seen in the spleen, with 3% and 3.5% of memory cells in the control-GFP and CD3-GFP population, respectively. Naïve cells accounted for the lowest percentage in this tissues, with 2.7% and 2.3% of cells in the control-GFP and CD3-GFP group respectively (figure 5.5B).

In both the bone marrow and the liver, the highest percentage (>82%) of cells isolated form the GFP^+ population, in both control-GFP and CD3-GFP populations, presented with an effector phenotype.

Figure 5.5C shows the proportions of naïve, effector and memory cells in the bone marrow. 1.5% and 1.7% of naïve cells were isolated from the control-GFP and the CD3-GFP populations, respectively. Memory cells accounted for 8.5% and 10.7% of all cells in the control-GFP and CD3-GFP populations respectively. 85.6% and 82.9% of all isolated control-GFP and CD3-GFP cells presented with an effector phenotype.

Similarly to the trends seen in the bone marrow, in the liver 86.7% of control-GFP cells and 92.3% of CD3-GFP cells presented with an effector phenotype. Less than 1% of adoptively transferred cells isolated from this tissue showed a naïve phenotype (control-GFP: 0.8%; CD3-GFP: 0.3%). Finally the percentage of memory cells in the isolate population of control-GFP cells was 6, compared to 4.1% of memory cells isolated from the CD3-GFP population (figure 5.5D).

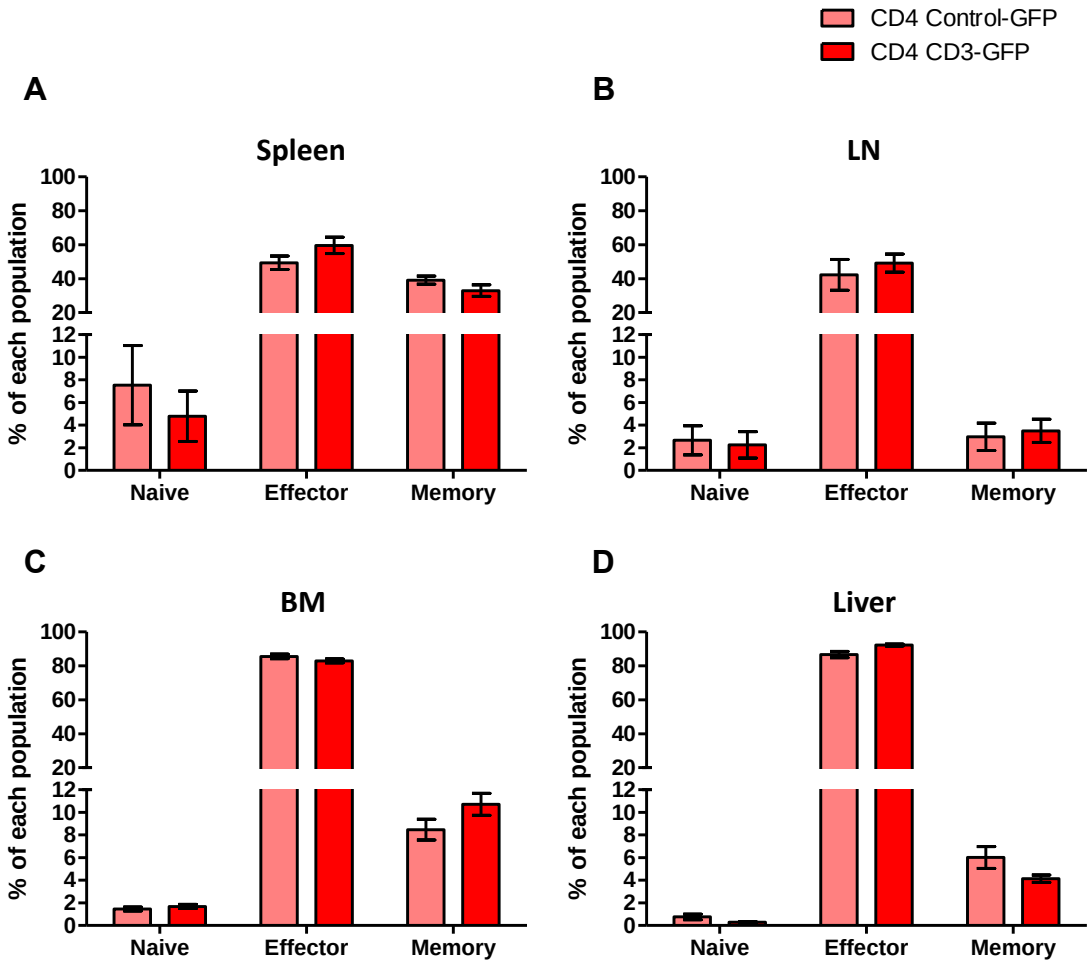

Figure 5.5 – Day 10 ex vivo differentiation status of the adoptively transferred cells. The differentiation profile was examined in adoptively transferred cells recovered from the (A) spleen, (B) inguinal lymph nodes (LN), (C) bone marrow (BM) and (D) liver. Transferred cells were identified as described in the gating strategy in figure 5.4 A. Cells were divided into naïve ($CD62L^+$ $CD127^+$), effector ($CD62L^-$ $CD127^-$), and memory cells ($CD62L^-$ $CD127^+$). Data from two independent experiments, n=9. The mean + SEM are shown.

5.4. CD3-overexpressing $CD4^+$ T cells are isolated in higher proportions compared to control-GFP $CD4^+$ T cells, in mice receiving a 2:1 mix of control-GFP to CD3-GFP cells

To determine whether CD3-overexpressing cells are capable of outcompeting control-GFP transduced cells when these are present in higher proportions, we decided to set up similar *in vivo* experiments as the ones described above, this time injecting twice as many control-GFP transduced cells compared to CD3-GFP transduced cells. Four different time points (day 5, 10, 15 and 20 post T cell transfer) allowed us to track the change in the relative numbers of control-GFP and CD3-GFP transduced populations over time.

On day 0 $CD45.2^+$ $Thy1.2^+$ C57Bl/6 recipients were sub lethally irradiated with 5.5 Gy; 2-3 hours post irradiation they were injected with a 2:1 mix of $CD45.1^+$ control-GFP $CD4^+$ and $Thy1.1^+$ CD3-GFP $CD4^+$ T cells. The total number of transduced cells in the injection mixture was 5×10^6. At 5, 10, 15 and 20 days post injection mice were sacrificed and the homing of GFP^+ $CD45.1^+$ and GFP^+ $Thy1.1^+$ cells was investigated in four tissues: spleen, inguinal LN, BM (from one tibia and one fibula) and liver. Mouse total weight was also monitored over time, and as per Home Office regulations and mice with > 20% body weight loss were sacrificed. Figure 5.6 shows a schematic representation of the experimental *in vivo* set up.

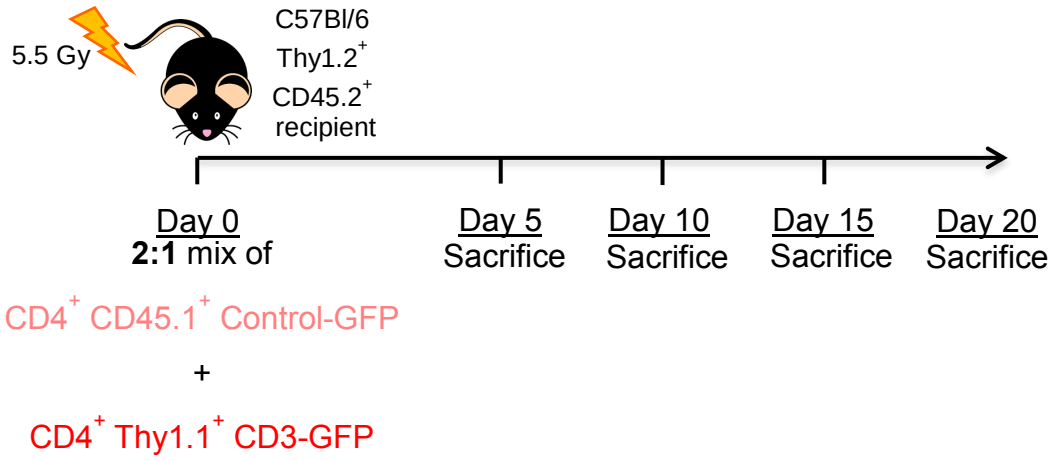

Figure 5.6 – Schematic representation of experimental set up for in vivo persistence, homing, differentiation and proliferation studies in a 2:1 competition environment.

$CD4^+$ T Cells were MACS sorted and transduced as described in chapter 2 sections 2.2.3 and 2.2.4, prior to injection on day 3 post transduction. Figure 5.7 shows typical purity of adoptively transferred cells, which was >95%. The injection mix was analysed by flow cytometry to verify the ratio of control-GFP to CD3-GFP transduced $CD4^+$ T cells (figure 5.7A). Summary data from the analysis of the injection mixtures used in the experiments is shown in figure 5.7B. On average in this set of experiments the injection mixtures contained 1.8 (1.7-2) times as many $CD4^+$ $CD45.1^+$ control-GFP cells, compared to CD3-GFP $CD4^+$ $Thy1.1^+$ cells.

The TCR expression level in the two experimental populations of $CD4^+$ T cells was also tracked by flow cytometry, both before injection and at the different experiments' end points (discussed later). At the time of injection, $CD4^+$ T cells transduced with the CD3-GFP vector expressed 3-3.8 times as much TCR as cells transduced with the control-GFP vector (figure 5.7C).

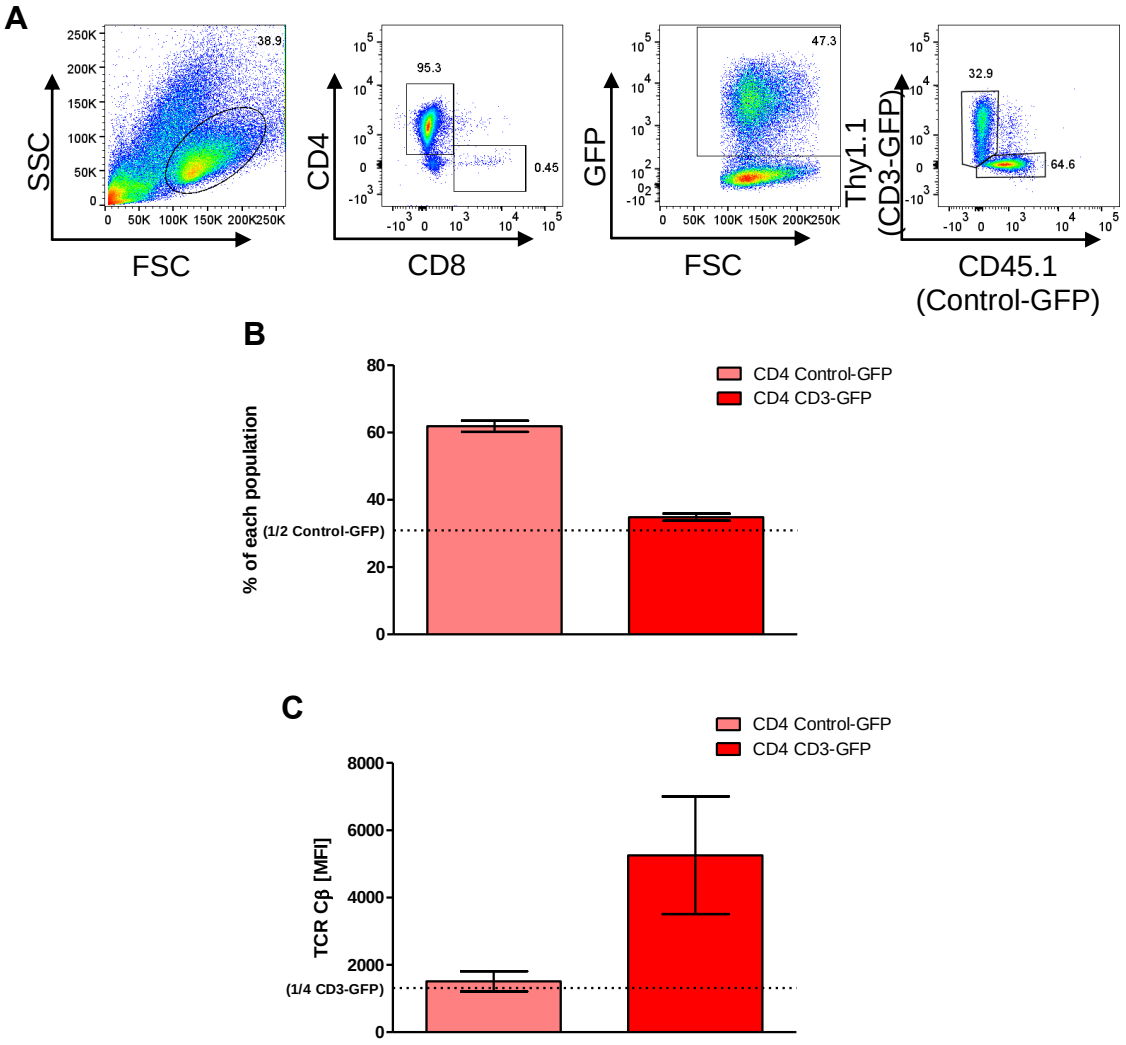

Figure 5.7 – Purity, transduction efficiency, injection mix ratio and TCR expression of the adoptively transferred cells, in the 2:1 competition experiments. (A) Typical purity, transduction efficiency and control-GFP:CD3-GFP ratio of the injection mix are shown. (B) The average proportion of Control-GFP and CD3-GFP CD4$^+$ T cells in the injection mix is shown. The proportion of control-GFP cells in the injection mix was twice that of CD3-GFP cells. (C) The TCR expression in the control-GFP and CD3-GFP transduced cells used for adoptive transfer was examined by looking at the median fluorescent intensity (MFI) of the TCR (constant β chain). Data from 3 independent experiments. SEM is shown.

The differentiation status based on CD127 and CD62L expression was also analysed before injection (figure 5.8A-C), and the proportions of naïve, effector and memory cells were similar to those seen in the previous experiments.

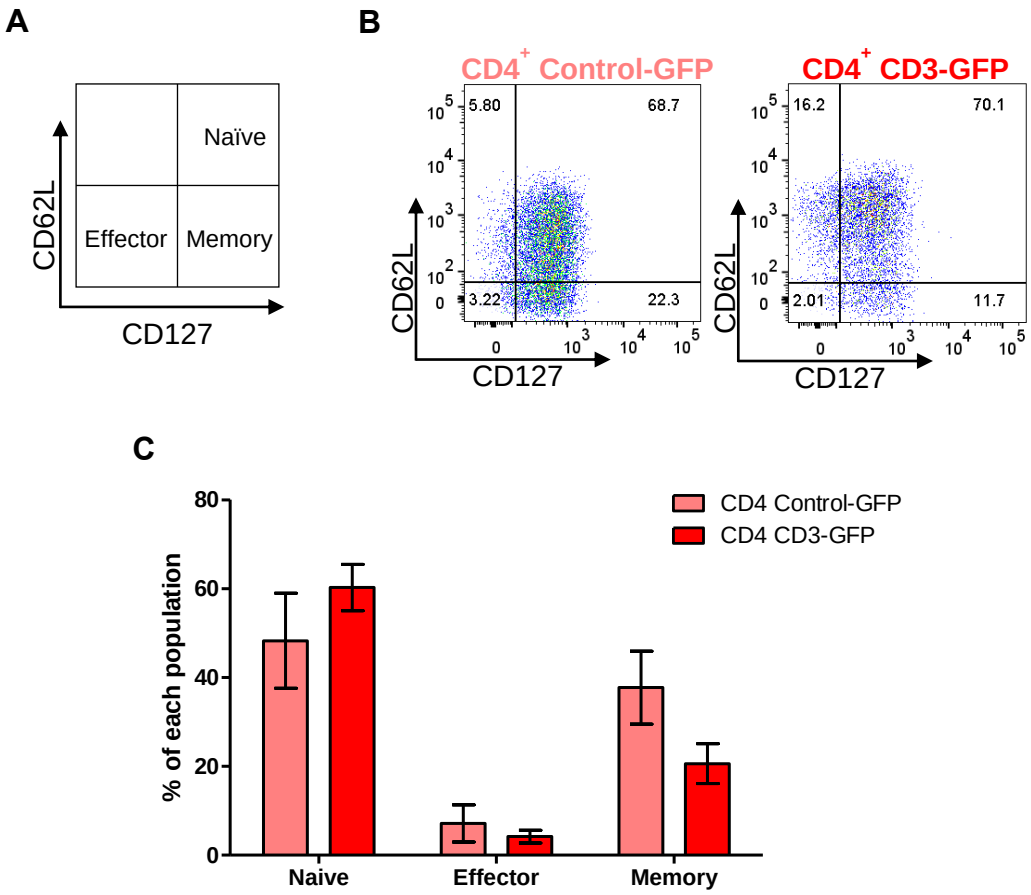

Figure 5.8 – Differentiation status of adoptively transferred cells, in the 2:1 competition experiments. (A) The differentiation status of the adoptively transferred cells was determined by examining CD62L and CD127 expression, as shown by the gating strategy diagram. (B) Representative plots of the differentiation profile seen in the two $CD4^+$ populations of adoptively transferred T cells are shown. (C) The average percentage of naïve, effector and memory cells in the adoptively transferred cells are shown. Data from 3 independent experiments. Mean + SEM are shown.

Figure 5.9 shows the changes from baseline weight seen in the recipient animals. In this set of experiments, two recipients lost more than 20% of their body weight (Home Office cut-off point).

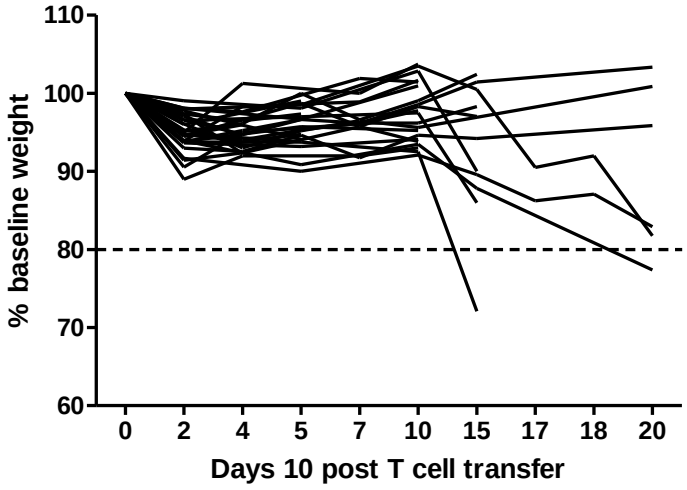

Figure 5.9 – Mice's body weight. The changes in mice weight are plotted as a function of time. Data from 3 independent experiments, n= 29.

On day 5, 10, 15 and 20 post adoptive T cell transfer, mice were sacrificed and single cell suspensions of the spleen, inguinal lymph nodes, bone marrow (pooled from one tibia and one fibula) and liver, were generated as described in chapter 2, section2.5.3. The proportion of CD45.1$^+$ control-GFP and Thy1.1$^+$ CD3-GFP CD4$^+$ T cells in each tissue was analysed. This allowed us to determine whether the accumulation of CD3-overexpressing CD4$^+$ T cells seen in the previous 1:1 competition experiments occurred in this context too. The flow cytometric gating strategy used for the analysis of the single cell suspensions was the same used for previous experiments (figure 5.4A).

The same trend was seen in all organs: by day 10 in the spleen, lymph nodes, bone marrow and liver the proportion of CD3-GFP cells in the total population of GFP$^+$ lymphocytes, was higher to that of control-GFP cells.

In the spleen (figure 5.10A) the percentage of control-GFP and CD3-GFP cells in the GFP$^+$ population at day 5 post T cell injection was similar to that seen in the injection mix. By day 10 the percentages had inverted, with now twice as much CD3-GFP cells (62.2%) compared to control-GFP cells (31.8%; $p \leq 0.0001$). At day 15 and day 20 the difference in the proportions of the two populations wasn't significant (day 15 control-GFP: 44.3%; CD3-GFP cells: 52.3%; day 20 control-GFP: 47.5%; CD3-GFP: 45.3%)

In the lymph nodes (figure 5.10B), at day 5 post T cell transfer the proportion of control-GFP cells was 1.5 fold higher compared to that of CD3-GFP cells (control-GFP:56.2%; CD3-GFP:37.1%; $p \leq 0.05$). At day 10 this difference was minimal with control-GFP cells accounting for 40.4% and CD3-GFP accounting for 45.7% of the total GFP$^+$ population. A negligible difference in the percentage of control-GFP and CD3-GFP cells isolated at day 15 was seen (control-GFP: 41.5%; CD3-GFP: 45.3%), and at day 20 a higher percentage of control-GFP cells (44.1%) was recovered, compared to the percentage of isolated CD3-GFP cells (34.6%; $p \leq 0.01$).

Similarly to the changes seen in the lymph nodes, in the bone marrow (figure 5.10C) 5 days post T cell transfer 2.6 fold more control-GFP cells were isolated, compared to the CD3-GFP cells (63.2% and 24.2% respectively; p≤0.001). However both at day 10 and 15 this difference was minimal, with CD3-GFP cells accounting for slightly more GFP^+ cells (day 10 control-GFP: 40%, CD3-GFP: 47.7%, p≤0.01; day 15 control-GFP: 44.7%, CD3-GFP: 47.6%). Equally to the trend seen in the lymph nodes, at day 20 the proportion of control-GFP cells was slightly higher (49.5%) to that of CD3-GFP cells (42.2%).

The trend seen in the liver was similar to that seen in the spleen, and it is shown in figure 5.10D. Five days post T cell transfer the proportion of control-GFP cells and CD3-GFP cells in the total GFP^+ population was similar to that seen in the injection mix (control-GFP: 57.5%, CD3-GFP: 39%; p ≤0.01). By day 10 the ratio of control-GFP and CD3-GFP cells had inverted, with control-GFP now accounting for less than half (30.6%) of the total GFP^+ population, compared to the CD3-GFP cells (65.1%; p ≤0.0001). This difference was seen at day 15 too, when the proportion of isolated control-GFP cells was 33.9%, compared to 64.2% of isolated CD3-GFP cells (p ≤0.001). Contrary to what was seen in the spleen, in the liver at day 20 the proportion of CD3-GFP cells in the GFP^+ population was still significantly higher to that of control-GFP; specifically CD3-GFP cells accounted for 55.7%, and control-GFP accounted for 38.2% of the total GFP^+ cells (p ≤0.01).

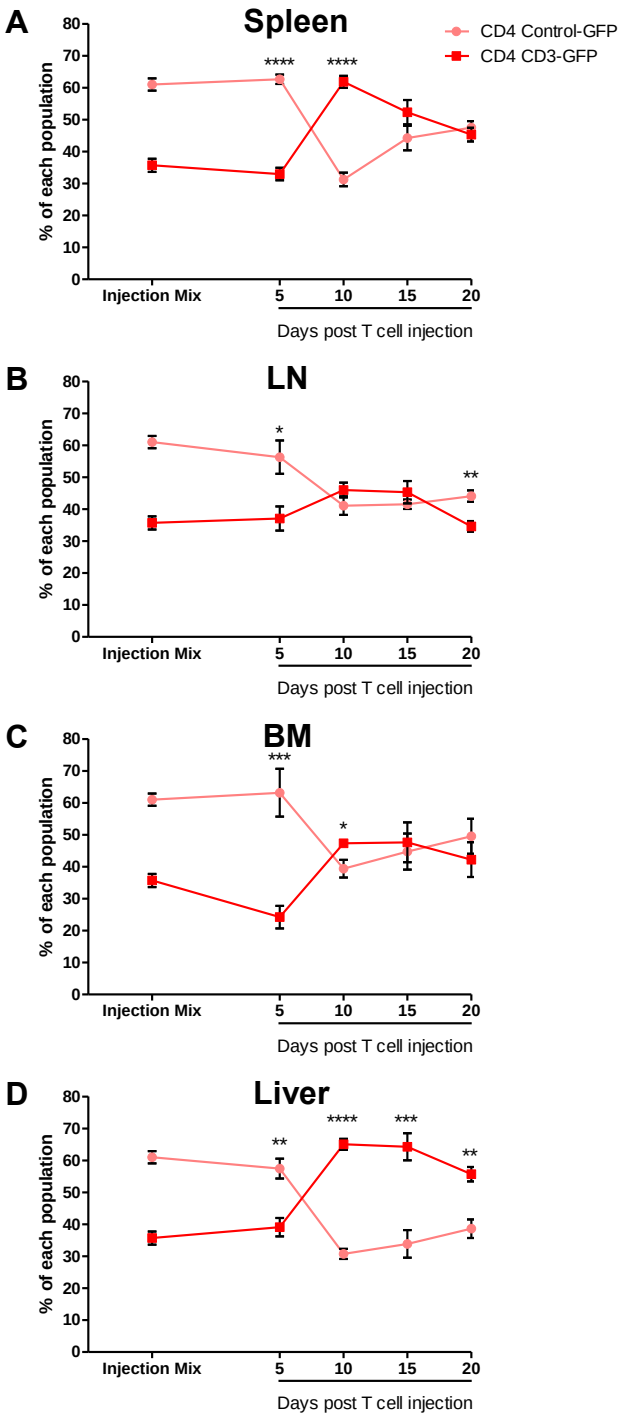

Figure 5.10 – Change in the proportion of control-GFP and CD3-GFP CD4+ T cell populations overtime, 2:1 competition experiments. The proportions of control-GFP and CD3-GFP T cells in to the total $CD4^+$ GFP^+ population isolated from the spleen (A), inguinal lymph nodes (B), bone marrow (C) and liver (D) were analysed and plotted as a function of time. The adoptively transferred cells were identified using the gating strategy described in figure 5.4 A. Data from 3 independent experiments. Day 5 n=6; day 10 n=16; day 15 n=6; day 20 n=5. (p=* ≤0.05; **≤0.01; ***≤0.001; ****≤0.0001; unpaired t test; mean + SEM are shown).

5.5. The level of TCR expression in the transduced $CD4^+$ T cells is down-regulated *in vivo*

TCR down-regulation is a regulatory feedback mechanism that occurs in T lymphocytes after TCR engagement, to dampen TCR signalling, and to prevent aberrant T cell activation. Recently, a study showed that higher affinity and avidity TCRs are down-regulated to a greater extent compared to lower affinity and avidity TCRs, when engaged by their cognate p:MHC complex.

To investigate if TCR down-regulation occurs in our system, and to determine if this altered *in vivo* T cell-persistence, we tracked the levels of TCR expression of our adoptively transferred cells over time (injection day, and day 5, 10, 15 and 20 post T cell transfer). The levels of TCR were measured by looking at the MFI of the anti-TCR constant β domain (Cβ).

CD3-GFP transduced $CD4^+$ T cells expressed on average 3-3.8 fold as much TCR compared to control-GFP $CD4^+$ cells (control-GFP TCR MFI: 1210-1807; CD3-GFP TCR MFI: 3510-7002). In all analysed organ this difference was lost by day 15, when both populations of cells expressed very similar levels of TCR.

Broadly speaking, the TCR MFI of both the control-TCR transduced and the CD3-GFP transduced $CD4^+$ T cells, increased early after adoptive transfer (between day 0 and day 5). The only exception was given by the TCR levels of the CD3-GFP transduced T cells isolated from the spleen, whose TCR levels slightly decreased between injection day and day 5. Moreover, no overall down-regulation in the levels of TCR expression was seen in the control-GFP transduced T cell population; the levels of TCR expression at day 10 were identical, or higher, to those seen at injection day.

In the spleen (figure 5.11A), 5 days post T cell transfer CD3-overexpressing cells expressed lower levels of TCR compared to the levels expressed on injection day. In particular, CD3-GFP cells expressed 1.9 folds more TCR compared to control-GFP cells.

From day 5 onwards the level of TCR expression on CD3-engineered $CD4^+$ T cells kept decreasing, and from day 15 onwards only a small difference in the level of TCR expressed by CD3-overexpressing and control-transduced $CD4^+$ T cells was seen.

In the lymph nodes (figure 5.11B) and bone marrow (figure 5.11C) a slightly different trend in TCR expression and down-regulation was seen. In particular, the levels of TCR expression were more varied, with a higher range of TCR expression in both transduced populations. Although in both tissues from day 5 to day 15 a gradual decrease in TCR expression was seen, this reduction was lower than that observed in the spleen. Moreover, between day 15 and day 20 a small increase in TCR expression was seen in both populations of transduced cells. Contrary to the spleen, the average level of TCR expressed in CD3-engineered $CD4^+$ T cells never reached that expressed in control-GFP cells.

Figure 5.11D shows summary data of the TCR expression kinetics in the liver. Analysis of TCR expression 5 days post T cell transfer showed a slight increase in TCR expression in both injected T cell populations. From day 5 onwards TCR expression gradually decreased until day 15, when 1.5 fold more TCR was expressed in CD3-engineered T cells compared to control-GFP T cells. Twenty days post T cell transfer this difference further decreased with CD3-GFP transduced $CD4^+$ T cells only expressing 1.4 fold more TCR compared to control-GFP transduced $CD4^+$ T cells.

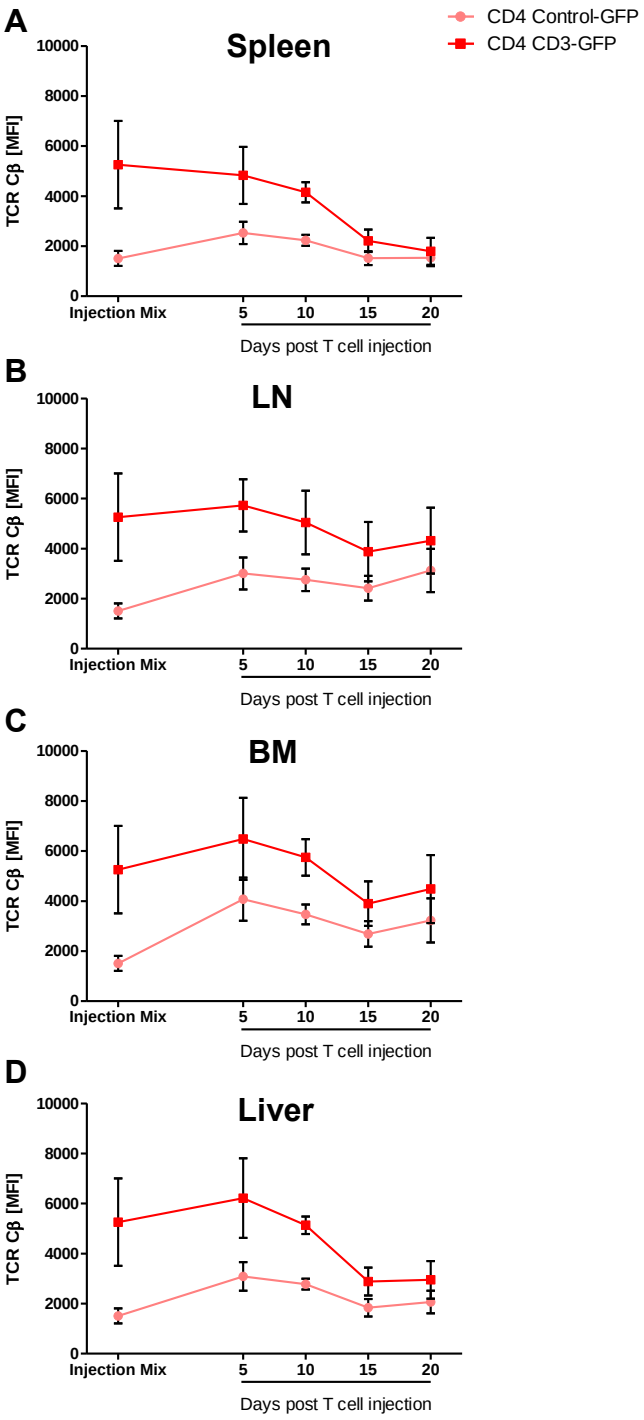

Figure 5.11 – TCR expression of control-GFP and CD3-GFP CD4+ T cells, 2:1 competition experiments. The TCR expression of the control-GFP and CD3-GFP T cells isolated from the different tissues at day 5, 10, 15 and 20 is plotted. The adoptively transferred cells were identified using the gating strategy described in figure 5.4 A. (A) Spleen; (B) inguinal lymph nodes; (C) bone marrow; (D) liver. Data from 3 independent experiments. Day 5 n=6; day 10 n=16; day 15 n=6; day 20 n=5. Mean + SEM are shown.

5.6. TCR down-regulation is not due to reduced expression of the retroviral transgene

TCR down-regulation may occur as a consequence of retroviral transgene expression loss. To investigate whether this was the case, the MFI of GFP was tracked over time. The gene coding for GFP, which was used as a marker of transduction, is found on the same retroviral vector as the CD3, or control, genes, and it's separated from them by an IRES sequence (figure 2.1). Thus, a loss of transgene expression will result in a loss of GFP expression too.

The GFP of the two transduced T cell populations, control-GFP and CD3-GFP, was analysed over time, in the four tissues: spleen, inguinal lymph nodes, bone marrow and liver (figure 5.12 A-D). In this set of experiments, no overall loss in GFP signal was seen over time, and the MFI of the GFP at day 20 was similar of higher than the MFI at injection. The expression levels of GFP from the control-GFP vector remained constant throughout the experiment. That of the fluorescent protein from the CD3-GFP retroviral construct, increased between day 0 and day 5, and decreased to reach the original value after day 5.

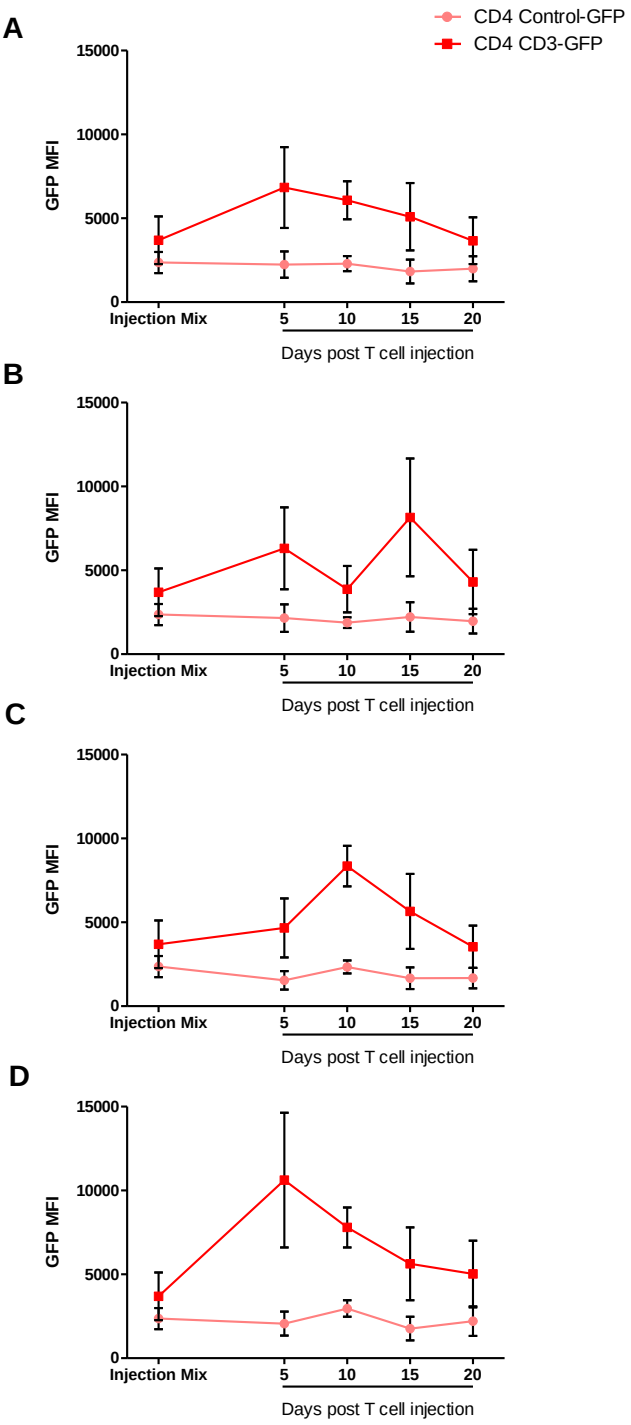

Figure 5.12 – GFP MFI of control-GFP and CD3-GFP CD4+ T cell populations, 2:1 competition experiments. The MFI of GFP in the population of control-GFP and CD3-GFP T cells isolated from the different tissues at day 5, 10, 15 and 20 is plotted. The adoptively transferred cells were identified using the gating strategy described in figure 5.4 A. (A) Spleen; (B) inguinal lymph nodes; (C) bone marrow; (D) liver. Data from 3 independent experiments. Day 5 n=6; day 10 n=16; day 15 n=6; day 20 n=5. Mean + SEM are shown.

5.7. Accumulation of gene-modified CD4$^+$ T cells is due to increased cell proliferation, not decreased cell death

These and previous experiments have shown that CD3 overexpression is associated with greater T cell accumulation both in a 1:1 and a 2:1 control-GFP to CD3:GFP competition environment. However so far the described experiments did not show whether this was due to increased cell proliferation or decreased cell death. To address this question, the percentage of Ki67$^+$ and Annexin V$^+$ cells in the two adoptively transferred populations was analysed throughout the experiment.

In the spleen (figure 5.13A) 5 days post T cell transfer the percentage of cells in the population transduced with the control-GFP vector expressing Ki67 (Ki67$^+$) and in the population transduced with the CD3-GFP vector was 16.4% and 19.4%, respectively. At day 10, a significantly higher proportion of proliferating cells were found in the CD3-GFP population (22.7%) compared to the percentage of proliferating cells in the control-GFP transduced cells (11.8%; $p \leq 0.01$). This difference was maintained until 15 days post T cell transfer, with Ki67$^+$ cells in the control-GFP and CD3-GFP populations accounting for 15.8% and 27.9%, respectively ($p \leq 0.05$). At the last time point analysed T cell proliferation had significantly reduced, with only 2.3% Ki67$^+$ cells found in the control-GFP population, compared to 3.7% Ki67$^+$ cells in the CD3-GFP transduced population.

Very similar proportions of proliferating cells were found in the lymph nodes (figure 5.13B) at 5 days post T cell transfer (control-GFP: 14.8%; CD3-GFP: 16.3%). The number of proliferating T cells increased in both transduced populations at day 10 (13.3% of control-GFP cells were Ki67$^+$, compared to 20.2% of CD3-GFP cells; $p \leq 0.05$) and continued until day 15, when 22.7% and 24.9% of the control-GFP and CD3-GFP populations were Ki67$^+$ respectively. After day 15 the rate of proliferation dropped, and at day 20 post T cell injection only 6.8% and 9.12% of the adoptive transferred T cells

isolated from the tissue were Ki67$^+$ in the control-GFP and CD3-GFP populations, respectively.

In the bone marrow (figure 5.13C) no significant difference in the proportion of proliferating cells were found at day 5 and 10 (Day 5 control-GFP: 10.6%, CD3-GFP: 15.3%; day 10 control-GFP: 6.9%, CD3-GFP: 14.2%). At day 15, twice as many Ki67$^+$ cells were found in the CD3-GFP population (34.8%), compared to the control-GFP population (17%; $p \leq 0.01$). However, by day 20 the proportion of proliferating cells had dramatically reduced in both populations (control-GFP: 0.12%; CD3-GFP: 0.2%)

The liver was the organ where the most dramatic differences in Ki67$^+$ expression was observed, among all the analysed organs (figure 5.13D). CD3-GFP cells isolated 5 days post adoptive transfer contained 17% of Ki67$^+$ cells, compared to 10.1% of proliferating cells in the control-GFP transduced population ($p \leq 0.05$). Five days later the percentage of Ki67$^+$ cells in the control-GFP population was 2.2 fold lower (18.3%) compared to that seen in CD3-GFP cells (40.9%; $p \leq 0.0001$). A similar difference in the proportion of Ki67 expressing cells was seen at day 15, with 24% of cells in the control-GFP population, and 49% of cells in the CD3-GFP population expressing Ki67$^+$ ($p \leq 0.05$). However, again by day 20 proliferation had dramatically reduced (control-GFP: 10.1%; CD3-GFP: 15.2%).

To determine the proportion of cell's undergoing apoptosis, the levels of Annexin V in the two different populations of transduced cells were tracked over time. Due to technical problems, no data from day 10 post T cell transfer was collected.

At injection no significant difference in the percentage of control-GFP and CD3-GFP cells undergoing apoptosis was seen, and 15.6% and 20.3% of cells in the control-GFP and CD3-GFP population respectively expressed Annexin V.

In the spleen (figure 5.13E) the overall levels of Annexin V$^+$ cells remained low (<22%) throughout the experiments. At day 5, 5.7% of control-GFP transduced cells and 16.7% of CD3-GFP cells were found positive for Annexin V expression ($p \leq 0.05$). This proportion

slightly decreased between day 5 and day 15 (control-GFP: 9%; CD3-GFP: 11%), and then marginally increased at day 20 (control-GFP: 12.2%; CD3-GFP: 22%).

Higher numbers of Annexin V^+ T cells were recovered from the lymph nodes in both groups (figure 5.13F) at day 5 post T cell transfer. 48% CD3-GFP transduced T cell population were Annexin V^+, compared to 25.2% of the control-GFP population. This had increased further at day 15 where both populations of Annexin V^+ cells increased and reached similar values (control-GFP: 52.8%; CD3-GFP: 56.7%), before decreasing at day 20. At this time point 29.1% and 36.4% of Annexin V^+ cells were recovered from the population of control-GFP and CD3-GFP cells, respectively.

The bone marrow (figure 5.13G) was the tissue from which the highest proportion of apoptotic cells was recovered. Already 5 days post adoptive transfer 51.4% and 57.9% of the T cells recovered from the control-GFP and the CD3-GFP populations were Annexin V^+, respectively. This proportion further increased, and at day 15 more than 60% of the cells from both populations were Annexin V^+ (control-GFP: 64.4%; CD3-GFP: 70.8%). However by day 20 post T cell transfer, the percentage of apoptotic cells dropped by 20% or more in both populations (control-GFP: 35.3%; CD3-GFP: 39.2%).

In the liver, a similar trend was observed. The proportion of apoptotic cells isolated 5 days after their adoptive transfer accounted for 12.9% and 16.1% of the population of cells transduced with the control-GFP and the CD3-GFP vectors respectively. However, this percentage decreased between day 5 and day 15, when the percentage of Annexin V^+ cells was 8.6% in the control-GFP population, and 12.1% in the CD3-GFP population. By day 20 only 2.48% and 2% of all cells in the control-GFP and CD3-GFP transduced population were positive for Annexin V.

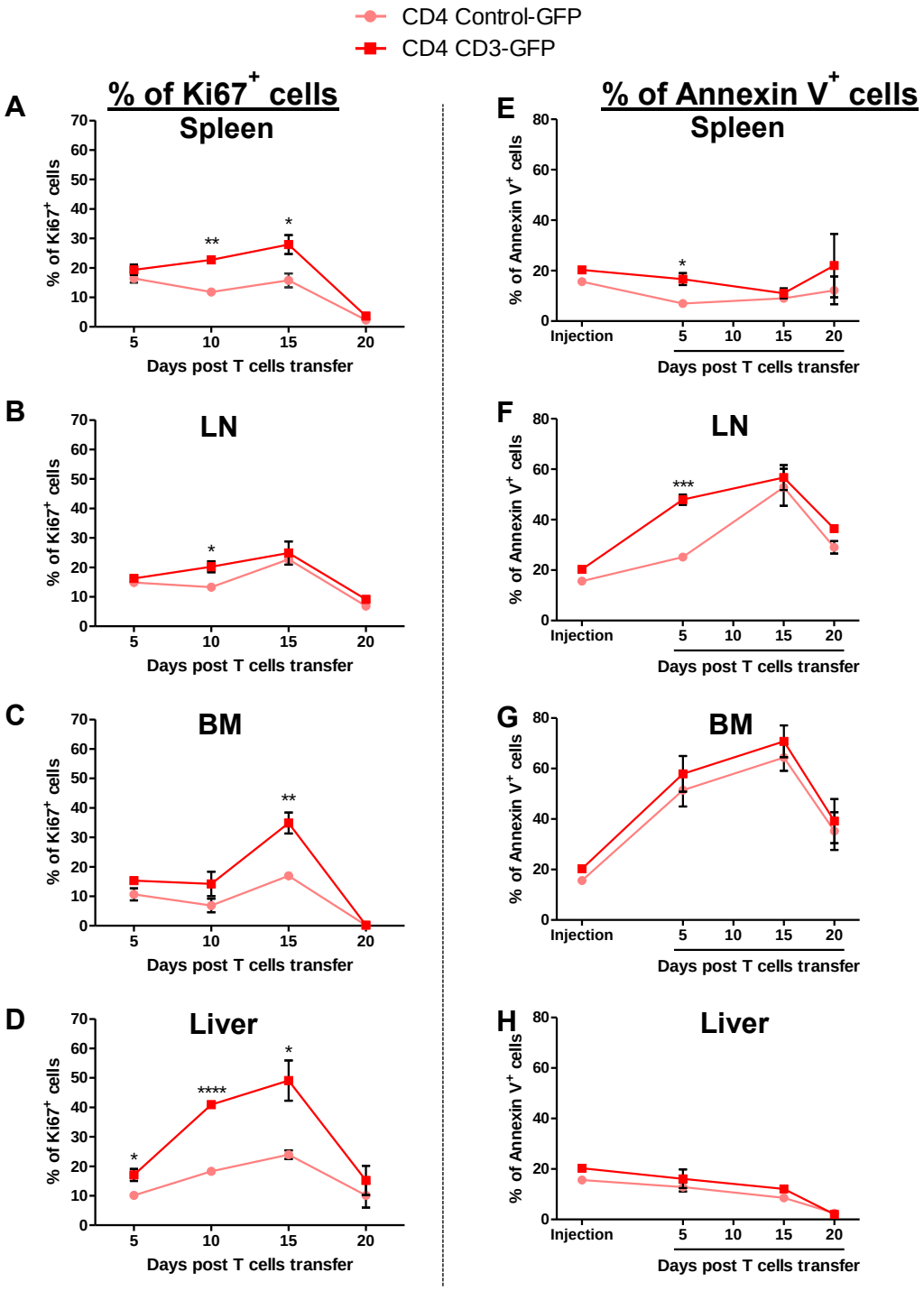

Figure 5.13 – Percentage of Ki67+ and Annexin V+ control-GFP and CD3-GFP cells, 2:1 experiments. The percentage of Ki67$^+$ (left) and Annexin V$^+$ (right) cells in the control-GFP and CD3-GFP populations overtime is shown. The adoptively transferred cells were identified using the gating strategy described in figure 5.4 A. (A, E) Spleen; (B, F) inguinal lymph nodes; (C, G) bone marrow; (D, H) liver. Data from one experiment. Day 5-15 n=3, day 20 n =2. No Annexin V data at day 10. (p=*≤0.05; **≤0.01; ***≤0.001; ****≤0.0001; unpaired t test; mean + SEM are shown).

5.8. The differentiation status of the cells is determined by their homing site and it changes over time

As in the non-competitive experiments, the expression of CD62L and CD127 were analysed in all organs, at the four different time points.

In all analysed tissues, no difference in CD127 and CD62L expression was seen between the two populations of transduced $CD4^+$ T cells. However different trends were seen among different organs.

In the spleen (figure 5.14 left) similar percentages of naïve and memory cells (35.1-37% and 29.4-38.5%, respectively) were isolated 5 days post T cell transfer. The percentage of effector cells was the lowest (7.9%-10%) of the three populations. However by day 10 both the proportion of effector and memory cells had increased with effector cells accounting for 46.1%-47.5% and 37.5-42.6%, respectively. There was a corresponding decrease in the percentage of naïve cells in both populations (6.8%-8.9%). The proportion of each population of differentiated cells further changed with time, and at day 15 the highest proportion of cells isolated from the spleen had a memory phenotype (39.5%-40.5%), followed by naïve (26%-34%), and finally effector (17.7%-23.8%) phenotypes. Five days later a similar trend to that of day 5 was seen, with naïve and memory cells presenting with the two highest proportions (31.2%-43.2% and 51%-59.6%, respectively), followed by effector cells (4.3%-6.8%).

Different trends were seen in the inguinal lymph nodes (figure 5.14 right). Five days post T cell transfer the majority of the cells retained a naïve phenotype (44.3%-44.9%), with the proportion of memory cells being between 19.7% and 30.6%. Effector cells were the smallest proportion of cells (9.4%-12.6%). By 10 days post T cell transfer similar proportions of naïve, effector and memory cells were found (36.5%-38.9%, 26%-27% and 27.9%-28.9%, respectively). The proportion of naïve cells isolated from the tissue at day 15 further increased (42.4%-43.6%), while that of effector cells and memory cells decreased (14.1%-19.6% and 25.4%-28.8%, respectively). The highest proportion of

naïve cells among the four different time points was recovered at day 20 post adoptive transfer (53.8%-60.7%). The proportion of memory cells at this time point was 34.6%and 42.8% in the two populations, while effector cells accounted for less than 2% (1.5%-1.9%).

Figure 5.15 right shows the changes in proportion of naïve, effector and memory cells in the bone marrow. At the first analysed time point the majority of the cells had a memory phenotype (36.8%-38%). The percentages of naïve and effector cells were similar (21.1%-23.4% and 19%-20.5%, respectively). Five days later (10 days post T cell transfer) memory cells still represented the highest proportion of cells (45.9%-46.8%), followed by effector cells (36.6%-37.5%), and finally naïve cells (11.4%-13.6%). At day 15 naïve and effector cells were recovered in similar percentages (23.2%-27.9% and 23%-24.8%, respectively), while the proportion of memory cells in the two transduced populations was slightly higher (34.4%-37.9%). At the last analysed time point the proportion of memory cells recovered from this tissue in both populations was the highest (57.6%-61.5%), followed by that of naïve cells (32.9%-38.7%). Effector cells accounted for 3.5% or less in both populations (2.5%-3.5%).

Lastly, the differentiation trends seen in the liver are summarised in figure 5.15 left. Similarly to the bone marrow, at day 5 post T cell transfer the majority of the cells had a memory phenotype (34.9%-49.2%); the second highest proportion was represented by naïve cells (23%-29.6%), whereas effector cells represented the lower proportion of cells (11%-13.8%). The proportion of effector and memory cells isolated at day 15 was similar (44.5%-47.5% and 42.8-42.9%, respectively), while naïve cells accounted for 6.1% and 7.9% of all cells. Five days later a similar trend was seen. Effector and memory cells were isolated in similar proportions (32.5%-39.6% and 40.3%-42.3%, respectively). Naïve cells were recovered in lower percentages from both populations (11.5%-16.7%). The majority of the cells isolated 20 days post adoptive transfer had a memory phenotype (69.6%-74.5%). Naïve and effector cells accounted for similar proportions in both populations (12%-16.3% and 12.8%-13%, respectively).

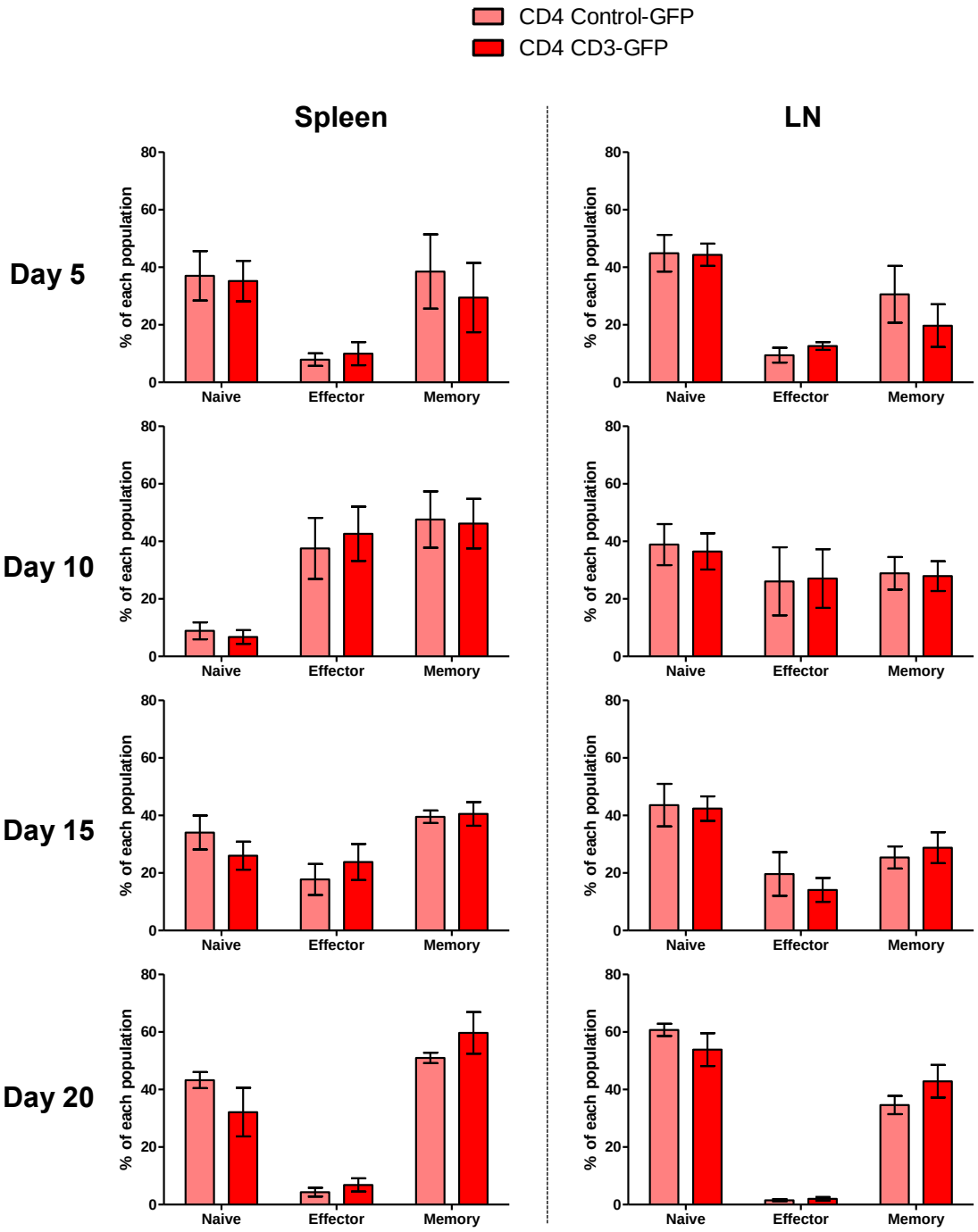

Figure 5.14 – Day 5-20 ex vivo differentiation status of the adoptively transferred cells. The differentiation status (naïve: $CD62L^+$ $CD127^+$; effector: $CD62L^-$ $CD127^-$; memory: $CD62L^-$ $CD127^+$) of the control-GFP and CD3-GFP $CD4^+$ T cells isolated from the spleen (left) and inguinal lymph nodes (right), at day 5, 10, 15 and 20 are shown. The adoptively transferred cells were identified using the gating strategy described in figure 5.4 A. Data from 3 independent experiments. Day 5 n=6; day 10 n=16; day 15 n=6; day 20 n=5. Mean + SEM are shown.

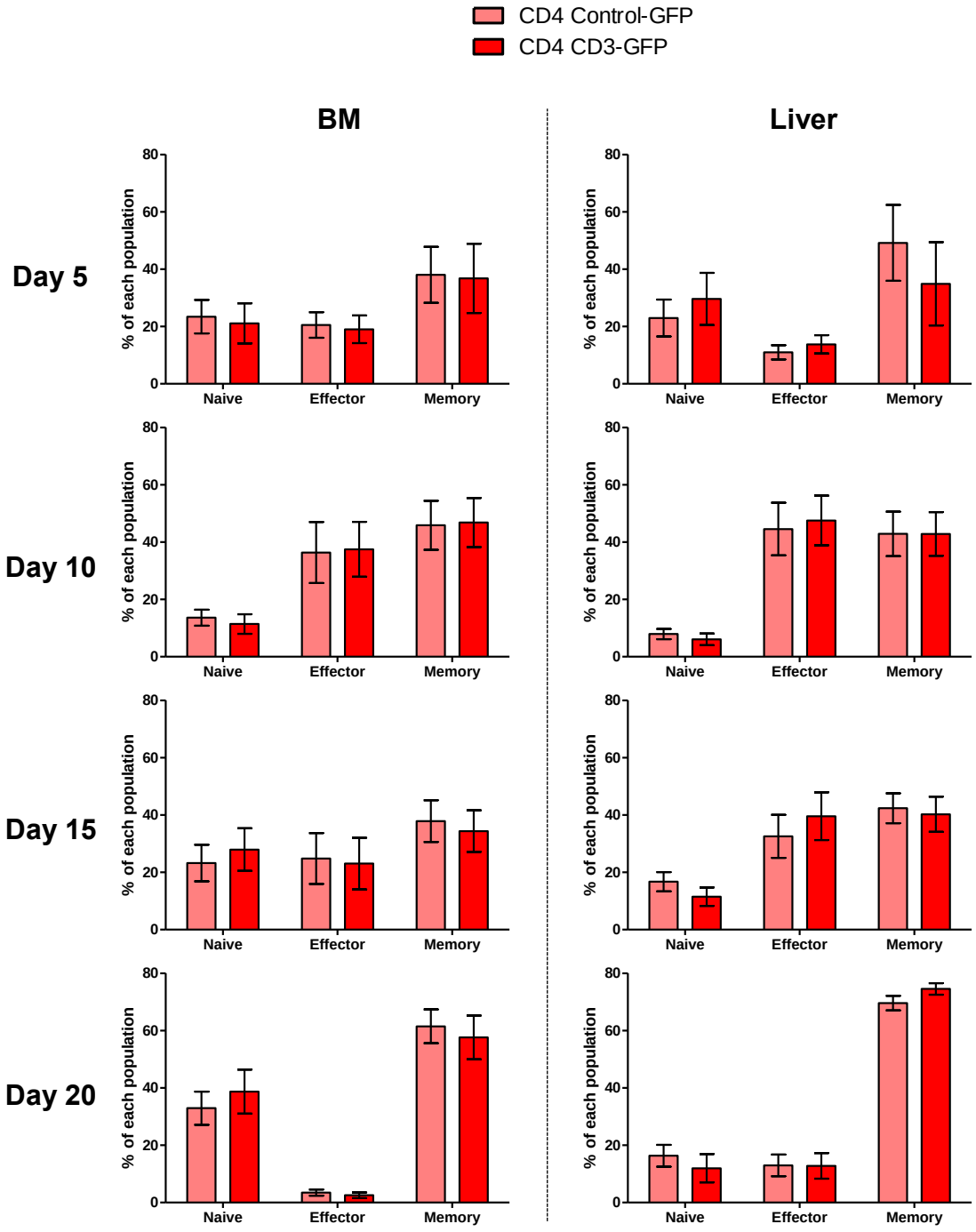

Figure 5.15 – Day 5-20 ex vivo differentiation status of the adoptively transferred cells. The differentiation status (naïve: $CD62L^+$ $CD127^+$; effector: $CD62L^-$ $CD127^-$; memory: $CD62L^-$ $CD127^+$) of the control-GFP and CD3-GFP $CD4^+$ T cells isolated from the bone marrow (left) and liver (right), at day 5, 10, 15 and 20 are shown. The adoptively transferred cells were identified using the gating strategy described in figure 5.4 A. Data from 3 independent experiments. Day 5 n=6; day 10 n=16; day 15 n=6; day 20 n=5. Mean + SEM are shown.

5.9. Acquisition of differentiation phenotypes is not associated with different levels of TCR expression

To determine whether acquisition of a particular differentiation profile (naïve, effector or memory phenotype) is associated with higher or lower TCR expression, the TCR expression levels were analysed in the three different T cell subsets (figure 5.16). As described previously, T cells were divided into naïve, effector and memory cells based on their expression of the markers CD62L and CD127.

All 3 differentiated subsets identified in the population of CD3-GFP transduced $CD4^+$ T cells expressed higher levels of TCR than $CD4^+$ T cells transduced with the control-GFP vector. However, in the two populations no difference in TCR expression was seen between naïve, effector and memory cells. The kinetics of TCR expression in the subsets of control-GFP and CD3-GFP cells are similar to the kinetics seen in the whole population of transduced cells.

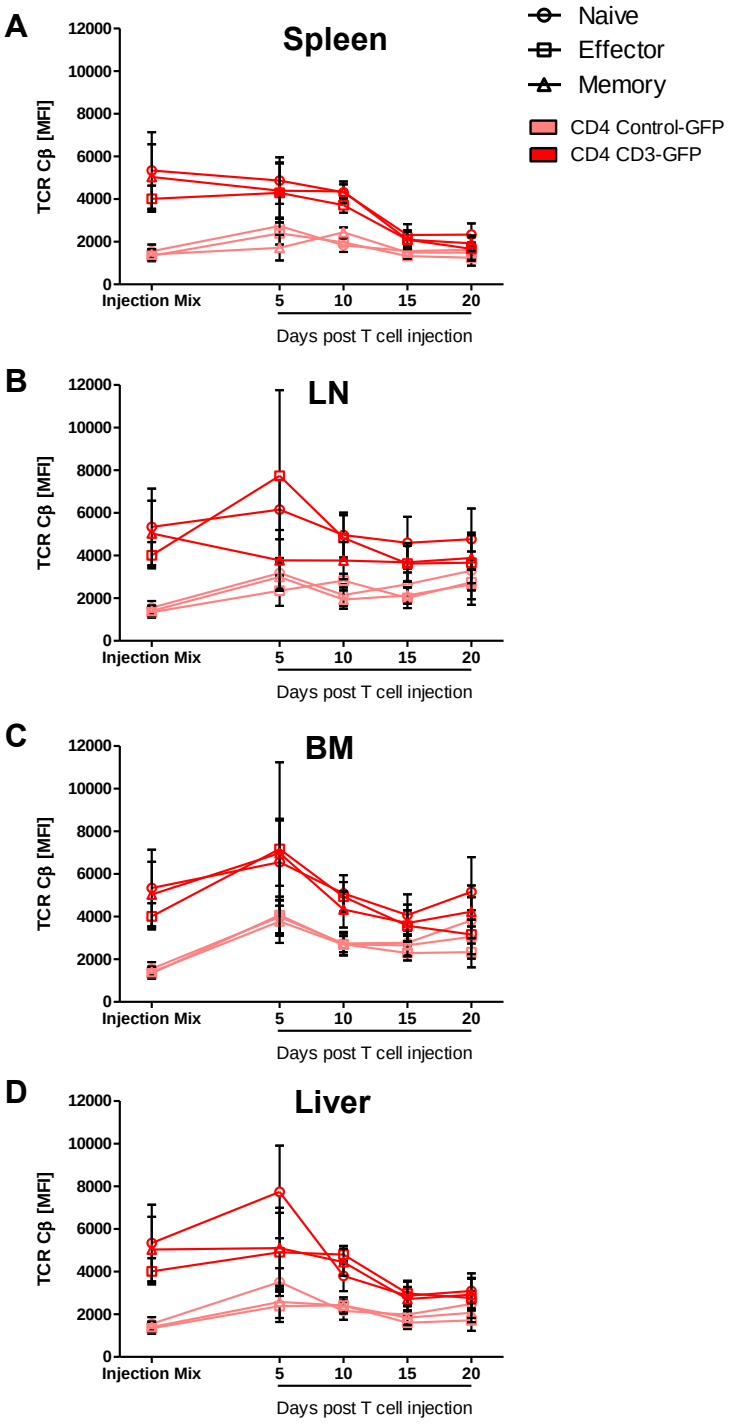

Figure 5.16 – TCR expression of naïve, effector and memory cells from the control-GFP and CD3-GFP CD4+ T cell populations, 2:1 competition experiments. The TCR expression of the naïve, effector and memory cells, of the control-GFP and CD3-GFP T cell populations isolated from the different tissues at day 5, 10, 15 and 20 is plotted. The adoptively transferred cells were identified using the gating strategy described in figure 5.4 A. (A) Spleen; (B) inguinal lymph nodes; (C) bone marrow; (D) liver. Data from 3 independent experiments. Day 5 n=6; day 10 n=16; day 15 n=6; day 20 n=5. Mean + SEM are plotted.

5.10. Physiological levels of TCR cannot promote CD4$^+$ T cell accumulation in a competitive environment, despite TCR down regulation in CD3-overexpressing CD4$^+$ T cells

The experiments described above show that after adoptive transfer, CD3-overexpressing CD4$^+$ T cells quickly down-regulated their TCR levels to that seen in control-GFP transduced cells. This down-regulation is associated with a loss of accumulation in 3 of the 4 analysed organs. To examine whether a higher proportion of CD3-overexpressing cells in the injection mix was associated with a greater loss of TCR expression and therefore reduced *in vivo* cell accumulation of this population, a different set of competition experiments were designed. It was postulated that a greater reduction in TCR expression may more rapidly reduce *in vivo* cell accumulation, allowing CD4$^+$ T cells expressing physiological levels of TCR (i.e. control-GFP T cells) to outcompete the population of CD3-overexpressing T cells.

In the following experiments host animals received an excess of CD3-GFP transduced T cells (a 1:2 mix of control-GFP to CD3-GFP cells), in order to test whether loss of organ-specific CD3-GFP T cell accumulation secondary to *in vivo* TCR down-modulation could be repopulated by the control-GFP transduced T cells. This could result in subsequent isolation of a relative increase in the number of control-GFP T cells in various organs. Previous experiments showed that control-GFP transduced cells, which express physiological levels of TCR overall did not down regulate their TCR expression *in vivo*.

On day 0 CD45.2$^+$ Thy1.2$^+$ C57Bl/6 recipients were sub lethally irradiated with 5.5 Gy and then 2-3 hours post irradiation they were injected with a 1:2 mix of CD45.1$^+$ control-GFP and Thy1.1$^+$ CD3-GFP CD4$^+$ T cells. The total number of transduced cells in the injection mixture was 5 x 10^6. At 5, 10 and 15 days post adoptive transfer mice were culled and the homing pattern of GFP$^+$ CD45.1$^+$ and GFP$^+$ Thy1.1$^+$ T cells was

investigated in four tissues: spleen, inguinal lymph nodes, bone marrow (from one tibia and one fibula) and liver. Mouse total weight was monitored over time, and as per Home Office regulations mice with > 20% body weight loss were culled. A schematic representation of the experimental *in vivo* set up is shown in figure 5.17.

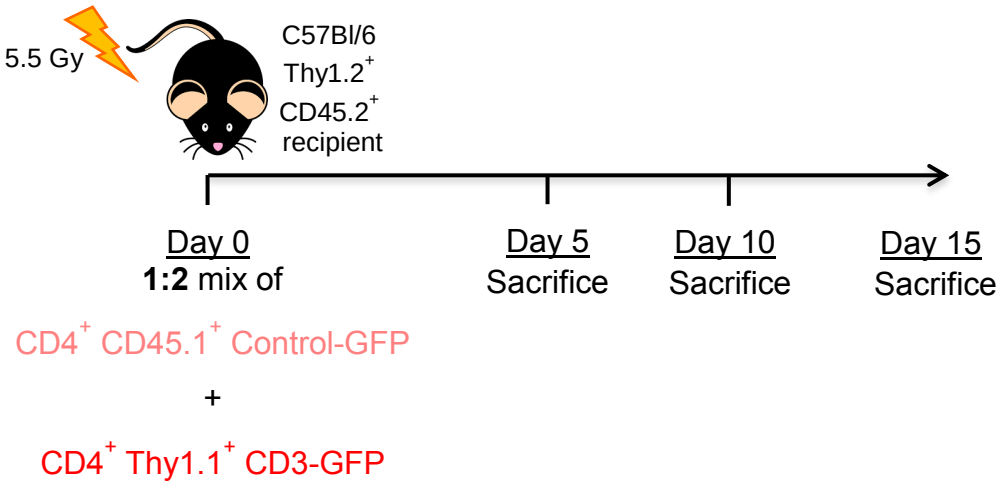

Figure 5.17 – Schematic representation of experimental set up for in vivo persistence, homing, differentiation and proliferation studies in a 1:2 competition environment.

$CD4^+$ T Cells were MACS sorted and transduced as described in chapter 2 sections 2.2.3 and 2.2.4, prior to injection on day 3 post transduction. Figure 5.18A shows typical purity of adoptively transferred cells, which was >97%. The number of cells from each population injected was calculated based on the transduction efficiency of the two populations, in order to inject a total of 2.5×10^6 transduced cells from each population. The injection mix was analysed by flow cytometry to verify the ratio of control-GFP to CD3-GFP cells (figure 5.18A). Summary data from the analysis of the injection mixtures used in all experiments is shown in figure 5.18B. On average in this set of experiments the injection mixture contained 1.75 times (1.6-1.9) as many $CD4^+$ $Thy1.1^+$ CD3-GFP cells (59.1%), compared to control-GFP $CD4^+$ $CD45.1^+$ cells (32.3%).

The expression of TCR in the two experimental populations of $CD4^+$ T cells was analysed before injection (figure 5.18C). On average $CD4^+$ T cells transduced with the CD3-GFP vector expressed 2 fold more TCR compared to T cells transduced with the control-GFP vector.

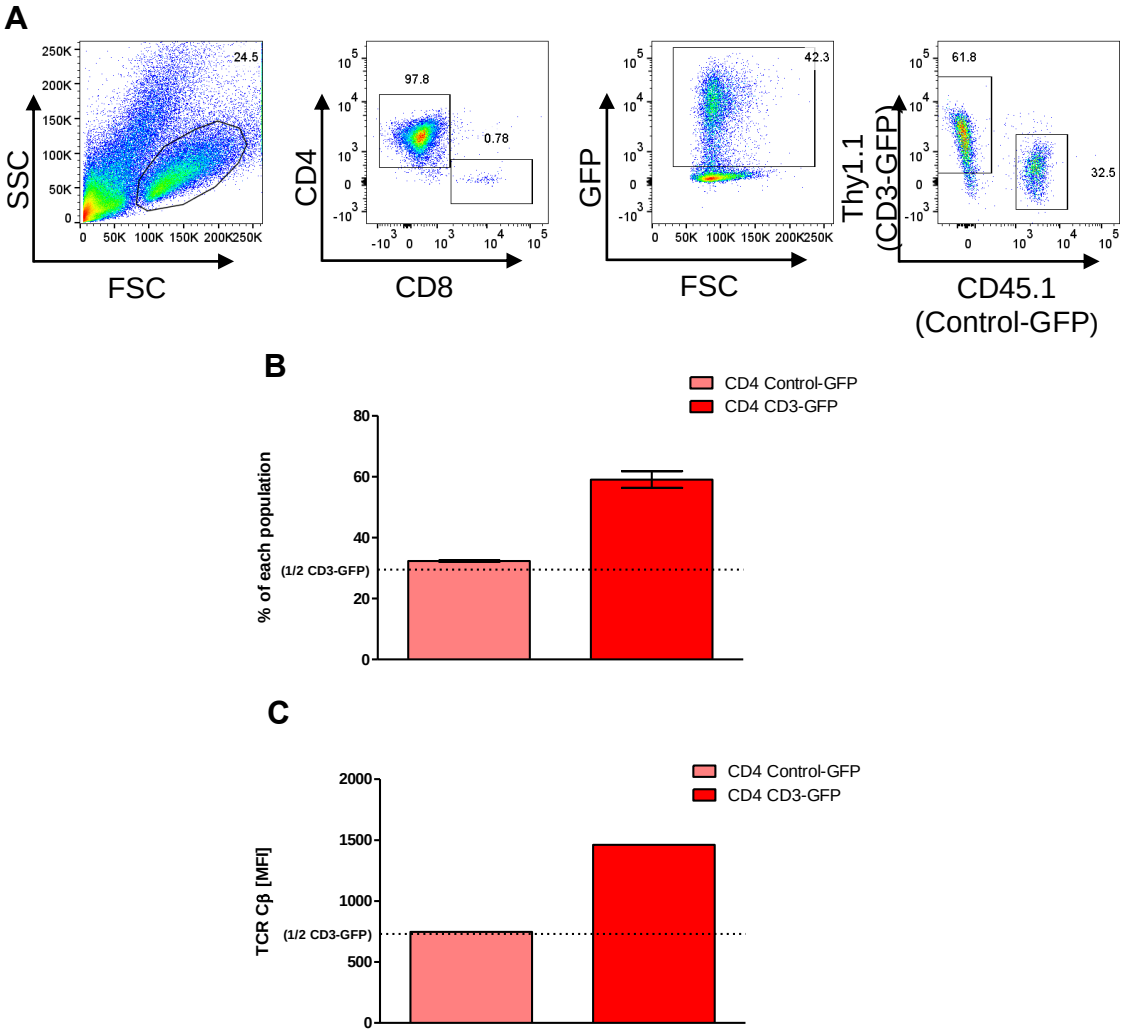

Figure 5.18 – Purity, transduction efficiency, injection mix ratio and TCR expression of the adoptively transferred cells, in the 1:2 competition experiments. (A) Typical purity, transduction efficiency and control-GFP:CD3-GFP ratio of the injection mix are shown. (B) The average proportion of Control-GFP and CD3-GFP cells in the injection mix is shown. The proportion of control-GFP cells in the injection mix was half that of CD3-GFP cells (SEM is shown). (C) The TCR expression in the control-GFP and CD3-GFP transduced cells used for adoptive transfer was examined by looking at the median fluorescent intensity (MFI) of the TCR (constant β chain). Data from 2 independent experiments.

The differentiation status based on CD127 and CD62L expression was also analysed before injection (figure 5.19). Figure 5.17B shows CD62L and CD127 expression in two representative populations of control-GFP and CD3-GFP transduced $CD4^+$ T cells. At the time of injection both populations contained similar proportions of naïve cells ($CD127^+$ $CD62L^+$; control-GFP: 50.5%; CD3-GFP: 45.4%); $CD127^-$ $CD62L^-$ effector cells (control-GFP: 6.3%; CD3-GFP: 7.6%) and $CD127^+$ $CD62L^-$ memory cells (control-GFP: 29.5%; CD3-GFP: 37.2%) (figure 5.19C). However there was a greater variation between experiments, compared to the previous set of experiments.

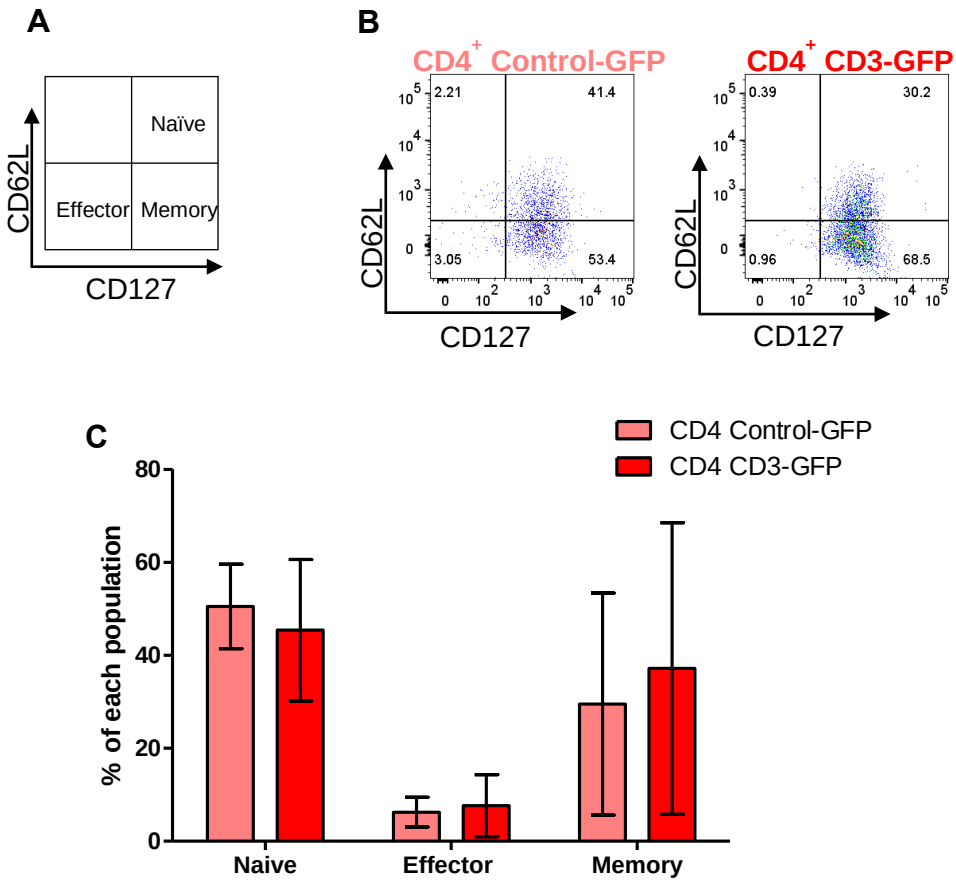

Figure 5.19 – Differentiation status of adoptively transferred cells, in the 1:2 competition experiments. (A) The differentiation status of the adoptively transferred cells was determined by examining CD62L and CD127 expression, as shown by this gating strategy diagram. (B) Representative plots of the differentiation profile seen in the two $CD4^+$ populations of adoptively transferred T cells are shown. (C) The average percentage of naïve, effector and memory cells in the adoptively transferred cells are shown. Mean + SEM are shown. Data from 2 independent experiments.

Figure 5.20 shows the changes from baseline weight observed in recipient animals, none of which lost more than 20% of their body weight.

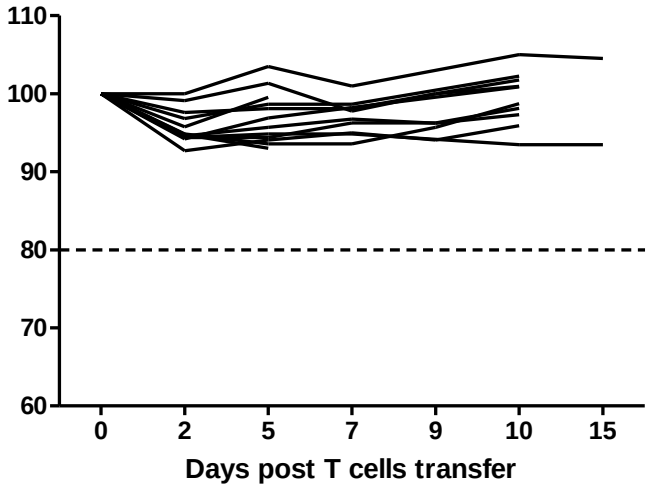

Figure 5.20 – Mice's body weight. The changes in mice weight are plotted as a function of time. Data from 2 independent experiments, n= 11.

On day 5, 10 and 15 post T cell transfer, mice were sacrificed and single cell suspensions of spleen, inguinal lymph nodes, bone marrow (pooled from one tibia and one fibula) and liver were generated, as described in chapter 2, section 2.5.3. The proportion of $CD45.1^+$ control-GFP and $Thy1.1^+$ CD3-GFP $CD4^+$ T cells in each tissue was analysed. The flow cytometric gating strategy used for the analysis of the single cell suspensions was the same used for previous experiments, and it is shown in figure 5.4A.

Figure 5.21A shows the control-GFP and CD3-GFP populations between injection day and day 15 in the spleen. At day 5 there was an increase in the proportion of CD3-GFP cells (78.1%), and a reciprocal decrease in the proportion of control-GFP cells (20.8%; $p \leq 0.01$). Five days later the marked difference between the seizes of the two populations decreased, with control-GFP cells accounting for 31.4%, and CD3-GFP cells accounting for 45.8% of the total population of $CD4^+$ GFP^+ cells ($p \leq 0.05$). However, 15 days after injection the percentage of recovered CD3-GFP cells (77.7%) was more than 4 times that of control-GFP cells (16.8%; $p \leq 0.001$).

Similarly, in the lymph nodes (figure 5.21B) after 5 days of *in vivo* exposure to "self" the percentage of CD3-GFP cells had increased (74.5%) relative to the composition of the injection mix, with the proportion of control-GFP cells decreasing to 21.1% ($p \leq 0.05$). At 10 days post adoptive transfer CD3-GFP cells accounted for 57.8% of the total population of isolated GFP^+ cells; control-GFP cells represented 36.5% of the total GFP^+ population ($p \leq 0.05$). As observed in the spleen, at the latest analysed time point a relative expansion of CD3-GFP cells compared to control-GFP cells had occurred, with 80.1% and 16.1% of CD3-GFP and control-GFP T cells, respectively, isolated from the GFP^+ population ($p \leq 0.001$).

The findings in the bone marrow were different. Contrary to the trend seen in the previous two analysed tissues, in the bone marrow (figure 5.21C) 5 days post initial cell transfer the percentage of CD3-GFP cells had decreased to 50.1% with a moderate increase in control-GFP cells to 40.5%, and this trend continued until day 10 with 42.2% of the remaining transferred cells belonging to the CD3-GFP subset and 50.4% control-GFP.

Analysis at day 15 revealed that this trend inverted after day 10, with 75.4% of CD3-GFP cells and 19.1% of control-GFP cells accounting for the total GFP^+ population ($p \leq 0.01$).

The trends in the liver (figure 5.21D) mirrored those of the spleen and the lymph nodes. At day 5 post T cell transfer CD3-GFP cells accounted for 74%, and control-GFP cells accounted for 25.3% of the total GFP^+ population ($p \leq 0.001$). By day 10 the percentage of CD3-GFP cells had dropped to 54.2%, and that of control-GFP had slightly increase to 26.9% ($p \leq 0.01$). Just like in the spleen and lymph nodes five days later the proportion of CD3-GFP cells isolated from the GFP^+ population was much greater to that of control-GFP cells (81.7% and 16.9%, respectively; $p \leq 0.01$).

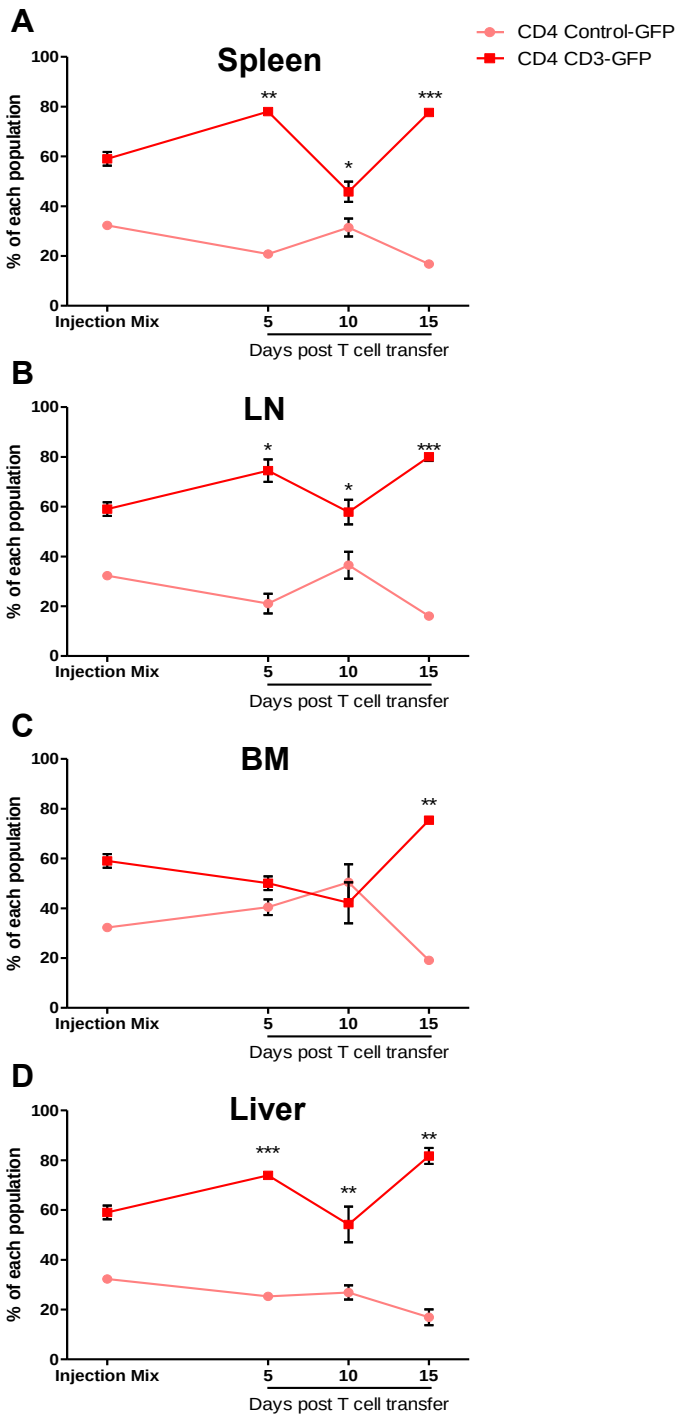

Figure 5.21 – Change in the proportion of control-GFP and CD3-GFP CD4+ T cell populations overtime, 1:2 experiments. The proportions of control-GFP and CD3-GFP T cells in to the total $CD4^+$ GFP^+ population isolated from the spleen (A), inguinal lymph nodes (B), bone marrow (C) and liver (D) were analysed and plotted as a function of time. The adoptively transferred cells were identified using the gating strategy described in figure 5.4 A. Data from 2 independent experiments. Day 5 n=2; day 10 n=7; day 15 n=2. (p=* ≤0.05; **≤0.01; ***≤0.001; unpaired t test. Mean + SEM are shown).

5.11. TCR downregulation trends are similar to those seen in a 2:1 competition settings

Again, the changes in TCR expression over time were tracked in this set of experiments too.

In the spleen at day 5 post T cell transfer, CD3-GFP cells expressed 1.9 times more endogenous TCR compared to control-GFP cells ($p \leq 0.05$). This difference decreased to 1.7 times at day 10 ($p \leq 0.01$) and 1.5 times at day 15 ($p \leq 0.05$) (figure 5.22A).

Figure 5.22B shows the changes in cell surface TCR density on the transduced cells homing to the lymph nodes. At 5 days post adoptive transfer, CD3-GFP T cells isolated from the lymph nodes expressed 1.4 fold higher TCR as control-GFP cells did. An increase in TCR expression in the CD3-GFP population was seen at day 10, with a 1.8 fold higher TCR expression compared to control-GFP cells. At the last time point of the analysis (day 15 post T cell transfer) the observed difference in TCR expression between the two populations decreased, with CD3-GFP cells expressing 1.6 times as much TCR as control-GFP transduced cells did.

In the bone marrow (figure 5.22C), the smallest differences in TCR expression between the two populations of T cells were seen. Already by 5 days post T cell transfer, CD3-GFP cells only expressed 1.3 times as much TCR as control-GFP cells did. This difference increased to 1.6 times at day 10 ($p \leq 0.01$), to then decrease again at day 15 when TCR expression in the cells transduced with the CD3-GFP vector was 1.4 folds that of control-GFP cells ($p \leq 0.05$).

In the liver (figure 5.22D), 5 days post adoptive transfer CD3-GFP cells expressed 2.3 fold higher TCR as control-GFP cells ($p \leq 0.01$); five days later CD3 over-expressing cells had down-regulated their TCR, and they expressed 1.9 times as much TCR as the control population ($p \leq 0.05$). Lastly, at day 15 CD3-GFP cells further down-regulated their

TCR and at this time point the difference in cell surface TCR expression was lowest, with CD3-GFP cells expressing 1.4 times as much TCR as control-GFP cells ($p \leq 0.01$).

GFP expression was confirmed over time (figure 5.23 A-D). In this instance the kinetics of GFP expression were different to the kinetics of TCR expression. TCR expression was observed to increase following injection (figure 5.22 A-D), whilst GFP expression was down-regulated in the majority of the populations between injection day and day 5. In all tissues GFP expression decreased in both populations of transduced cells between day 5 and day 10. After day 10 the expression trends were different in the different tissues, and in the two populations of transduced cells. The GFP MFI in the CD3-GFP transduced cells increased in the spleen, whereas it decreased in all the other tissues. In the control-GFP transduced population, GFP expression remained stable in the lymph nodes and bone marrow, and it increased in the spleen and liver.

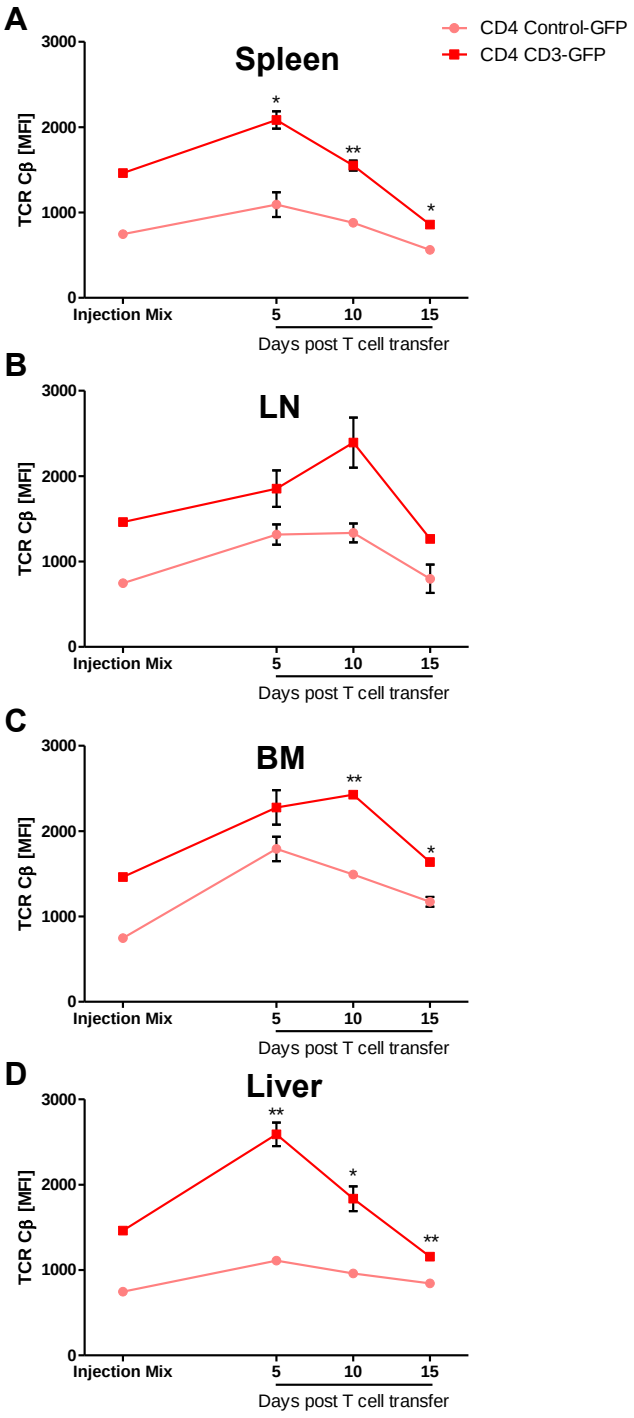

Figure 5.22 – TCR expression of control-GFP and CD3-GFP cells, 1:2 experiments. The TCR expression (MFI) of the control-GFP and CD3-GFP T cells isolated from the different tissues at day 5, 10 and 15 is plotted. The adoptively transferred cells were identified using the gating strategy described in figure 5.4 A. (A) Spleen; (B) inguinal lymph nodes; (C) bone marrow; (D) liver. Data from 1 experiments. Day 5-15 n=2. (p=*≤0.05; **≤0.01; unpaired t test. Mean + SEM are shown).

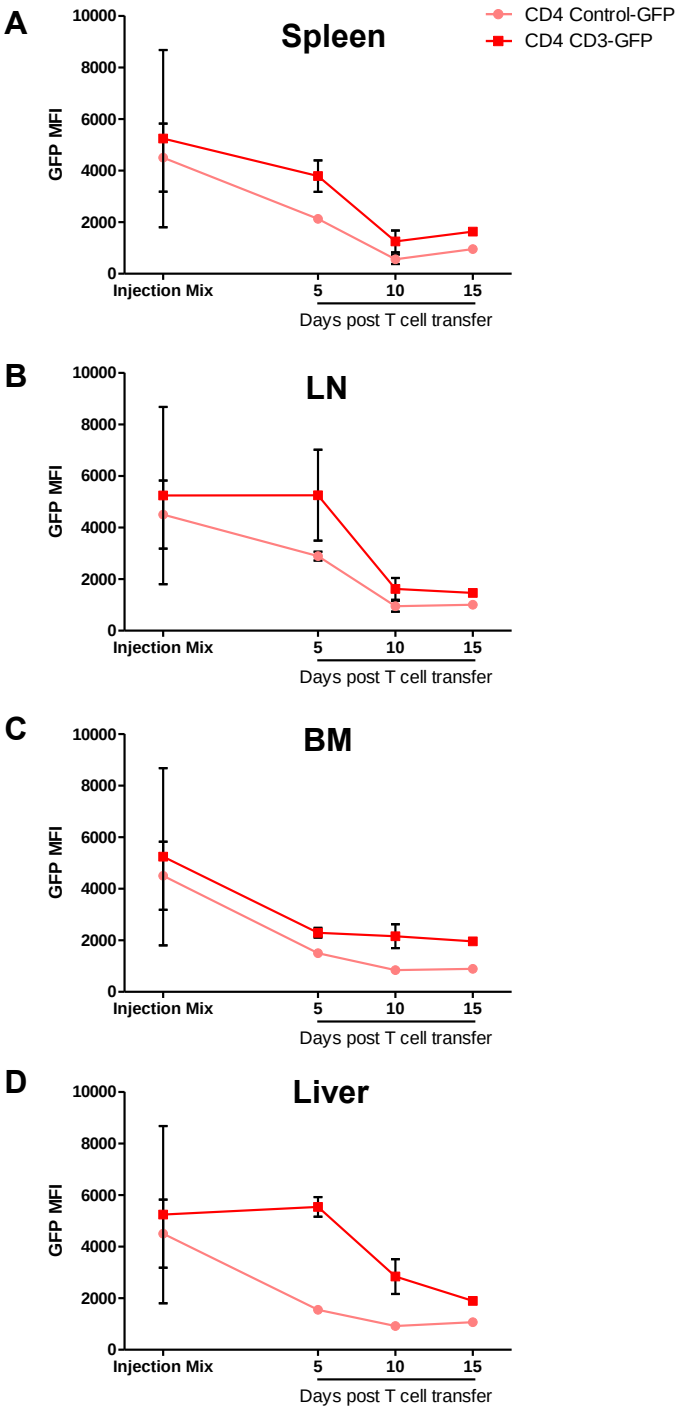

Figure 5.23 – GFP MFI of control-GFP and CD3-GFP CD4+ T cell populations, 1:2 competition experiments. The MFI of GFP in the population of control-GFP and CD3-GFP T cells isolated from the different tissues at day 5, 10, 15 and 20 is plotted. The adoptively transferred cells were identified using the gating strategy described in figure 5.4 A. (A) Spleen; (B) inguinal lymph nodes; (C) bone marrow; (D) liver. Data from 2 independent experiments. Day 5 =2, day 10 n=7, day 15 n=2. Mean + SEM are shown.

5.12. CD3-overexpressing and control-transduced CD4$^+$ T cells have similar rates of cell proliferation and cell death in a 1:2 competitive *in vivo* environment

The trends in cell accumulation and TCR down-regulation that were seen in the 1:2 control-GFP to CD3-GFP competition environment, were different to those seen when the proportion of control-GFP cells in the injection mix was twice as that of CD3-GFP cells. To determine whether this difference in accumulation was due to a higher rate of proliferation or a lower rate of cell death, the proportion of proliferating and apoptotic cells in the two different populations were analysed.

In the spleen (figure 5.24A) no significant difference in the percentage of proliferating cells was seen at any of the time points, between the two populations. At day 5 between 9.5% and 11.1% of cells in the control-GFP and CD3-GFP populations respectively, were found to be positive for Ki67. These percentages marginally increased at day 10 (control-GFP: 11.2%; CD3-GFP: 13.6%), to then decrease again by day 15 (control-GFP: 5.7%; CD3-GFP: 8.4%).

In the lymph nodes (figure 5.24B) less than 20% of all GFP$^+$ cells were Ki67$^+$ by day 5 post T cell transfer (control-GFP: 15%; CD3-GFP: 16.9%). These proportions decreased further at 10 days post T cell transfer (control-GFP: 10%; CD3-GFP: 12.9%), and by day 15 post injection the percentage of Ki67$^+$ cells in the two populations were identical (11.2%).

The initial trend seen in the bone marrow (figure 5.24C) was identical to that seen in other tissues, with the percentage of proliferating cells dropping below 20% in both populations (control-GFP: 10.9%; CD3-GFP: 12.7%) at day 5 post infusion. However, after day 5 the percentage of proliferating cells in the CD3-GFP cells started to increase (12.9%) compared to that observed in the control-GFP cells (8.8%) (day 10), and at day 15 the difference was even greater with the proportion of proliferating cells in the CD3-

GFP population being 13.3%, compared to 7.6% of proliferating cells in the control population. However, these values were not significantly different.

The changes described above for the bone marrow were more pronounced in the liver (figure 5.24D). Cells isolated from both populations at day 5 contained very similar proportions of proliferating cells (control-GFP: 9%; CD3-GFP: 10.2%). At day 10, 26% of CD3-GFP cells were proliferating, compared to 15.9% of proliferating cells in the control-population ($p \leq 0.01$). Five days later 22.6% of CD3-GFP cells were $Ki67^+$, whereas the control-GFP population contained 15% of proliferating cells.

The percentage of apoptotic cells was similar between the two populations in the different organs.

In the spleen (5.24E) at day 5 on average 34.2% of cells in the CD3-GFP population were positive for Annexin V, compared to 15.1% of Anenxin V^+ cells isolated from the control-GFP population. Ten days post T cell transfer, 19.4% and 12.9% of all cells from the CD3-GFP and control-GFP population respectively, were identified as positive for Annexin V. At day 15 the percentages of apoptotic cells from the control-GFP and the CD3-GFP populations was 6.8% and 8.2%, respectively.

No difference in Annexin V expression was seen between the two transduced populations isolated from the lymph nodes, at any of the analysed time points (figure 5.24F). In both populations the percentage of apoptotic cells increased between injection day and day 5 post T cell transfer, when in the population of control-GFP cells 25% of cells were apoptotic, and 31.7% of CD3-GFP cells were positive for Annexin V. Five days later 29.4% of all CD3-GFP cells and 32.3% of all control-GFP cells were apoptotic. Similar percentages were seen at day 15, with 25.4% of control-GFP and 26% of CD3-GFP cells undergoing apoptosis.

The bone marrow (figure 5.24G) contained the highest percentage of apoptotic cells of all tissues. By day 5, 74.1% and 85.1% of cells from the control-GFP and the CD3-GFP respectively were found positive for Annexin V. A marginal decrease was seen at day 10

(control-GFP: 51%; CD3-GFP: 53.5%), followed by another increase in Annexin V expression at day 15, when 70% of control-GFP cells and 78.3% of CD3-GFP cells were apoptotic. This higher proportion of Annexin V^+ cell is in line with previous reports where a higher turnover rate was shown for T cells in the bone marrow as compared with spleen and lymph nodes (Parretta et al., 2008).

In the liver (figure 5.24H) the levels of apoptotic cells were not statistically different and remained below 10% in both populations, throughout the analysis.

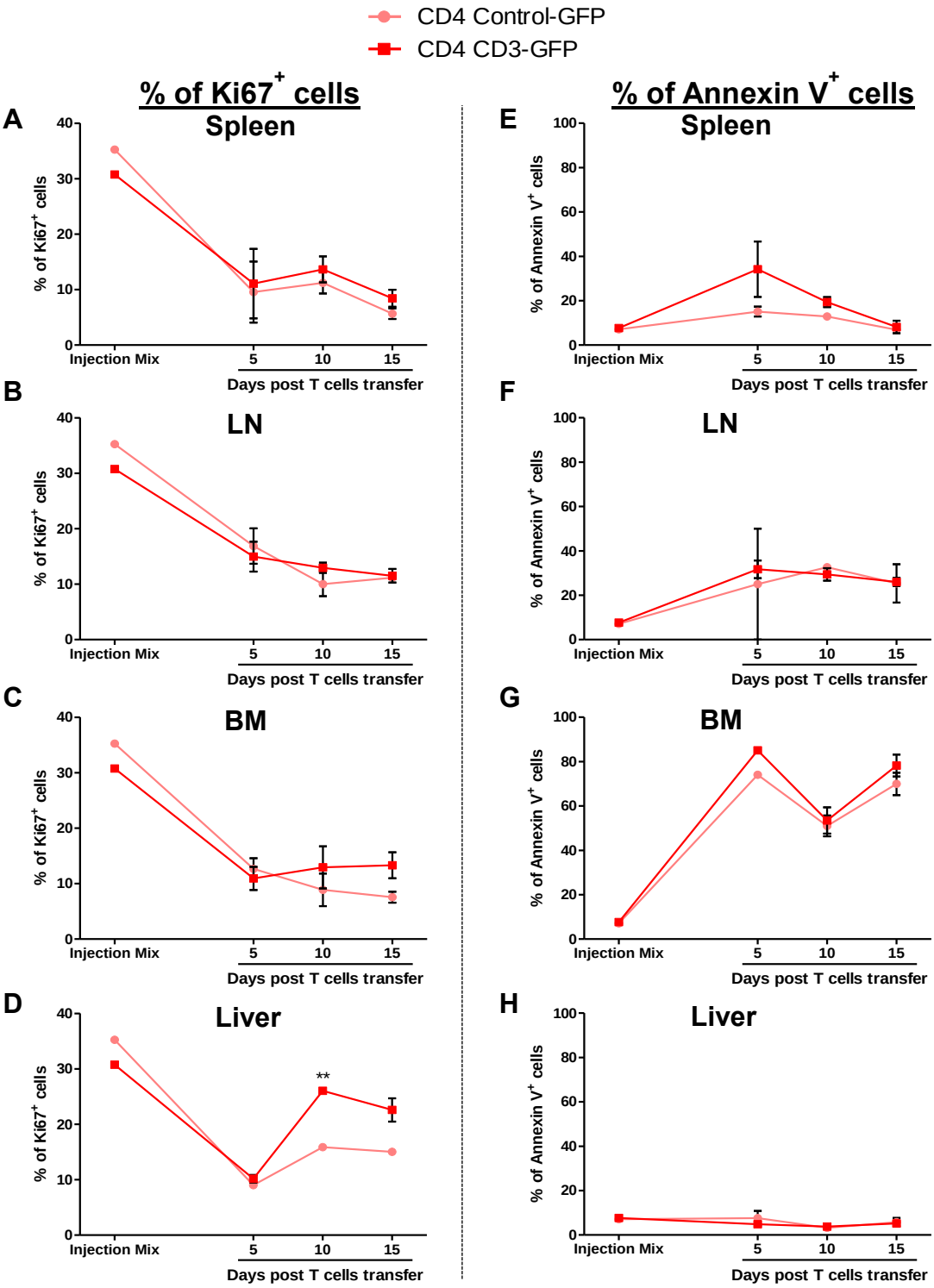

Figure 5.24 – Percentage of Ki67+ and Annexin V+ control-GFP and CD3-GFP cells, 1:2 experiments. The percentage of Ki67⁺ (left) and Annexin V⁺ (right) cells in the control-GFP and CD3-GFP populations overtime is shown. The adoptively transferred cells were identified using the gating strategy described in figure 5.4 A. (A, E) Spleen; (B, F) inguinal lymph nodes; (C, G) bone marrow; (D, H) liver. Data from one experiment. Day 5-15 n=2. (p=**≤0.01; unpaired t test. Mean + SEM are shown).

5.13. The differentiation profile of the adoptively transferred cells in a 1:2 competition context is influenced by the homing of the cells, and it's different from that seen in a 2:1 competition

As seen in the previous experiments, the differentiation profile of the transduced cells isolated from the four analysed tissues was determined by the homing site of the cells. The percentages of naïve, effector and memory cells in the two populations of transduced cells were not affected by CD3 over-expression, but were different according to the organ from which they were re-isolated.

On average in the spleen (figure 5.25 left) 5 days after adoptive transfer, the percentage of effector cells and memory cells was similar (effector cells: 42.3%-47.8%; memory cells: 37.9%-45.7%), whereas a lower proportion of naïve cells were recovered (2.8%-8%). The proportion of memory cells increased with time and at day 10, 66.8%-71.8% of memory cells were recovered. At the same time point the percentage of effector cells in the populations was 20.4%-24.2%; that of naïve cells was 2.9%-4.4%. At the last analysed time point (day 15 post T cell transfer) the same trend was seen, with memory cells representing the highest proportion of cells (61.1%-63.2%), followed by effector cells (28%-28.3%) and naïve cells (6.7%-8.7%).

The trends seen in the lymph nodes are shown in figure 5.25 right. At day 5 post adoptive transfer the highest proportion of cells in the two transduced populations were memory cells (46.7%-55%), followed by effector cells (31.1%-38.9%), and naïve cells (4.2%-8.4%). Five days later the proportions of effector and memory cells were similar and were 37.2%-41.8% and 37%-37.1%, respectively. At this time point naïve cells accounted for 14% of the total populations. Fifteen days post adoptive transfer memory cells accounted for more than 60% of the total population (65.9%-73.8%), whereas the percentages of naïve and effector cells were lower (9.5%-13.6% and 15%-16%, respectively).

The proportion of naïve, effector and memory cells in the bone marrow (figure 5.26 left) were similar 5 days post T cell transfer (24.1%-36.8%, 17.9%-22.5% and 19.1%-28.4%, respectively). At day 10 post T cell transfer, memory cells represented the highest proportion of cells (56.7%-60.2%), followed by effector cells (31.7%-33.1%) and lastly naïve cells (4.6%-5.3%). Analysis of the cells isolated at the last time point, revealed that the majority of transduced cells had acquired a memory phenotype (50.2%-51.5%). The proportion of naïve cells was 23%-23.5%, and that of effector cells was 17.8%-18.7%.

The differentiation trends of the cells homing to the liver are depicted in figure 5.26 right. Memory and effector cells represented the main populations isolated 5 days post T cell transfer (49.6%-52.5% and 43.3%-45.3%, respectively). The proportion of naïve cells was between 2.3% and 4.8%. Similar percentages were seen at day 10 (naïve cells: 2.7%-5.4%; effector cells: 39.8%-42%; memory cells: 51.2%-55.3%). The same trend was again seen five days later, with memory cells accounting for 65.6%-66.9%, effector cells accounting for 28.4%-29.15%, and naïve cells accounting for 4%-4.7% of the total GFP^+ populations.

Finally, the TCR expression levels in naïve, effector and memory cells from the two populations of transduced cells were analysed as before (figure 5.27). Again, no difference in the level of TCR expression was observed on naïve, effector and memory cells from the same transduced population. As expected, naïve, effector and memory cells isolated form the CD3-GFP transduced $CD4^+$ T cells expressed higher levels of TCR compared to their counterparts in the control-GFP transduced population. The kinetics of TCR expression were similar to those seen in the whole populations of control-GFP and CD3-GFP transduced populations (figure 5.22).

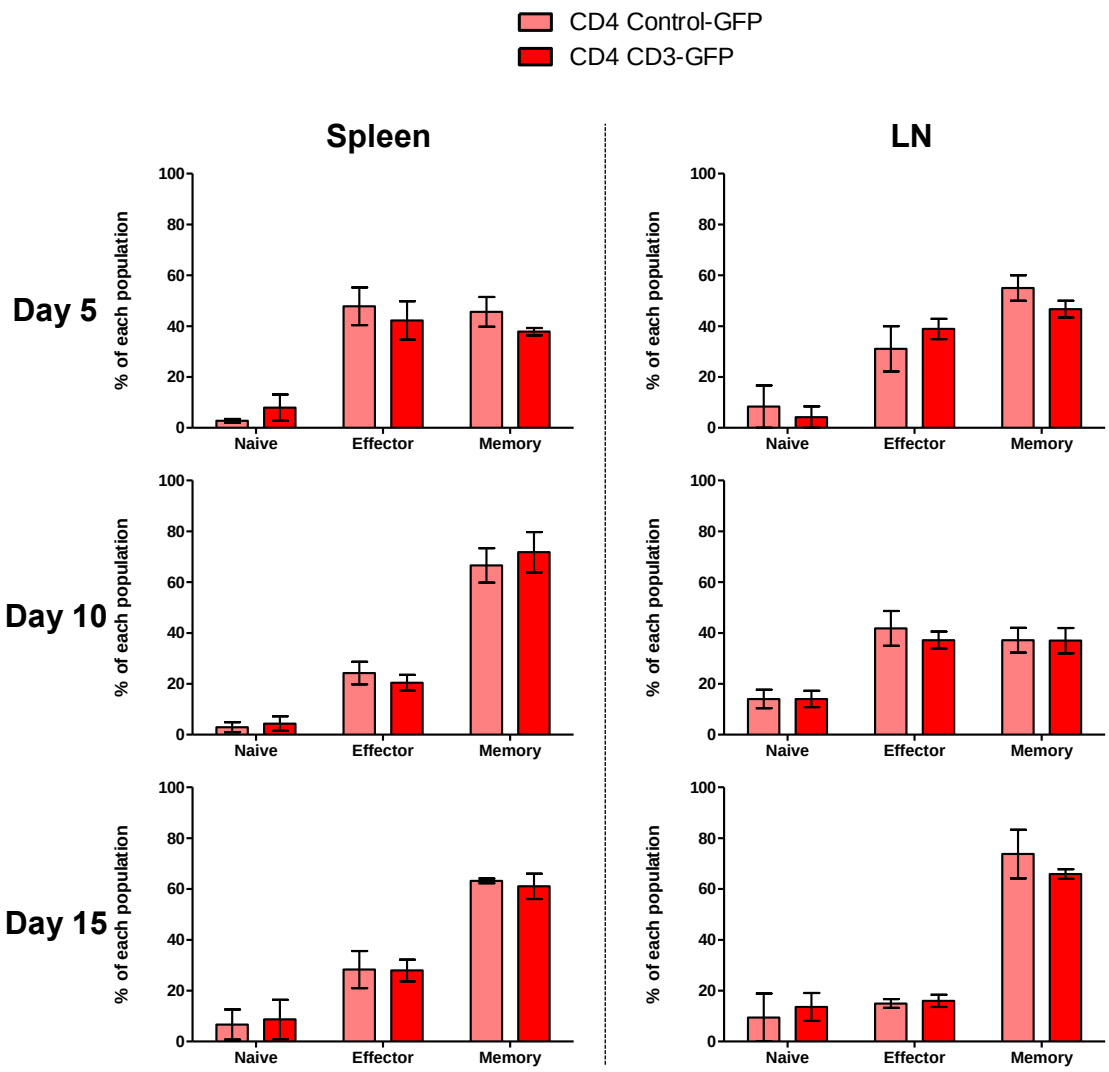

Figure 5.25 – Day 5-15 ex vivo differentiation status of the adoptively transferred cells. The differentiation status of the control-GFP and CD3-GFP T cells isolated from the spleen (left) and inguinal lymph nodes (right), at day 5, 10, 15 and 20 are shown. The adoptively transferred cells were identified using the gating strategy described in figure 5.4 A. Data from one experiment. Day 5-15 n=2. Mean + SEM are shown.

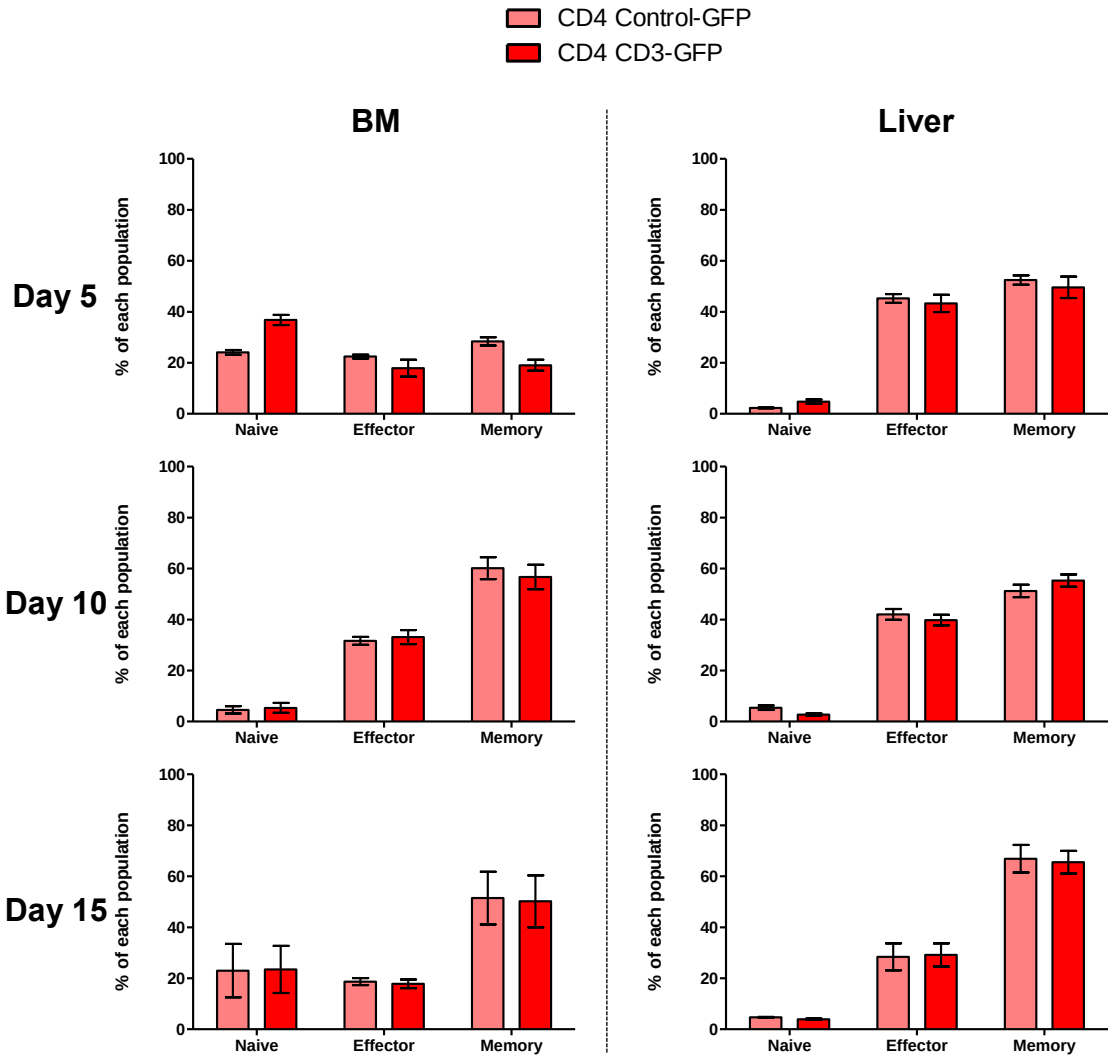

Figure 5.26 – Day 5-15 *ex vivo* differentiation status of the adoptively transferred cells. The differentiation status of the control-GFP and CD3-GFP T cells isolated from the bone marrow (left) and liver (right), at day 5, 10, 15 and 20 are shown. The adoptively transferred cells were identified using the gating strategy described in figure 5.4 A. Data from one experiment. Day 5-15 n=2. Mean + SEM are shown.

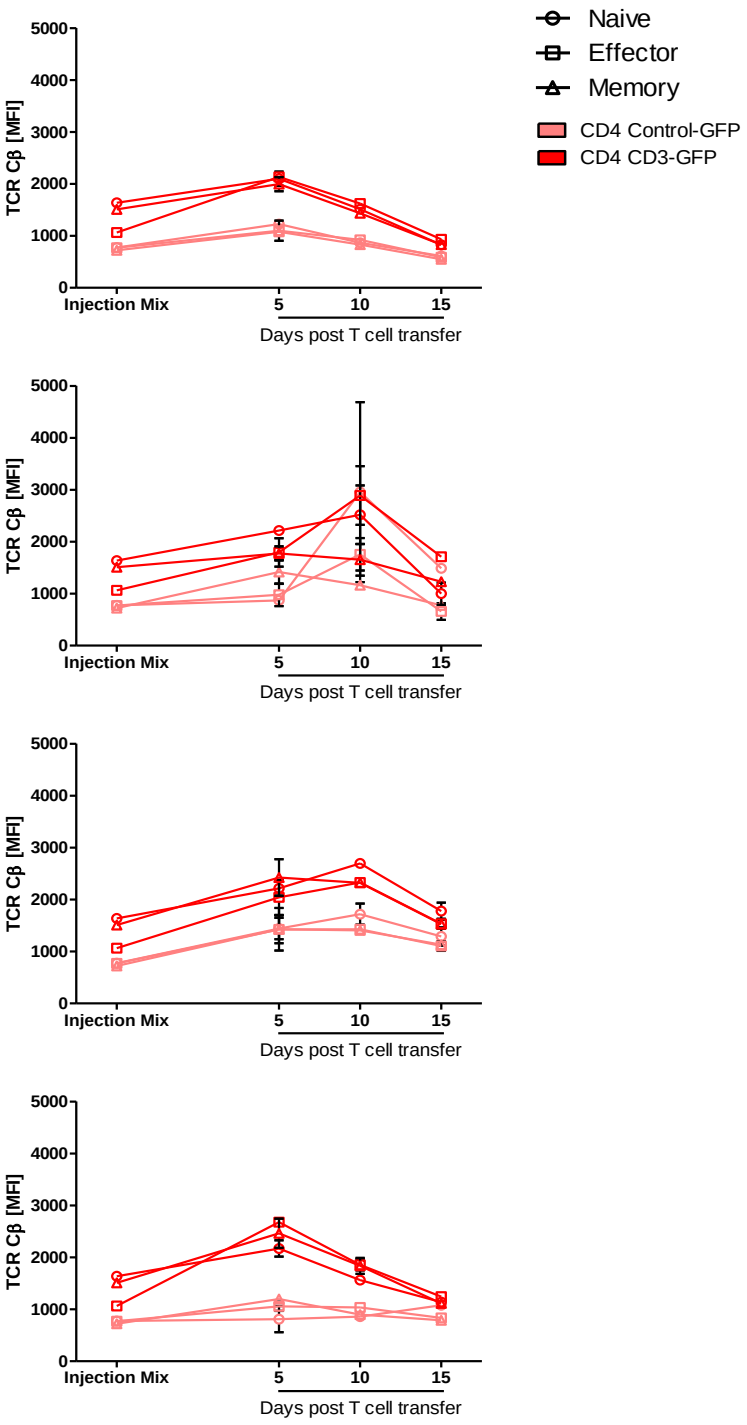

Figure 5.27 – TCR expression of naïve, effector and memory cells from the control-GFP and CD3-GFP CD4+ T cell populations, 1:2 competition experiments. The TCR expression of the naïve, effector and memory cells, of the control-GFP and CD3-GFP T cell populations isolated from the different tissues at day 5, 10, 15 and 20 is plotted. The adoptively transferred cells were identified using the gating strategy described in figure 5.4 A. (A) Spleen; (B) inguinal lymph nodes; (C) bone marrow; (D) liver. Data from 1 independent experiments. Day 5-15 n=2. Mean + SEM are shown.

5.14. Summary and discussion

The aim of the experiments described in this chapter was to determine whether the accumulation of CD3-overexpressing $CD4^+$ T cells seen in a non-competition setting (chapter 4), was also observed in a competitive environment. CD3-overexpressing $CD4^+$ T cells were co-transferred with control-GFP transduced $CD4^+$ T cells into lymphopenic syngeneic recipients. Three different ratios of control-GFP:CD3-GFP were used (1:1, 2:1 and 1:2) to study the behaviour of CD3-overexpressing cells. Transfer of injection mixes containing different proportions of control-GFP and CD3-GFP cells means that CD3-overexpressing cells have to compete with similar, higher or lower proportions of competitor cells for survival signals (self-p:MHC complexes and cytokines), which might result in different CD3-GFP T cells' survival and differentiation outcomes. How the persistence of control-GFP and CD3-GFP transduced cells varies over time was tracked by sacrificing recipient animals at different time points (5, 10, 15 and 20 days after adoptive transfer), and looking in the spleen, inguinal lymph nodes, bone marrow and liver. The proportion of proliferating and apoptotic cells in each one of the transferred populations was also analysed by looking at the expression of Ki67 and Annexin V respectively. This allowed us to determine whether the difference in cell accumulation was a consequence of increased/decreased cell proliferation, or increased/decreased cell death. The kinetics of TCR expression was also analysed over time to investigate how these related to cell's persistence. Finally the differentiation status of the transferred cells homing to the spleen, lymph nodes, bone marrow and liver was examined.

In the first set of experiments irradiated mice received a 1:1 mix of control-GFP:CD3-GFP cells. We found that 10 days post adoptive transfer, CD3-overexpressing $CD4^+$ T cells are found in significantly higher percentages compared to $CD4^+$ T cells that express physiological levels of TCR and CD3. Both cell populations were analysed before injection for purity and differentiation status. In both cases they were >95% pure, and both populations contained the same proportion of naïve, effector and memory cells. Thus we concluded that the difference in the percentages of isolated cells was due to

different *in vivo* behaviours of the two populations, rather than the consequence of a difference in purity or activation status acquired before injection. This difference in accumulation however did not translated into a difference in activation status. Cells isolated at day 10 had the same differentiation phenotype, independent of level of TCR/CD3 expression (e.g. either control-GFP or CD3-GFP transduced). Specifically, in all four of the analysed tissues, the majority of the cells (over 40%) had an effector phenotype, with this proportion being 85% or higher in the bone marrow and liver.

The kinetics of this accumulation were studied further in a second set of experiments. Recipient mice received a 2:1 mix of control-GFP:CD3-GFP transduced $CD4^+$ T cells, and their accumulation in the four tissues was analysed over time, from day 5 to day 20 post T cell injection. This set of experiments was designed to study the behaviour of CD3-overexpressing T cells when their access to survival signal is limited by an increased number of competitor cells (control-GFP $CD4^+$ T cells). The purity of both injected populations was over 95% and the activation status of the cells was similar, with the majority of the cells retaining a naïve phenotype. Increased TCR expression in the CD3-GFP transduced cells was confirmed before injection, and CD3-overexpressing $CD4^+$ T cells expressed on average 4 fold higher TCR compared to control-GFP transduced cells. Isolation of the transferred cells at the four different time points showed that although at day 5 the population of control-GFP cells still accounted for the majority of cells within the GFP^+ population, by day 10 their percentage had fallen, with CD3-GFP transduced cells representing the highest proportion of GFP^+ cells. After day 10, the percentage of CD3-GFP cells gradually decreased until day 20 when it reached similar or lower numbers then the control-GFP population. The only exception was in the liver, where at day 20 an accumulation of CD3-GFP cells was observed.

Interestingly, the initial increase in the proportion of CD3-overexpressing T cells in the GFP^+ population, was not associated with the kinetics of TCR expression. Indeed, from day 5 onwards CD3-overexpressing cells started to gradually down-regulate their TCR levels. This decrease carried on until day 20 in the spleen, where the TCR expression

levels of control-GFP and CD3-GFP T cells were indistinguishable. In other tissues the TCR expression levels plateaued at day 15 post T cell transfer, when it reached similar levels to that seen in the control-GFP population. In all 4 tissues, an initial increase in TCR expression was observed between day 0 and day 5 in the control-GFP transduced T cells. After day 5 TCR down-regulation occurred in the control cells, but at a much lower extent to that seen in CD3-GFP transduced T cells. For example, in the spleen a 3 fold decrease in TCR expression is seen in the CD3-GFP population, between injection day and day 20. On the contrary, no overall down-regulation is seen in control-GFP cells, with TCR expression levels at day 20 being identical or higher to those seen at injection day.

The accumulation of CD3-overexpressing $CD4^+$ T cells seen in the mice receiving the 2:1 ratio of cells, is a consequence of increased cell proliferation in this population. A higher proportion of $Ki67^+$ cells is found in the $CD4^+$ population transduced with the CD3-GFP vector. This increase in proliferating cells began after day 5, and it was seen until day 15, after which both transduced populations equilibrated at similar proportions of proliferating cells. The proportion of apoptotic cells on the other hand, was similar in the two populations at all analysed time points, with the exception of day 5 in the spleen and lymph nodes, when the percentage of Annexin V^+ T cells within the CD3-overexpressing population of $CD4^+$ T cells was higher.

As previously discussed, the driver of this proliferation is unknown. Increased proliferation may be a consequence of stronger interactions with self-p:MHC complexes, or stronger ligand-independent TCR signalling. As previously mentioned CD5 can be used to indirectly verify the strength of T cell interaction with self, with high CD5 expression triggered by stronger self-p:MHC interactions. Indeed, Mandl and colleagues have shown that polyclonal $CD5^{hi}$ $CD4^+$ T cells have higher proliferation rates compared to $CD5^{lo}$ $CD4^+$ T cells. This resulted in $CD5^{hi}$ $CD4^+$ T cells outcompeting $CD5^{lo}$ cells in an infection model, in which the two populations were initially transferred in a 1:1 ratio. The different proliferative ability was not attributed to different cell-intrinsic proliferation

abilities, as observed *in vitro* responses were similar in the two populations. Interestingly, the same $CD5^{hi}$ clones that dominated the anti-infectious response, showed stronger interaction with self (Mandl et al., 2013). Thus, if self-p:MHC interaction is driving the observed T cell proliferation and CD3-overexpressing T cells interact more strongly with self, we would expect our CD3-overexpressing $CD4^+$ T cells to express higher levels of CD5 compared to the control-GFP transduced population.

Although marked TCR down-regulation was seen in the CD3-GFP transduced population, their proliferation continued until day 15; after this time point the proportion of proliferating cells decreased. Interestingly day 15 is the time point when the TCR expression of the two populations reach similar levels. Thus, our data supports the hypothesis that higher levels of endogenous TCR expression, even if only marginally higher, can still promote preferential T cell proliferation. As soon as the CD3-overexpressing T cells lose this advantage, their proliferative capacity returns to baseline levels as seen in the control-GFP transduced $CD4^+$ population.

How CD3-overexpressing T cells out-proliferate control-GFP transduced T cells is not known. Three main models of T cell competition for “space” have been proposed (Takada et al., 2009a). In the first case “intraclonal competition” between T cell clones recognising the same self-p:MHC complex, regulates the survival of clones with the same specificity, but does not interfere with the maintenance of clones of different specificity. The second proposed mechanism is based on the promiscuity of the TCR (“interclonal dominance through promiscuity” model). More promiscuous TCRs, capable of recognising multiple self-p:MHC complexes, can out-compete T cell clones that are less promiscuous, by preventing them from interacting with their self-p:MHC complexes. Finally, in the last proposed model, some T cell clones can outcompete other clones through interclonal competition for survival signals (“interclonal dominance through fitness” model). In this model T cell clones only compete with their cognate self-p:MHC complex, but these different TCR:self-p:MHC interactions lead to acquisition of different survival capacities by some clones, for example allowing some of them to compete more

effectively for other survival signals, such as cytokines. Indeed, Agenes and colleagues showed that OT1 cells (H-2K^{b}-restricted) co-transferred with P14 cells (H-2D^{b}-restricted) into P14 recipients, proliferate whereas P14 cells do not. Moreover they also used parabiotic pairs of OT1 Rag$^{-/-}$ and K^{b}-sufficient or K-^{b}-mutant mice to demonstrate that OT1 cells prevented homeostatic proliferation of P14 cells, even in the presence of K^{b}-deficient APCs, which OT1 cells cannot interact with. This difference in proliferative capacity was a consequence of the higher ability of OT1 cells to access IL-7 and IL-2, compared to P14 cells (Agenes et al., 2008).

It is possible that increasing the TCR levels on T cell clones, may render them more promiscuous, as their increased avidity may allow them to bind more self-p:MHC complexes. However whether increased TCR expression confers increased ability to compete for other survival signals, is not known. Thus, in our model the interclonal dominance through promiscuity model alone, or a combination of this model with the "interclonal dominance through fitness" one, may be promoting the observed increased cell proliferation. Alternatively, increased TCR expression may not lead to increased promiscuity, but simply stronger activation signals, leading to increased proliferation and higher cell numbers, which outcompete the lower proliferating cells.

In the third set of experiments, where the mice received twice as much CD3-GFP transduced CD4^{+} T cells, compared to control-GFP transduced CD4^{+} T cells, the percentage of CD3-overexpressing CD4^{+} T cells, remained higher than that of control-GFP T cells throughout the majority of the experiments. One exception was the bone marrow at day 10 post T cell transfer, when the percentage of control-GFP T cells was slightly higher than that of CD3-GFP T cells; however, after a further 5 days the proportion of CD3-overexpressing cells was almost 4 fold higher than the control-GFP cells. In the other 3 analysed tissues, throughout the analysis the proportion of CD3-GFP cells in the total GFP^{+} population was between 4.8 and 5 folds higher than the control-GFP cells, a diversion from the original 1:2 ratio seen in the injection mix. This difference in the behaviour of the cells may be attributed to the different TCR down-regulation seen

in the adoptively transferred cells in these experiments. Although TCR down-regulation in the CD3-overexpressing $CD4^+$ T cells still occurs, the extent of the down modulation is almost 4 times less that seen in the 2:1 competition experiments. The greatest down-regulation is seen in the spleen, and the difference in TCR expression between injection day and day 15 post T cell transfer is 1.7 times lower, compared to the 3 fold decrease seen in the 2:1 competition experiments. Why a difference in the extent of the TCR down-regulation is seen is unknown. However this could be partially explained by the fact that in this setting CD3-overexpressing $CD4^+$ T cells do not always contain a higher percentage of proliferating cells. Indeed in the spleen and inguinal lymph nodes, both populations of transduced cells contain similar proportions of proliferating ($Ki67^+$) cells throughout the analysis. In the bone marrow similar percentages of $Ki67^+$ cells are seen until day 10; whereas in the liver after day 5 CD3-overexpression leads to increased proliferation levels. As with the 2:1 set of competitions experiments, the levels of Annexin V^+ are similar between the two populations. Since no difference in cell proliferation or cell death was seen in the spleen and lymph nodes, the increase in the proportion of CD3-overexpressing $CD4^+$ T cells in the total GFP^+ population could be explained by control-GFP transduced cells migrating outside of these tissues. On the other two tissues (bone marrow and liver) it could be explained by the higher percentage of proliferating cells in the CD3-GFP transduced population.

Why the proportion of CD3-overexpressing T cells is not downregulated overtime as seen in the previous 2:1 competition set of experiments, is unknown. Notably this data is from one single experiment, thus replicate experiments should be performed to confirm these findings.

Transfer of CD3-overexpressing cells at an advantageous percentage compared to the other population of experimental T cells, means they will have a competitive advantage over the control-GFP transduced T cells. $CD4^+$ T cells expressing physiological levels of TCR have to compete with the CD3-overexpressing population of T cells for survival signals in order to expand. However as previously mentioned, CD3-GFP transduced T

cell may outcompete their competitor population both in terms of access to self-p:MHC complexes and any other potential survival signals. This may drive the persistence of the CD3-overexpressing population, but prevent the persistence of the control-GFP population. Alternatively, since control-GFP T cells may not be able to access survival signals in the tissues where CD3-GFP T cells are also present, they may have migrated out of those organs and into other tissues where less competition was present.

Analysis of trafficking receptors would indicate whether this is the case or not. For example, analysis of the expression pattern of the sphingosine-1-phosphate receptor 1 (S1PR1) would indicate whether control-GFP transduced cells have a higher rate of egress from the lymphoid organs. S1PR1 recognises the phospholipid sphingosine-1-phosphate (S1P) which is present in the lymph and blood, and promotes T cell egress from various lymphoid tissues (Cyster, 2005). Up-regulation of this receptor on T cells promotes their migration out of secondary lymphoid organs, thus we could expect control-GFP cells to express more S1PR1 compared to CD3-overexpressing $CD4^+$ T cells. Moreover, it has previously been reported that $CD4^+$ T cell maintenance in the periphery is dependent on, and occurs in secondary lymphoid organs, such as Peyer's patches, in which $CD4^+$ T cells receive specific survival signals (Dai et al., 2001). Thus, analysis of other secondary lymphoid tissues may reveal different homing patterns of control-GFP $CD4^+$ T cells to the CD3-GFP $CD4^+$ T cells.

Down-regulation of retroviral transgene expression has been previously reported (Lindermann et al., 2002; Burns et al., 2009). Thus, to confirm that TCR down-regulation was not due to loss of CD3 overexpression after loss of retroviral transgene expression, the levels of GFP expression were tracked over time. The gene coding for GFP is found on the same retroviral vector as the CD3, or iCre-control, genes. Thus, a loss of the transgene will result in a loss of GFP expression too. Although the kinetics of GFP and TCR expression are different, GFP expression was maintained throughout the experiment, suggesting the transgene is still expressed and TCR down-regulation is the consequence of a TCR specific down modulation. Moreover previous experiments from

our in which the same CD3-GFP vector was used, have shown that 35 days post adoptive T cell transfer T cells co-transduced with the CD3-GFP and the F5-TCR vectors, still expressed higher levels of F5-TCR (Vβ11) compared to cells transduced with the TCR alone, suggesting the CD3 transgene is still expressed (Ahmadi et al., 2011). The difference in TCR and GFP expression kinetics can be explained by the fact that the two genes (CD3/iCre and GFP) are regulated by different promoters. The CD3/iCre and GFP genes are separated by an IRES element. The CD3/iCre genes are found upstream of IRES and their translation relies on a 5' cap-dependent mechanism; GFP is found downstream of IRES, thus its translation is initiated at the IRES site, in a cap-independent manner. In addition to being regulated by two different mechanisms, the efficiency of translation of the two genes is also different. In particular, it is known that the translation initiation of the gene downstream of an IRES element is less efficient than that of the upstream gene (Mizuguchi et al., 2000). Therefore, differences in the MFI of GFP and TCR, as a surrogate for CD3, may be explained by different translational kinetics.

The subsequent differentiation status of the transferred cells seemed to be affected by the proportion at which the two populations of $CD4^+$ T cells were transferred (1:1, 2:1 or 1:2). Indeed, in the 3 different sets of experiments, different activation profiles were seen in the 4 analysed tissues. Moreover, as in chapter 4, whether the phenotype acquired by the T cell was a consequence of their migration to a specific tissue or whether it was acquired somewhere else which then drives the T cell migration, is not known. However, no differences in the proportion of recovered naïve, effector and memory cells, was seen between the two populations in any of the tissues, at any time point. This suggests that TCR expression levels do not alter the differentiation profile of transduced $CD4^+$ T cells.

The majority of the T cells re-isolated from tissues of mice which received a 1:1 mix of transduced cells 10 days post T cell transfer, had an effector phenotype. Effector cells do not express the lymph node homing receptor L-selectin (CD62L), and therefore preferentially migrate between the blood and splenic compartments, but also enter

peripheral organs, such as the liver. The effector cells isolated from the lymph node, may either be newly differentiated cells that are about to egress, or they may be recruited to these lymphoid organs via CD62L independent mechanisms, including E-selectin and α4β1 (Brinkman et al., 2013).

Acquisition of an effector phenotype *in vivo* suggests that the T cells have engaged with their cognate p:MHC complex. This may simply be an interaction between the TCR and self-p:MHC complex. In a physiological context this may promote T cell survival. In a lymphopenic context, this interaction in addition to higher exposure to survival factors, and/or inflammatory cytokines (due to the initial conditioning regime) may drive T cell activation and acquisition of the effector phenotype.

What the findings of the 2:1 and 1:2 competition experiments have demonstrated is that T cell differentiation *in vivo* is a very plastic phenomenon. Indeed, the phenotype of the cells in the different organs changes with time. Broadly speaking in all analysed organs, 5 days post T cell transfer the majority of the cells that were isolated had a naïve or memory phenotype. Five days later the proportion of effector cells had increased, to then subsequently decrease again. By day 15 and day 20 post T cell transfer the majority of the isolated cells again had a naïve or memory phenotype. This may suggest that after T cell transfer into lymphopenic animals, the transduced cells started to expand and acquire an effector like' phenotype. However, further lymphopenia induced proliferation, lack of appropriate signals (e.g. foreign antigens), or repopulation of the lymphoid compartment, may drive the cells to revert their differentiation to a naïve or memory phenotype. Indeed, Goldrath and colleagues showed that once the lymphoid compartment has been repopulated following lymphopenia, and T cell proliferation ceases, T cells return to a naïve phenotype (Goldrath et al., 2000).

The trafficking pattern of the transferred gene-modified T cells is likely to be determined by multiple *in vivo* factors. All the analysed organs function as lymphoid organs, through which naïve cells continuously recirculate. Effector cells need to traffic to those organs to encounter their cognate p:MHC complex, and memory cells home here. As previously

described memory T cells do not express CD62L. Thus more specifically they can be identified as effector memory T cells. It has been previously reported that effector memory T cells can indeed migrate to non-classical lymphoid tissues (e.g. the liver) and reside there as long lived memory cells (Masopust et al., 2001).

Interestingly the phenotype of the cells isolated at day 20 post T cell transfer was similar to that seen in the population of $CD4^+$ cells isolated from untreated mice (figure 4.12). In untreated mice, the majority of the $CD4^+$ T cells isolated from the spleen and inguinal lymph nodes had a naïve phenotype. However, the majority of the $CD4^+$ population isolated from the bone marrow and liver of untreated mice had a memory phenotype. Transferred $CD4^+$ T cells with similar phenotypes were recovered from the injected mice 20 days post T cell transfer. It is possible that longer exposure to "self" in the absence of foreign antigens, may result in reversion of the phenotype of the transduced cells to that seen in untreated animals. Alternatively, it may be that only cells with those specific phenotypes were capable of repopulating the lymphocyte niche in those tissues. In some cases a lower proportion of naïve cells, and a higher proportion of memory cells were seen in the populations of transduced cells. This may have been a consequence of memory formation due to LIP, as described in the previous chapter.

One model of T cell differentiation suggests that memory and effector cells are generated simultaneously upon T cell activation. What determines whether a cell will acquire a memory or effector phenotype, is the extent of the activation stimulus: fully activated cells will become effector cells; whereas cells that encounter their cognate antigen but are not fully activated will differentiate into memory cells. Thus, higher TCR expression may correlate with T cell receiving a stronger activation signal, leading to a preferential differentiation into effector cells, rather than memory cells; and vice versa. To test whether this is the case in our *in vivo* model, the TCR levels on naïve, effector and memory cells from both control-GFP and CD3-GFP transduced populations were analysed. Although all 3 differentiated subsets in the CD3-GFP transduced population expressed higher levels of TCR than control-GFP transduced cells, no significant

difference in TCR expression was seen among the 3 subsets in either one of the transduced populations. Naïve, effector and memory cells all expressed similar levels of TCR, thus in this model, the level of TCR expression did not seem to influence their differentiation.

To conclude, this set of experiments has shown that CD3 overexpression led to increased expression of endogenous TCR, and was sufficient to drive proliferation and promote T cell persistence, even in disadvantageous, competitive environments. However, increased TCR levels were not readily maintained *in vivo*. $CD4^+$ T cells transduced with the CD3-GFP vector gradually down-regulated their TCR, until it reached expression levels similar to those seen in control $CD4^+$ T cells. The extent of down-regulation was also associated with the levels of proliferation: higher proliferation led to greater TCR down-regulation. Lastly, the levels of TCR expression in $CD4^+$ T cells did not influence the differentiation status of those cells.

6. Conclusions and future work

The experiments described in this thesis have explored phenotypic and behavioural differences between $CD4^+$ T cells and $CD8^+$ T cells. In particular, differences were analysed before and after T cells were transduced with a retroviral vector encoding the CD3 ε, δ, γ, and ζ chains (CD3-GFP vector), or a control vector (control-GFP). This transduction was used to increase TCR expression on the surface of the T cell. Indeed, transduction with the CD3-GFP vector led to a significant and similar increase in TCR expression, in both $CD4^+$ and $CD8^+$ T cells.

The amount of CD3 within a cell determines the amount of TCR that will be expressed on the cell's surface. Moreover, one of the main factors influencing TCR avidity is the density of TCR. Thus, increasing the amount of CD3 available in a T cell, will increase the amount of TCR that can be expressed, and the cell's functional avidity. Increased functional avidity following transduction with the CD3-GFP vector was previously shown in $CD8^+$ T cells.

Initial *in vitro* experiments showed that *ex vivo* untreated $CD4^+$ T cells expressed significantly higher levels of TCR (and CD3) than untreated $CD8^+$ T cells. This difference in TCR expression was maintained even after transduction with the CD3-GFP vector. The increase in TCR was similar in both $CD4^+$ and $CD8^+$ T cells, suggesting TCR is not a rate limiting factor in $CD8^+$ T cells. The biological and functional reason behind the difference in TCR expression levels in $CD4^+$ and $CD8^+$ T cells was not investigated in this project. We hypothesise that the different levels of interaction of $CD4^+$ and $CD8^+$ T cells with the lower expressed MHC-II and the higher expressed MHC-I molecules respectively, may influence the levels of TCR on T cells. More frequent interactions of $CD8^+$ T cells with the almost-ubiquitously expressed MHC-I, may drive down-regulation of TCR on this subset, compared to $CD4^+$ T cells.

Future experiments aimed at investigating the levels of basal CD3ζ phosphorylation could help us determine whether increased interaction with self, leading to higher CD3ζ

phosphorylation, is indeed playing a role in modulating TCR expression levels in the periphery. If this is the case, we would expect $CD8^+$ T cells to have higher level of basal CD3ζ phosphorylation.

However, the higher TCR expression in $CD4^+$ T cells may lead to higher avidity interactions with MHC-II molecules, although less frequent, and similar levels of CD3ζ phosphorylation. Thus, to further dissect the level of interaction of $CD4^+$ and $CD8^+$ T cells with "self", future experiments could be aimed at examining the expression of CD5 on the T cell subsets. Higher avidity interactions between TCR and self-p:MHC complexes have been shown by others to correlate with higher CD5 expression. Therefore $CD4^+$ T cells may have increased CD5 expression, compared to $CD8^+$ T cells, due to their increased TCR expression.

We have shown that the increased TCR expression was associated with higher intracellular calcium concentration and higher CD107a concentration, both at steady-state and after polyclonal stimulation. Whether this was a direct result of higher TCR expression, was not investigated in this project. Future experiments analysing calcium concentration and CD107a expression in $CD4^+$ and $CD8^+$ T cells expressing the same level of TCR, would help understand whether this is the case or not. In particular, a recent study has shown that increased levels of CD5 correlate with increased calcium signalling (Freitas et al., 2017). Thus, TCR expression and calcium signalling might indeed be correlated.

Unexpectedly, increasing the levels of TCR expression did not alter the functional avidity (triggering threshold and amount of cytokines produced) of either bulk $CD4^+$ T cells or TCR-transduced $CD4^+$ T cells as previously demonstrated by our lab (Ahmadi et al., 2011; Nicholson, unpublished data). However, in this thesis MHC-II restricted TCR responses were analysed, whereas previous work was carried out with the F5-TCR, a MHC-I restricted TCR. We hypothesised that the lack of a difference is a consequence of experimental limitations, rather than a lack of differences attributed by the increased CD3 and TCR expression. In the case of the bulk $CD4^+$ T cell population, the lack of a

common known antigen that could be used for stimulation, and the consequent use of a high affinity anti-CD3 antibody for stimulation, may have masked subtle differences between the two populations of CD3-GFP and control-GFP transduced cells. In the case of TCR-transduced $CD4^+$ T cells, the use of suboptimal conditions for stimulation (low number of APCs, mixed with a high number of bystander cells) may have prevented effective stimulation of the target population, providing false negative results. In both cases, improved stimulatory conditions may lead to different conclusions. The use of superantigens such as staphylococcal enterotoxins, and the use of a cleaner population of APCs, may lead to different functional avidity profiles in bulk and TCR-transduced $CD4^+$ T cells, respectively.

Following adoptive transfer *in vivo*, it was demonstrated that the persistence of the $CD4^+$ T cells transduced with the CD3-GFP was superior to that of $CD4^+$ T cells transduced with the control-GFP vector or $CD8^+$ T cells transduced with the CD3-GFP vector. This suggested that increased TCR expression provided T cells with a persistence advantage over the other experimental populations of T cells. To test this further, adoptive transfer of $CD4^+$ and $CD8^+$ T cells expressing the same density of TCR, would indicate whether the difference in persistence is a sole consequence of different levels of TCR expression.

This project has shown that increased, supraphysiological TCR expression in $CD4^+$ T cells cannot be maintained *in vivo*. By 20 days post initial T cell transfer, the $CD4^+$ T cells transduced with the CD3-GFP vector had down modulated the expression of their TCR, to levels similar to those seen in the control-GFP population. Since this downregulation was not seen in the control-GFP population, we hypothesised that this was a consequence of increasing the levels of TCR to supraphysiological levels. Increased TCR expression may result in stronger interaction with self-p:MHC complexes, leading to aberrant T cell signalling. To prevent abnormal T cell activation and potential auto-reactivity and toxicity, regulatory mechanisms drive TCR downregulation to physiological levels. To confirm that this is a consequence of TCR:self-p:MHC interaction, future experiments should be carried out in MHC-II deficient mice. In this case $CD4^+$ T cells

would not be able to interact with self-MHC and it would be predicted that no TCR down-regulation would be observed.

Moreover, to investigate whether TCR downregulation is indeed a mechanism to prevent aberrant T cell activation and development of toxicity, genetically modified $CD4^+$ T cells could be used. Two mechanisms are known to drive TCR downregulation: one is dependent on the kinases p56-lck and p59-fyn; the second one is induced by PKC and is dependent on a di-leucine motif in the CD3γ chain. Mutant T cells lacking either p56-lck or the di-leucine CD3γ motif are unable to downregulate their TCR following stimulation. These mutant $CD4^+$ T cells could be used as donor cells, and their TCR expression and ability to induce toxicity *in vivo* tracked overtime. If TCR downregulation is impaired and supraphysiological levels of TCR are indeed able to induce auto-reactivity in T cells, recipient mice would present with progressively higher severity scoring.

Finally, future experiments should concentrate on investigating whether the observed TCR downregulation is permanent or not. *Ex vivo* CD3-GFP transduced $CD4^+$ T cells could be cultivated *in vitro* following their isolation from a variety of tissues. Their expression of TCR could be monitored to determine whether constant TCR:self-p:MHC interactions are needed to maintain the levels of TCR low; or whether the downregulation is a permanent feature.

7. Bibliography

Acuto, O., V. Di Bartolo and F. Michel. "Tailoring T-Cell Receptor Signals by Proximal Negative Feedback Mechanisms." *Nat Rev Immunol* 8, no. 9 (2008): 699-712.

Agenès, Fabien, Jean-Pierre Dangy and Jörg Kirberg. "T Cell Receptor Contact to Restricting Mhc Molecules Is a Prerequisite for Peripheral Interclonal T Cell Competition." *The Journal of Experimental Medicine* 205, no. 12 (2008): 2735-2743.

Ahmadi, M., J. W. King, S. A. Xue, C. Voisine, A. Holler, G. P. Wright, J. Waxman, E. Morris and H. J. Stauss. "Cd3 Limits the Efficacy of Tcr Gene Therapy in Vivo." *Blood* 118, no. 13 (2011): 3528-37.

Akl, H., B. Badran, G. Dobirta, G. Manfouo-Foutsop, M. Moschitta, M. Merimi, A. Burny, P. Martiat and K. E. Willard-Gallo. "Progressive Loss of Cd3 Expression after Htlv-I Infection Results from Chromatin Remodeling Affecting All the Cd3 Genes and Persists Despite Early Viral Genes Silencing." *Virol J* 4, (2007): 85.

Alarcon, B, B Berkhout, J Breitmeyer and C Terhorst. "Assembly of the Human T Cell Receptor-Cd3 Complex Takes Place in the Endoplasmic Reticulum and Involves Intermediary Complexes between the Cd3-Gamma.Delta.Epsilon Core and Single T Cell Receptor Alpha or Beta Chains." *Journal of Biological Chemistry* 263, no. 6 (1988): 2953-2961.

Alarcon, Balbino, Jose Ramon Regueiro , Antonio Arnaiz-Villena and Cox Terhorst "Familial Defect in the Surface Expression of the T-Cell Receptor–Cd3 Complex." *New England Journal of Medicine* 319, no. 18 (1988): 1203-1208.

Algarra, Ignacio, Teresa Cabrera and Federico Garrido. "The Hla Crossroad in Tumor Immunology." *Human Immunology* 61, no. 1 (2000): 65-73.

Almeida, A. R., B. Rocha, A. A. Freitas and C. Tanchot. "Homeostasis of T Cell Numbers: From Thymus Production to Peripheral Compartmentalization and the Indexation of Regulatory T Cells." *Semin Immunol* 17, no. 3 (2005): 239-49.

Antony, Paul Andrew and Nicholas P. Restifo. "Cd4(+)Cd25(+) T Regulatory Cells, Immunotherapy of Cancer, and Interleukin-2." *Journal of immunotherapy (Hagerstown, Md.: 1997)* 28, no. 2 (2005): 120-128.

Appleby, L. J., N. Nausch, F. Heard, L. Erskine, C. D. Bourke, N. Midzi, T. Mduluza, J. E. Allen and F. Mutapi. "Down Regulation of the Tcr Complex Cd3ζ-Chain on Cd3+ T Cells: A Potential Mechanism for Helminth-Mediated Immune Modulation." *Front Immunol* 6,(2015).

Ardouin, Laurence, Claude Boyer, Anne Gillet, Jeannine Trucy, Anne-Marie Bernard, Jacques Nunes, Jérôme Delon, Alain Trautmann, Hai-Tao He, Bernard Malissen and Marie Malissen. "Crippling of Cd3-Z Itams Does Not Impair T Cell Receptor Signaling." *Immunity* 10, no. 4 (1999): 409-420.

Bach, Fritz H., Marilyn L. Bach and Paul M. Sondel. "Differential Function of Major Histocompatibility Complex Antigens in T-Lymphocyte Activation." *Nature* 259, no. 5541 (1976): 273-281.

Baldwin, K. K., B. P. Trenchak, J. D. Altman and M. M. Davis. "Negative Selection of T Cells Occurs Throughout Thymic Development." *J Immunol* 163, no. 2 (1999): 689-98.

Baniyash, Michal. "Tcr [Zeta]-Chain Downregulation: Curtailing an Excessive Inflammatory Immune Response." *Nat Rev Immunol* 4, no. 9 (2004): 675-687.

Bendle, G. M., C. Linnemann, A. I. Hooijkaas, L. Bies, M. A. de Witte, A. Jorritsma, A. D. Kaiser, N. Pouw, R. Debets, E. Kieback, W. Uckert, J. Y. Song, J. B. Haanen and T. N. Schumacher. "Lethal Graft-Versus-Host Disease in Mouse Models of T Cell Receptor Gene Therapy." *Nat Med* 16, no. 5 (2010): 565-70, 1p following 570.

Bennett, S. R., F. R. Carbone, F. Karamalis, R. A. Flavell, J. F. Miller and W. R. Heath. "Help for Cytotoxic-T-Cell Responses Is Mediated by Cd40 Signalling." *Nature* 393, no. 6684 (1998): 478-80.

Bennett, S. R., F. R. Carbone, F. Karamalis, R. A. Flavell, J. F. Miller and W. R. Heath. "Help for Cytotoxic-T-Cell Responses Is Mediated by Cd40 Signalling." *Nature* 393, no. 6684 (1998): 478-80.

Berg, L., J. Rönnelid, L. Klareskog and A. Bucht. "Down-Regulation of the T Cell Receptor Cd3ζ Chain in Rheumatoid Arthritis (Ra) and Its Influence on T Cell Responsiveness." *Clin Exp Immunol* 120, no. 1 (2000): 174-82.

Berke, G. "The Ctl's Kiss of Death." *Cell* 81, no. 1 (1995): 9-12.

Bevan, M. J. "Cross-Priming for a Secondary Cytotoxic Response to Minor H Antigens with H-2 Congenic Cells Which Do Not Cross-React in the Cytotoxic Assay." *The Journal of Experimental Medicine* 143, no. 5 (1976): 1283-1288.

Biswas P., Mantelli B., Sica A., Malnati M., Panzeri C., Saccani A., Hasson H., Vecchi A., Saniabadi A., Lusso P., Lazzarin A. and Beretta A. “Expression of CD4 on human peripheral blood neutrophils.” *Blood* 101(11):4452-6.

Blattman, J. N., R. Antia, D. J. Sourdive, X. Wang, S. M. Kaech, K. Murali-Krishna, J. D. Altman and R. Ahmed. "Estimating the Precursor Frequency of Naive Antigen-Specific Cd8 T Cells." *J Exp Med* 195, no. 5 (2002): 657-64.

Blichfeldt, E., L. A. Munthe, J. S. Rotnes and B. Bogen. "Dual T Cell Receptor T Cells Have a Decreased Sensitivity to Physiological Ligands Due to Reduced Density of Each T Cell Receptor." *Eur J Immunol* 26, no. 12 (1996): 2876-84.

Brinkman, C. Colin, Sherin J. Rouhani, Nithya Srinivasan and Victor H. Engelhard. "Peripheral Tissue Homing Receptors Enable T Cell Entry into Lymph Nodes and Affect the Anatomical Distribution of Memory Cells." *The Journal of Immunology* 191, no. 5 (2013): 2412-2425.

Brocker, T. "Survival of Mature Cd4 T Lymphocytes Is Dependent on Major Histocompatibility Complex Class Ii-Expressing Dendritic Cells." *J Exp Med* 186, no. 8 (1997): 1223-32.

Brocker, T. and K. Karjalainen. "Signals through T Cell Receptor-Zeta Chain Alone Are Insufficient to Prime Resting T Lymphocytes." *J Exp Med* 181, no. 5 (1995): 1653-9.

Bromley, S. K. and M. L. Dustin. "Stimulation of Naive T-Cell Adhesion and Immunological Synapse Formation by Chemokine-Dependent and -Independent Mechanisms." *Immunology* 106, no. 3 (2002): 289-98.

Bronstein-Sitton, N., L. Cohen-Daniel, I. Vaknin, A. V. Ezernitchi, B. Leshem, A. Halabi, Y. Houri-Hadad, E. Greenbaum, Z. Zakay-Rones, L. Shapira and M. Baniyash. "Sustained Exposure to Bacterial Antigen Induces Interferon-Gamma-Dependent T Cell Receptor Zeta Down-Regulation and Impaired T Cell Function." *Nat Immunol* 4,

no. 10 (2003): 957-64.

Buchholz, Veit R., Michael Flossdorf, Inge Hensel, Lorenz Kretschmer, Bianca Weissbrich, Patricia Gräf, Admar Verschoor, Matthias Schiemann, Thomas Höfer and Dirk H. Busch. "Disparate Individual Fates Compose Robust Cd8(+) T Cell Immunity." *Science* 340, no. 6132 (2013): 630-635.

Bunse, Mario, Gavin M. Bendle, Carsten Linnemann, Laura Bies, Stephan Schulz, Ton N. Schumacher and Wolfgang Uckert. "Rnai-Mediated Tcr Knockdown Prevents Autoimmunity in Mice Caused by Mixed Tcr Dimers Following Tcr Gene Transfer." *Molecular Therapy* 22, no. 11 (2014): 1983-1991.

Burns, W. R., Z. Zheng, S. A. Rosenberg and R. A. Morgan. "Lack of Specific Gamma-Retroviral Vector Long Terminal Repeat Promoter Silencing in Patients Receiving Genetically Engineered Lymphocytes and Activation Upon Lymphocyte Restimulation." *Blood* 114, no. 14 (2009): 2888-99.

Call, Matthew E., Jason Pyrdol, Martin Wiedmann and Kai W. Wucherpfennig. "The Organizing Principle in the Formation of the T Cell Receptor-Cd3 Complex." *Cell* 111, no. 7 (2002): 967-979.

Call, Matthew E., Jason Pyrdol and Kai W. Wucherpfennig. "Stoichiometry of the T-Cell Receptor–Cd3 Complex and Key Intermediates Assembled in the Endoplasmic Reticulum." *The EMBO Journal* 23, no. 12 (2004): 2348-2357.

Call, Matthew E. and Kai W. Wucherpfennig. "Molecular Mechanisms for the Assembly of the T Cell Receptor–Cd3 Complex." *Molecular Immunology* 40, no. 18 (2004): 1295-1305.

Campbell, James J., Kristine E. Murphy, Eric J. Kunkel, Christopher E. Brightling, Dulce Soler, Zhimin Shen, Judie Boisvert, Harry B. Greenberg, Mark A. Vierra, Stuart B. Goodman, Mark C. Genovese, Andrew J. Wardlaw, Eugene C. Butcher and Lijun Wu. "Ccr7 Expression and Memory T Cell Diversity in Humans." *The Journal of Immunology* 166, no. 2 (2001): 877-884.

Cantor, H and E A Boyse. "Functional Subclasses of T-Lymphocytes Bearing Different Ly Antigens. I. The Generation of Functionally Distinct T-Cell Subclasses Is a Differentiative Process Independent of Antigen." *The Journal of Experimental Medicine* 141, no. 6 (1975): 1376-1389.

Cantor, H. and E. A. Boyse. "Regulation of Cellular and Humoral Immune Responses by T-Cell Subclasses." *Cold Spring Harb Symp Quant Biol* 41 Pt 1, (1977): 23-32.

Carrasco, Yolanda R., Almudena R. Ramiro, César Trigueros, Virginia G. de Yébenes, Marina García-Peydró and María L. Toribio. "An Endoplasmic Reticulum Retention Function for the Cytoplasmic Tail of the Human Pre–T Cell Receptor (Tcr) A Chain: Potential Role in the Regulation of Cell Surface Pre-Tcr Expression Levels." *The Journal of Experimental Medicine* 193, no. 9 (2001): 1045-1058.

Chakraborty, Arup K. and Arthur Weiss. "Insights into the Initiation of Tcr Signaling." *Nat Immunol* 15, no. 9 (2014): 798-807.

Chen, Lieping and Dallas B. Flies. "Molecular Mechanisms of T Cell Co-Stimulation and Co-Inhibition." *Nat Rev Immunol* 13, no. 4 (2013): 227-242.

Cheon D.J., Orsulic S. (2011) “Mouse models of cancer” Annu Rev Pathol, 6:95-119.

Chu, D.H., van Oers N.S., Malissen M., Harris J., Elder M. and Weiss A. (1999)
“Pre-T cell receptor signals are responsible for the down-regulation of Syk protein tyrosine kinase expression”. J. Immunol. 163:2610

Clarke, S. R. and A. Y. Rudensky. "Survival and Homeostatic Proliferation of Naive Peripheral Cd4+ T Cells in the Absence of Self Peptide:Mhc Complexes." *J Immunol* 165, no. 5 (2000): 2458-64.

Clay, T. M., M. C. Custer, J. Sachs, P. Hwu, S. A. Rosenberg and M. I. Nishimura. "Efficient Transfer of a Tumor Antigen-Reactive Tcr to Human Peripheral Blood Lymphocytes Confers Anti-Tumor Reactivity." *J Immunol* 163, no. 1 (1999): 507-13.

Cohen, C. J., Y. F. Li, M. El-Gamil, P. F. Robbins, S. A. Rosenberg and R. A. Morgan. "Enhanced Antitumor Activity of T Cells Engineered to Express T-Cell Receptors with a Second Disulfide Bond." *Cancer Res* 67, no. 8 (2007): 3898-903.

Cohen, C. J., Y. Zhao, Z. Zheng, S. A. Rosenberg and R. A. Morgan. "Enhanced Antitumor Activity of Murine-Human Hybrid T-Cell Receptor (Tcr) in Human Lymphocytes Is Associated with Improved Pairing and Tcr/Cd3 Stability." *Cancer Res* 66, no. 17 (2006): 8878-86.

Cooper, Laurence J. N., Michael Kalos, Deborah A. Lewinsohn, Stanley R. Riddell and Philip D. Greenberg. "Transfer of Specificity for Human Immunodeficiency Virus Type 1 into Primary Human T Lymphocytes by Introduction of T-Cell Receptor Genes." *Journal of Virology* 74, no. 17 (2000): 8207-8212.

Corthay, Alexandre, Dag K. Skovseth, Katrin U. Lundin, Egil Røsjø, Hilde Omholt, Peter O. Hofgaard, Guttorm Haraldsen and Bjarne Bogen. "Primary Antitumor Immune Response Mediated by Cd4+ T Cells." *Immunity* 22, no. 3 (2005): 371-383.

Crispe, I. N. "The Liver as a Lymphoid Organ." *Annu Rev Immunol* 27, (2009): 147-63.

Curtsinger, Julie M. and Matthew F. Mescher. "Inflammatory Cytokines as a Third Signal for T Cell Activation." *Current Opinion in Immunology* 22, no. 3 (2010): 333-340.

Cyster, J. G. "Lymphoid Organ Development and Cell Migration." *Immunol Rev* 195, (2003): 5-14.

Cyster, J. G. "Chemokines, Sphingosine-1-Phosphate, and Cell Migration in Secondary Lymphoid Organs." *Annu Rev Immunol* 23, (2005): 127-59.

D'Souza, Warren N. and Stephen M. Hedrick. "Cutting Edge: Latecomer Cd8 T Cells Are Imprinted with a Unique Differentiation Program." *The Journal of Immunology* 177, no. 2 (2006): 777-781.

Dadi , Harjit K., Amos J. Simon and Chaim M. Roifman "Effect of Cd3δ Deficiency on Maturation of A/B and Γ/Δ T-Cell Lineages in Severe Combined Immunodeficiency." *New England Journal of Medicine* 349, no. 19 (2003): 1821-1828.

Daeron, M. (1997). "Fc receptor biology". Annu. Rev. Immunol. 15:203.

Dai, Zhenhua and Fadi G. Lakkis. "Cutting Edge: Secondary Lymphoid Organs Are Essential for Maintaining the Cd4, but Not Cd8, Naive T Cell Pool." *The Journal of Immunology* 167, no. 12 (2001): 6711-6715.

Dardalhon, V., A. Awasthi, H. Kwon, G. Galileos, W. Gao, R. A. Sobel, M. Mitsdoerffer, T. B. Strom, W. Elyaman, I. C. Ho, S. Khoury, M. Oukka and V. K. Kuchroo. "Il-4 Inhibits Tgf-Beta-Induced Foxp3+ T Cells and, Together with Tgf-Beta, Generates Il-9+ Il-10+ Foxp3(-) Effector T Cells." *Nat Immunol* 9, no. 12 (2008): 1347-55.

Dave, Vibhuti P. "Hierarchical Role of Cd3 Chains in Thymocyte Development." *Immunological Reviews* 232, no. 1 (2009): 22-33.

Davis, M. M. and P. J. Bjorkman. "T-Cell Antigen Receptor Genes and T-Cell Recognition." *Nature* 334, no. 6181 (1988): 395-402.

Davis, M. M., J. J. Boniface, Z. Reich, D. Lyons, J. Hampl, B. Arden and Y. Chien. "Ligand Recognition by Alpha Beta T Cell Receptors." *Annu Rev Immunol* 16, (1998): 523-44.

Davis, S. J. and P. A. van der Merwe. "The Kinetic-Segregation Model: Tcr Triggering and Beyond." *Nat Immunol* 7, no. 8 (2006): 803-9.

de Saint Basile, G., F. Geissmann, E. Flori, B. Uring-Lambert, C. Soudais, M. Cavazzana-Calvo, A. Durandy, N. Jabado, A. Fischer and F. Le Deist. "Severe Combined Immunodeficiency Caused by Deficiency in Either the Delta or the Epsilon Subunit of Cd3." *J Clin Invest* 114, no. 10 (2004): 1512-7.

de Witte, M. A., A. Jorritsma, A. Kaiser, M. D. van den Boom, M. Dokter, G. M. Bendle, J. B. Haanen and T. N. Schumacher. "Requirements for Effective Antitumor Responses of Tcr Transduced T Cells." *J Immunol* 181, no. 7 (2008): 5128-36.

den Braber I., Mugwagwa T., Vrisekoop N., Westera L., Mögling R., de Boer A.B., Willems N., Schrijver E.H., Spierenburg G., Gaiser K., Mul E., Otto S.A., Ruiter A.F., Ackermans M..T, Miedema F., Borghans J.A., de Boer R.J., Tesselaar K. “Maintenance of peripheral naive T cells is sustained by thymus output in mice but not humans”. *Immunity*, (2012) 36(2):288-97.

Di Rosa, Francesca and Thomas Gebhardt. "Bone Marrow T Cells and the Integrated Functions of Recirculating and Tissue-Resident Memory T Cells." *Frontiers in Immunology* 7, (2016): 51.

Dighe, Anand S., Elizabeth Richards, Lloyd J. Old and Robert D. Schreiber. "Enhanced in Vivo Growth and Resistance to Rejection of Tumor Cells Expressing Dominant Negative Ifnγ Receptors." *Immunity* 1, no. 6 (1994): 447-456.

Dong, C. and R. A. Flavell. "Control of T Helper Cell Differentiation--in Search of Master Genes." *Sci STKE* 2000, no. 49 (2000): pe1.

Dorfman, J. R., I. Stefanova, K. Yasutomo and R. N. Germain. "Cd4+ T Cell Survival Is Not Directly Linked to Self-Mhc-Induced Tcr Signaling." *Nat Immunol* 1, no. 4 (2000): 329-35.

Doyle, Carolyn and Jack L. Strominger. "Interaction between Cd4 and Class Ii Mhc Molecules Mediates Cell Adhesion." *Nature* 330, no. 6145 (1987): 256-259.

Dudley, M. E., J. R. Wunderlich, P. F. Robbins, J. C. Yang, P. Hwu, D. J. Schwartzentruber, S. L. Topalian, R. Sherry, N. P. Restifo, A. M. Hubicki, M. R. Robinson, M. Raffeld, P. Duray, C. A. Seipp, L. Rogers-Freezer, K. E. Morton, S. A. Mavroukakis, D. E. White and S. A. Rosenberg. "Cancer Regression and Autoimmunity in Patients after Clonal Repopulation with Antitumor Lymphocytes." *Science* 298, no. 5594 (2002): 850-4.

Dudley, M. E., J. R. Wunderlich, J. C. Yang, R. M. Sherry, S. L. Topalian, N. P. Restifo, R. E. Royal, U. Kammula, D. E. White, S. A. Mavroukakis, L. J. Rogers, G. J. Gracia, S. A. Jones, D. P. Mangiameli, M. M. Pelletier, J. Gea-Banacloche, M. R. Robinson, D. M. Berman, A. C. Filie, A. Abati and S. A. Rosenberg. "Adoptive Cell Transfer Therapy Following Non-Myeloablative but Lymphodepleting Chemotherapy for the Treatment of Patients with Refractory Metastatic Melanoma." *J Clin Oncol* 23, no. 10 (2005): 2346-57.

Dudley, M. E., J. C. Yang, R. Sherry, M. S. Hughes, R. Royal, U. Kammula, P. F. Robbins, J. Huang, D. E. Citrin, S. F. Leitman, J. Wunderlich, N. P. Restifo, A. Thomasian, S. G. Downey, F. O. Smith, J. Klapper, K. Morton, C. Laurencot, D. E. White and S. A. Rosenberg. "Adoptive Cell Therapy for Patients with Metastatic Melanoma: Evaluation of Intensive Myeloablative Chemoradiation Preparative Regimens." *J Clin Oncol* 26, no. 32 (2008): 5233-9.

Dummer, W., A. G. Niethammer, R. Baccala, B. R. Lawson, N. Wagner, R. A. Reisfeld and A. N. Theofilopoulos. "T Cell Homeostatic Proliferation Elicits Effective Antitumor Autoimmunity." *J Clin Invest* 110, no. 2 (2002): 185-92.

Dunn, G. P., A. T. Bruce, H. Ikeda, L. J. Old and R. D. Schreiber. "Cancer Immunoediting: From Immunosurveillance to Tumor Escape." *Nat Immunol* 3, no. 11 (2002): 991-8.

Duong, C. P., C. S. Yong, M. H. Kershaw, C. Y. Slaney and P. K. Darcy. "Cancer Immunotherapy Utilizing Gene-Modified T Cells: From the Bench to the Clinic." *Mol*

Immunol 67, no. 2 Pt A (2015): 46-57.

Dustin, M. L., A. K. Chakraborty and A. S. Shaw. "Understanding the Structure and Function of the Immunological Synapse." *Cold Spring Harb Perspect Biol* 2, no. 10 (2010): a002311.

Dustin, M. L. and D. R. Colman. "Neural and Immunological Synaptic Relations." *Science* 298, no. 5594 (2002): 785-9.

Dworacki, G., N. Meidenbauer, I. Kuss, T. K. Hoffmann, W. Gooding, M. Lotze and T. L. Whiteside. "Decreased Zeta Chain Expression and Apoptosis in Cd3+ Peripheral Blood T Lymphocytes of Patients with Melanoma." *Clin Cancer Res* 7, no. 3 Suppl (2001): 947s-957s.

Eberlein, T. J., M. Rosenstein and S. A. Rosenberg. "Regression of a Disseminated Syngeneic Solid Tumor by Systemic Transfer of Lymphoid Cells Expanded in Interleukin 2." *J Exp Med* 156, no. 2 (1982): 385-97.

Ehrlich, P. "Über Den Jetzigen Stand Der Karzinomforschung." *Beiträge zur experimentellen Pathologie und Chemotherapie*, (1909): 117–164.

Elder M.E., Skoda-Smith S., Kadlecek T.A., Wang F., Wu J. Weiss A. (2001). “Distinct T cell developmental consequences in humans and mice expressing identical mutations in the DLAARN motif of ZAP-70”. J. Immunol. 166:656.

Eleftheriadis, T., C. Kartsios, E. Yiannaki, P. Kazila, G. Antoniadi, V. Liakopoulos and D. Markala. "Chronic Inflammation and T Cell Zeta-Chain Downregulation in Hemodialysis Patients." *Am J Nephrol* 28, no. 1 (2008): 152-7.

Ernst, Bettina, Dong-Sup Lee, Jennifer M. Chang, Jonathan Sprent and Charles D. Surh. "The Peptide Ligands Mediating Positive Selection in the Thymus Control T Cell Survival and Homeostatic Proliferation in the Periphery." *Immunity* 11, no. 2 (1999): 173-181.

Eyerich, Stefanie, Kilian Eyerich, Davide Pennino, Teresa Carbone, Francesca Nasorri, Sabatino Pallotta, Francesca Cianfarani, Teresa Odorisio, Claudia Traidl-Hoffmann, Heidrun Behrendt, Stephen R. Durham, Carsten B. Schmidt-Weber and Andrea Cavani. "Th22 Cells Represent a Distinct Human T Cell Subset Involved in Epidermal Immunity and Remodeling." *The Journal of Clinical Investigation* 119, no. 12 (2009):

3573-3585.

Fazilleau, Nicolas, Linda Mark, Louise J. McHeyzer-Williams and Michael G. McHeyzer-Williams. "Follicular Helper T Cells: Lineage and Location." *Immunity* 30, no. 3 (2009): 324-335.

Fernandes, Ricardo A., Chao Yu, Alexandre M. Carmo, Edward J. Evans, P. Anton van der Merwe and Simon J. Davis. "What Controls T Cell Receptor Phosphorylation?" *Cell* 142, no. 5 (2010): 668-669.

Ferreira, Cristina, Thomas Barthlott, Sylvie Garcia, Rose Zamoyska and Brigitta Stockinger. "Differential Survival of Naive Cd4 and Cd8 T Cells." *The Journal of Immunology* 165, no. 7 (2000): 3689-3694.

Feske, Stefan. "Calcium Signalling in Lymphocyte Activation and Disease." *Nat Rev Immunol* 7, no. 9 (2007): 690-702.

Finke, J. H., A. H. Zea, J. Stanley, D. L. Longo, H. Mizoguchi, R. R. Tubbs, R. H. Wiltrout, J. J. O'Shea, S. Kudoh, E. Klein and et al. "Loss of T-Cell Receptor Zeta Chain and P56lck in T-Cells Infiltrating Human Renal Cell Carcinoma." *Cancer Res* 53, no. 23 (1993): 5613-6.

Finkel, T H, P Marrack, J W Kappler, R T Kubo and J C Cambier. "Alpha Beta T Cell Receptor and Cd3 Transduce Different Signals in Immature T Cells. Implications for Selection and Tolerance." *The Journal of Immunology* 142, no. 9 (1989): 3006-3012.

Finney, Helene M., Arne N. Akbar and Alastair D. G. Lawson. "Activation of Resting Human Primary T Cells with Chimeric Receptors: Costimulation from Cd28, Inducible Costimulator, Cd134, and Cd137 in Series with Signals from the Tcrζ Chain." *The Journal of Immunology* 172, no. 1 (2004): 104-113.

Foulds, K. E., L. A. Zenewicz, D. J. Shedlock, J. Jiang, A. E. Troy and H. Shen. "Cutting Edge: Cd4 and Cd8 T Cells Are Intrinsically Different in Their Proliferative Responses." *J Immunol* 168, no. 4 (2002): 1528-32.

Freitas, Claudia M. Tellez, Garrett J. Hamblin, Carlee M. Raymond and K. Scott Weber. "Naïve Helper T Cells with High Cd5 Expression Have Increased Calcium Signaling." PLoS ONE 12, no. 5 (2017): e0178799.

Fu, G., S. Vallee, V. Rybakin, M. V. McGuire, J. Ampudia, C. Brockmeyer, M. Salek, P. R. Fallen, J. A. Hoerter, A. Munshi, Y. H. Huang, J. Hu, H. S. Fox, K. Sauer, O. Acuto and N. R. Gascoigne. "Themis Controls Thymocyte Selection through Regulation of T Cell Antigen Receptor-Mediated Signaling." *Nat Immunol* 10, no. 8 (2009): 848-56.

Gabrilovich, D. I. and S. Nagaraj. "Myeloid-Derived Suppressor Cells as Regulators of the Immune System." *Nat Rev Immunol* 9, no. 3 (2009): 162-74.

Gallegos, Alena M., Huizhong Xiong, Ingrid M. Leiner, Boze Susac, Michael S. Glickman, Eric G. Pamer and Jeroen W. J. van Heijst. "Control of T Cell Antigen Reactivity Via Programmed Tcr Downregulation." *Nat Immunol* 17, no. 4 (2016): 379-386.

Gallucci, S., M. Lolkema and P. Matzinger. "Natural Adjuvants: Endogenous Activators of Dendritic Cells." *Nat Med* 5, no. 11 (1999): 1249-55.

Gattinoni, L., S. E. Finkelstein, C. A. Klebanoff, P. A. Antony, D. C. Palmer, P. J. Spiess, L. N. Hwang, Z. Yu, C. Wrzesinski, D. M. Heimann, C. D. Surh, S. A. Rosenberg and N. P. Restifo. "Removal of Homeostatic Cytokine Sinks by Lymphodepletion Enhances the Efficacy of Adoptively Transferred Tumor-Specific Cd8+ T Cells." *J Exp Med* 202, no. 7 (2005a): 907-12.

Gattinoni, L., C. A. Klebanoff, D. C. Palmer, C. Wrzesinski, K. Kerstann, Z. Yu, S. E. Finkelstein, M. R. Theoret, S. A. Rosenberg and N. P. Restifo. "Acquisition of Full Effector Function in Vitro Paradoxically Impairs the in Vivo Antitumor Efficacy of Adoptively Transferred Cd8+ T Cells." *J Clin Invest* 115, no. 6 (2005b): 1616-26.

Ge, Qing, Varada P. Rao, Bryan K. Cho, Herman N. Eisen and Jianzhu Chen. "Dependence of Lymphopenia-Induced T Cell Proliferation on the Abundance of Peptide/ Mhc Epitopes and Strength of Their Interaction with T Cell Receptors." *Proceedings of the National Academy of Sciences* 98, no. 4 (2001): 1728-1733.

Geppert, T. D. and P. E. Lipsky. "Antigen Presentation by Interferon-Gamma-Treated Endothelial Cells and Fibroblasts: Differential Ability to Function as Antigen-Presenting Cells Despite Comparable Ia Expression." *J Immunol* 135, no. 6 (1985): 3750-62.

Gerlach, Carmen, Jan C. Rohr, Leïla Perié, Nienke van Rooij, Jeroen W. J. van Heijst, Arno Velds, Jos Urbanus, Shalin H. Naik, Heinz Jacobs, Joost B. Beltman, Rob J. de Boer and Ton N. M. Schumacher. "Heterogeneous Differentiation Patterns of

Individual Cd8⁺ T Cells." *Science* 340, no. 6132 (2013): 635-639.

Gerlinger , Marco, Andrew J. Rowan , Stuart Horswell , James Larkin , David Endesfelder , Eva Gronroos , Pierre Martinez , Nicholas Matthews , Aengus Stewart , Patrick Tarpey , Ignacio Varela , Benjamin Phillimore , Sharmin Begum , Neil Q. McDonald , Adam Butler , David Jones , Keiran Raine , Calli Latimer , Claudio R. Santos , Mahrokh Nohadani , Aron C. Eklund , Bradley Spencer-Dene , Graham Clark , Lisa Pickering , Gordon Stamp , Martin Gore , Zoltan Szallasi , Julian Downward , P. Andrew Futreal and Charles Swanton "Intratumor Heterogeneity and Branched Evolution Revealed by Multiregion Sequencing." *New England Journal of Medicine* 366, no. 10 (2012): 883-892.

Goldrath, Ananda W., Lisa Y. Bogatzki and Michael J. Bevan. "Naive T Cells Transiently Acquire a Memory-Like Phenotype During Homeostasis-Driven Proliferation." *The Journal of Experimental Medicine* 192, no. 4 (2000): 557-564.

Gommeaux, J., C. Gregoire, P. Nguessan, M. Richelme, M. Malissen, S. Guerder, B. Malissen and A. Carrier. "Thymus-Specific Serine Protease Regulates Positive Selection of a Subset of Cd4+ Thymocytes." *Eur J Immunol* 39, no. 4 (2009): 956-64.

Gong, Michael C., Jean-Baptiste Latouche, Anja Krause, Warren D. W. Heston, Neil H. Bander and Michel Sadelain. "Cancer Patient T Cells Genetically Targeted to Prostate-Specific Membrane Antigen Specifically Lyse Prostate Cancer Cells and Release Cytokines in Response to Prostate-Specific Membrane Antigen." *Neoplasia (New York, N.Y.)* 1, no. 2 (1999): 123-127.

Grakoui, Arash, Shannon K. Bromley, Cenk Sumen, Mark M. Davis, Andrey S. Shaw, Paul M. Allen and Michael L. Dustin. "The Immunological Synapse: A Molecular Machine Controlling T Cell Activation." *Science* 285, no. 5425 (1999): 221-227.

Grandjean, I., L. Duban, E. A. Bonney, E. Corcuff, J. P. Di Santo, P. Matzinger and O. Lantz. "Are Major Histocompatibility Complex Molecules Involved in the Survival of Naive Cd4+ T Cells?" *J Exp Med* 198, no. 7 (2003): 1089-102.

Greaves, Mel and Carlo C. Maley. "Clonal Evolution in Cancer." *Nature* 481, no. 7381 (2012): 306-313.

Greenberg, P D, D E Kern and M A Cheever. "Therapy of Disseminated Murine

Leukemia with Cyclophosphamide and Immune Lyt-1+,2- T Cells. Tumor Eradication Does Not Require Participation of Cytotoxic T Cells." *The Journal of Experimental Medicine* 161, no. 5 (1985): 1122-1134.

Haks, Mariëlle C., Elsa Pépin, Jeroen H.N. van den Brakel, Sigrid A.A. Smeele, Stanley M. Belkowski, Helmut W.H.G. Kessels, Paul Krimpenfort and Ada M. Kruisbeek. "Contributions of the T Cell Receptor–Associated Cd3γ–Itam to Thymocyte Selection." *The Journal of Experimental Medicine* 196, no. 1 (2002): 1-13.

Haley P.J. “Species differences in the structure and function of the immune system”. Toxicology (2003) 188(1):49-71.

Haribhai, D., J. B. Williams, S. Jia, D. Nickerson, E. G. Schmitt, B. Edwards, J. Ziegelbauer, M. Yassai, S. H. Li, L. M. Relland, P. M. Wise, A. Chen, Y. Q. Zheng, P. M. Simpson, J. Gorski, N. H. Salzman, M. J. Hessner, T. A. Chatila and C. B. Williams. "A Requisite Role for Induced Regulatory T Cells in Tolerance Based on Expanding Antigen Receptor Diversity." *Immunity* 35, no. 1 (2011): 109-22.

Harrington, L. E., K. M. Janowski, J. R. Oliver, A. J. Zajac and C. T. Weaver. "Memory Cd4 T Cells Emerge from Effector T-Cell Progenitors." *Nature* 452, no. 7185 (2008): 356-60.

Hassan, J. and D. J. Reen. "Il-7 Promotes the Survival and Maturation but Not Differentiation of Human Post-Thymic Cd4+ T Cells." *Eur J Immunol* 28, no. 10 (1998): 3057-65.

Hawiger, D., K. Inaba, Y. Dorsett, M. Guo, K. Mahnke, M. Rivera, J. V. Ravetch, R. M. Steinman and M. C. Nussenzweig. "Dendritic Cells Induce Peripheral T Cell Unresponsiveness under Steady State Conditions in Vivo." *J Exp Med* 194, no. 6 (2001): 769-79.

Healy, C. G., J. W. Simons, M. A. Carducci, T. L. DeWeese, M. Bartkowski, K. P. Tong and W. E. Bolton. "Impaired Expression and Function of Signal-Transducing Zeta Chains in Peripheral T Cells and Natural Killer Cells in Patients with Prostate Cancer." *Cytometry* 32, no. 2 (1998): 109-19.

Heemskerk, B., P. Kvistborg and T. N. Schumacher. "The Cancer Antigenome." *Embo j* 32, no. 2 (2013): 194-203.

Heemskerk, M. H., R. S. Hagedoorn, M. A. van der Hoorn, L. T. van der Veken, M. Hoogeboom, M. G. Kester, R. Willemze and J. H. Falkenburg. "Efficiency of T-Cell Receptor Expression in Dual-Specific T Cells Is Controlled by the Intrinsic Qualities of the Tcr Chains within the Tcr-Cd3 Complex." *Blood* 109, no. 1 (2007): 235-43.

Hildemann, Steven K., Jens Eberlein, Bennett Davenport, Tom T. Nguyen, Francisco Victorino and Dirk Homann. "High Efficiency of Antiviral Cd4(+) Killer T Cells." *PLoS ONE* 8, no. 4 (2013): e60420.

Hinrichs, C. S., Z. A. Borman, L. Cassard, L. Gattinoni, R. Spolski, Z. Yu, L. Sanchez-Perez, P. Muranski, S. J. Kern, C. Logun, D. C. Palmer, Y. Ji, R. N. Reger, W. J. Leonard, R. L. Danner, S. A. Rosenberg and N. P. Restifo. "Adoptively Transferred Effector Cells Derived from Naive Rather Than Central Memory Cd8+ T Cells Mediate Superior Antitumor Immunity." *Proc Natl Acad Sci U S A* 106, no. 41 (2009): 17469-74.

Hofmann, M. W., S. Honing, D. Rodionov, B. Dobberstein, K. von Figura and O. Bakke. "The Leucine-Based Sorting Motifs in the Cytoplasmic Domain of the Invariant Chain Are Recognized by the Clathrin Adaptors Ap1 and Ap2 and Their Medium Chains." *J Biol Chem* 274, no. 51 (1999): 36153-8.

Holler, P. D., L. K. Chlewicki and D. M. Kranz. "Tcrs with High Affinity for Foreign Pmhc Show Self-Reactivity." *Nat Immunol* 4, no. 1 (2003): 55-62.

Holst, Jeff, Haopeng Wang, Kelly Durick Eder, Creg J. Workman, Kelli L. Boyd, Zachary Baquet, Harvir Singh, Karen Forbes, Andrzej Chruscinski, Richard Smeyne, Nicolai S. C. van Oers, Paul J. Utz and Dario A. A. Vignali. "Scalable Signaling Mediated by T Cell Antigen Receptor-Cd3 Itams Ensures Effective Negative Selection and Prevents Autoimmunity." *Nat Immunol* 9, no. 6 (2008): 658-666.

Huang, A. Y., P. Golumbek, M. Ahmadzadeh, E. Jaffee, D. Pardoll and H. Levitsky. "Role of Bone Marrow-Derived Cells in Presenting Mhc Class I-Restricted Tumor Antigens." *Science* 264, no. 5161 (1994): 961-5.

Hunder , Naomi N., Herschel Wallen , Jianhong Cao , Deborah W. Hendricks , John Z. Reilly , Rebecca Rodmyre , Achim Jungbluth , Sacha Gnjatic , John A. Thompson and Cassian Yee "Treatment of Metastatic Melanoma with Autologous Cd4+ T Cells

against Ny-Eso-1." *New England Journal of Medicine* 358, no. 25 (2008): 2698-2703.

Hung, K., R. Hayashi, A. Lafond-Walker, C. Lowenstein, D. Pardoll and H. Levitsky. "The Central Role of Cd4(+) T Cells in the Antitumor Immune Response." *J Exp Med* 188, no. 12 (1998): 2357-68.

Huppa, Johannes B., Markus Axmann, Manuel A. Mortelmaier, Bjorn F. Lillemeier, Evan W. Newell, Mario Brameshuber, Lawrence O. Klein, Gerhard J. Schutz and Mark M. Davis. "Tcr-Peptide-Mhc Interactions in Situ Show Accelerated Kinetics and Increased Affinity." *Nature* 463, no. 7283 (2010): 963-967.

Intlekofer, A. M., N. Takemoto, E. J. Wherry, S. A. Longworth, J. T. Northrup, V. R. Palanivel, A. C. Mullen, C. R. Gasink, S. M. Kaech, J. D. Miller, L. Gapin, K. Ryan, A. P. Russ, T. Lindsten, J. S. Orange, A. W. Goldrath, R. Ahmed and S. L. Reiner. "Effector and Memory Cd8+ T Cell Fate Coupled by T-Bet and Eomesodermin." *Nat Immunol* 6, no. 12 (2005): 1236-44.

Itoh, Yasushi, Bernhard Hemmer, Roland Martin and Ronald N. Germain. "Serial Tcr Engagement and Down-Modulation by Peptide:Mhc Molecule Ligands: Relationship to the Quality of Individual Tcr Signaling Events." *The Journal of Immunology* 162, no. 4 (1999): 2073-2080.

Jacks T., Fazeli A., Schmitt E.M., Bronson R.T., Goodell M.A., et al. (1992) “Effects of an Rb mutation in the mouse” Nature, 359:295–300.

Jameson, Stephen C. "Maintaining the Norm: T-Cell Homeostasis." *Nat Rev Immunol* 2, no. 8 (2002): 547-556.

Jenkins, M. R. and G. M. Griffiths. "The Synapse and Cytolytic Machinery of Cytotoxic T Cells." *Curr Opin Immunol* 22, no. 3 (2010): 308-13.

Johnson, L. A., R. A. Morgan, M. E. Dudley, L. Cassard, J. C. Yang, M. S. Hughes, U. S. Kammula, R. E. Royal, R. M. Sherry, J. R. Wunderlich, C. C. Lee, N. P. Restifo, S. L. Schwarz, A. P. Cogdill, R. J. Bishop, H. Kim, C. C. Brewer, S. F. Rudy, C. VanWaes, J. L. Davis, A. Mathur, R. T. Ripley, D. A. Nathan, C. M. Laurencot and S. A. Rosenberg. "Gene Therapy with Human and Mouse T-Cell Receptors Mediates Cancer Regression and Targets Normal Tissues Expressing Cognate Antigen." *Blood* 114, no. 3 (2009): 535-46.

Jorritsma, A., R. Gomez-Eerland, M. Dokter, W. van de Kasteele, Y. M. Zoet, Doxiadis, II, N. Rufer, P. Romero, R. A. Morgan, T. N. Schumacher and J. B. Haanen. "Selecting Highly Affine and Well-Expressed Tcrs for Gene Therapy of Melanoma." *Blood* 110, no. 10 (2007): 3564-72.

Joshi, N. S., W. Cui, A. Chandele, H. K. Lee, D. R. Urso, J. Hagman, L. Gapin and S. M. Kaech. "Inflammation Directs Memory Precursor and Short-Lived Effector Cd8(+) T Cell Fates Via the Graded Expression of T-Bet Transcription Factor." *Immunity* 27, no. 2 (2007): 281-95.

Kaech, S. M., E. J. Wherry and R. Ahmed. "Effector and Memory T-Cell Differentiation: Implications for Vaccine Development." *Nat Rev Immunol* 2, no. 4 (2002): 251-62.

Kassiotis, George, Rose Zamoyska and Brigitta Stockinger. "Involvement of Avidity for Major Histocompatibility Complex in Homeostasis of Naive and Memory T Cells." *The Journal of Experimental Medicine* 197, no. 8 (2003): 1007-1016.

Kerkar, S. P., L. Sanchez-Perez, S. Yang, Z. A. Borman, P. Muranski, Y. Ji, D. Chinnasamy, A. D. Kaiser, C. S. Hinrichs, C. A. Klebanoff, C. D. Scott, L. Gattinoni, R. A. Morgan, S. A. Rosenberg and N. P. Restifo. "Genetic Engineering of Murine Cd8+ and Cd4+ T Cells for Preclinical Adoptive Immunotherapy Studies." *J Immunother* 34, no. 4 (2011): 343-52.

Kessels, H. W., M. C. Wolkers, M. D. van den Boom, M. A. van der Valk and T. N. Schumacher. "Immunotherapy through Tcr Gene Transfer." *Nat Immunol* 2, no. 10 (2001): 957-61.

Khong, H. T. and N. P. Restifo. "Natural Selection of Tumor Variants in the Generation of "Tumor Escape" Phenotypes." *Nat Immunol* 3, no. 11 (2002): 999-1005.

Kirberg, J., A. Berns and H. von Boehmer. "Peripheral T Cell Survival Requires Continual Ligation of the T Cell Receptor to Major Histocompatibility Complex-Encoded Molecules." *J Exp Med* 186, no. 8 (1997): 1269-75.

Klebanoff, C. A., L. Gattinoni, P. Torabi-Parizi, K. Kerstann, A. R. Cardones, S. E. Finkelstein, D. C. Palmer, P. A. Antony, S. T. Hwang, S. A. Rosenberg, T. A. Waldmann and N. P. Restifo. "Central Memory Self/Tumor-Reactive Cd8+ T Cells

Confer Superior Antitumor Immunity Compared with Effector Memory T Cells." *Proc Natl Acad Sci U S A* 102, no. 27 (2005): 9571-6.

Klein, Ludger, Bruno Kyewski, Paul M. Allen and Kristin A. Hogquist. "Positive and Negative Selection of the T Cell Repertoire: What Thymocytes See and Don't See." *Nature reviews. Immunology* 14, no. 6 (2014): 377-391.

Knipping, Friederike, Mark J. Osborn, Karl Petri, Jakub Tolar, Hanno Glimm, Christof von Kalle, Manfred Schmidt and Richard Gabriel. "Genome-Wide Specificity of Highly Efficient Talens and Crispr/Cas9 for T Cell Receptor Modification." *Molecular Therapy. Methods & Clinical Development* 4, (2017): 213-224.

Koebel, C. M., W. Vermi, J. B. Swann, N. Zerafa, S. J. Rodig, L. J. Old, M. J. Smyth and R. D. Schreiber. "Adaptive Immunity Maintains Occult Cancer in an Equilibrium State." *Nature* 450, no. 7171 (2007): 903-7.

Kohrt, H. E., N. Nouri, K. Nowels, D. Johnson, S. Holmes and P. P. Lee. "Profile of Immune Cells in Axillary Lymph Nodes Predicts Disease-Free Survival in Breast Cancer." *PLoS Med* 2, no. 9 (2005): e284.

Kondrack, R. M., J. Harbertson, J. T. Tan, M. E. McBreen, C. D. Surh and L. M. Bradley. "Interleukin 7 Regulates the Survival and Generation of Memory Cd4 Cells." *J Exp Med* 198, no. 12 (2003): 1797-806.

Kong, S., S. Sengupta, B. Tyler, A. J. Bais, Q. Ma, S. Doucette, J. Zhou, A. Sahin, B. S. Carter, H. Brem, R. P. Junghans and P. Sampath. "Suppression of Human Glioma Xenografts with Second-Generation Il13r-Specific Chimeric Antigen Receptor-Modified T Cells." *Clin Cancer Res* 18, no. 21 (2012): 5949-60.

Kono, K., F. Salazar-Onfray, M. Petersson, J. Hansson, G. Masucci, K. Wasserman, T. Nakazawa, P. Anderson and R. Kiessling. "Hydrogen Peroxide Secreted by Tumor-Derived Macrophages Down-Modulates Signal-Transducing Zeta Molecules and Inhibits Tumor-Specific T Cell-and Natural Killer Cell-Mediated Cytotoxicity." *Eur J Immunol* 26, no. 6 (1996): 1308-13.

Kuball, J., M. L. Dossett, M. Wolfl, W. Y. Ho, R. H. Voss, C. Fowler and P. D. Greenberg. "Facilitating Matched Pairing and Expression of Tcr Chains Introduced into Human T Cells." *Blood* 109, no. 6 (2007): 2331-8.

Kurt, R. A., W. J. Urba, J. W. Smith and D. D. Schoof. "Peripheral T Lymphocytes from Women with Breast Cancer Exhibit Abnormal Protein Expression of Several Signaling Molecules." *Int J Cancer* 78, no. 1 (1998): 16-20.

Kurts, C., H. Kosaka, F. R. Carbone, J. F. Miller and W. R. Heath. "Class I-Restricted Cross-Presentation of Exogenous Self-Antigens Leads to Deletion of Autoreactive Cd8(+) T Cells." *J Exp Med* 186, no. 2 (1997): 239-45.

Kurts, Christian, Bruce W. S. Robinson and Percy A. Knolle. "Cross-Priming in Health and Disease." *Nat Rev Immunol* 10, no. 6 (2010): 403-414.

Kuss, I., H. Rabinowich, W. Gooding, R. Edwards and T. L. Whiteside. "Expression of Zeta in T Cells Prior to Interleukin-2 Therapy as a Predictor of Response and Survival in Patients with Ovarian Carcinoma." *Cancer Biother Radiopharm* 17, no. 6 (2002): 631-40.

Kuss, I., T. Saito, J. T. Johnson and T. L. Whiteside. "Clinical Significance of Decreased Zeta Chain Expression in Peripheral Blood Lymphocytes of Patients with Head and Neck Cancer." *Clin Cancer Res* 5, no. 2 (1999): 329-34.

Labrecque, N., L. S. Whitfield, R. Obst, C. Waltzinger, C. Benoist and D. Mathis. "How Much Tcr Does a T Cell Need?" *Immunity* 15, no. 1 (2001): 71-82.

Lalor, Patricia F., Philip Shields, Allister J. Grant and David H. Adams. "Recruitment of Lymphocytes to the Human Liver." *Immunol Cell Biol* 80, no. 1 (2002): 52-64.

Landsverk, O. J., O. Bakke and T. F. Gregers. "Mhc Ii and the Endocytic Pathway: Regulation by Invariant Chain." *Scand J Immunol* 70, no. 3 (2009): 184-93.

Lee, Kyeong-Hee, Aaron R. Dinner, Chun Tu, Gabriele Campi, Subhadip Raychaudhuri, Rajat Varma, Tasha N. Sims, W. Richard Burack, Hui Wu, Julia Wang, Osami Kanagawa, Mary Markiewicz, Paul M. Allen, Michael L. Dustin, Arup K. Chakraborty and Andrey S. Shaw. "The Immunological Synapse Balances T Cell Receptor Signaling and Degradation." *Science* 302, no. 5648 (2003): 1218-1222.

Lenschow, D.J., T. L. Walunas, and J. A. Bluestone. (1996) “CD28/B7 system of T cell costimulation”. Annu. Rev. Immunol. 14:233.

Lennerz, V., M. Fatho, C. Gentilini, R. A. Frye, A. Lifke, D. Ferel, C. Wolfel, C. Huber and T. Wolfel. "The Response of Autologous T Cells to a Human Melanoma Is Dominated by Mutated Neoantigens." *Proc Natl Acad Sci U S A* 102, no. 44 (2005): 16013-8.

Li, Y., R. Moysey, P. E. Molloy, A. L. Vuidepot, T. Mahon, E. Baston, S. Dunn, N. Liddy, J. Jacob, B. K. Jakobsen and J. M. Boulter. "Directed Evolution of Human T-Cell Receptors with Picomolar Affinities by Phage Display." *Nat Biotechnol* 23, no. 3 (2005): 349-54.

Lindemann, C., A. J. Schilz, B. Emons, C. Baum, R. Low, A. A. Fauser, K. Kuehlcke and H. G. Eckert. "Down-Regulation of Retroviral Transgene Expression During Differentiation of Progenitor-Derived Dendritic Cells." *Exp Hematol* 30, no. 2 (2002): 150-7.

Liossis, S. N., X. Z. Ding, G. J. Dennis and G. C. Tsokos. "Altered Pattern of Tcr/Cd3-Mediated Protein-Tyrosyl Phosphorylation in T Cells from Patients with Systemic Lupus Erythematosus. Deficient Expression of the T Cell Receptor Zeta Chain." *J Clin Invest* 101, no. 7 (1998): 1448-57.

Löhning, Max, Ahmed N. Hegazy, Daniel D. Pinschewer, Dorothea Busse, Karl S. Lang, Thomas Höfer, Andreas Radbruch, Rolf M. Zinkernagel and Hans Hengartner. "Long-Lived Virus-Reactive Memory T Cells Generated from Purified Cytokine-Secreting T Helper Type 1 and Type 2 Effectors." *The Journal of Experimental Medicine* 205, no. 1 (2008): 53-61.

Love, PE, EW Shores, MD Johnson, ML Tremblay, EJ Lee, A Grinberg, SP Huang, A Singer and H Westphal. "T Cell Development in Mice That Lack the Zeta Chain of the T Cell Antigen Receptor Complex." *Science* 261, no. 5123 (1993): 918-921.

Love, Paul E., Jan Lee and Elizabeth W. Shores. "Critical Relationship between Tcr Signaling Potential and Tcr Affinity During Thymocyte Selection." *The Journal of Immunology* 165, no. 6 (2000): 3080-3087.

Lu, Y. C., X. Yao, J. S. Crystal, Y. F. Li, M. El-Gamil, C. Gross, L. Davis, M. E. Dudley, J. C. Yang, Y. Samuels, S. A. Rosenberg and P. F. Robbins. "Efficient Identification of Mutated Cancer Antigens Recognized by T Cells Associated with Durable Tumor Regressions." *Clin Cancer Res* 20, no. 13 (2014): 3401-10.

Lyubchenko, T. A., G. A. Wurth and A. Zweifach. "Role of Calcium Influx in Cytotoxic T

Lymphocyte Lytic Granule Exocytosis During Target Cell Killing." *Immunity* 15, no. 5 (2001): 847-59.

Malissen, B. and P. Bongrand. "Early T Cell Activation: Integrating Biochemical, Structural, and Biophysical Cues." *Annu Rev Immunol* 33, (2015): 539-61.

Malissen, M., A. Gillet, L. Ardouin, G. Bouvier, J. Trucy, P. Ferrier, E. Vivier and B. Malissen. "Altered T Cell Development in Mice with a Targeted Mutation of the Cd3-Epsilon Gene." *Embo j* 14, no. 19 (1995): 4641-53.

Mandl, Judith N., João P. Monteiro, Nienke Vrisekoop and Ronald N. Germain. "T Cell Positive Selection Uses Self-Ligand Binding Strength to Optimize Repertoire Recognition of Foreign Antigens." *Immunity* 38, no. 2 (2013): 263-274.

Martin, B., C. Becourt, B. Bienvenu and B. Lucas. "Self-Recognition Is Crucial for Maintaining the Peripheral Cd4+ T-Cell Pool in a Nonlymphopenic Environment." *Blood* 108, no. 1 (2006): 270-7.

Masopust, David, Vaiva Vezys, Amanda L. Marzo and Leo Lefrançois. "Preferential Localization of Effector Memory Cells in Nonlymphoid Tissue." *Science* 291, no. 5512 (2001): 2413-2417.

Matsuda, M., M. Petersson, R. Lenkei, J. L. Taupin, I. Magnusson, H. Mellstedt, P. Anderson and R. Kiessling. "Alterations in the Signal-Transducing Molecules of T Cells and Nk Cells in Colorectal Tumor-Infiltrating, Gut Mucosal and Peripheral Lymphocytes: Correlation with the Stage of the Disease." *Int J Cancer* 61, no. 6 (1995): 765-72.

Matsuda, Satoshi, Yoshihiro Miwa, Yasuko Hirata, Akiko Minowa, Junko Tanaka, Eisuke Nishida and Shigeo Koyasu. "Negative Feedback Loop in T-Cell Activation through Mapk-Catalyzed Threonine Phosphorylation of Lat." *The EMBO Journal* 23, no. 13 (2004): 2577-2585.

Maude, Shannon L., Noelle Frey, Pamela A. Shaw, Richard Aplenc, David M. Barrett, Nancy J. Bunin, Anne Chew, Vanessa E. Gonzalez, Zhaohui Zheng, Simon F. Lacey, Yolanda D. Mahnke, Jan J. Melenhorst, Susan R. Rheingold, Angela Shen, David T. Teachey, Bruce L. Levine, Carl H. June, David L. Porter and Stephan A. Grupp. "Chimeric Antigen Receptor T Cells for Sustained Remissions in Leukemia." *New*

England Journal of Medicine 371, no. 16 (2014): 1507-1517.

Maul-Pavicic, Andrea, Samuel C. C. Chiang, Anne Rensing-Ehl, Birthe Jessen, Cyril Fauriat, Stephanie M. Wood, Sebastian Sjöqvist, Markus Hufnagel, Ilka Schulze, Thilo Bass, Wolfgang W. Schamel, Sebastian Fuchs, Hanspeter Pircher, Christie-Ann McCarl, Katsuhiko Mikoshiba, Klaus Schwarz, Stefan Feske, Yenan T. Bryceson and Stephan Ehl. "Orai1-Mediated Calcium Influx Is Required for Human Cytotoxic Lymphocyte Degranulation and Target Cell Lysis." *Proceedings of the National Academy of Sciences of the United States of America* 108, no. 8 (2011): 3324-3329.

Maurice, M. M., A. C. Lankester, A. C. Bezemer, M. F. Geertsma, P. P. Tak, F. C. Breedveld, R. A. van Lier and C. L. Verweij. "Defective Tcr-Mediated Signaling in Synovial T Cells in Rheumatoid Arthritis." *J Immunol* 159, no. 6 (1997): 2973-8.

McKeithan, T W. "Kinetic Proofreading in T-Cell Receptor Signal Transduction." *Proceedings of the National Academy of Sciences* 92, no. 11 (1995): 5042-5046.

McNeil, L. K., T. K. Starr and K. A. Hogquist. "A Requirement for Sustained Erk Signaling During Thymocyte Positive Selection in Vivo." *Proc Natl Acad Sci U S A* 102, no. 38 (2005): 13574-9.

Mizoguchi, H., J. J. O'Shea, D. L. Longo, C. M. Loeffler, D. W. McVicar and A. C. Ochoa. "Alterations in Signal Transduction Molecules in T Lymphocytes from Tumor-Bearing Mice." *Science* 258, no. 5089 (1992): 1795-8.

Mizuguchi, Hiroyuki, Zhili Xu, Akiko Ishii-Watabe, Eriko Uchida and Takao Hayakawa. "Ires-Dependent Second Gene Expression Is Significantly Lower Than Cap-Dependent First Gene Expression in a Bicistronic Vector." *Molecular Therapy* 1, no. 4 (2000): 376-382.

Mohan, James F. and Emil R. Unanue. "Unconventional Recognition of Peptides by T Cells and the Implications for Autoimmunity." *Nat Rev Immunol* 12, no. 10 (2012): 721-728.

Monks, Colin R. F., Benjamin A. Freiberg, Hannah Kupfer, Noah Sciaky and Abraham Kupfer. "Three-Dimensional Segregation of Supramolecular Activation Clusters in T Cells." *Nature* 395, no. 6697 (1998): 82-86.

Mora, J. R. and U. H. von Andrian. "T-Cell Homing Specificity and Plasticity: New Concepts and Future Challenges." *Trends Immunol* 27, no. 5 (2006): 235-43.

Morgan, R. A., N. Chinnasamy, D. Abate-Daga, A. Gros, P. F. Robbins, Z. Zheng, M. E. Dudley, S. A. Feldman, J. C. Yang, R. M. Sherry, G. Q. Phan, M. S. Hughes, U. S. Kammula, A. D. Miller, C. J. Hessman, A. A. Stewart, N. P. Restifo, M. M. Quezado, M. Alimchandani, A. Z. Rosenberg, A. Nath, T. Wang, B. Bielekova, S. C. Wuest, N. Akula, F. J. McMahon, S. Wilde, B. Mosetter, D. J. Schendel, C. M. Laurencot and S. A. Rosenberg. "Cancer Regression and Neurological Toxicity Following Anti-Mage-A3 Tcr Gene Therapy." *J Immunother* 36, no. 2 (2013): 133-51.

Morgan, R. A., M. E. Dudley, J. R. Wunderlich, M. S. Hughes, J. C. Yang, R. M. Sherry, R. E. Royal, S. L. Topalian, U. S. Kammula, N. P. Restifo, Z. Zheng, A. Nahvi, C. R. de Vries, L. J. Rogers-Freezer, S. A. Mavroukakis and S. A. Rosenberg. "Cancer Regression in Patients after Transfer of Genetically Engineered Lymphocytes." *Science* 314, no. 5796 (2006): 126-9.

Mosmann, T. R., H. Cherwinski, M. W. Bond, M. A. Giedlin and R. L. Coffman. "Two Types of Murine Helper T Cell Clone. I. Definition According to Profiles of Lymphokine Activities and Secreted Proteins." *J Immunol* 136, no. 7 (1986): 2348-57.

Murata, S., K. Sasaki, T. Kishimoto, S. Niwa, H. Hayashi, Y. Takahama and K. Tanaka. "Regulation of Cd8+ T Cell Development by Thymus-Specific Proteasomes." *Science* 316, no. 5829 (2007): 1349-53.

Nakagawa, T., W. Roth, P. Wong, A. Nelson, A. Farr, J. Deussing, J. A. Villadangos, H. Ploegh, C. Peters and A. Y. Rudensky. "Cathepsin L: Critical Role in Ii Degradation and Cd4 T Cell Selection in the Thymus." *Science* 280, no. 5362 (1998): 450-3.

Nakamura, Haruhiko, Hisashi Saji, Akihiko Ogata, Makoto Hosaka, Masaru Hagiwara, Norihiko Kawasaki, Chimori Konaka and Harubumi Kato. "Immunologic Parameters as Significant Prognostic Factors in Lung Cancer." *Lung Cancer* 37, no. 2 (2002): 161-169.

Neefjes, Jacques, Marlieke L. M. Jongsma, Petra Paul and Oddmund Bakke. "Towards a Systems Understanding of Mhc Class I and Mhc Class Ii Antigen Presentation." *Nat Rev Immunol* 11, no. 12 (2011): 823-836.

Norment, Anne M., Russell D. Salter, Peter Parham, Victor H. Engelhard and Dan R. Littman. "Cell-Cell Adhesion Mediated by Cd8 and Mhc Class I Molecules." *Nature* 336, no. 6194 (1988): 79-81.

O'Shea, J. J. and W. E. Paul. "Mechanisms Underlying Lineage Commitment and Plasticity of Helper Cd4+ T Cells." *Science* 327, no. 5969 (2010): 1098-102.

Otsuji, Mizuto, Yoshimitsu Kimura, Tomohiko Aoe, Yasuhiro Okamoto and Takashi Saito. "Oxidative Stress by Tumor-Derived Macrophages Suppresses the Expression of Cd3 Z Chain of T-Cell Receptor Complex and Antigen-Specific T-Cell Responses." *Proceedings of the National Academy of Sciences* 93, no. 23 (1996): 13119-13124.

Overwijk, W. W., M. R. Theoret, S. E. Finkelstein, D. R. Surman, L. A. de Jong, F. A. Vyth-Dreese, T. A. Dellemijn, P. A. Antony, P. J. Spiess, D. C. Palmer, D. M. Heimann, C. A. Klebanoff, Z. Yu, L. N. Hwang, L. Feigenbaum, A. M. Kruisbeek, S. A. Rosenberg and N. P. Restifo. "Tumor Regression and Autoimmunity after Reversal of a Functionally Tolerant State of Self-Reactive Cd8+ T Cells." *J Exp Med* 198, no. 4 (2003): 569-80.

Palmer, E. and D. Naeher. "Affinity Threshold for Thymic Selection through a T-Cell Receptor-Co-Receptor Zipper." *Nat Rev Immunol* 9, no. 3 (2009): 207-13.

Parcej, David and Robert Tampe. "Abc Proteins in Antigen Translocation and Viral Inhibition." *Nat Chem Biol* 6, no. 8 (2010): 572-580.

Parretta, Elisabetta, Giuliana Cassese, Angela Santoni, John Guardiola, Antonia Vecchio and Francesca Di Rosa. "Kinetics of in Vivo Proliferation and Death of Memory and Naive Cd8 T Cells: Parameter Estimation Based on 5-Bromo-2′-Deoxyuridine Incorporation in Spleen, Lymph Nodes, and Bone Marrow." *The Journal of Immunology* 180, no. 11 (2008): 7230-7239.

Pelletier M., Maggi L., Micheletti A., Lazzeri E., Tamassia N., Costantini C., Cosmi L., Lunardi C., Annunziato F., Romagnani S., Cassatella MA. “Evidence for a cross-talk between human neutrophils and Th17 cells.” *Blood* 2010 Jan 14;115(2):335-43.

Perez-Diez, Ainhoa, Nathalie T. Joncker, Kyungho Choi, William F. N. Chan, Colin C. Anderson, Olivier Lantz and Polly Matzinger. "Cd4 Cells Can Be More Efficient at Tumor Rejection Than Cd8 Cells." *Blood* 109, no. 12 (2007): 5346-5354.

Pickart, Cecile M. and Michael J. Eddins. "Ubiquitin: Structures, Functions,

Mechanisms." *Biochimica et Biophysica Acta (BBA) - Molecular Cell Research* 1695, no. 1 (2004): 55-72.

Pinzon-Charry, A., T. Maxwell and J. A. Lopez. "Dendritic Cell Dysfunction in Cancer: A Mechanism for Immunosuppression." *Immunol Cell Biol* 83, no. 5 (2005): 451-61.

Pitcher, Lisa A., Meredith A. Mathis, Srividya Subramanian, Jennifer A. Young, Edward K. Wakeland, Paul E. Love and Nicolai S. C. van Oers. "Selective Expression of the 21-Kilodalton Tyrosine-Phosphorylated Form of Tcr Z Promotes the Emergence of T Cells with Autoreactive Potential." *The Journal of Immunology* 174, no. 10 (2005a): 6071-6079.

Pitcher, L. A., M. A. Mathis, J. A. Young, L. M. DeFord, B. Purtic, C. Wulfing and N. S. van Oers. "The Cd3 Gamma Epsilon/Delta Epsilon Signaling Module Provides Normal T Cell Functions in the Absence of the Tcr Zeta Immunoreceptor Tyrosine-Based Activation Motifs." *Eur J Immunol* 35, no. 12 (2005b): 3643-54.

Polic, B., D. Kunkel, A. Scheffold and K. Rajewsky. "How Alpha Beta T Cells Deal with Induced Tcr Alpha Ablation." *Proc Natl Acad Sci U S A* 98, no. 15 (2001): 8744-9.

Provasi, E., P. Genovese, A. Lombardo, Z. Magnani, P. Q. Liu, A. Reik, V. Chu, D. E. Paschon, L. Zhang, J. Kuball, B. Camisa, A. Bondanza, G. Casorati, M. Ponzoni, F. Ciceri, C. Bordignon, P. D. Greenberg, M. C. Holmes, P. D. Gregory, L. Naldini and C. Bonini. "Editing T Cell Specificity Towards Leukemia by Zinc Finger Nucleases and Lentiviral Gene Transfer." *Nat Med* 18, no. 5 (2012): 807-815.

Qin, Zhihai and Thomas Blankenstein. "Cd4+ T Cell–Mediated Tumor Rejection Involves Inhibition of Angiogenesis That Is Dependent on Ifnγ Receptor Expression by Nonhematopoietic Cells." *Immunity* 12, no. 6 (2000): 677-686.

Qureshi, O. S., Y. Zheng, K. Nakamura, K. Attridge, C. Manzotti, E. M. Schmidt, J. Baker, L. E. Jeffery, S. Kaur, Z. Briggs, T. Z. Hou, C. E. Futter, G. Anderson, L. S. Walker and D. M. Sansom. "Trans-Endocytosis of Cd80 and Cd86: A Molecular Basis for the Cell-Extrinsic Function of Ctla-4." *Science* 332, no. 6029 (2011): 600-3.

R., Neta, Perlstein R., Vogel S. N., G. D. Ledney and J. Abrams. "Role of Interleukin 6 (Il-6) in Protection from Lethal Irradiation and in Endocrine Responses to Il-1 and Tumor Necrosis Factor." *The Journal of Experimental Medicine* 175, no. 3 (1992):

689-694.

Rabinowitz, J. D., C. Beeson, C. Wulfing, K. Tate, P. M. Allen, M. M. Davis and H. M. McConnell. "Altered T Cell Receptor Ligands Trigger a Subset of Early T Cell Signals." *Immunity* 5, no. 2 (1996): 125-35.

Raphael, I., S. Nalawade, T. N. Eagar and T. G. Forsthuber. "T Cell Subsets and Their Signature Cytokines in Autoimmune and Inflammatory Diseases." *Cytokine* 74, no. 1 (2015): 5-17.

Rathmell, J. C., E. A. Farkash, W. Gao and C. B. Thompson. "Il-7 Enhances the Survival and Maintains the Size of Naive T Cells." *J Immunol* 167, no. 12 (2001): 6869-76.

Recio, María J., Miguel Angel Moreno-Pelayo, Sara S. Kiliç, Alberto C. Guardo, Ozden Sanal, Luis M. Allende, Verónica Pérez-Flores, Angeles Mencía, Silvia Modamio-Høybjør, Elena Seoane and José R. Regueiro. "Differential Biological Role of Cd3 Chains Revealed by Human Immunodeficiencies." *The Journal of Immunology* 178, no. 4 (2007): 2556-2564.

Reddy, Sai T. "Immunology: The Patterns of T-Cell Target Recognition." *Nature* 547, no. 7661 (2017): 36-38.

Restifo, N. P. and L. Gattinoni. "Lineage Relationship of Effector and Memory T Cells." *Curr Opin Immunol* 25, no. 5 (2013): 556-63.

Rieux-Laucat , Frédéric, Claire Hivroz , Annick Lim , Véronique Mateo , Isabelle Pellier , Françoise Selz , Alain Fischer and Françoise Le Deist "Inherited and Somatic Cd3ζ Mutations in a Patient with T-Cell Deficiency." *New England Journal of Medicine* 354, no. 18 (2006): 1913-1921.

Robbins, P. F., M. E. Dudley, J. Wunderlich, M. El-Gamil, Y. F. Li, J. Zhou, J. Huang, D. J. Powell, Jr. and S. A. Rosenberg. "Cutting Edge: Persistence of Transferred Lymphocyte Clonotypes Correlates with Cancer Regression in Patients Receiving Cell Transfer Therapy." *J Immunol* 173, no. 12 (2004): 7125-30.

Robbins, P. F., R. A. Morgan, S. A. Feldman, J. C. Yang, R. M. Sherry, M. E. Dudley, J. R. Wunderlich, A. V. Nahvi, L. J. Helman, C. L. Mackall, U. S. Kammula, M. S. Hughes, N. P. Restifo, M. Raffeld, C. C. Lee, C. L. Levy, Y. F. Li, M. El-Gamil, S. L.

Schwarz, C. Laurencot and S. A. Rosenberg. "Tumor Regression in Patients with Metastatic Synovial Cell Sarcoma and Melanoma Using Genetically Engineered Lymphocytes Reactive with Ny-Eso-1." *J Clin Oncol* 29, no. 7 (2011): 917-24.

Roberts, Joseph L., Jens Peter H. Lauritsen, Myriah Cooney, Roberta E. Parrott, Elisa O. Sajaroff, Chan M. Win, Michael D. Keller, Jeffery H. Carpenter, Juan Carabana, Michael S. Krangel, Marcella Sarzotti, Xiao-Ping Zhong, David L. Wiest and Rebecca H. Buckley. "T(−) B(+) Nk(+) Severe Combined Immunodeficiency Caused by Complete Deficiency of the Cd3ζ Subunit of the T-Cell Antigen Receptor Complex." *Blood* 109, no. 8 (2007): 3198-3206.

Rock, Kenneth L., Colette Gramm, Lisa Rothstein, Karen Clark, Ross Stein, Lawrence Dick, Daniel Hwang and Alfred L. Goldberg. "Inhibitors of the Proteasome Block the Degradation of Most Cell Proteins and the Generation of Peptides Presented on Mhc Class I Molecules." *Cell* 78, no. 5 (1994): 761-771.

Roelse, J., M. Gromme, F. Momburg, G. Hammerling and J. Neefjes. "Trimming of Tap-Translocated Peptides in the Endoplasmic Reticulum and in the Cytosol During Recycling." *J Exp Med* 180, no. 5 (1994): 1591-7.

Romieu-Mourez, R., M. Francois, M. N. Boivin, J. Stagg and J. Galipeau. "Regulation of Mhc Class Ii Expression and Antigen Processing in Murine and Human Mesenchymal Stromal Cells by Ifn-Gamma, Tgf-Beta, and Cell Density." *J Immunol* 179, no. 3 (2007): 1549-58.

Rosenberg, S. A. and M. E. Dudley. "Cancer Regression in Patients with Metastatic Melanoma after the Transfer of Autologous Antitumor Lymphocytes." *Proc Natl Acad Sci U S A* 101 Suppl 2, (2004): 14639-45.

Rosenberg, S. A., M. T. Lotze, L. M. Muul, S. Leitman, A. E. Chang, S. E. Ettinghausen, Y. L. Matory, J. M. Skibber, E. Shiloni, J. T. Vetto and et al. "Observations on the Systemic Administration of Autologous Lymphokine-Activated Killer Cells and Recombinant Interleukin-2 to Patients with Metastatic Cancer." *N Engl J Med* 313, no. 23 (1985): 1485-92.

Rosenberg, S. A., P. Spiess and R. Lafreniere. "A New Approach to the Adoptive Immunotherapy of Cancer with Tumor-Infiltrating Lymphocytes." *Science* 233, no. 4770 (1986): 1318-21.

Rudolph, M. G., R. L. Stanfield and I. A. Wilson. "How Tcrs Bind Mhcs, Peptides, and Coreceptors." *Annu Rev Immunol* 24, (2006): 419-66.

Sadelain, Michel, Renier Brentjens and Isabelle Riviere. "The Basic Principles of Chimeric Antigen Receptor (Car) Design." *Cancer discovery* 3, no. 4 (2013): 388-398.

Saito, T., T. Yokosuka and A. Hashimoto-Tane. "Dynamic Regulation of T Cell Activation and Co-Stimulation through Tcr-Microclusters." *FEBS Lett* 584, no. 24 (2010): 4865-71.

Sakaguchi, S., N. Sakaguchi, M. Asano, M. Itoh and M. Toda. "Immunologic Self-Tolerance Maintained by Activated T Cells Expressing Il-2 Receptor Alpha-Chains (Cd25). Breakdown of a Single Mechanism of Self-Tolerance Causes Various Autoimmune Diseases." *J Immunol* 155, no. 3 (1995): 1151-64.

Salio, Mariolina, Salvatore Valitutti and Antonio Lanzavecchia. "Agonist-Induced T Cell Receptor Down-Regulation: Molecular Requirements and Dissociation from T Cell Activation." *European Journal of Immunology* 27, no. 7 (1997): 1769-1773.

Sallusto, F., J. Geginat and A. Lanzavecchia. "Central Memory and Effector Memory T Cell Subsets: Function, Generation, and Maintenance." *Annu Rev Immunol* 22, (2004): 745-63.

Sallusto, F., D. Lenig, R. Forster, M. Lipp and A. Lanzavecchia. "Two Subsets of Memory T Lymphocytes with Distinct Homing Potentials and Effector Functions." *Nature* 401, no. 6754 (1999): 708-12.

Saveanu, L., O. Carroll, V. Lindo, M. Del Val, D. Lopez, Y. Lepelletier, F. Greer, L. Schomburg, D. Fruci, G. Niedermann and P. M. van Endert. "Concerted Peptide Trimming by Human Erap1 and Erap2 Aminopeptidase Complexes in the Endoplasmic Reticulum." *Nat Immunol* 6, no. 7 (2005): 689-97.

Savoldo, B., C. A. Ramos, E. Liu, M. P. Mims, M. J. Keating, G. Carrum, R. T. Kamble, C. M. Bollard, A. P. Gee, Z. Mei, H. Liu, B. Grilley, C. M. Rooney, H. E. Heslop, M. K. Brenner and G. Dotti. "Cd28 Costimulation Improves Expansion and Persistence of Chimeric Antigen Receptor-Modified T Cells in Lymphoma Patients." *J Clin Invest* 121, no. 5 (2011): 1822-6.

Schatz, D. G., M. A. Oettinger and M. S. Schlissel. "V(D)J Recombination: Molecular Biology and Regulation." *Annu Rev Immunol* 10, (1992): 359-83.

Schluns, K. S., W. C. Kieper, S. C. Jameson and L. Lefrancois. "Interleukin-7 Mediates the Homeostasis of Naive and Memory Cd8 T Cells in Vivo." *Nat Immunol* 1, no. 5 (2000): 426-32.

Schmidt, A., N. Oberle and P. H. Krammer. "Molecular Mechanisms of Treg-Mediated T Cell Suppression." *Front Immunol* 3, (2012): 51.

Schoenberger, S. P., R. E. Toes, E. I. van der Voort, R. Offringa and C. J. Melief. "T-Cell Help for Cytotoxic T Lymphocytes Is Mediated by Cd40-Cd40l Interactions." *Nature* 393, no. 6684 (1998): 480-3.

Schreiber, R. D., L. J. Old and M. J. Smyth. "Cancer Immunoediting: Integrating Immunity's Roles in Cancer Suppression and Promotion." *Science* 331, no. 6024 (2011): 1565-70.

Schumacher, T. N. and R. D. Schreiber. "Neoantigens in Cancer Immunotherapy." *Science* 348, no. 6230 (2015): 69-74.

Schwartz, R. H. "T Cell Anergy." *Annu Rev Immunol* 21, (2003): 305-34.

Seddon, B. and R. Zamoyska. "Tcr Signals Mediated by Src Family Kinases Are Essential for the Survival of Naive T Cells." *J Immunol* 169, no. 6 (2002): 2997-3005.

Segura, I., C. Delmelle-Wibaut, M. Janssens, Y. Cleuter, A. van den Broeke, R. Kettmann and K. E. Willard-Gallo. "Human Immunodeficiency Virus Type 2 Produces a Defect in Cd3-Gamma Gene Transcripts Similar to That Observed for Human Immunodeficiency Virus Type 1." *J Virol* 73, no. 6 (1999): 5207-13.

Seliger, B., M. J. Maeurer and S. Ferrone. "Antigen-Processing Machinery Breakdown and Tumor Growth." *Immunol Today* 21, no. 9 (2000): 455-64.

Serwold, Thomas, Federico Gonzalez, Jennifer Kim, Richard Jacob and Nilabh Shastri. "Eraap Customizes Peptides for Mhc Class I Molecules in the Endoplasmic Reticulum." *Nature* 419, no. 6906 (2002): 480-483.

Sewell, Andrew K. "Why Must T Cells Be Cross-Reactive?" *Nat Rev Immunol* 12, no. 9 (2012): 669-677.

Shahinian, A., K. Pfeffer, K. P. Lee, T. M. Kundig, K. Kishihara, A. Wakeham, K. Kawai, P. S. Ohashi, C. B. Thompson and T. W. Mak. "Differential T Cell Costimulatory Requirements in Cd28-Deficient Mice." *Science* 261, no. 5121 (1993): 609-12.

Shankaran, V., H. Ikeda, A. T. Bruce, J. M. White, P. E. Swanson, L. J. Old and R. D. Schreiber. "Ifngamma and Lymphocytes Prevent Primary Tumour Development and Shape Tumour Immunogenicity." *Nature* 410, no. 6832 (2001): 1107-11.

Shinkai, Yoichi, Gary Rathbun, Kong-Peng Lam, Eugene M. Oltz, Valerie Stewart, Monica Mendelsohn, Jean Charron, Milton Datta, Faith Young, Alan M. Stall and Frederick W. Alt. "Rag-2-Deficient Mice Lack Mature Lymphocytes Owing to Inability to Initiate V(D)J Rearrangement." *Cell* 68, no. 5 (1992): 855-867.

Shores, Elizabeth W., Tom Tran, Alexander Grinberg, Connie L. Sommers, Howard Shen and Paul E. Love. "Role of the Multiple T Cell Receptor (Tcr)-Z Chain Signaling Motifs in Selection of the T Cell Repertoire." *The Journal of Experimental Medicine* 185, no. 5 (1997): 893-900.

Sigal, L. J., S. Crotty, R. Andino and K. L. Rock. "Cytotoxic T-Cell Immunity to Virus-Infected Non-Haematopoietic Cells Requires Presentation of Exogenous Antigen." *Nature* 398, no. 6722 (1999): 77-80.

Simms, P. E. and T. M. Ellis. "Utility of Flow Cytometric Detection of Cd69 Expression as a Rapid Method for Determining Poly- and Oligoclonal Lymphocyte Activation." *Clinical and Diagnostic Laboratory Immunology* 3, no. 3 (1996): 301-304.

Smith, K., B. Seddon, M. A. Purbhoo, R. Zamoyska, A. G. Fisher and M. Merkenschlager. "Sensory Adaptation in Naive Peripheral Cd4 T Cells." *J Exp Med* 194, no. 9 (2001): 1253-61.

Smith, K., B. Seddon, M. A. Purbhoo, R. Zamoyska, A. G. Fisher and M. Merkenschlager. "Sensory Adaptation in Naive Peripheral Cd4 T Cells." *J Exp Med* 194, no. 9 (2001): 1253-61.

Smith-Garvin, J. E., G. A. Koretzky and M. S. Jordan. "T Cell Activation." *Annu Rev Immunol* 27, (2009): 591-619.

Snapper, C. M. and F. D. Finkelman. (1999). “Immunoglobulin class switching”. Fundamental Immunology. W. E. Paul, ed. Lippincott-Raven, Philadelphia, p. 831.

Soudais, Claire, Jean-Pierre de Villartay, Francoise Le Deist, Alain Fischer and Barbara Lisowska-Grospierre. "Independent Mutations of the Human Cd3-[Epsi] Gene Resulting in a T Cell Receptor/Cd3 Complex Immunodeficiency." *Nat Genet* 3, no. 1 (1993): 77-81.

Stanislawski, T., R. H. Voss, C. Lotz, E. Sadovnikova, R. A. Willemsen, J. Kuball, T. Ruppert, R. L. Bolhuis, C. J. Melief, C. Huber, H. J. Stauss and M. Theobald. "Circumventing Tolerance to a Human Mdm2-Derived Tumor Antigen by Tcr Gene Transfer." *Nat Immunol* 2, no. 10 (2001): 962-70.

Stefanova, I., J. R. Dorfman and R. N. Germain. "Self-Recognition Promotes the Foreign Antigen Sensitivity of Naive T Lymphocytes." *Nature* 420, no. 6914 (2002): 429-34.

Stefanova, I., M. W. Saville, C. Peters, F. R. Cleghorn, D. Schwartz, D. J. Venzon, K. J. Weinhold, N. Jack, C. Bartholomew, W. A. Blattner, R. Yarchoan, J. B. Bolen and I. D. Horak. "Hiv Infection--Induced Posttranslational Modification of T Cell Signaling Molecules Associated with Disease Progression." *J Clin Invest* 98, no. 6 (1996): 1290-7.

Stinchcombe, J. C., G. Bossi, S. Booth and G. M. Griffiths. "The Immunological Synapse of Ctl Contains a Secretory Domain and Membrane Bridges." *Immunity* 15, no. 5 (2001): 751-61.

Strong, J., Q. Wang and N. Killeen. "Impaired Survival of T Helper Cells in the Absence of Cd4." *Proc Natl Acad Sci U S A* 98, no. 5 (2001): 2566-71.

Surh, C. D. and J. Sprent. "Homeostasis of Naive and Memory T Cells." *Immunity* 29, no. 6 (2008): 848-62.

Sussman, Jeffrey J., Juan S. Bonifacino, Jennifer Lippincott-Schwartz, Allan M. Weissman, Takashi Saito, Richard D. Klausner and Jonathan D. Ashwell. "Failure to Synthesize the T Cell Cd3-Z Chain: Structure and Function of a Partial T Cell

Receptor Complex." *Cell* 52, no. 1 (1988): 85-95.

Sutton, V. R., J. E. Davis, M. Cancilla, R. W. Johnstone, A. A. Ruefli, K. Sedelies, K. A. Browne and J. A. Trapani. "Initiation of Apoptosis by Granzyme B Requires Direct Cleavage of Bid, but Not Direct Granzyme B-Mediated Caspase Activation." *J Exp Med* 192, no. 10 (2000): 1403-14.

Szymczak, A. L., C. J. Workman, Y. Wang, K. M. Vignali, S. Dilioglou, E. F. Vanin and D. A. Vignali. "Correction of Multi-Gene Deficiency in Vivo Using a Single 'Self-Cleaving' 2a Peptide-Based Retroviral Vector." *Nat Biotechnol* 22, no. 5 (2004): 589-94.

Takada, Kensuke and Stephen C. Jameson. "Naive T Cell Homeostasis: From Awareness of Space to a Sense of Place." *Nat Rev Immunol* 9, no. 12 (2009a): 823-832.

Takada, K. and S. C. Jameson. "Self-Class I Mhc Molecules Support Survival of Naive Cd8 T Cells, but Depress Their Functional Sensitivity through Regulation of Cd8 Expression Levels." *J Exp Med* 206, no. 10 (2009b): 2253-69.

Tammana, S., X. Huang, M. Wong, M. C. Milone, L. Ma, B. L. Levine, C. H. June, J. E. Wagner, B. R. Blazar and X. Zhou. "4-1bb and Cd28 Signaling Plays a Synergistic Role in Redirecting Umbilical Cord Blood T Cells against B-Cell Malignancies." *Hum Gene Ther* 21, no. 1 (2010): 75-86.

Tan, J. T., E. Dudl, E. LeRoy, R. Murray, J. Sprent, K. I. Weinberg and C. D. Surh. "Il-7 Is Critical for Homeostatic Proliferation and Survival of Naive T Cells." *Proc Natl Acad Sci U S A* 98, no. 15 (2001): 8732-7.

Tanchot, Corinne, Armelle Le Campion, Bruno Martin, Sandrine Léaument, Nicole Dautigny and Bruno Lucas. "Conversion of Naive T Cells to a Memory-Like Phenotype in Lymphopenic Hosts Is Not Related to a Homeostatic Mechanism That Fills the Peripheral Naive T Cell Pool." *The Journal of Immunology* 168, no. 10 (2002): 5042-5046.

Tanchot, C., F. A. Lemonnier, B. Perarnau, A. A. Freitas and B. Rocha. "Differential Requirements for Survival and Proliferation of Cd8 Naive or Memory T Cells." *Science* 276, no. 5321 (1997): 2057-62.

Tarakhovsky, A., S. B. Kanner, J. Hombach, J. A. Ledbetter, W. Muller, N. Killeen and K. Rajewsky. "A Role for Cd5 in Tcr-Mediated Signal Transduction and Thymocyte Selection." *Science* 269, no. 5223 (1995): 535-7.

Terabe, M. and J. A. Berzofsky. "Immunoregulatory T Cells in Tumor Immunity." *Curr Opin Immunol* 16, no. 2 (2004): 157-62.

Thomas, S., S. A. Xue, C. R. Bangham, B. K. Jakobsen, E. C. Morris and H. J. Stauss. "Human T Cells Expressing Affinity-Matured Tcr Display Accelerated Responses but Fail to Recognize Low Density of Mhc-Peptide Antigen." *Blood* 118, no. 2 (2011): 319-29.

Tokgoz, Huseyin, Umran Caliskan, Sevgi Keles, İsmail Reisli, Isabel Sánchez Guiu and Neil V. Morgan. "Variable Presentation of Primary Immune Deficiency: Two Cases with Cd3 Gamma Deficiency Presenting with Only Autoimmunity." *Pediatric Allergy and Immunology* 24, no. 3 (2013): 257-262.

Trimble, L. A. and J. Lieberman. "Circulating Cd8 T Lymphocytes in Human Immunodeficiency Virus-Infected Individuals Have Impaired Function and Downmodulate Cd3 Zeta, the Signaling Chain of the T-Cell Receptor Complex." *Blood* 91, no. 2 (1998): 585-94.

Ungefroren, H., M. Voss, W. V. Bernstorff, A. Schmid, B. Kremer and H. Kalthoff. "Immunological Escape Mechanisms in Pancreatic Carcinoma." *Ann N Y Acad Sci* 880, (1999): 243-51.

Valitutti, Salvatore, Sabina Muller, Marina Cella, Elisabetta Padovan and Antonio Lanzavecchia. "Serial Triggering of Many T-Cell Receptors by a Few Peptide–Mhc Complexes." *Nature* 375, no. 6527 (1995): 148-151.

Valitutti, S., S. Muller, M. Salio and A. Lanzavecchia. "Degradation of T Cell Receptor (Tcr)-Cd3-Zeta Complexes after Antigenic Stimulation." *J Exp Med* 185, no. 10 (1997): 1859-64.

van den Broek, M. E., D. Kagi, F. Ossendorp, R. Toes, S. Vamvakas, W. K. Lutz, C. J. Melief, R. M. Zinkernagel and H. Hengartner. "Decreased Tumor Surveillance in Perforin-Deficient Mice." *J Exp Med* 184, no. 5 (1996): 1781-90.

van der Bruggen, P., C. Traversari, P. Chomez, C. Lurquin, E. De Plaen, B. Van den Eynde, A. Knuth and T. Boon. "A Gene Encoding an Antigen Recognized by Cytolytic T Lymphocytes on a Human Melanoma." *Science* 254, no. 5038 (1991): 1643-7.

van der Merwe, P. A. and O. Dushek. "Mechanisms for T Cell Receptor Triggering." *Nat Rev Immunol* 11, no. 1 (2011): 47-55.

van Oers, N. S., N. Killeen and A. Weiss. "Zap-70 Is Constitutively Associated with Tyrosine-Phosphorylated Tcr Zeta in Murine Thymocytes and Lymph Node T Cells." *Immunity* 1, no. 8 (1994): 675-85.

Vardhana, Santosha, Kaushik Choudhuri, Rajat Varma and Michael L. Dustin. "Essential Role of Ubiquitin and Tsg101 Protein in Formation and Function of the Central Supramolecular Activation Cluster." *Immunity* 32, no. 4 (2010): 531-540.

Varma, Rajat, Gabriele Campi, Tadashi Yokosuka, Takashi Saito and Michael L. Dustin. "T Cell Receptor-Proximal Signals Are Sustained in Peripheral Microclusters and Terminated in the Central Supramolecular Activation Cluster." *Immunity* 25, no. 1 (2006): 117-127.

Veldhoen, M., C. Uyttenhove, J. van Snick, H. Helmby, A. Westendorf, J. Buer, B. Martin, C. Wilhelm and B. Stockinger. "Transforming Growth Factor-Beta 'Reprograms' the Differentiation of T Helper 2 Cells and Promotes an Interleukin 9-Producing Subset." *Nat Immunol* 9, no. 12 (2008): 1341-6.

Verdegaal, E. M., N. F. de Miranda, M. Visser, T. Harryvan, M. M. van Buuren, R. S. Andersen, S. R. Hadrup, C. E. van der Minne, R. Schotte, H. Spits, J. B. Haanen, E. H. Kapiteijn, T. N. Schumacher and S. H. van der Burg. "Neoantigen Landscape Dynamics During Human Melanoma-T Cell Interactions." *Nature* 536, no. 7614 (2016): 91-5.

Verdegaal, E. M., N. F. de Miranda, M. Visser, T. Harryvan, M. M. van Buuren, R. S. Andersen, S. R. Hadrup, C. E. van der Minne, R. Schotte, H. Spits, J. B. Haanen, E. H. Kapiteijn, T. N. Schumacher and S. H. van der Burg. "Neoantigen Landscape Dynamics During Human Melanoma-T Cell Interactions." *Nature* 536, no. 7614 (2016): 91-5.

Viola, A. and A. Lanzavecchia. "T Cell Activation Determined by T Cell Receptor Number

and Tunable Thresholds." *Science* 273, no. 5271 (1996): 104-6.

Wan, Y. Y. and R. A. Flavell. "How Diverse--Cd4 Effector T Cells and Their Functions." *J Mol Cell Biol* 1, no. 1 (2009): 20-36.

Wang, Baoping, Ninghai Wang, Mariolina Salio, Arlene Sharpe, Deborah Allen, Jian She and Cox Terhorst. "Essential and Partially Overlapping Role of Cd3γ and Cd3δ for Development of Aβ and Γδ T Lymphocytes." *The Journal of Experimental Medicine* 188, no. 7 (1998): 1375-1380.

Wang, N., B. Wang, M. Salio, D. Allen, J. She and C. Terhorst. "Expression of a Cd3 Epsilon Transgene in Cd3 Epsilon(Null) Mice Does Not Restore Cd3 Gamma and Delta Expression but Efficiently Rescues T Cell Development from a Subpopulation of Prothymocytes." *International Immunology* 10, no. 12 (1998): 1777-1788.

Waring, P. and A. Mullbacher. "Cell Death Induced by the Fas/Fas Ligand Pathway and Its Role in Pathology." *Immunol Cell Biol* 77, no. 4 (1999): 312-7.

Weninger, W., M. A. Crowley, N. Manjunath and U. H. von Andrian. "Migratory Properties of Naive, Effector, and Memory Cd8(+) T Cells." *J Exp Med* 194, no. 7 (2001): 953-66.

Whiteside, T. L. "Down-Regulation of Zeta-Chain Expression in T Cells: A Biomarker of Prognosis in Cancer?" *Cancer Immunol Immunother* 53, no. 10 (2004): 865-78.

Whitmire, Jason K., Richard A. Flavell, Iqbal S. Grewal, Christian P. Larsen, Thomas C. Pearson and Rafi Ahmed. "Cd40-Cd40 Ligand Costimulation Is Required for Generating Antiviral Cd4 T Cell Responses but Is Dispensable for Cd8 T Cell Responses." *The Journal of Immunology* 163, no. 6 (1999): 3194-3201.

Willard-Gallo, K. E., C. Delmelle-Wibaut, I. Segura-Zapata, M. Janssens, L. Willems and R. Kettmann. "Modulation of Cd3-Gamma Gene Expression after Hiv Type 1 Infection of the We17/10 T Cell Line Is Progressive and Occurs in Concert with Decreased Production of Viral P24 Antigen." *AIDS Res Hum Retroviruses* 12, no. 8 (1996): 715-25.

Willard-Gallo, K. E., M. Furtado, A. Burny and S. M. Wolinsky. "Down-Modulation of Tcr/Cd3 Surface Complexes after Hiv-1 Infection Is Associated with Differential

Expression of the Viral Regulatory Genes." *Eur J Immunol* 31, no. 4 (2001): 969-79.

Williams, M. A. and M. J. Bevan. "Effector and Memory Ctl Differentiation." *Annu Rev Immunol* 25, (2007): 171-92.

Witherden, D., N. van Oers, C. Waltzinger, A. Weiss, C. Benoist and D. Mathis. "Tetracycline-Controllable Selection of Cd4(+) T Cells: Half-Life and Survival Signals in the Absence of Major Histocompatibility Complex Class Ii Molecules." *J Exp Med* 191, no. 2 (2000): 355-64.

Wofford, J. A., H. L. Wieman, S. R. Jacobs, Y. Zhao and J. C. Rathmell. "Il-7 Promotes Glut1 Trafficking and Glucose Uptake Via Stat5-Mediated Activation of Akt to Support T-Cell Survival." *Blood* 111, no. 4 (2008): 2101-11.

Wojciechowski, S., P. Tripathi, T. Bourdeau, L. Acero, H. L. Grimes, J. D. Katz, F. D. Finkelman and D. A. Hildeman. "Bim/Bcl-2 Balance Is Critical for Maintaining Naive and Memory T Cell Homeostasis." *J Exp Med* 204, no. 7 (2007): 1665-75.

Wong, P., G. M. Barton, K. A. Forbush and A. Y. Rudensky. "Dynamic Tuning of T Cell Reactivity by Self-Peptide-Major Histocompatibility Complex Ligands." *J Exp Med* 193, no. 10 (2001): 1179-87.

Wooldridge, Linda, Hugo A. van den Berg, Meir Glick, Emma Gostick, Bruno Laugel, Sarah L. Hutchinson, Anita Milicic, Jason M. Brenchley, Daniel C. Douek, David A. Price and Andrew K. Sewell. "Interaction between the Cd8 Coreceptor and Major Histocompatibility Complex Class I Stabilizes T Cell Receptor-Antigen Complexes at the Cell Surface." *Journal of Biological Chemistry* 280, no. 30 (2005): 27491-27501.

Xie, Ying, Akgül Akpinarli, Charles Maris, Edward L. Hipkiss, Malcolm Lane, Eun-Kyung M. Kwon, Pawel Muranski, Nicholas P. Restifo and Paul Andrew Antony. "Naive Tumor-Specific Cd4⁺ T Cells Differentiated in Vivo Eradicate Established Melanoma." *The Journal of Experimental Medicine* 207, no. 3 (2010): 651-667.

Xing, Y. and K. A. Hogquist. "T-Cell Tolerance: Central and Peripheral." *Cold Spring Harb Perspect Biol* 4, no. 6 (2012).

Xu, C., E. Gagnon, M. E. Call, J. R. Schnell, C. D. Schwieters, C. V. Carman, J. J. Chou

and K. W. Wucherpfennig. "Regulation of T Cell Receptor Activation by Dynamic Membrane Binding of the Cd3epsilon Cytoplasmic Tyrosine-Based Motif." *Cell* 135, no. 4 (2008): 702-13.

Xue, Shao-An, Liquan Gao, Daniel Hart, Roopinder Gillmore, Waseem Qasim, Adrian Thrasher, Jane Apperley, Boris Engels, Wolfgang Uckert, Emma Morris and Hans Stauss. "Elimination of Human Leukemia Cells in <Em>Nod/Scid</Em> Mice by <Em>Wt1-Tcr</Em> Gene–Transduced Human T Cells." *Blood* 106, no. 9 (2005): 3062-3067.

Yewdell, J. W. and S. M. Haeryfar. "Understanding Presentation of Viral Antigens to Cd8+ T Cells in Vivo: The Key to Rational Vaccine Design." *Annu Rev Immunol* 23, (2005): 651-82.

York, Ian A., Shih-Chung Chang, Tomo Saric, Jennifer A. Keys, Janice M. Favreau, Alfred L. Goldberg and Kenneth L. Rock. "The Er Aminopeptidase Erap1 Enhances or Limits Antigen Presentation by Trimming Epitopes to 8-9 Residues." *Nat Immunol* 3, no. 12 (2002): 1177-1184.

Youngblood, B., J. S. Hale and R. Ahmed. "T-Cell Memory Differentiation: Insights from Transcriptional Signatures and Epigenetics." *Immunology* 139, no. 3 (2013): 277-84.

Zambrano-Zaragoza, José Francisco, Enrique Jhonatan Romo-Martínez, Ma de Jesús Durán-Avelar, Noemí García-Magallanes and Norberto Vibanco-Pérez. "Th17 Cells in Autoimmune and Infectious Diseases." *International Journal of Inflammation* 2014, (2014): 651503.

Zea, A. H., M. T. Ochoa, P. Ghosh, D. L. Longo, W. G. Alvord, L. Valderrama, R. Falabella, L. K. Harvey, N. Saravia, L. H. Moreno and A. C. Ochoa. "Changes in Expression of Signal Transduction Proteins in T Lymphocytes of Patients with Leprosy." *Infect Immun* 66, no. 2 (1998): 499-504.

Zhang, D. H., L. Cohn, P. Ray, K. Bottomly and A. Ray. "Transcription Factor Gata-3 Is Differentially Expressed in Murine Th1 and Th2 Cells and Controls Th2-Specific Expression of the Interleukin-5 Gene." *J Biol Chem* 272, no. 34 (1997): 21597-603.

Zhong, X. S., M. Matsushita, J. Plotkin, I. Riviere and M. Sadelain. "Chimeric Antigen Receptors Combining 4-1bb and Cd28 Signaling Domains Augment

Pi3kinase/Akt/Bcl-Xl Activation and Cd8+ T Cell-Mediated Tumor Eradication." *Mol Ther* 18, no. 2 (2010): 413-20.

Zhu, M. L., A. Nagavalli and M. A. Su. "Aire Deficiency Promotes Trp-1-Specific Immune Rejection of Melanoma." *Cancer Res* 73, no. 7 (2013): 2104-16.

8. Appendix

pMP71 CD3-IRES-GFP retroviral construct

TCAAGGTTAG GAACAGAGAG ACAGGAGAAT ATGGGCCAAA CAGGATATCT
GTGGTAAGCA GTTCCTGCCC CGGCTCAGGG CCAAGAACAG TTGGAACAGC
AGAATATGGG CCAAACAGGA TATCTGTGGT AAGCAGTTCC TGCCCCGGCT
CAGGGCCAAG AACAGATGGT CCCCAGATGC GGTCCCGCCC TCAGCAGTTT
CTAGAGAACC ATCAGATGTT TCCAGGGTGC CCCAAGGACC TGAAATGACC
CTGTGCCTTA TTTGAACTAA CCAATCAGTT CGCTTCTCGC TTCTGTTCGC
GCGCTTCTGC TCCCCGAGCT CAATAAAAGA GCCCACAACC CCTCACTCGG
CGCGCCAGTC CTCCGATTGA CTGCGTCGCC CGGGTACCCG TATTCCCAAT
AAAGCCTCTT GCTGTTTGCA TCCGAATCGT GGACTCGCTG ATCCTTGGGA
GGGTCTCCTC AGATTGATTG ACTGCCCACC TCGGGGGTCT TTCATTTGGA
GGTTCCACCG AGATTTGGAG ACCCCTGCCC AGGGACCACC GACCCCCCCG
CCGGGAGGTA AGCTGGCCAG CGGTCGTTTC GTGTCTGTCT CTGTCTTTGG
GCGTGTTTGT GCCGGCATCT AATGTTTGCG CCTGCGTCTG TACTAGTTGG
CTAACTAGAT CTGTATCTGG CGGTCCCGCG GAAGAACTGA CGAGTTCGTA
TTCCCGGCCG CAGCCCCTGG GAGACGTCCC AGCGGCCTCG GGGGCCCGTT
TTGTGGCCCA TTCTGTATCA GTTAACCTAC CCGAGTCGGA CTTTTTGGAG
CTCCGCCACT GTCCGAGGGG TACGTGGCTT TGTTGGGGGA CGAGAGACAG
AGACACTTCC CGCCCCCGTC TGAATTTTTG CTTTCGGTTT TACGCCGAAA
CCGCGCCGCG CGTCTTGTCT GCTGCAGCAT CGTTCTGTGT TGTCTCTGTC
TGACTGTGTT TCTGTATTTG TCTGAAAATT AGCTCGACAA AGTTAAGTAA
TAGTCCCTCT CTCCAAGCTC ACTTACAGGC GGCCGCATGA AGTGGAAAGT
GTCTGTTCTC GCCTGCATCC TCCACGTGCG GTTCCCAGGA GCAGAGGCAC
AGAGCTTTGG TCTGCTGGAT CCCAAACTCT GCTACTTGCT AGATGGAATC
CTCTTCATCT ACGGAGTCAT CATCACAGCC CTGTACCTGA GAGCAAAATT
CAGCAGGAGT GCAGAGACTG CTGCCAACCT GCAGGACCCC AACCAGCTCT
ACAATGAGCT CAATCTAGGG CGAAGAGAGG AATATGACGT CTTGGAGAAG
AAGCGGGCTC GGGATCCAGA GATGGGAGGC AAACAGCAGA GGAGGAGGAA
CCCCCAGGAA GGCGTATACA ATGCACTGCA GAAAGACAAG ATGGCAGAAG
CCTACAGTGA GATCGGCACA AAAGGCGAGA GGCGGAGAGG CAAGGGGCAC
GATGGCCTTT ACCAGGGTCT CAGCACTGCC ACCAAGGACA CCTGTGATGC
CCTGCATATG CAGACCCTGG CCCCTCGCGT GAAGCAGACT TTGAATTTTG
ACCTTCTCAA GTTGGCGGGA GACGTGGAGT CCAACCCAGG GCCCATGCGG
TGGAACACTT TCTGGGGCAT CCTGTGCCTC AGCCTCCTAG CTGTTGGCAC
TTGCCAGGAC GATGCCGAGA ACATTGAATA CAAAGTCTCC ATCTCAGGAA
CCAGTGTAGA GTTGACGTGC CCTCTAGACA GTGACGAGAA CTTAAAATGG
GAAAAAAATG GCCAAGAGCT GCCTCAGAAG CATGATAAGC ACCTGGTGCT
CCAGGATTTC TCGGAAGTCG AGGACAGTGG CTACTACGTC TGCTACACAC
CAGCCTCAAA TAAAAACACG TACTTGTACC TGAAAGCTCG AGTGTGTGAG
TACTGTGTGG AGGTGGACCT GACAGCAGTA GCCATAATCA TCATTGTTGA
CATCTGTATC ACTCTGGGCT TGCTGATGGT CATTTATTAC TGGAGCAAGA
ATAGGAAGGC CAAGGCCAAG CCTGTGACCC GAGGAACCGG TGCTGGTAGC
AGGCCCAGAG GGCAAAACAA GGAGCGGCCA CCACCTGTTC CCAACCCAGA
CTATGAGCCC ATCCGCAAAG GCCAGCGGGA CCTGTATTCT GGCCTGAATC
AGAGAGCAGT CGAGGGCAGA GGAAGTCTGC TAACATGCGG TGACGTCGAG
GAGAATCCTG GCCCAATGGA ACACAGCGGG ATTCTGGCTA GTCTGATACT
GATTGCTGTT CTCCCCCAAG GGAGCCCCTT CAAGGTACAA GTGACCGAAT
ATGAGGACAA AGTATTTGTG ACCTGCAATA CCAGCGTCAT GCATCTAGAT

GGAACGGTGG AAGGATGGTT TGCAAAGAAT AAAACACTCA ACTTGGGCAA
AGGCGTTCTG GACCCACGAG GGATATATCT GTGTAATGGG ACAGAGCAGC
TGGCAAAGGT GGTGTCTTCT GTGCAAGTCC ATTACCGAAT GTGCCAGAAC
TGTGTGGAGC TAGACTCGGG CACCATGGCT GGTGTCATCT TCATTGACCT
CATCGCAACT CTGCTCCTGG CTTTGGGCGT CTACTGCTTT GCAGGACATG
AGACCGGAAG GCCTTCTGGG GCTGCTGAGG TTCAAGCACT GCTGAAGAAT
GAGCAGCTGT ATCAGCCTCT TCGAGATCGT GAAGATACCC AGTACAGCCG
TCTTGGAGGG AACTGGCCCC GGAACAAGAA ATCTCAATGT ACTAACTACG
CTTTGTTGAA ACTCGCTGGC GATGTTGAAA GTAACCCCGG TCCTATGGAG
CAGAGGAAGG GTCTGGCTGG CCTCTTCCTG GTGATCTCTC TTCTTCAAGG
CACTGTAGCC CAGACAAATA AAGCAAAGAA TTTGGTACAA GTGGATGGCA
GCCGAGGAGA CGGTTCTGTA CTTCTGACTT GTGGCTTGAC TGACAAGACT
ATCAAGTGGC TTAAAGACGG GAGCATAATA AGTCCTCTAA ATGCAACTAA
AAACACATGG AATCTGGGCA ACAATGCCAA AGACCCTCGA GGCACGTATC
AGTGTCAAGG AGCAAAGGAG ACATCAAACC CCCTGCAAGT GTATTACAGA
ATGTGTGAAA ACTGCATTGA GCTAAACATA GGCACCATAT CCGGCTTTAT
CTTCGCTGAG GTCATCAGCA TCTTCTTCCT TGCTCTTGGT GTATATCTCA
TTGCGGGACA GGATGGAGTT CGCCAGTCAA GAGCTTCAGA CAAGCAGACT
CTGTTGCAAA ATGAACAGCT GTACCAGCCC CTCAAGGACC GGGAATATGA
CCAGTACAGC CATCTCCAAG GAAACCAACT GAGGAAGAAG GTCGACCTCG
AGATCCGCCC CTCTCCCTCC CCCCCCCCTA ACGTTACTGG CCGAAGCCGC
TTGGAATAAG GCCGGTGTGC GTTTGTCTAT ATGTTATTTT CCACCATATT
GCCGTCTTTT GGCAATGTGA GGGCCCGGAA ACCTGGCCCT GTCTTCTTGA
CGAGCATTCC TAGGGGTCTT TCCCCTCTCG CCAAAGGAAT GCAAGGTCTG
TTGAATGTCG TGAAGGAAGC AGTTCCTCTG GAAGCTTCTT GAAGACAAAC
AACGTCTGTA GCGACCCTTT GCAGGCAGCG GAACCCCCCA CCTGGCGACA
GGTGCCTCTG CGGCCAAAAG CCACGTGTAT AAGATACACC TGCAAAGGCG
GCACAACCCC AGTGCCACGT TGTGAGTTGG ATAGTTGTGG AAAGAGTCAA
ATGGCTCTCC TCAAGCGTAT TCAACAAGGG GCTGAAGGAT GCCCAGAAGG
TACCCCATTG TATGGGATCT GATCTGGGGC CTCGGTGCAC ATGCTTTACA
TGTGTTTAGT CGAGGTTAAA AAAACGTCTA GGCCCCCCGA ACCACGGGGA
CGTGGTTTTC CTTTGAAAAA CACGATGATA ATATGGCCAC AACCATGGTG
AGCAAGGGCG AGGAGCTGTT CACCGGGGTG GTGCCCATCC TGGTCGAGCT
GGACGGCGAC GTAAACGGCC ACAAGTTCAG CGTGTCCGGC GAGGGCGAGG
GCGATGCCAC CTACGGCAAG CTGACCCTGA AGTTCATCTG CACCACCGGC
AAGCTGCCCG TGCCCTGGCC CACCCTCGTG ACCACCCTGA CCTACGGCGT
GCAGTGCTTC AGCCGCTACC CCGACCACAT GAAGCAGCAC GACTTCTTCA
AGTCCGCCAT GCCCGAAGGC TACGTCCAGG AGCGCACCAT CTTCTTCAAG
GACGACGGCA ACTACAAGAC CCGCGCCGAG GTGAAGTTCG AGGGCGACAC
CCTGGTGAAC CGCATCGAGC TGAAGGGCAT CGACTTCAAG GAGGACGGCA
ACATCCTGGG GCACAAGCTG GAGTACAACT ACAACAGCCA CAACGTCTAT
ATCATGGCCG ACAAGCAGAA GAACGGCATC AAGGTGAACT TCAAGATCCG
CCACAACATC GAGGACGGCA GCGTGCAGCT CGCCGACCAC TACCAGCAGA
ACACCCCCAT CGGCGACGGC CCCGTGCTGC TGCCCGACAA CCACTACCTG
AGCACCCAGT CCGCCCTGAG CAAAGACCCC AACGAGAAGC GCGATCACAT
GGTCCTGCTG GAGTTCGTGA CCGCCGCCGG GATCACTCTC GGCATGGACG
AGCTGTACAG AATTCGAGCA TCTTACCGCC ATTTATTCCC ATATTTGTTC

TGTTTTTCTT GATTTGGGTA TACATTTAAA TGTTAATAAA ACAAAATGGT
GGGGCAATCA TTTACATTTT ATGGGATATG TAATTACTAG TTCAGGTGTA
TTGCCACAAG ACAAACATGT TAAGAAACTT TCCCGTTATT TACGCTCTGT
TCCTGTTAAT CAACCTCTGG ATTACAAAAT TTGTGAAAGA TTGACTGATA
TTCTTAACTA TGTTGCTCCT TTTACGCTGT GTGGATATGC TGCTTTAATG
CCTCTGTATC ATGCTATTGC TTCCCGTACG GCTTTCGTTT TCTCCTCCTT
GTATAAATCC TGGTTGCTGT CTCTTTATGA GGAGTTGTGG CCCGTTGTCC
GTCAACGTGG CGTGGTGTGC TCTGTGTTTG CTGACGCAAC CCCCACTGGC
TGGGGCATTG CCACCACCTG TCAACTCCTT TCTGGGACTT TCGCTTTCCC
CCTCCCGATC GCCACGGCAG AACTCATCGC CGCCTGCCTT GCCCGCTGCT
GGACAGGGGC TAGGTTGCTG GGCACTGATA ATTCCGTGGT GTTGTCGGGG
AAGCTGACGT CCTTTCCATG GCTGCTCGCC TGTGTTGCCA ACTGGATCCT
GCGCGGGACG TCCTTCTGCT ACGTCCCTTC GGCTCTCAAT CCAGCGGACC
TCCCTTCCCG AGGCCTTCTG CCGGTTCTGC GGCCTCTCCC GCGTCTTCGC
TTTCGGCCTC CGACGAGTCG GATCTCCCTT TGGGCCGCCT CCCCGCCTGT
TTCGCCTCGG CGTCCGGTCC GTGTTGCTTG GTCGTCACCT GTGCAGAATT
GCGAACCATG GATTCCACCG TGAACTTTGT CTCCTGGCAT GCAAATCGTC
AACTTGGCAT GCCAAGAATT CGGATCCAAG CTTAGGCCTG CTCGCTTTCT
TGCTGTCCCA TTTCTATTAA AGGTTCCTTT GTTCCCTAAG TCCAACTACT
AAACTGGGGG ATATTATGAA GGGCCTTGAG CATCTGGATT CTGCCTAGCG
CTAAGCTTCC TAACACGAGC CATAGATAGA ATAAAAGATT TTATTTAGTC
TCCAGAAAAA GGGGGGAATG AAAGACCCCA CCTGTAGGTT TGGCAAGCTA
GCTTAAGTAA GCCATTTTGC AAGGCATGGA AAAATACATA ACTGAGAATA
GAGAAGTTCA GATCAAGGTT AGGAACAGAG AGACAGGAGA ATATGGGCCA
AACAGGATAT CTGTGGTAAG CAGTTCCTGC CCCGGCTCAG GGCCAAGAAC
AGTTGGAACA GCAGAATATG GGCCAAACAG GATATCTGTG GTAAGCAGTT
CCTGCCCCGG CTCAGGGCCA AGAACAGATG GTCCCCAGAT GCGGTCCCGC
CCTCAGCAGT TTCTAGAGAA CCATCAGATG TTTCCAGGGT GCCCCAAGGA
CCTGAAATGA CCCTGTGCCT TATTTGAACT AACCAATCAG TTCGCTTCTC
GCTTCTGTTC GCGCGCTTCT GCTCCCCGAG CTCAATAAAA GAGCCCACAA
CCCCTCACTC GGCGCGCCAG TCCTCCGATA GACTGCGTCG CCCGGGGTAC
CCGTATTCCC AATAAAGCCT CTTGCTGTTT GCATCCGAAT CGTGGACTCG
CTGATCCTTG GGAGGGTCTC CTCAGATTGA TTGACTGCCC ACCTCGGGGG
TCTTTCATTC TCGAGAGCTT TGGCGTAATC ATGGTCATAG CTGTTTCCTG
TGTGAAATTG TTATCCGCTC ACAATTCCAC ACAACATACG AGCCGGAAGC
ATAAAGTGTA AAGCCTGGGG TGCCTAATGA GTGAGCTAAC TCACATTAAT
TGCGTTGCGC TCACTGCCCG CTTTCCAGTC GGGAAACCTG TCGTGCCAGC
TGCATTAATG AATCGGCCAA CGCGCGGGGA GAGGCGGTTT GCGTATTGGG
CGCTCTTCCG CTTCCTCGCT CACTGACTCG CTGCGCTCGG TCGTTCGGCT
GCGGCGAGCG GTATCAGCTC ACTCAAAGGC GGTAATACGG TTATCCACAG
AATCAGGGGA TAACGCAGGA AAGAACATGT GAGCAAAAGG CCAGCAAAAG
GCCAGGAACC GTAAAAAGGC CGCGTTGCTG GCGTTTTTCC ATAGGCTCCG
CCCCCCTGAC GAGCATCACA AAAATCGACG CTCAAGTCAG AGGTGGCGAA
ACCCGACAGG ACTATAAAGA TACCAGGCGT TTCCCCCTGG AAGCTCCCTC
GTGCGCTCTC CTGTTCCGAC CCTGCCGCTT ACCGGATACC TGTCCGCCTT
TCTCCCTTCG GGAAGCGTGG CGCTTTCTCA ATGCTCACGC TGTAGGTATC
TCAGTTCGGT GTAGGTCGTT CGCTCCAAGC TGGGCTGTGT GCACGAACCC

CCCGTTCAGC CCGACCGCTG CGCCTTATCC GGTAACTATC GTCTTGAGTC
CAACCCGGTA AGACACGACT TATCGCCACT GGCAGCAGCC ACTGGTAACA
GGATTAGCAG AGCGAGGTAT GTAGGCGGTG CTACAGAGTT CTTGAAGTGG
TGGCCTAACT ACGGCTACAC TAGAAGGACA GTATTTGGTA TCTGCGCTCT
GCTGAAGCCA GTTACCTTCG GAAAAAGAGT TGGTAGCTCT TGATCCGGCA
AACAAACCAC CGCTGGTAGC GGTGGTTTTT TTGTTTGCAA GCAGCAGATT
ACGCGCAGAA AAAAAGGATC TCAAGAAGAT CCTTTGATCT TTTCTACGGG
GTCTGACGCT CAGTGGAACG AAAACTCACG TTAAGGGATT TTGGTCATGA
GATTATCAAA AAGGATCTTC ACCTAGATCC TTTTAAATTA AAAATGAAGT
TTTAAATCAA TCTAAAGTAT ATATGAGTAA ACTTGGTCTG ACAGTTACCA
ATGCTTAATC AGTGAGGCAC CTATCTCAGC GATCTGTCTA TTTCGTTCAT
CCATAGTTGC CTGACTCCCC GTCGTGTAGA TAACTACGAT ACGGGAGGGC
TTACCATCTG GCCCCAGTGC TGCAATGATA CCGCGAGACC CACGCTCACC
GGCTCCAGAT TTATCAGCAA TAAACCAGCC AGCCGGAAGG GCCGAGCGCA
GAAGTGGTCC TGCAACTTTA TCCGCCTCCA TCCAGTCTAT TAATTGTTGC
CGGGAAGCTA GAGTAAGTAG TTCGCCAGTT AATAGTTTGC GCAACGTTGT
TGCCATTGCT GCTGGCATCG TGGTGTCACG CTCGTCGTTT GGTATGGCTT
CATTCAGCTC CGGTTCCCAA CGATCAAGGC GAGTTACATG ATCCCCCATG
TTGTGCAAAA AAGCGGTTAG CTCCTTCGGT CCTCCGATCG TTGTCAGAAG
TAAGTTGGCC GCAGTGTTAT CACTCATGGT TATGGCAGCA CTGCATAATT
CTCTTACTGT CATGCCATCC GTAAGATGCT TTTCTGTGAC TGGTGAGTAC
TCAACCAAGT CATTCTGAGA ATAGTGTATG CGGCGACCGA GTTGCTCTTG
CCCGGCGTCA ATACGGGATA ATACCGCGCC ACATAGCAGA ACTTTAAAAG
TGCTCATCAT TGGAAAACGT TCTTCGGGGC GAAAACTCTC AAGGATCTTA
CCGCTGTTGA GATCCAGTTC GATGTAACCC ACTCGTGCAC CCAACTGATC
TTCAGCATCT TTTACTTTCA CCAGCGTTTC TGGGTGAGCA AAAACAGGAA
GGCAAAATGC CGCAAAAAAG GGAATAAGGG CGACACGGAA ATGTTGAATA
CTCATACTCT TCCTTTTTCA ATATTATTGA AGCATTTATC AGGGTTATTG
TCTCATGAGC GGATACATAT TTGAATGTAT TTAGAAAAAT AAACAAATAG
GGGTTCCGCG CACATTTCCC CGAAAAGTGC CACCTGACGT CTAAGAAACC
ATTATTATCA TGACATTAAC CTATAAAAAT AGGCGTATCA CGAGGCCCTT
TCGTCTTCAA GCTGCCTCGC GCGTTTCGGT GATGACGGTG AAAACCTCTG
ACACATGCAG CTCCCGGAGA CGGTCACAGC TTGTCTGTAA GCGGATGCCG
GGAGCAGACA AGCCCGTCAG GGCGCGTCAG CGGGTGTTGG CGGGTGTCGG
GGCGCAGCCA TGACCCAGTC ACGTAGCGAT AGTTACTATG CGGCATCAGA
GCAGATTGTA CTGAGAGTGC ACCATATGCG GTGTGAAATA CCGCACAGAT
GCGTAAGGAG AAAATACCGC ATCAGGCGCC ATTCGCCATT CAGGCTGCGC
AACTGTTGGG AAGGGCGATC GGTGCGGGCC TCTTCGCTAT TACGCCAGCT
GGCGAAAGGG GGATGTGCTG CAAGGCGATT AAGTTGGGTA ACGCCAGGGT
TTTCCCAGTC ACGACGTTGT AAAACGACGG CCAGTGAATT AGTACTCTAG
CTTAAGTAAG CCATTTTGCA AGGCATGGAA AAATACATAA CTGAGAATAG
AGAAGTTCAG A

pMP71 invertedCre-IRES-GFP retroviral construct

AGCATCGTTC TGTGTTGTCT CTGTCTGACT GTGTTTCTGT ATTTGTCTGA
AAATTAGCTC GACAAAGTTA GTATAGTCCC TCTCTCCAAG CTCACTTACA
GGCGGCCGCT CGAGATCGCC ATCTTCCAGC AGGCGCACCA TTGCCCCTGT
TTCACTATCC AGGTTACGGA TATAGTTCAT GACAATATTT ACATTGGTCC
AGCCACCAGC TTGCATGATC TCCGGTATTG AAACTCCAGC GCGGGCCATA
TCTCGCGCGG CTCCGACACG GGCACTGTGT CCAGACCAGG CCAGGTATCT
CTGACCAGAG TCATCCTTAG CGCCGTAAAT CAATCGATGA GTTGCTTCAA
AAATCCCTTC CAGGGCGCGA GTTGATAGCT GGCTGGTGGC AGATGGCGCG
GCAACACCAT TTTTTCTGAC CCGGCAAAAC AGGTAGTTAT TCGGATCATC
AGCTACACCA GAGACGGAAA TCCATCGCTC GACCAGTTTA GTTACCCCCA
GGCTAAGTGC CTTCTCTACA CCTGCGGTGC TAACCAGCGT TTTCGTTCTG
CCAATATGGA TTAACATTCT CCCACCGTCA GTACGTGAGA TATCTTTAAC
CCTGATCCTG GCAATTTCGG CTATACGTAA CAGGGTGTTA TAAGCAATCC
CCAGAAATGC CAGATTACGT ATATCCTGGC AGCGATCGCT ATTTTCCATG
AGTGAACGAA CCTGGTCGAA ATCAGTGCGT TCGAACGCTA GAGCCTGTTT
TGCACGTTCA CCGGCATCAA CGTTTTCTTT TCGGATCCGC CGCATAACCA
GTGAAACAGC ATTGCTGTCA CTTGGTCGTG GCAGCCCGGA CCGACGATGA
AGCATGTTTA GCTGGCCCAA ATGTTGCTGG ATAGTTTTTA CTGCCAGACC
GCGCGCCTGA AGATATAGAA GATAATCGCG AACATCTTCA GGTTCTGCGG
GAAACCATTT CCGGTTATTC AACTTGCACC ATGCCGCCCA CGACCGGCAA
ACGGACAGAA GCATTTTCCA GGTATGCTCA GAAAACGCCT GGCGATCCCT
GAACATGTCC ATCAGGTTCT TGCGAACCTC ATCACTCGTT GCATCGACCG
GTAATGCAGG CAAATTTTGG TGTACGGTCA GTAAATTGGC CATGGTGGCG
GCTCAGAATT CTTTGCCAAG TCGACCTCGA GATCCGCCCC TCTCCCTCCC
CCCCCCCTAA CGTTACTGGC CGAAGCCGCT TGGAATAAGG CCGGTGTGCG
TTGTCTATAT GTTATTTTCC ACCATATTGC CGTCTTTTGG CAATGTGAGG
GCCCGGAAAC CTGGCCCTGT CTTCTTGACG AGCATTCCTA GGGGTCTTTC
CCCTCTCGCC AAAGGAATGC AAGGTCTGTT GAATGTCGTG AAGGAAGCAG
TTCCTCTGGA AGCTTCTTGA AGACAAACAA CGTCTGTAGC GACCCTTTGC
AGGCAGCGGA ACCCCCCACC TGGCGACAGG TGCCTCTGCG GCCAAAAGCC
ACGTGTATAA GATACACCTG CAAAGGCGGC ACAACCCCAG TGCCACGTTG
TGAGTTGGAT AGTTGTGGAA AGAGTCAAAT GGCTCTCCTC AAGCGTATTC
AACAAGGGGC TGAAGGATGC CCAGAAGGTA CCCCATTGTA TGGGATCTGA
TCTGGGGCCT CGGTGCACAT GCTTTACATG TGTTTAGTCG AGGTTAAAAA
AACGTCTAGG CCCCCCGAAC CACGGGGACG TGGTTTTCCT TTGAAAAACA
CGATGATAAT ATGGCCACAA CCATGGTGAG CAAGGGCGAG GAGCTGTTCA
CCGGGGTGGT GCCCATCCTG GTCGAGCTGG ACGGCGACGT AAACGGCCAC
AAGTTCAGCG TGTCCGGCGA GGGCGAGGGC GATGCCACCT ACGGCAAGCT
GACCCTGAAG TTCATCTGCA CCACCGGCAA GCTGCCCGTG CCCTGGCCCA
CCCTCGTGAC CACCCTGACC TACGGCGTGC AGTGCTTCAG CCGCTACCCC
GACCACATGA AGCAGCACGA CTTCTTCAAG TCCGCCATGC CCGAAGGCTA
CGTCCAGGAG CGCACCATCT TCTTCAAGGA CGACGGCAAC TACAAGACCC
GCGCCGAGGT GAAGTTCGAG GGCGACACCC TGGTGAACCG CATCGAGCTG
AAGGGCATCG ACTTCAAGGA GGACGGCAAC ATCCTGGGGC ACAAGCTGGA
GTACAACTAC AACAGCCACA ACGTCTATAT CATGGCCGAC AAGCAGAAGA
ACGGCATCAA GGTGAACTTC AAGATCCGCC ACAACATCGA GGACGGCAGC
GTGCAGCTCG CCGACCACTA CCAGCAGAAC ACCCCCATCG GCGACGGCCC
CGTGCTGCTG CCCGACAACC ACTACCTGAG CACCCAGTCC GCCCTGAGCA
AAGACCCCAA CGAGAAGCGC GATCACATGG TCCTGCTGGA GTTCGTGACC
GCCGCCGGGA TCACTCTCGG CATGGACGAG CTGTACAGAA TTCGAGCATC
TTACCGCCAT TTATTCCCAT ATTTGTTCTG TTTTTCTTGA TTTGGGTATA
CATTTAAATG TTAATAAAAC AAAATGGTGG GGCAATCATT TACATTTTAT
GGGATATGTA ATTACTAGTT CAGGTGTATT GCCACAAGAC AAACATGTTA

AGAAACTTTC CCGTTATTTA CGCTCTGTTC CTGTTAATCA ACCTCTGGAT
TACAAAATTT GTGAAAGATT GACTGATATT CTTAACTATG TTGCTCCTTT
TACGCTGTGT GGATATGCTG CTTTAATGCC TCTGTATCAT GCTATTGCTT
CCCGTACGGC TTTCGTTTTC TCCTCCTTGT ATAAATCCTG GTTGCTGTCT
CTTTATGAGG AGTTGTGGCC CGTTGTCCGT CAACGTGGCG TGGTGTGCTC
TGTGTTTGCT GACGCAACCC CCACTGGCTG GGGCATTGCC ACCACCTGTC
AACTCCTTTC TGGGACTTTC GCTTTCCCCC TCCCGATCGC CACGGCAGAA
CTCATCGCCG CCTGCCTTGC CCGCTGCTGG ACAGGGGCTA GGTTGCTGGG
CACTGATAAT TCCGTGGTGT TGTCGGGGAA GCTGACGTCC TTTCCATGGC
TGCTCGCCTG TGTTGCCAAC TGGATCCTGC GCGGGACGTC CTTCTGCTAC
GTCCCTTCGG CTCTCAATCC AGCGGACCTC CCTTCCCGAG GCCTTCTGCC
GGTTCTGCGG CCTCTCCCGC GTCTTCGCTT TCGGCCTCCG ACGAGTCGGA
TCTCCCTTTG GGCCGCCTCC CCGCCTGTTT CGCCTCGGCG TCCGGTCCGT
GTTGCTTGGT CGTCACCTGT GCAGAATTGC GAACCATGGA TTCCACCGTG
AACTTTGTCT CCTGGCATGC AAATCGTCAA CTTGGCATGC CAAGAATTCG
GATCCAAGCT TAGGCCTGCT CGCTTTCTTG CTGTCCCATT TCTATTAAAG
GTTCCTTTGT TCCCTAAGTC CAACTACTAA ACTGGGGGAT ATTATGAAGG
GCCTTGAGCA TCTGGATTCT GCCTAGCGCT AAGCTTCCTA ACACGAGCCA
TAGATAGAAT AAAAGATTTT ATTTAGTCTC CAGAAAAAGG GGGGAATGAA
AGACCCCACC TGTAGGTTTG GCAAGCTAGC TTAAGTAAGC CATTTTGCAA
GGCATGGAAA AATACATAAC TGAGAATAGA GAAGTTCAGA TCAAGGTTAG
GAACAGAGAG ACAGGAGAAT ATGGGCCAAA CAGGATATCT GTGGTAAGCA
GTTCCTGCCC CGGCTCAGGG CCAAGAACAG TTGGAACAGC AGAATATGGG
CCAAACAGGA TATCTGTGGT AAGCAGTTCC TGCCCCGGCT CAGGGCCAAG
AACAGATGGT CCCCAGATGC GGTCCCGCCC TCAGCAGTTT CTAGAGAACC
ATCAGATGTT TCCAGGGTGC CCCAAGGACC TGAAATGACC CTGTGCCTTA
TTTGAACTAA CCAATCAGTT CGCTTCTCGC TTCTGTTCGC GCGCTTCTGC
TCCCCGAGCT CAATAAAAGA GCCCACAACC CCTCACTCGG CGCGCCAGTC
CTCCGATAGA CTGCGTCGCC CGGGGTACCC GTATTCCCAA TAAAGCCTCT
TGCTGTTTGC ATCCGAATCG TGGACTCGCT GATCCTTGGG AGGGTCTCCT
CAGATTGATT GACTGCCCAC CTCGGGGGTC TTTCATTCTC GAGAGCTTTG
GCGTAATCAT GGTCATAGCT GTTTCCTGTG TGAAATTGTT ATCCGCTCAC
AATTCCACAC AACATACGAG CCGGAAGCAT AAAGTGTAAA GCCTGGGGTG
CCTAATGAGT GAGCTAACTC ACATTAATTG CGTTGCGCTC ACTGCCCGCT
TTCCAGTCGG GAAACCTGTC GTGCCAGCTG CATTAATGAA TCGGCCAACG
CGCGGGGAGA GGCGGTTTGC GTATTGGGCG CTCTTCCGCT TCCTCGCTCA
CTGACTCGCT GCGCTCGGTC GTTCGGCTGC GGCGAGCGGT ATCAGCTCAC
TCAAAGGCGG TAATACGGTT ATCCACAGAA TCAGGGGATA ACGCAGGAAA
GAACATGTGA GCAAAAGGCC AGCAAAAGGC CAGGAACCGT AAAAAGGCCG
CGTTGCTGGC GTTTTTCCAT AGGCTCCGCC CCCCTGACGA GCATCACAAA
AATCGACGCT CAAGTCAGAG GTGGCGAAAC CCGACAGGAC TATAAAGATA

CCAGGCGTTT CCCCCTGGAA GCTCCCTCGT GCGCTCTCCT GTTCCGACCC
TGCCGCTTAC CGGATACCTG TCCGCCTTTC TCCCTTCGGG AAGCGTGGCG
CTTTCTCAAT GCTCACGCTG TAGGTATCTC AGTTCGGTGT AGGTCGTTCG
CTCCAAGCTG GGCTGTGTGC ACGAACCCCC CGTTCAGCCC GACCGCTGCG
CCTTATCCGG TAACTATCGT CTTGAGTCCA ACCCGGTAAG ACACGACTTA
TCGCCACTGG CAGCAGCCAC TGGTAACAGG ATTAGCAGAG CGAGGTATGT
AGGCGGTGCT ACAGAGTTCT TGAAGTGGTG GCCTAACTAC GGCTACACTA
GAAGGACAGT ATTTGGTATC TGCGCTCTGC TGAAGCCAGT TACCTTCGGA
AAAAGAGTTG GTAGCTCTTG ATCCGGCAAA CAAACCACCG CTGGTAGCGG
TGGTTTTTTT GTTTGCAAGC AGCAGATTAC GCGCAGAAAA AAAGGATCTC
AAGAAGATCC TTTGATCTTT TCTACGGGGT CTGACGCTCA GTGGAACGAA
AACTCACGTT AAGGGATTTT GGTCATGAGA TTATCAAAAA GGATCTTCAC
CTAGATCCTT TTAAATTAAA AATGAAGTTT TAAATCAATC TAAAGTATAT
ATGAGTAAAC TTGGTCTGAC AGTTACCAAT GCTTAATCAG TGAGGCACCT
ATCTCAGCGA TCTGTCTATT TCGTTCATCC ATAGTTGCCT GACTCCCCGT
CGTGTAGATA ACTACGATAC GGGAGGGCTT ACCATCTGGC CCCAGTGCTG
CAATGATACC GCGAGACCCA CGCTCACCGG CTCCAGATTT ATCAGCAATA
AACCAGCCAG CCGGAAGGGC CGAGCGCAGA AGTGGTCCTG CAACTTTATC
CGCCTCCATC CAGTCTATTA ATTGTTGCCG GGAAGCTAGA GTAAGTAGTT
CGCCAGTTAA TAGTTTGCGC AACGTTGTTG CCATTGCTGC TGGCATCGTG
GTGTCACGCT CGTCGTTTGG TATGGCTTCA TTCAGCTCCG GTTCCCAACG
ATCAAGGCGA GTTACATGAT CCCCCATGTT GTGCAAAAAA GCGGTTAGCT
CCTTCGGTCC TCCGATCGTT GTCAGAAGTA AGTTGGCCGC AGTGTTATCA
CTCATGGTTA TGGCAGCACT GCATAATTCT CTTACTGTCA TGCCATCCGT
AAGATGCTTT TCTGTGACTG GTGAGTACTC AACCAAGTCA TTCTGAGAAT
AGTGTATGCG GCGACCGAGT TGCTCTTGCC CGGCGTCAAT ACGGGATAAT
ACCGCGCCAC ATAGCAGAAC TTTAAAAGTG CTCATCATTG GAAAACGTTC
TTCGGGGCGA AAACTCTCAA GGATCTTACC GCTGTTGAGA TCCAGTTCGA
TGTAACCCAC TCGTGCACCC AACTGATCTT CAGCATCTTT TACTTTCACC
AGCGTTTCTG GGTGAGCAAA AACAGGAAGG CAAAATGCCG CAAAAAAGGG
AATAAGGGCG ACACGGAAAT GTTGAATACT CATACTCTTC CTTTTTCAAT
ATTATTGAAG CATTTATCAG GGTTATTGTC TCATGAGCGG ATACATATTT
GAATGTATTT AGAAAAATAA ACAAATAGGG GTTCCGCGCA CATTTCCCCG
AAAAGTGCCA CCTGACGTCT AAGAAACCAT TATTATCATG ACATTAACCT
ATAAAAATAG GCGTATCACG AGGCCCTTTC GTCTTCAAGC TGCCTCGCGC
GTTTCGGTGA TGACGGTGAA AACCTCTGAC ACATGCAGCT CCCGGAGACG
GTCACAGCTT GTCTGTAAGC GGATGCCGGG AGCAGACAAG CCCGTCAGGG
CGCGTCAGCG GGTGTTGGCG GGTGTCGGGG CGCAGCCATG ACCCAGTCAC
GTAGCGATAG TTACTATGCG GCATCAGAGC AGATTGTACT GAGAGTGCAC
CATATGCGGT GTGAAATACC GCACAGATGC GTAAGGAGAA AATACCGCAT
CAGGCGCCAT TCGCCATTCA GGCTGCGCAA CTGTTGGGAA GGGCGATCGG
TGCGGGCCTC TTCGCTATTA CGCCAGCTGG CGAAAGGGGG ATGTGCTGCA
AGGCGATTAA GTTGGGTAAC GCCAGGGTTT TCCCAGTCAC GACGTTGTAA
AACGACGGCC AGTGAATTAG TACTCTAGCT TAAGTAAGCC ATTTTGCAAG
GCATGGAAAA ATACATAACT GAGAATAGAG AAGTTCAGAT CAAGGTTAGG
AACAGAGAGA CAGGAGAATA TGGGCCAAAC AGGATATCTG TGGTAAGCAG
TTCCTGCCCC GGCTCAGGGC CAAGAACAGT TGGAACAGCA GAATATGGGC
CAAACAGGAT ATCTGTGGTA AGCAGTTCCT GCCCCGGCTC AGGGCCAAGA
ACAGATGGTC CCCAGATGCG GTCCCGCCCT CAGCAGTTTC TAGAGAACCA
TCAGATGTTT CCAGGGTGCC CCAAGGACCT GAAATGACCC TGTGCCTTAT
TTGAACTAAC CAATCAGTTC GCTTCTCGCT TCTGTTCGCG CGCTTCTGCT
CCCCGAGCTC AATAAAAGAG CCCACAACCC CTCACTCGGC GCGCCAGTCC
TCCGATTGAC TGCGTCGCCC GGGTACCCGT ATTCCCAATA AAGCCTCTTG
CTGTTTGCAT CCGAATCGTG GACTCGCTGA TCCTTGGGAG GGTCTCCTCA
GATTGATTGA CTGCCCACCT CGGGGGTCTT TCATTTGGAG GTTCCACCGA

GATTTGGAGA CCCCTGCCCA GGGACCACCG ACCCCCCCGC CGGGAGGTAA
GCTGGCCAGC GGTCGTTTCG TGTCTGTCTC TGTCTTTGGG CGTGTTTGTG
CCGGCATCTA ATGTTTGCGC CTGCGTCTGT ACTAGTTGGC TAACTAGATC
TGTATCTGGC GGTCCCGCGG AAGAACTGAC GAGTTCGTAT TCCCGGCCGC
AGCCCCTGGG AGACGTCCCA GCGGCCTCGG GGGCCCGTTT TGTGGCCCAT
TCTGTATCAG TTAACCTACC CGAGTCGGAC TTTTTGGAGC TCCGCCACTG
TCCGAGGGGT ACGTGGCTTT GTTGGGGGAC GAGAGACAGA GACACTTCCC
GCCCCCGTCT GAATTTTTGC TTTCGGTTTT ACGCCGAAAC CGCGCCGCGC
GTCTTGTCTG CTGC

pMP71 TRP1-TCR-IRES-CD19 retroviral construct

AGCATCGTTCTGTGTTGTCTCTGTCTGACTGTGTTTCTGTATTTGTCTGAAAATTAGCTCG
ACAAAGTTAAGTAATAGTCCCTCTCTCCAAGCTCACTTACAGGCGGCCGCGCCACCCCCGG
ACCATGGTGCTGGCTCTGCTGCCTGTGCTGGGCATCCACTTTCTGCTGAGAGATGCCCAGG
CCCAGAGCGTGACACAGCCTGATGCTAGAGTGACCGTGTCCGAGGGCGCCAGCCTGCAGCT
GAGATGCAAGTACAGCAGCAGCGTGACCCCCTACCTGTTTTGGTACGTGCAGTACCCCAGA
CAGGGACTGCAGCTGCTGCTGAAGTACTACAGCGGCGACCCTGTGGTGCAGGGCGTGAACG
GATTCGAGGCCGAGTTCAGCAAGAGCAACAGCAGCTTCCACCTGAGAAAGGCCTCCGTGCA
TTGGAGCGACAGCGCCGTGTACTTCTGCGCCGTGTCCAGCAACAACAACAGAATCTTCTTC
GGCGACGGCACCCAGCTGGTCGTGAAGCCCAACATCCAGAACCCCGAGCCTGCCGTGTACC
AGCTGAAGGACCCTAGAAGCCAGGACAGCACCCTGTGCCTGTTCACCGACTTCGACAGCCA
GATCAACGTGCCCAAGACCATGGAAAGCGGCACCTTCATCACCGATAAGTGCGTGCTGGAC
ATGAAGGCCATGGACAGCAAGTCCAACGGCGCTATCGCCTGGTCCAACCAGACCAGCTTCA
CATGCCAGGACATCTTCAAAGAGACAAACGCCACCTACCCCAGCAGCGACGTGCCATGTGA
CGCCACCCTGACCGAGAAGTCCTTCGAGACAGACATGAACCTGAACTTCCAGAACCTGAGC
GTGATGGGCCTGAGAATCCTGCTGCTGAAAGTGGCCGGCTTCAACCTGCTGATGACCCTGA
GACTGTGGTCCAGCGGCTCTGGCGCCACGAACTTCTCTCTGTTAAAGCAAGCAGGAGACGT
GCAAGAAAACCCCGGTCCCATGCTGTACTCCCTGCTGGCTTTCCTGCTGGGAATGTTCCTG
GGCGTGTCCGCCCAGACCATCCACCAGTGGCCTGTGGCCGAGATCAAGGCTGTGGGCAGCC
CTCTGTCTCTGGGCTGCACCATCAAGGGCAAGAGCAGCCCCAACCTGTACTGGTACTGGCA
GGCTACCGGCGGCACACTGCAGCAGCTGTTCTACAGCATCACCGTGGGCCAGGTGGAAAGC
GTGGTGCAGCTGAACCTGTCCGCCAGCAGACCCAAGGACGACCAGTTCATCCTGAGCACCG
AGAAACTGCTGCTGAGCCACAGCGGCTTCTACCTGTGTGCTTGGAGCCCTGGCCACCAGGA
CACCCAGTACTTTGGCCCTGGCACAAGACTGCTGGTGCTGGAAGATCTGAGAAACGTGACC
CCTCCCAAGGTGTCCCTGTTCGAGCCTAGCAAGGCTGAGATCGCCAACAAGCAGAAAGCCA
CCCTCGTGTGCCTGGCCAGAGGCTTCTTCCCCGACCACGTGGAACTGTCTTGGTGGGTCAA
CGGCAAAGAGGTGCACTCCGGCGTGTGCACAGACCCCCAGGCCTACAAAGAGAGCAACTAC
AGCTACTGCCTGAGCAGCAGACTGAGAGTGTCCGCCACCTTCTGGCACAACCCCAGAAACC
ACTTCAGGTGCCAGGTGCAGTTTCACGGCCTGAGCGAAGAGGACAAGTGGCCTGAGGGCAG
CCCAAAGCCCGTGACCCAGAACATCTCTGCCGAGGCTTGGGGCAGAGCCGACTGCGGCATT
ACAAGCGCTAGCTACCAGCAGGGGGTGCTGAGCGCCACCATCCTGTACGAGATTCTGCTGG
GCAAGGCCACCCTGTACGCCGTGCTGGTGTCTACCCTGGTCGTGATGGCCATGGTCAAGAG
AAAGAACTCCTGAGTCGACACGCGTACGTCGCGACCGCGGACATGTACAGAGCTCGAGCGG
GATCAATTCCGCCCCCCCCCTAACGTTACTGGCCGAAGCCGCTTGGAATAAGGCCGGTGTG
CGTTTGTCTATATGTTATTTTCCACCATATTGCCGTCTTTTGGCAATGTGAGGGCCCGGAA
ACCTGGCCCTGTCTTCTTGACGAGCATTCCTAGGGGTCTTTCCCCTCTCGCCAAAGGAATG
CAAGGTCTGTTGAATGTCGTGAAGGAAGCAGTTCCTCTGGAAGCTTCTTGAAGACAAACAA
CGTCTGTAGCGACCCTTTGCAGGCAGCGGAACCCCCCACCTGGCGACAGGTGCCTCTGCGG
CCAAAAGCCACGTGTATAAGATACACCTGCAAAGGCGGCACAACCCCAGTGCCACGTTGTG
AGTTGGATAGTTGTGGAAAGAGTCAAATGGCTCTCCTCAAGCGTATTCAACAAGGGGCTGA
AGGATGCCCAGAAGGTACCCCATTGTATGGGATCTGATCTGGGGCCTCGGTGCACATGCTT
TACATGTGTTTAGTCGAGGTTAAAAAACGTCTAGGCCCCCCGAACCACGGGGACGTGGTTT
TCCTTTGAAAAACACGATAATAATGCCACCATGCCATCTCCTCTCCCTGTCTCCTTCCTCC
TCTTTCTTACCTTAGTAGGAGGCAGGCCCCAGAAGTCCTTACTGGTGGAGGTAGAAGAGGG
AGGCAATGTTGTGCTGCCATGCCTCCCGGACTCCTCACCTGTCTCTTCTGAGAAGCTGGCT
TGGTATCGAGGTAACCAGTCAACACCCTTCCTGGAGCTGAGCCCCGGGTCCCCTGGCCTGG
GATTGCACGTGGGGTCCCTGGGCATCTTGCTAGTGATTGTCAATGTCTCAGACCATATGGG
GGGCTTCTACCTGTGCCAGAAGAGGCCCCCTTTCAAGGACATCTGGCAGCCTGCCTGGACA
GTGAACGTGGAGGATAGTGGGGAGATGTTCCGGTGGAATGCTTCAGACGTCAGGGACCTGG
ACTGTGACCTAAGGAACAGGTCCTCTGGGAGCCACAGGTCCACTTCTGGTTCCCAGCTGTA
TGTGTGGGCTAAAGACCATCCTAAGGTCTGGGGAACAAAGCCTGTATGTGCCCCTCGGGGG
AGCAGTTTGAATCAGAGTCTAATCAACCAAGACCTCACTGTGGCACCCGGCTCCACACTTT
GGCTGTCCTGTGGGGTACCCCCTGTCCCAGTGGCCAAAGGCTCCATCTCCTGGACCCATGT
GCATCCTAGGAGACCTAATGTTTCACTACTGAGCCTAAGCCTTGGGGGAGAGCACCCGGTC

AGAGAGATGTGGGTTTGGGGGTCTCTTCTGCTTCTGCCCCAAGCCACAGCTTTAGATGAAG
GCACCTATTATTGTCTCCGAGGAAACCTGACCATCGAGAGGCACGTGAAGGTCATTGCAAG
GTCAGCAGTGTGGCTCTGGCTGTTGAGAACTGGTGGATGGATAGTCCCAGTGGTGACTTTA
GTATATGTCATCTTCTGTATGGTTTCTCTGGTGGCTTTTCTCTATTGTCAAAGAGCCTTTA
TCCTGAGAAGGAAAAGGAAGCGAATGACTGACCCCGCCAGGAGATTCTTCAAAGTGACGTG
ATCCGGATTAGTCCAATTTGTTAAAGACAGGATATCAGTGGTCCAGGCTCTAGTTTTGACT
CAACAATATCACCAGCTGAAGCCTATAGAGTGAATTCGGATCCAAGCTTAGGCCTGCTCGC
TTTCTTGCTGTCCCATTTCTATTAAAGGTTCCTTTGTTCCCTAAGTCCAACTACTAAACTG
GGGGATATTATGAAGGGCCTTGAGCATCTGGATTCTGCCTAGCGCTAAGCTTCCTAACACG
AGCCATAGATAGAATAAAAGATTTTATTTAGTCTCCAGAAAAAGGGGGGAATGAAAGACCC
CACCTGTAGGTTTGGCAAGCTAGCTTAAGTAAGCCATTTTGCAAGGCATGGAAAAATACAT
AACTGAGAATAGAGAAGTTCAGATCAAGGTTAGGAACAGAGAGACAGGAGAATATGGGCCA
AACAGGATATCTGTGGTAAGCAGTTCCTGCCCCGGCTCAGGGCCAAGAACAGTTGGAACAG
CAGAATATGGGCCAAACAGGATATCTGTGGTAAGCAGTTCCTGCCCCGGCTCAGGGCCAAG
AACAGATGGTCCCCAGATGCGGTCCCGCCCTCAGCAGTTTCTAGAGAACCATCAGATGTTT
CCAGGGTGCCCCAAGGACCTGAAATGACCCTGTGCCTTATTTGAACTAACCAATCAGTTCG
CTTCTCGCTTCTGTTCGCGCGCTTCTGCTCCCCGAGCTCAATAAAAGAGCCCACAACCCCT
CACTCGGCGCGCCAGTCCTCCGATAGACTGCGTCGCCCGGGGTACCCGTATTCCCAATAAA
GCCTCTTGCTGTTTGCATCCGAATCGTGGACTCGCTGATCCTTGGGAGGGTCTCCTCAGAT
TGATTGACTGCCCACCTCGGGGGTCTTTCATTCTCGAGAGCTTTGGCGTAATCATGGTCAT
AGCTGTTTCCTGTGTGAAATTGTTATCCGCTCACAATTCCACACAACATACGAGCCGGAAG
CATAAAGTGTAAAGCCTGGGGTGCCTAATGAGTGAGCTAACTCACATTAATTGCGTTGCGC
TCACTGCCCGCTTTCCAGTCGGGAAACCTGTCGTGCCAGCTGCATTAATGAATCGGCCAAC
GCGCGGGGAGAGGCGGTTTGCGTATTGGGCGCTCTTCCGCTTCCTCGCTCACTGACTCGCT
GCGCTCGGTCGTTCGGCTGCGGCGAGCGGTATCAGCTCACTCAAAGGCGGTAATACGGTTA
TCCACAGAATCAGGGGATAACGCAGGAAAGAACATGTGAGCAAAAGGCCAGCAAAAGGCCA
GGAACCGTAAAAAGGCCGCGTTGCTGGCGTTTTTCCATAGGCTCCGCCCCCCTGACGAGCA
TCACAAAAATCGACGCTCAAGTCAGAGGTGGCGAAACCCGACAGGACTATAAAGATACCAG
GCGTTTCCCCCTGGAAGCTCCCTCGTGCGCTCTCCTGTTCCGACCCTGCCGCTTACCGGAT
ACCTGTCCGCCTTTCTCCCTTCGGGAAGCGTGGCGCTTTCTCAATGCTCACGCTGTAGGTA
TCTCAGTTCGGTGTAGGTCGTTCGCTCCAAGCTGGGCTGTGTGCACGAACCCCCCGTTCAG
CCCGACCGCTGCGCCTTATCCGGTAACTATCGTCTTGAGTCCAACCCGGTAAGACACGACT
TATCGCCACTGGCAGCAGCCACTGGTAACAGGATTAGCAGAGCGAGGTATGTAGGCGGTGC
TACAGAGTTCTTGAAGTGGTGGCCTAACTACGGCTACACTAGAAGGACAGTATTTGGTATC
TGCGCTCTGCTGAAGCCAGTTACCTTCGGAAAAAGAGTTGGTAGCTCTTGATCCGGCAAAC
AAACCACCGCTGGTAGCGGTGGTTTTTTTGTTTGCAAGCAGCAGATTACGCGCAGAAAAAA
AGGATCTCAAGAAGATCCTTTGATCTTTTCTACGGGGTCTGACGCTCAGTGGAACGAAAAC
TCACGTTAAGGGATTTTGGTCATGAGATTATCAAAAAGGATCTTCACCTAGATCCTTTTAA
ATTAAAAATGAAGTTTTAAATCAATCTAAAGTATATATGAGTAAACTTGGTCTGACAGTTA
CCAATGCTTAATCAGTGAGGCACCTATCTCAGCGATCTGTCTATTTCGTTCATCCATAGTT
GCCTGACTCCCCGTCGTGTAGATAACTACGATACGGGAGGGCTTACCATCTGGCCCCAGTG
CTGCAATGATACCGCGAGACCCACGCTCACCGGCTCCAGATTTATCAGCAATAAACCAGCC
AGCCGGAAGGGCCGAGCGCAGAAGTGGTCCTGCAACTTTATCCGCCTCCATCCAGTCTATT
AATTGTTGCCGGGAAGCTAGAGTAAGTAGTTCGCCAGTTAATAGTTTGCGCAACGTTGTTG
CCATTGCTGCTGGCATCGTGGTGTCACGCTCGTCGTTTGGTATGGCTTCATTCAGCTCCGG
TTCCCAACGATCAAGGCGAGTTACATGATCCCCCATGTTGTGCAAAAAAGCGGTTAGCTCC
TTCGGTCCTCCGATCGTTGTCAGAAGTAAGTTGGCCGCAGTGTTATCACTCATGGTTATGG
CAGCACTGCATAATTCTCTTACTGTCATGCCATCCGTAAGATGCTTTTCTGTGACTGGTGA
GTACTCAACCAAGTCATTCTGAGAATAGTGTATGCGGCGACCGAGTTGCTCTTGCCCGGCG
TCAATACGGGATAATACCGCGCCACATAGCAGAACTTTAAAAGTGCTCATCATTGGAAAAC
GTTCTTCGGGGCGAAAACTCTCAAGGATCTTACCGCTGTTGAGATCCAGTTCGATGTAACC
CACTCGTGCACCCAACTGATCTTCAGCATCTTTTACTTTCACCAGCGTTTCTGGGTGAGCA
AAAACAGGAAGGCAAAATGCCGCAAAAAAGGGAATAAGGGCGACACGGAAATGTTGAATAC
TCATACTCTTCCTTTTTCAATATTATTGAAGCATTTATCAGGGTTATTGTCTCATGAGCGG
ATACATATTTGAATGTATTTAGAAAAATAAACAAATAGGGGTTCCGCGCACATTTCCCCGA

AAAGTGCCACCTGACGTCTAAGAAACCATTATTATCATGACATTAACCTATAAAAATAGGC
GTATCACGAGGCCCTTTCGTCTTCAAGCTGCCTCGCGCGTTTCGGTGATGACGGTGAAAAC
CTCTGACACATGCAGCTCCCGGAGACGGTCACAGCTTGTCTGTAAGCGGATGCCGGGAGCA
GACAAGCCCGTCAGGGCGCGTCAGCGGGTGTTGGCGGGTGTCGGGGCGCAGCCATGACCCA
GTCACGTAGCGATAGTTACTATGCGGCATCAGAGCAGATTGTACTGAGAGTGCACCATATG
CGGTGTGAAATACCGCACAGATGCGTAAGGAGAAAATACCGCATCAGGCGCCATTCGCCAT
TCAGGCTGCGCAACTGTTGGGAAGGGCGATCGGTGCGGGCCTCTTCGCTATTACGCCAGCT
GGCGAAAGGGGGATGTGCTGCAAGGCGATTAAGTTGGGTAACGCCAGGGTTTTCCCAGTCA
CGACGTTGTAAAACGACGGCCAGTGAATTAGTACTCTAGCTTAAGTAAGCCATTTTGCAAG
GCATGGAAAAATACATAACTGAGAATAGAGAAGTTCAGATCAAGGTTAGGAACAGAGAGAC
AGGAGAATATGGGCCAAACAGGATATCTGTGGTAAGCAGTTCCTGCCCCGGCTCAGGGCCA
AGAACAGTTGGAACAGCAGAATATGGGCCAAACAGGATATCTGTGGTAAGCAGTTCCTGCC
CCGGCTCAGGGCCAAGAACAGATGGTCCCCAGATGCGGTCCCGCCCTCAGCAGTTTCTAGA
GAACCATCAGATGTTTCCAGGGTGCCCCAAGGACCTGAAATGACCCTGTGCCTTATTTGAA
CTAACCAATCAGTTCGCTTCTCGCTTCTGTTCGCGCGCTTCTGCTCCCCGAGCTCAATAAA
AGAGCCCACAACCCCTCACTCGGCGCGCCAGTCCTCCGATTGACTGCGTCGCCCGGGTACC
CGTATTCCCAATAAAGCCTCTTGCTGTTTGCATCCGAATCGTGGACTCGCTGATCCTTGGG
AGGGTCTCCTCAGATTGATTGACTGCCCACCTCGGGGGTCTTTCATTTGGAGGTTCCACCG
AGATTTGGAGACCCCTGCCCAGGGACCACCGACCCCCCCGCCGGGAGGTAAGCTGGCCAGC
GGTCGTTTCGTGTCTGTCTCTGTCTTTGGGCGTGTTTGTGCCGGCATCTAATGTTTGCGCC
TGCGTCTGTACTAGTTGGCTAACTAGATCTGTATCTGGCGGTCCCGCGGAAGAACTGACGA
GTTCGTATTCCCGGCCGCAGCCCCTGGGAGACGTCCCAGCGGCCTCGGGGGCCCGTTTTGT
GGCCCATTCTGTATCAGTTAACCTACCCGAGTCGGACTTTTTGGAGCTCCGCCACTGTCCG
AGGGGTACGTGGCTTTGTTGGGGGACGAGAGACAGAGACACTTCCCGCCCCCGTCTGAATT
TTTGCTTTCGGTTTTACGCCGAAACCGCGCCGCGCGTCTTGTCTGCTGC